Methane emissions from rice paddies; experiments and modelling

Peter M. van Bodegom

Methane emissions from rice paddies; experiments and modelling

Peter M. van Bodegom

N$\mathcal{W}$O

Stellingen

1. Het is goed mogelijk seizoensemissies van methaan uit rijstvelden te voorspellen met een vereenvoudigd procesmodel.
   Dit proefschrift

2. De beschikbaarheid van ruimtelijke agronomische informatie is meer limiterend voor regionale methaanemissieschattingen dan de nauwkeurigheid van procesmodellen.
   Dit proefschrift

3. Het veilig stellen van voedselzekerheid heeft een hogere prioriteit dan terugdringing van het broeikasgaseffect bij het manipuleren van methaanemissies uit rijstvelden.

4. Emissiebeperkende maatregelen dienen ter plaatse van de emissie genomen te worden.

5. De oorzaak van het mislukken van diverse 'extension programs' zit al in de naam.

6. Aannames in wetenschappelijk werk zijn belangrijker dan de resultaten zelf.

7. Onderzoek doen is als de vlinder van Lorenz.

8. Landen in ontwikkeling op het gebied van bestuur en beleid hebben de meeste baat bij ontwikkelingshulp.

9. In een modernistische organisatie verzandt beleid gericht op randvoorwaarden in meer regels.

10. De enige passende infrastructurele uitbreidingen voor Nederland zijn die voor een kennisinfrastructuur.

11. Nederlanders hebben geen teveel aan individuele vrijheid, maar hoogstens een tekort aan schaamte.

12. Juridificatie van het verzekeringswezen ondermijnt de samenleving.

Stellingen bij het proefschrift 'Methane emissions from rice paddies; experiments and modelling' van Peter M. van Bodegom
Wageningen, 13 oktober 2000

Acknowledgements

Table of contents

Abstract

This thesis describes model development and experimentation on the comprehension and prediction of methane (CH_4) emissions from rice paddies. The large spatial and temporal variability in CH_4 emissions and the dynamic non-linear relationships between processes underlying CH_4 emissions impairs the applicability of empirical relations. Mechanistic concepts are therefore starting point of analysis throughout the thesis.

The process of CH_4 production was investigated by soil slurry incubation experiments at different temperatures and with additions of different electron donors and acceptors. Temperature influenced conversion rates and the competitiveness of microorganisms. The experiments were used to calibrate and validate a mechanistic model on CH_4 production that describes competition for acetate and H_2/CO_2, inhibition effects and chemolithotrophic reactions. The redox sequence leading eventually to CH_4 production was well predicted by the model, calibrating only the maximum conversion rates.

Gas transport through paddy soil and rice plants was quantified by experiments in which the transport of SF_6 was monitored continuously by photoacoustics. A mechanistic model on gas transport in a flooded rice system based on diffusion equations was validated by these experiments and could explain why most gases are released via plant mediated transport. Variability in root distribution led to highly variable gas transport.

Experiments showed that CH_4 oxidation in the rice rhizosphere was oxygen (O_2) limited. Rice rhizospheric O_2 consumption was dominated by chemical iron oxidation, and heterotrophic and methanotrophic respiration. The most abundant methanotrophs and heterotrophs were isolated and kinetically characterised. Based upon these experiments it was hypothesised that CH_4 oxidation mainly occurred at microaerophilic, low acetate conditions not very close to the root surface. A mechanistic rhizosphere model that combined production and consumption of O_2, carbon and iron compounds with iron adsorption kinetics and diffusive transport in a rice plant and rhizosphere, confirmed this hypothesis. Oxidation of CH_4 depended on acetate and O_2 concentrations and on variables influencing competition between methanotrophs and chemical iron oxidation. Oxidation of CH_4 also depended on root growth dynamics and was intrinsically dynamic.

The process-based concepts were simplified in a field scale model on CH_4 emissions by dividing a rice paddy into a rhizosphere compartment and a bulk soil compartment. The field scale model was validated by independent CH_4 emission measurements from fields in the Philippines, China and Indonesia in different seasons and with different inorganic and organic fertiliser additions. The model predicted CH_4 emissions well with only few generally available site-specific input parameters. A sensitivity analysis showed that the model was very sensitive to the description of substrate supply.

The field scale model was coupled to a Geographic Information System to scale up regional CH_4 emissions from rice paddies, as was the aim of the overall project. Regional CH_4 emission estimates were however affected by the applied interpolation technique and by data resolution effects in a case study for the island of Java, Indonesia. The scaling effects were induced by the combination of a loss of information on heterogeneities and by non-linear model responses. Data availability and not model uncertainty, which was small for the field scale model developed in this thesis, limits upscaling of CH_4 emissions from rice paddies to regions.

General introduction

1.1 Methane emissions and rice production

The greenhouse effect

Since the late 1980s there is an increased public concern on the impact of human activities on the environment. One of the issues is global warming; the enhanced greenhouse effect. The global climate is controlled by the balance of heating by incoming short-wave solar radiation and cooling by long-wave infrared radiation into space. Part of the outgoing infrared radiation is trapped by radiatively active gases, the so-called greenhouse gases. This leads to an increased global temperature; the basic greenhouse effect. Without this basic greenhouse effect, mean global temperature would be about -18°C (Houghton et al., 1995), making life in its present form virtually impossible.

The concentration of greenhouse gases in the atmosphere increases since the onset of industrialisation due to human activities. This enhanced greenhouse effect is of concern, because it may cause additional global warming, change weather patterns and cause more extreme weather events like storms, floods and droughts. The most important contributions to enhanced greenhouse effect are caused by carbon dioxide, CO_2 (62%), methane, CH_4 (20%) and nitrous oxide, N_2O (4%). Man-made chlorofluorocarbons (CFC's) also contribute to the enhanced greenhouse effect (Houghton et al., 1995). These are estimated values and the uncertainties in the estimates are large, although the greenhouse gases have been subject to many research projects since the late 1980s. The enhanced greenhouse effect is difficult to detect, because it is small compared to the background of the much larger basic greenhouse effect and because of the large natural variation in temperature and weather. Yet, 'the balance of evidence suggests a discernible human influence on global climate' (IPCC, 1995). Reducing or even stabilising greenhouse gas emissions will however most probably slow down economic growth or human welfare, which makes it politically difficult to carry out.

Table 1.1:   Estimated atmospheric methane budget in Tg CH_4 yr^1 (1 Tg=10^{12} g) (Houghton et al., 1995)

Sources			Sinks		
Natural			*Atmosphere*		
	Wetlands	115 (55-150)		Troposphere	445 (360-530)
	Other	45 (25-140)		Stratosphere	40 (32-48)
Anthropogenic			*Soils*		30 (15-45)
	Fossil fuel related	100 (70-120)			
	Cattle (Enteric fermentation)	85 (65-100)			
	Rice paddies	60 (20-100)			
	Biomass burning	40 (20-80)			
	Landfills	40 (20-70)			
	Other	50 (35-110)			
Total		535 (410-660)	*Total*		515 (430-600)

Global methane emissions

Methane has been recognised as one of the principal greenhouse gases and methane concentrations doubled in the last century (a percentual increase larger than those of CO_2 and N_2O). Methane is not only a potent greenhouse gas, but it is also chemically active in the atmosphere influencing atmospheric concentrations of several important species like hydroxyl radicals (OH•), ozone and carbon monoxide (Cicerone and Oremland, 1988). About 2/3 of the current atmospheric methane sources is anthropogenic (Table 1.1), whereas its major sink, the reaction with OH• in the atmosphere, is only indirectly influenced by human activities. Although the individual sources of global methane emissions have been identified, there are large uncertainties in the individual source strength estimates (Table 1.1). This is mainly because experimental data show a large variation that is hard to relate to easily measurable variables due to interacting underlying processes, discussed below. The net atmospheric CH_4 increase is estimated at 37 (35-40) Tg yr^{-1} (Houghton et al., 1995) and is probably related to rising human activities, among which rice production is very important.

Rice production

Rice is one of world's most important food crops and is the dominant food crop in the humid subtropics and humid and subhumid tropics. Rice growing systems are categorised into upland, irrigated, rainfed and deepwater rice. Upland rice fields contribute 14% to total rice production (Neue and Roger, 1994) and are never flooded. Deepwater rice, on the contrary, has long growing seasons with more than half a meter of water. Rainfed rice has an irregular water supply. In the last decades many rainfed rice fields have been transformed into irrigated rice fields to increase rice production. Irrigated rice is concentrated mainly in the humid and subhumid subtropics and humid tropics. It contributes to 76% of the global rice production on 54% of the rice harvested area (Neue and Roger, 1994).

From 1951 to 1990 the harvested area of rice increased from 104 to 146 million ha and rice production increased even faster under influence of the green revolution; from 171 to 519 million tons of rough rice (IRRI, 1991). The green revolution mainly affected irrigated rice systems that are now characterised by high cropping intensity and intensive use of agrochemicals, like pesticides and inorganic fertilisers. Improved rice varieties have been developed for irrigated rice lands. They have a short growth duration, relatively short stem, high tillering capacity and incorporated resistance to several biological stress factors and some tolerance for adverse soil conditions (Hossain, 1996). These characteristics allow multiple rice cropping per year. The change in harvested area, yield and adoption of improved rice varieties have been far from uniform across Asia (IRRI, 1991). The determining factor for the adoption of improved rice varieties is the degree of water control (David and Otsuka, 1994). Rice cultivation environments with a lesser degree of water control have far more diverse conditions than described above for irrigated rice systems, ranging from aerobic to anaerobic, organically to inorganically fertilised and from tall traditional varieties to improved rice varieties.

Methane emissions from rice fields

Methane emission is the outcome of the balance between methane production, oxidation and transport (Segers, 1998). Methane production is a microbiological process, that

occurs when organic matter is degraded anaerobically and w hen most alternative terminal electron acceptors -nitrate, ferric iron and sulphate- have been depleted (Conrad, 1993). Flooded rice fields have anaerobic soil conditions. Methane oxidation is also a microbiological process and needs oxygen in addition to methane and occurs therefore only at aerobic/anaerobic interfaces. In rice fields, such interfaces exist in the rhizosphere (i.e. soil influenced by the nearby presence of roots) and at the soil -water interface. Methane transport can occur via diffusion, g as bubble release (called ebullition) and via the aerenchyma of vascular plants. Rice plants have such aerenchyma (e.g. Jackson and Armstrong, 1999). The three processes depend upon each other and are influenced by a number of interacting factors like wate r and nutrient management, vegetation (cultivar), soil characteristics and temperature.

Wetland rice fields, and especially irrigated rice fields, thus provide favourable conditions for methane release. The first global estimate of the methane source stren gth of rice paddies was 190 Tg yr^{-1} and was based on anaerobic incubation of paddy soil samples (Koyama, 1963). Since then, many scientific efforts have been made to improve the upscaling technique (for a review, see Denier van der Gon et al. (2000)) with which global or regional emission estimates have been improved. The most recent global emission estimate, that considers different rice ecosystems, is 60 Tg yr^{-1} (Table 1.1). However, this estimate is still highly tentative, as expressed by the large range (20-100 Tg yr^{-1}) in Table 1.1.

1.2 The project 'upscaling and downscaling of regional methane sources'

A more accurate estimate of methane emissions from some major sources is needed to reduce the uncertainty in the global methane budget. The project 'Up scaling and downscaling of regional methane sources - rice agriculture as a case study' started in 1995 with as main objective to reduce the uncertainty in one major methane source. The project team consisted of air chemists, land use change modellers, agro nomists, soil scientists and microbiologists. The project was supported financially by the Dutch National Research Program on Global Air Pollution and Climate Change (NRP project no. 951202) and was co-ordinated by Hugo Denier van der Gon.

Two regions where rice agriculture is the dominant methane source, were chosen for case studies, because i) rice paddies are an important anthropogenic source of methane, ii) this methane source is manageable and iii) the current source strength is highly uncertain. By improving the estimate from rice paddies, the uncertainty in the estimates for other CH$_4$ sources might be reduced as well. A better source strength estimate might also help to evaluate the impact and cost-benefit analysis of mitigation technologies.

For this purpose, both a bottom-up scaling methodology (upscaling) and a top-down scaling methodology (downscaling) for methane emissions from rice paddies were applied and compared in this project. In the upscaling approach, small scale flux measurements were aggregated to a regional scale. In this project a field scale model on methane emissions from rice paddies was developed based on microbiological, plant physiological, soil chemical and soil physical processes. The model was used in combination with a Geographic Information System (GIS) for upscaling while accounting for scaling effects. The downscaling approach used atmospheric transport and chemistry to deduce information on methane sources and sinks from the temporal and spatial variation of atmospheric me thane mixing ratios as measured by global air

sampling networks. In this project regional source apportionment was deduced by inverse modelling. Some of the variables controlling methane emissions from rice fields may change considerably on time scales larger than one season. For such variables, the rate of change and its impacts on emissions have to be quantified. For this purpose, temporal scaling -estimating past or future magnitudes based upon current estimates - was also included in the project.

Direct validation of methane emissions at regional scales is hardly possible. Therefore, the different methodologies to estimate the methane source strength were compared to obtain a quantitative evaluation of the precision and reliability of the calculated source strength estimates at the regional scale and to evaluate the scaling procedure itself. Such a comparison may help to constrain the source strength estimate and to cost -effectively reducing greenhouse gas emissions.

1.3 This thesis

This thesis is one out of three PhD theses that were written as part of the above mentioned project. The other two theses are on the downscaling approach (Houweling, 2000) and on temporal scaling (Verburg, 2000). The aims of this thesis are:

i) Development of a process-based model that can be coupled to a GIS for the calculation and prediction of methane emissions from rice paddies at a regional scale. Empirical relationships only explain part of the encountered variability in methane emissions (Walter et al., 1996) and are difficult to extrapolate beyond the region for which they were developed. Processes are reproducible and repeatable. A model applied at a regional scale thus needs to be process-based to allow better extrapolation possibilities to other regions and to limit the increase in uncertainty.

ii) Understanding and quantifying the role of controlling factors affecting methane emissions from rice paddies by experiments and models. A mechanistic understanding allows the application of a process-based model under various environmental conditions (different soils or temperature regimes) and management practices (water, nutrient, rice crop growth and cultivar management), and can indicate how methane emissions will change under changing conditions (e.g. by mitigation). Experiments were designed and performed based upon literature analysis in combination with uncertainty analysis of available models.

Most chapters of this thesis are to be published as individual research papers. Therefore, each of the chapters contains a separate introduction into the subject under consideration. In Chapter 2, the processes leading to methane emissions from rice paddies -methane production, oxidation and transport- are introduced, described and summarised in a computer model that predicts methane emissions at the field scale level. This model was developed so that only a few parameters, e.g. from a GIS, are needed to allow an emission calculation while the model is still process-based. These characteristics make the model suitable for upscaling purposes. A sensitivity analysis of the field scale model to regional input parameters is presented in Chapter 3. One of the attempts to use the model for upscaling purposes is described in Chapter 4 for the case study of the island of Java. Such an effort is important, because it couples models to databases and allows, using this combination, a better emission estimate. This integration of models and databases was one of the principal aims of the project, introduced above. A control of

spatial and temporal variability is a key issue in upscaling and is emphasised in this Chapter 4.

The other chapters in this thesis, Chapters 5 to 9, deal with quantification of the underlying processes: methane production, oxidation and transport. The quantification was carried out by a combination of experiments and model development to deal efficiently with the gaps in knowledge and to remain close to the objectives. The processes leading to methane production are treated in Chapters 5 and 6. Chapter 5 presents an experimental study on the effects of temperature and alternative electron acceptors on methane production. In Chapter 6, a mechanistic model on the processes determining methane production is presented and validated. The mechanisms of gas transport through a rice paddy system were investigated by experiments and mechanistic modelling (Chapter 7). The final process of importance, methane oxidation, is the subject of Chapters 8 and 9. An experimental basis for the process is treated first (Chapter 8) and then combined with information on methane production and methane transport to come to a mechanistic model that explains methane oxidation at a single root (Chapter 9).

At first sight, an analysis of processes at a detailed scale may not seem appropriate for the overall aim of the project. There are however profound reasons that make such an analysis necessary for the aims of upscaling methane emissions to regional scales. Firstly, one has to be sure that the simplifications made in the field scale model are acceptable (to avoid that inappropriate regional estimates are made). Therefore, the outcome of the mechanistic models is compared with the description in the simplified model (Chapter 10). Secondly, the interactions between the processes may lead to unexpected resul ts. It is important to consider these interactions to allow a general application of the field scale model. These interactions are an important reason for choosing a process -based approach instead of an empirical approach. Initial attempts to couple the pr ocesses are described in Chapter 9. Thirdly, understanding the underlying processes leading to methane emissions allows a more thorough and quantitative analysis of mitigation

Chapter

A process-based model for methane emission predictions from flooded rice paddies

H.A.C. Denier van der Gon[1,2], R. Wassmann[3] and J.M. Metra-Corton[4]

[1]Laboratory of Microbiology, Wageningen University (WU),
H. van Suchtelenweg 4, 6703 CT Wageningen, The Netherlands.
[2]Department of Theoretical Production Ecology (WU).
[3]Soil and Water Sciences Division, International Rice Research Institute, Los Baños, Philippines.
[4]Agronomy, Soil and Plant Physiology Division, Philippine Rice Research Institute,
Muñoz, Nueva Ecija, Philippines.

A process-based model for methane emission predictions from flooded rice paddies

Abstract

Estimation and prediction of methane emission from flooded rice paddies is impaired by the large spatial and temporal variability in methane emissions and by the dynamic non-linear relations between processes underlying methane emissions. This paper describes a process-based model on methane emission prediction from flooded rice paddies that can be used for extrapolation. The model is divided into two compartments; rhizosphere -which is a function of root length density- and bulk soil. The production of carbon substrates drives methane emission and originates from soil organic matter mineralisation, organic fertiliser decomposition -in both compartments- and root exudation and root decay -in the rhizosphere compartment only. It is assumed that the methanogens are completely outcompeted for acetate by nitrate and iron reducers, but that competition takes place with sulphate reducers. Produced methane is transported to the root surface in the rhizosphere or the soil-water interface in the bulk soil. Transport time coefficients are different for the two compartments. Part of the methane is oxidised; a constant fraction of produced methane in the bulk soil, whereas the oxidation fraction varies according to root activity dynamics in the rhizosphere. The remaining methane is emitted to the atmosphere. The model was validated with independent field measurements of methane emissions at sites in the Philippines, China and Indonesia with only few generally available site-specific input parameters. The model predicts methane emission dynamics and total seasonal methane emission for the sites, in different seasons and under different inorganic and organic fertiliser conditions. A sensitivity analysis on model assumptions showed that the assumptions made in this model are reasonable and that the division into two compartments was necessary to obtain good results with this model. The combination of proper prediction and the necessity of few input parameters allows model application at regional and global scales.

2.1 Introduction

Methane is one of the principal greenhouse gases and rice paddy fields are among the most important sources of atmospheric methane (Houghton et al., 1996). Precise estimates of global methane emissions from rice paddies are however not available and depend on the approaches, techniques and databases used. One principal cause for uncertainties in global estimates results from the large intrinsic spatial and temporal variability in methane emissions. This variation in methane emissions is only partly explained by correlations with environmental variables (Walter et al., 1996). This is attributed to the diurnal and seasonal dynamic and non-linear interactions between processes underlying methane emissions. A process-based model, quantifying the functional relationships between methane emissions and the most important underlying processes, methane production, oxidation and transport, may improve insight in these

relations and may thus contribute to a reduction of the uncertainties in global methane emission estimates from rice paddies.

This paper presents a process-based model that predicts seasonal methane emissions from flooded rice fields that can be applied at large scales using Geographic Information System (GIS). Such a model must be simple –by lack of mechanistic knowledge-, balanced and process-based -to cope with encountered variability and to avoid site specific calibrations. In addition, such a model should use only a few site characteristics as input parameters to avoid an excessively high data demand for the GIS and to allow scenario analyses at a larger spatial and temporal scale.

For this particular objective, other models on methane emissions from wetlands, including rice paddies -developed for different objectives and with different degrees of mechanistic detail- seem less suitable. Some models use methane emission data to parameterise empirical relations for some of the underlying processes (Hosono and Nouchi, 1997; Huang et al., 1998), which may be problematic for extrapolation to larger scales due to the non-linear interactions and the number of fitted parameters. Some more process-based models (Arah and Stephen, 1998; Walter et al., 1996) describe all processes as mechanistically as possible, although mechanistic knowledge on the spatial characteristics of driving variables, especially for methane production and gas transport, is scarce. Some parameters therefore have to be calibrated for each site specifically, particularly on methane production potential and plant transport characteristics. This necessary calibration limits the extrapolation possibilities of the models. Other process-based models emphasise methane production, whereas the descriptions of methane oxidation and methane transport are highly simplified (Cao et al., 1995; James, 1993).

The processes leading to methane emissions are highly different for the rhizosphere and the remaining part of the soil, the bulk soil (see section 2.1). In our model, the soil is therefore divided into two compartments, a rhizosphere and a bulk soil, without considering soil layers. This distinction allows an efficient and well-balanced approach for constructing a simple process-based model, because use can be made of the process differences between each compartment. With these two compartments, the variability can be decreased more efficiently than with a soil layer model, because differences between soil layers are smaller than differences between rhizosphere and bulk soil. The model was validated against independent experimental data collected by an automatic measurement system based on the closed chamber technique (Wassmann et al., 1994) in flooded rice fields at two sites in the Philippines, one site in China and one site in Indonesia, while using only generally available site specific parameters. A sensitivity analysis of the model was carried out to evaluate the assumptions made in the model. This sensitivity analysis was also helpful in obtaining insight in important gaps of knowledge.

2.2 Model description
Two model compartments: bulk soil and rhizosphere

Methane emissions from rice fields are strongly influenced by the presence of the rice plants. Methane emissions are higher with than without rice plants (Holzapfel-Pschorn et al., 1986) and methane emissions are dominated by plant mediated emissions (Schütz et al., 1989b). Recognition of the importance of rice plants has led to the development of correlative models between methane emissions and plant parameters (e.g. Sass et al.,

1990; Watanabe et al., 1994), although such correlations could not always be found (e.g. Denier van der Gon and Neue, 1996; Watanabe et al., 1995a). For a better quantitative understanding of the rice plant influence, the various processes by which the plant modifies methane emissions must be considered. The model quantifies these different processes of plant influence in a separate compartment: the rhizosphere. All other processes leading to methane emissions occur in a bulk soil compartment. The processes occur independently in both compartments outlined in Figure 2.1 and differ in some characteristics for the compartments: Organic matter in the rhizosphere is not only released by soil mineralisation and straw and stubble decomposition, but also by root exudation and root decay. Methane is transported by plant mediated transport in the rhizosphere, while ebullition and diffusion are the major transport routes in the bulk soil. The oxygen used for methane oxidation in the rhizosphere comes from Root Oxygen Release (ROL), whereas oxygen enters the bulk soil by diffusion through the soil-water interface. Before describing these processes in more detail, the distribution of the soil between the compartments during the season is treated.
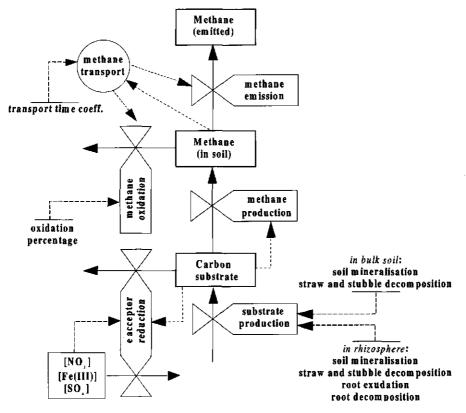
Figure 2.1: Relational diagram of the flow of carbon for each compartment in the model

The rice crop influences the processes underlying methane emissions via its roots. In general, the uptake and release of solutes and gases depend on the root length density (RLD) (Armstrong and Beckett, 1987; Kirk and Solivas, 1997). RLD is empirically related

to its maximum root length density (RLD_{max}) based on data by Beyrouty et al (1988), Drenth et al. (1991), Kang et al. (1995), Slaton et al. (1990) and Teo et al. (1995) and fitted by minimising the Mean Square Error (MSE) to a cumulative logistic growth curve up to RLD_{max} and an exponential decrease after RLD_{max} (Figure 2.2) as from that moment on roots start to decay:

$$RLD = \frac{RLD_{max}}{1+K \cdot e^{-rgr \cdot time'}} \qquad \text{For RLD} < \text{RLD}_{max}$$

$$RLD = \frac{RLD_{max}}{1+K \cdot e^{-rgr \cdot time'_{mor}}} \cdot e^{-k_{mor}(time' - time'_{mor})} \qquad \text{For RLD} \geq \text{RLD}_{ma} \qquad (2.1)$$

in which *time'* is the relative time (time divided by the total length of the plant growing season) and *rgr* (relative growth rate), K ((RLD_{max}-$RLD_{t=0}$)/$RLD_{t=0}$), k_{mor} (relative root mortality rate) and *time'$_{mor}$* (relative time at which roots start to die) are dimensionless empirical parameters (Table 2.1).
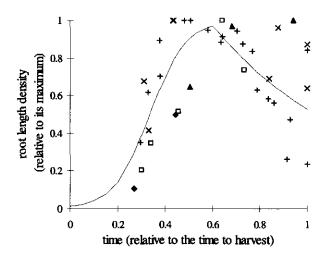
Figure 2.2:   Time course of relative root length density during the growth of the rice crop as derived from literature (crosses; Beyrouty et al. (1988), filled diamonds; Drenth et al. (1991), filled triangles; Kang et al. (1995), pluses; Slaton et al. (1990), open squares; Teo et al. (1995)). Time is taken relative to the time of harvest. If there are no data on the length of the season, the length of the growing season is estimated from data on climate and cultivar.

At good crop performance and at normal plant densities, almost all methane is emitted via the plant around RLD_{max} (Schütz et al., 1989b; Wassmann et al., 1996a). It can thus be assumed that the fraction of the soil under influence of the rhizosphere compartment (*F_rhizosphere*) is a function of RLD_{max}:

$$F\_rhizosphere = \frac{RLD}{RLD_{max}} \qquad (2.2)$$

With a change in RLD during the season, the contribution of the rhizosphere compartment changes. *F_rhizosphere* is zero in absence of plants, i.e. before transplanting. The fraction of the bulk soil is one minus *F_rhizosphere*. The model is not subdivided into

different soil layers, as initial soil conditions are constant throughout the soil upto the rooting depth by puddling. Heterogeneities with depth formed during the season under influence of the rice plant are accounted for by the development of the rhizosphere compartment. All compounds are expressed in local within-compartment concentrations and are thus not affected by such heterogeneities. Methane transport rates may be affected by the use of depth-averaged parameter values. This has no large implications as the model is not sensitive to transport parameter values (Chapter 3).

Table 2.1: General process model parameters kept constant at all conditions

Parameter	Description	Value	Unit
K	Relative rice biomass increase	85.5	-
rgr	Rice relative growth rate	13.3	-
k_{mor}	Relative root mortality rate	$1.30 \ 10^{-7}$	s^{-1}
$time'_{mor}$	Relative time of mortality start	0.6	-
R_{min}	Initial soil mineralisation parameter	$1.25.10^{-4}$	$s^{-0.415}$
S_{min}	Relative soil mineralisation decrease	0.585	-
Q_{10}	Temperature correction factor	2.85	-
R_{fert}	Initial straw decomposition parameter	$5.77.10^{-2}$	$s^{-0.623}$
S_{fert}	Relative straw decomposition decrease	0.377	-
B_{exu}	Baseline root exudation rate	$0.85.10^{-6}$	mol m^{-3} s^{-1}
A_{exu}	Maximum root exudation rate increase	$4.41.10^{-6}$	mol m^{-3} s^{-1}
$time'_{max}$	Moment of maximum root exudation	0.552	-
σ	Relative rate of root exudation change	0.14	-
$K_{d,root}$	Root decomposition constant	$6.5.10^{-8}$	s^{-1}
k_{reox}	Relative reoxidation rate	e$^-$ acc dependent	s^{-1}
$\tau_{rhizosphere}$	Rhizosphere transport time coefficient	9.10^3	s
τ_{bulk}	Bulk soil transport time coefficient	$1.08.10^6$	s
B_{oxi}	Baseline methane oxidation	0.10	-
A_{oxi}	Maximum methane oxidation increase	0.63	-

Carbon substrate production

Methane emissions are driven by the production of a carbon substrate, mainly acetate, CO_2/H_2 and formate (in mol C m^{-3} s^{-1}), for methane production. Carbon substrates are produced by anaerobic soil organic matter mineralisation and decomposition of added organic material (in both compartments) and by root exudation and root decay (in the rhizosphere compartment only). These production rates need to be modelled explicitly to allow the prediction of methane emissions. It is assumed that carbon substrates are converted in the same compartment as they are produced. This seems reasonable as the turnover time of CO_2/H_2 and probably for formate as well is around 1 minute (Conrad et al., 1989a,b). The turnover time of acetate, and thus the possibilities for transport and exchange between compartments, is larger. In absence of plants and at the start of the season, when methane production and the rhizosphere compartment are very small, turnover times of acetate are 10-16 hours (Krumböck and Conrad, 1991; Schütz et al., 1989a; Sigren et al., 1997), which is equivalent to a maximum diffusion distance of about 7.5 mm. When methane production is important and when exchange may occur, i.e. while the rhizosphere compartment is well developed, turnover times of acetate are less

than 1.5 hours; max. 2 mm (Sigren et al., 1997).

Anaerobic soil organic matter mineralisation releases small organic compounds by the breakdown of soil organic matter. Soil mineralisation rates are not constant, but decrease during the season due to a decrease in easily accessible organic material. This can be taken into account by the use of a multi-component model in which organic substrates are partitioned into several components according to their resistance to mineralisation. Each component follows first-order kinetics but with a different relative decomposition coefficient (e.g. Jenkinson et al, 1992; Parton et al., 1987). The principal problem with such models is that the quantities of the individual components cannot be determined directly by analytical fractionation procedures (Paustian et al., 1992). As a consequence, the components have to be reconstructed indirectly by fitting. An alternative approach is to define one pool of substrates, but decrease its relative mineralisation rate over time (Yang, 1996). The 2nd approach needs fewer parameters to describe mineralisation, P_{min}(in mol C m^{-3} s^{-1}), and is independent of whether the systems is aerobic or anaerobic. This approach was therefore used as default in this study and leads to (Yang, 1996):

$$P_{min} = C_{min} \cdot (1\text{-}S_{min}) \cdot K_{d_{min}} \cdot e^{-K_{d_{min}} \cdot time} \tag{2.3}$$

in which C_{min} is the soil organic carbon pool (mol C m^{-3}) and:
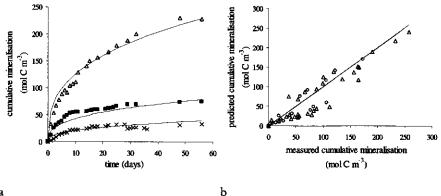
$$K_{d_{min}} = R_{min} \cdot time^{-S_{min}} \tag{2.4}$$

R_{min} (s^{Smin-1}) and S_{min}(-) are parameters that have to be determined experimentally.
Temperature influence on mineralisation rates is described using a Q_{10} value, defined as the relative increase in reaction rates at a temperature increase of 10°C:

$$P_{minT} = P_{minT_{ref}} \cdot Q_{10}^{\frac{T-T_{ref}}{10}} \tag{2.5}$$

The reference temperature (T_{ref}) in this study is 30°C. For a rice soil the R_{min}, S_{min} and Q_{10} are taken from soil incubation studies (Chapter 5) by minimising MSE (Table 2.1).

a   b

Figure 2.3:   a) Calibrated (based upon Eq. 2.3-2.5) (lines) and measured cumulative mineralisation in an incubation study with rice paddy soil at 14 °C (crosses), 20 °C (filled squares) and 30°C (open triangles). b) Validation of the calibrated mineralisation model with independent data presented by Tsutsuki and Ponnamperuma (1987) (triangles) and Inubushi et al. (1997) (circles).

Measured and calculated mineralisation rates at different temperatures are depicted in Figure 2.3a. The same empirical parameter values can describe anaerobic soil mineralisation rates in rice paddy soils presented by Tsutsuki and Ponnamperuma (1987) and Inubushi et al. (1997) (Figure 2.3b). It is therefore concluded that this description may be applied to rice paddy soils in general.
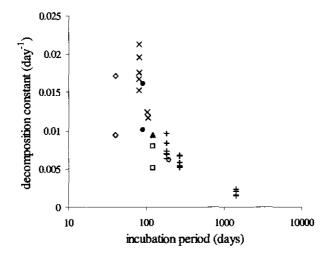
Figure 2.4:   Decomposition constants for the decomposition of rice straw calculated from literature after different incubation periods (crosses; Watanabe (1981), pluses; Neue and Scharpenseel (1987), open diamonds; Murthy et al. (1991), open squares; Acharya (1935), filled triangles; Watanabe et al. (1998), filled circles; Singh et al. (1992), open circle; Saini (1989)).

Organic fertilisers are sometimes added as extra substrates in rice paddies. The most common organic fertilisers are green manure and rice straw. Organic material from the previous crop, stubble and dead roots, is an additional source of organic material. The decomposition of such compounds, P_{fert} (in mol C m^{-3} s^{-1}) is usually described as a first-order decomposition rate:

$$P_{fert} = C_{fert} \cdot K_{d_{fert}} \cdot e^{-K_{d_{fert}} \cdot (time-t\_added)} \qquad (2.6)$$

in which C_{fert} (mol C m^{-3}) is the organic fertiliser applied at time t_added (s) and $K_{d, fert}$ (s^{-1}) the relative decomposition rate is considered as a constant. Analysis of data on $K_{d, fert}$ for rice straw(Acharya, 1935; Murthy et al., 1991; Neue and Scharpenseel, 1987; Saini, 1989; Singh et al., 1992; Watanabe, 1984; Watanabe et al., 1998) shows however a clear relationship between incubation period and $K_{d_{fert}}$ (Figure 2.4). The decomposability of organic material changes with time. To account for this change, the decomposition rate of organic fertilisers is described similarly to the soil mineralisation rate with R_{fert} and S_{fert} instead of using Eq. 2.6:

$$P_{fert} = C_{fert} \cdot (1-S_{fert}) \cdot K_{d_{fert}} \cdot e^{-K_{d_{fert}} \cdot (time-t\_added)} \text{ and } K_{d_{fert}} = R_{fert} \cdot time^{-S_{fert}} \qquad (2.7)$$

R_{fert} and S_{fert} were determined for rice straw by minimising the MSE for the data in Figure 2.4 (Table 2.1). Other organic fertilisers will have different values for R_{fert} and S_{fert} Organic

fertiliser decomposition rate is assumed to have a Q_{10} of 2.

Root exudation is passive and active release of carbon compounds from the rice roots into the soil. Root exudation changes during the season and is affected by environmental conditions. Mineral deficiencies (Kludze and Delaune, 1995b) and low radiation intensity (Butterbach-Bahl, 1992) decrease root exudation, while root exudation increases under the influence of a low redox potential (Sass and Fisher, 1995), drought stress (Turner, 1986) and in the presence of organic fertilisers (Sass et al., 1991b). However, quantitative information on these influences is scarce and can therefore not be incorporated in the model. Only information on a well growing cultivar IR72 (Kludze, pers. comm.; Minoda and Kimura, 1994; Minoda et al., 1996; Lu et al., 1999) is available to construct a gaussian curve -by minimising MSE- that describes the change in root exudation rate, P_{exu} (mol C m^{-3} s^{-1}) during the season (Figure 2.5):

$$P_{exu} = B_{exu} + A_{exu} \cdot \exp(-0.5 \cdot ((time'-time'_{max})/\sigma)^2) \tag{2.8}$$

in which B_{exu} is the baseline root exudation rate at transplanting and A_{exu} is the maximum increase in root exudation rate. This maximum is obtained if the $time'=time'_{max}$ and the relative rate of change to and from the maximum is expressed by σ (Table 2.1). This curve can thus describe the decrease in root activity after anthesis, but may apply only to IR72. A change in the size of the rhizosphere compartment also influences the total amount of root exudation in the soil as root exudation rate is expressed per m^3.
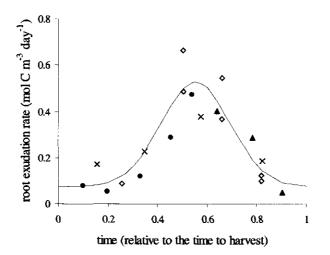
Figure 2.5:   Fitted and measured root exudation rates from a IR72 rice cultivar at different moments during the growing season (crosses; Kludze pers. comm., open diamonds; Minoda et al. (1996), filled triangles; Minoda and Kimura (1994), filled circles; Lu et al. (1999)).

Finally, organic substrates can be produced by rice root decay. This is mainly important at the end of the season, as can be seen from the change in the size of the rhizosphere compartment (Figure 2.2). As quantitative data are scarce, root mortality is determined from this curve as a first-order decay with k_{mor} as exponent starting at $time'_{mor}$. Root

decomposition (in mol C m^{-3} s^{-1}), releasing carbon substrates, is also approached by a first-order decay:

$$P_{root} = K_{d_{root}} \cdot \text{(pool of dead roots)} \tag{2.9}$$

$K_{d, root}$ is the decomposition constant for roots (Table 2.1), estimated from Saini (1989) and is assumed to have a Q_{10} of 2. Changes in the *pool of dead roots* (in mol m^{-3}) is equal to the difference between root mortality and root decomposition rates.

Methane production

Some simplified models (e.g. Cao et al., 1995) relate methane production to the redox potential (Eh) to avoid a difficult mechanistic description of methane production. There are several reasons not to choose the easily measurable parameter Eh as a determining parameter in this model: 1) Eh is the resultant of all kinds of compounds, which makes it difficult to investigate specific effects e.g. the addition of inorganic fertilisers or dynamic water tables in rainfed systems. 2) Eh is a spatially averaged value, not taking into account gradients of electron acceptors or other heterogeneities. 3) Methanogens, methane producing bacteria, are able to modify Eh to generate a favourable environment (Fetzer and Conrad, 1993). 4) The critical Eh value for methane production varies considerably from +150 to -200mV (Devai and Delaune, 1996; Masscheleyn et al., 1993; Mayer and Conrad, 1990, Peters and Conrad, 1995; Wang et al., 1992; 1993) and seems to vary with the type of electron acceptors present in the soil. All these values are far below the threshold value of +420 mV given by Fetzer and Conrad (1993). 5) Eh is hard to predict as Ratering and Conrad (1998) showed that concentration changes in iron(II) and especially in sulphate did not follow Eh changes.

Therefore an approach is chosen in which the underlying parameters and processes itself are used: It is assumed that all available substrate is consumed directly either by methanogens or by other anaerobic bacteria using alternative electron acceptors (all conversion rates in mol m^{-3} s^{-1}). No severe substrate accumulation occurs, which seems, based on experimental data (e.g. Achtnich et al., 1995b; Rothfuss and Conrad, 1993), reasonable in periods that methane production is predominant.

Simulation time starts after flooding the soil and thus is oxygen absent in the bulk soil. Oxygen concentrations in the rhizosphere are low (Gilbert and Frenzel, 1995) and it is assumed that these concentrations are too low to inhibit methane production or to allow reoxidation of electron acceptors or aerobic respiration. It is assumed that all oxygen is consumed by methane oxidisers, which can operate at these low oxygen concentrations because of their high affinity for oxygen (Frenzel et al., 1990). NO$_3^-$ is thus the first electron acceptor to be reduced :

$$\frac{d[NO_3]}{dtime} = -v_{NO3} \cdot \sum P_x \tag{2.10a}$$

in which v_{NO3} is a stoichiometry factor for the carbon substrate needed to reduce NO$_3^-$ and $\sum P_x = P_{min} + P_{fert}$ or $\sum P_x = P_{min} + P_{fert} + P_{exu} + P_{root}$ for the bulk soil and rhizosphere, respectively. After NO$_3^-$, Fe(III) is reduced:

$$\frac{d[Fe(III)]}{dtime} = -v_{Fe} \cdot \sum P_x \tag{2.10b}$$

Methanogens and sulphate reducers are outcompeted by nitrate reducers (Achtnich et al., 1995a; Westermann and Ahring, 1987) and by iron reducers (Lovley and Phillips, 1986; 1987). In addition, methane production is inhibited by accumulated NO and N$_2$O

(Klüber and Conrad, 1998). Methane production and sulphate reduction therefore start after NO_3^- and Fe(III) disappearance. Sulphate reducers outcompete methanogens for H_2/formate, but some competition is possible for acetate (Achtnich et al., 1995a; Westermann and Ahring, 1987). In addition H_2S can inhibit methanogenic activity at high concentrations. All these interactions are summarised by:

$$\frac{d[SO_4^{2-}]}{dtime} = -v_{SO4} \cdot \frac{[SO_4^{2-}]}{[SO_4^{2-}]_{t=0}} \cdot \sum P_x \tag{2.10c}$$

$$\frac{d[CH_4]}{dtime} = v_{CH4} \cdot \frac{[SO_4^{2-}]_{t=0} - [SO_4^{2-}]}{[SO_4^{2-}]_{t=0}} \cdot \sum P_x - CH_4 \_ transport \_ rate \tag{2.11a}$$

After all alternative electron acceptors have been reduced, all substrate is converted by methanogens:

$$\frac{d[CH_4]}{dtime} = v_{CH4} \cdot \sum P_x - CH_4 \_ transport \_ rate \tag{2.11b}$$

The *CH_4_transport_rate* is treated in next section. Eq. 2.10 and 2.11 are independent of the mechanism involved in the inhibition of methane production, whether it is by specific inhibition, by competition or by a methanogenic biomass limitation at the start of the season. The model does not specifically incorporate pH effects, as soil pH changes are highly correlated to Eh changes (Tsutsuki and Ponnamperuma, 1987). After alternative electron acceptor depletion, soils have a pH of around 7 (Tsutsuki and Ponnamperuma, 1987), at which methanogenesis is around its optimum value (Minami, 1989; Wang et al., 1993). Inhibiting effects by salinity are not treated either, as such effects happen under extreme conditions only (Denier van der Gon and Neue, 1995b).

Under aerobic conditions, methane production stops and reduced electron acceptors (e^- acc_{red}) are reoxidised. Reoxidation rates (*reoxi_rate*) (in mol m^{-3} s^{-1}) of ferrous iron, sulphide and FeS are described by first order kinetics:

$$reoxi \_ rate = k_{reox} \cdot [e^- acc_{red}] \tag{2.12}$$

in which k_{reox} is the relative reoxidation constant of $1.27 \ 10^{-4} \ s^{-1}$, $5.6 \ 10^{-6} \ s^{-1}$ and $7.6 \ 10^{-7} \ s^{-1}$ for ferous iron, sulphide and FeS, respectively (Chapter 3). Other reoxidation processes are not treated for reasons given elsewhere (Chapter 3).

Methane transport
In the model, produced methane is transported to an anaerobic/aerobic interface; the root surface in the rhizosphere compartment or the soil-water interface in the bulk soil compartment. Different transport mechanisms of gases in rice paddies, plant mediated transport, diffusion through the soil and ebullition, to these interfaces are lumped into a transport time coefficient, τ, which is the average period (in s) between production and the moment of reaching the interface:

$$CH_4 \_ transport \_ rate = \frac{[CH_4]}{\tau} \tag{2.13}$$

in which (CH_4) is the methane concentration (in mol m^{-3}) in a compartment. Transport time coefficients depend on path length and diffusion coefficient, which are assumed to be constant under flooded conditions. The τs differ for each compartment. Eq. 2.13 implies that methane produced in one compartment cannot leave the system through an other compartment. In reality, some methane produced in the bulk soil may however leave the system through the plant if the roots capture gas bubbles formed in the bulk

soil. Diffusion calculations taking into account transport resistances indicate that methane transport from bulk soil to rhizosphere will be small (data not shown). Even if such exchange occurs, it will automatically be taken into account as experimental data are used to estimate this time coefficient. The opposite will not occur because transport through the plant is faster than transport through the soil.

In the rhizosphere compartment, transport will mainly take place via plant mediated transport. The time coefficient for plant mediated transport was found to be smaller than 3 hours after the introduction of a temperature change (Sass et al., 1991a) and 2-3 hours after an introduction of a change in light conditions (Byrnes et al., 1995), respectively. The $\tau_{rhizosphere}$ is thus set at 2.5 hours in the model (Table 2.1).

There are no data available from which the time coefficient of transport by ebullition or diffusion through the bulk soil can be calculated directly. However, Watanabe and Kimura (1995) and Kimura and Minami (1995) calculated, using the same dataset, that the maximum period between methane production and emission was 11-14 days at the start of the growing season. At the start of the season, transport through the soil dominates the methane transport completely (Schütz et al., 1989b; Wassmann et al., 1996a). In the model, it is therefore assumed that τ_{bulk} is 12.5 days (Table 2.1). From the large difference in time coefficients of the two compartments and the seasonal change in contribution of the compartments (Eq. 2.2), the seasonal trends in conductance (Hosono and Nouchi, 1997) and in turnover times (Watanabe and Kimura, 1995; Kimura and Minami, 1995) can be calculated and understood.

In an aerobic period, at drainage, τ_{bulk} decreases as more pores for transport become available, releasing entrapped methane to the atmosphere. This results in a fast release of methane at the start of drainage that tails off afterwards. This change in τ_{bulk} during the release can be described by an empirical beta function:

$$\tau_{bulk} = \frac{release\_time.\frac{(v-1)!.(w-1)!}{(v+w-1)!}}{r\_time^{v-1}.(1-\ r\_time)^{w-1}} \tag{2.14}$$

in which *release_time* is the period of methane release (7 days). *v* (5) and *w* (8) determine the curve shape and are estimated from Denier van der Gon et al. (1996). *r_time* is *time/release_time*, between 0 and 1.

Methane oxidation

At aerobic/anaerobic interfaces part of the methane is oxidised to CO_2 by methanotrophic bacteria in the presence of oxygen. Anaerobic methane oxidation is neglected for reasons given in Chapter 3. Methane oxidation can be measured by a mass balance approach, comparing potential methane production in the absence of oxygen with the actual plant mediated methane emission (e.g. Holzapfel-Pschorn et al., 1985; Sass et al., 1992). This method overestimates methane oxidation as methanogenic activity is enhanced in such anaerobic incubations. Estimates with this method are much higher than those obtained by in-situ experiments with 100% N_2, while these experiments produce an upper boundary for methane oxidation estimates (Denier van der Gon and Neue, 1996). The second commonly used method is to measure methane oxidation in presence of specific inhibitors of methanotrophic activity. Problems with this method are that various inhibitors also partly inhibit methane production (Frenzel and Bosse, 1996;

Oremland and Culbertson, 1992; Oremland and Taylor, 1975) and that the higher oxygen concentrations in the soil can also reduce methane production in various ways. These interfering effects seem to be limited in short-term incubations (King, 1996) and estimates obtained by this method are not higher than those obtained by in-situ experiments with 100% N_2. Therefore specific inhibitor experiments are used to estimate methane oxidation.

Methane oxidation is limited by oxygen availability. Oxygen is released into the rhizosphere through ROL, which changes during the season (Kludze et al., 1994; Satpathy et al., 1997; Wang et al., 1997) as a function of root activity. Seasonal changes in root exudation rates also depend on root activity. Therefore, a similar gaussian curve as for root exudation (Eq. 2.8) is chosen for methane oxidation in the rhizosphere, adjusting parameter B and A (Table 2.1) such that the seasonal average oxidation in the rhizosphere equals to the average found by use of specific inhibitors, which is $32\pm8\%$ of methane produced (Banker et al., 1995; Bosse and Frenzel, 1997; 1998; Denier van der Gon and Neue, 1996; Epp and Chanton, 1993; Gilbert and Frenzel, 1995; Sigren et al., 1997; Tyler et al., 1997). As this curve depends on root activity, which may be cultivar dependent, it may only be appropriate for IR72.

Oxygen diffuses into the bulk soil at the soil-water interface. At this interface, where methane and oxygen gradients meet, methane oxidation rates are high and fairly constant at 70-95% of the locally produced methane (Banker et al., 1995; Butterbach-Bahl et al., 1997; Conrad and Rothfuss, 1991; Epp and Chanton, 1993; Gilbert and Frenzel, 1995; Schütz et al, 1989b). However, only 10-20% of the methane emission from the bulk soil passes this soil-water interface by diffusion (Rothfuss and Conrad, 1993; Schütz et al., 1989b). The remaining emission from the bulk soil is transported by ebullition. Gas bubbles for ebullition are formed in anaerobic soil and hardly comes into contct with oxygen during transport to the atmosphere and will thus not be oxidised. Therefore, only diffusive flux through the soil can lead to methane oxidation. The average fraction that is oxidised the bulk soil can be calculated from these arguments at $37\pm19\%$ of the produced methane, based on the data above. This fraction is not significantly different from the oxidation of $28\pm11\%$ of produced methane transported by ebullition and sediment diffusion, calculated by Tyler et al. (1997).

The remaining methane from each compartment is directly released from the interface into the atmosphere, thus assuming no transport limitation inside the plant or in the water layer on top of the soil. Methane emission is calculated as the sum of the methane released from the rhizosphere and the bulk soil. The model was written in FST (Rappoldt and van Kraalingen, 1996) and is available upon request.

2.3 Model validation
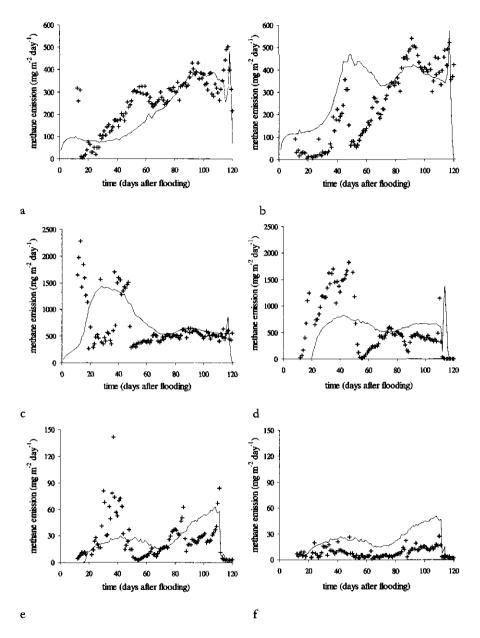
For model validation, model performance was compared to field data on daily methane emissions collected at various sites: Maligaya (MA) of the Philippine Rice Research Institute, Los Baños (LB) of the International Rice Research Institute in the Philippines, Beijing (BG) of the Institute of Crop Breeding and Cultivation in China and Jakenan (JK) of the Central Research Institute for Food Crops in Indonesia (Figure 2.6). Diurnal pattens in methane emissions cannot be predicted by the model, given its objectives and simplified nature. At all sites methane emissions were measured with an automatic closed chamber technique described in detail by Wassmann et al. (1994). Site specific

experimental conditions are described elsewhere (Metra-Corton et al., 1995; Metra-Corton et al., 2000, Buendia et al, 2000; Setyanto et al., 2000; Wang et al., 2000).

Table 2.2:   Site specific input parameters

	Maligaya	Los Baños	Beijing	Jakenan
Soil carbon content (%)	1.21	1.86	0.99	0.48
Dithionite extractable iron (%)	1.15	2.27	0.56	0.18
Daily temperature (°C)	23.5-31.8	22.8-28.3	8.2-29.1	25.3-30.3
Rice cultivar	IR72	IR72	IR72	IR72
Yield (tons ha⁻¹)	5.1-5.3	3.5-5.4	6.9	7.4
Water management	Cont. flooded	Cont. flooded	mid-season drainage	Cont. flooded
Growing season length (days)	120-121	121	149	103
Fertiliser management	urea, KCl, solophos	urea	urea	urea

All process parameters were kept at the constant values presented in Table 2.1 for all model runs. These values were not derived from the experimental data used for validation. These experimental sites represent therefore a truly independent validation of the model. All site specific input parameters are shown in Table 2.2. Soil organic carbon and dithionite extractable iron can be found in soil maps. Daily temperature was measured at the site, but can in general be found in weather inventories. The rice cultivar was in all cases IR72, because this is the only variety for which root activity data are known. Fertilization, water management and length of the growing season were obtained from the site, but can in general be found in agricultural databases. All sites were drained at the end of the season. All site specific parameters can thus be obtained from generally available databases, facilitating extrapolation of this process-based model for use in regional and global studies. All other parameters were always kept at their default values presented in Table 2.1.
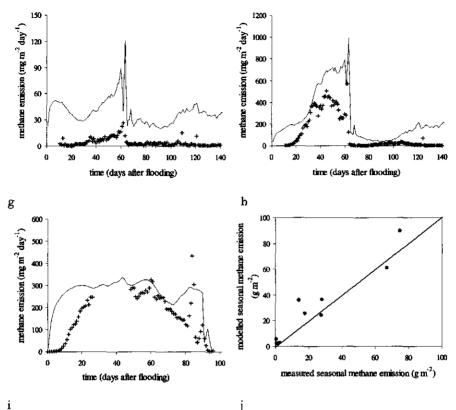
The model was validated under various conditions. Two seasons for Maligaya, wet season 1994 (MA94) data and wet season 1996 (MA96) data, were used in the validation set to test the representation of interseasonal variations in methane emissions by the model (Figure 2.6a,b). The model predicted well the different methane emissions in both seasons, which occurred mainly under influence of different temperatures. The effects of organic fertilisation, in this case rice straw, was tested at various sites; at Maligaya (compare Figure 2.6b and 2.6c), Los Baños (compare Figure 2.6d and 2.6e) and at Beijing (compare Figure 2.6g and 2.6h). The addition of straw, and thus of extra carbon substrate, causes a tremendous increase in methane emissions especially during the 1st half of the season. The model could well predict well both the magnitude and the timing of methane emission increase. The total increase is slightly underestimated at Los Baños and slightly overestimated at Beijing, but the differences with measured methane emissions are not significant (at P<0.05). The performance of the model with a different inorganic fertiliser than urea. $CO(NH_2)_2$, was tested by including a treatment with $(NH_4)_2SO_4$. Sulphate additions reduce methane production as described by Eq. 2.10 and lead to a reduction in both measured and modelled methane emissions (compare Figure 2.6e and Figure 2.6f). The inhibiting effects of sulphate were slightly underestimated by

the model, which is probably due to the neglect of the recycling of sulfurous compounds
within the rice paddy.

Figure 2.6   (continued next page)

i   j

<u>Figure 2.6:</u>   Model validation. Comparison of measured (pluses) and modelled (lines) methane emissions at different locations, with different seasons and treatments for a) MA 94 control, b) MA 96 control, c) MA 96 with straw, d) LB 97 with straw, e) LB 97 control, f) LB 97 with $(NH_4)_2SO_4$, g) BG 97 control, h) BG 97 with straw and i) JK 96 control. Note the different scales at the y-axes. j) Comparison of modelled seasonal methane emissions and measured seasonal methane emissions.
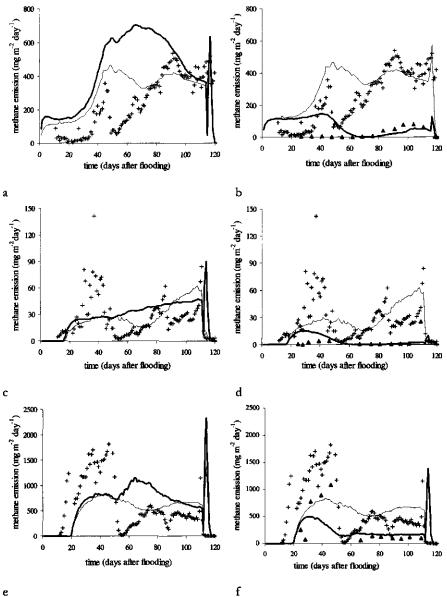
In the validation set, four sites in different countries differing tremendously in soil characteristics but with the same management and rice cultivar were compared (Figure 2.6b,e,g,i). Both the absolute amounts and the patterns in the highly different methane emissions at the various sites could be well predicted by the model. Only the methane emissions predicted for BG97 were significantly higher (at $P<0.05$) than the measured methane emissions, but BG97 control was a very low emitter and this overestimation will thus hardly influence model estimates if the model is extrapolated to regional scales.

In all situations, except for BG97 control, the seasonal patterns in methane emission during the rice growth season were well described by the model and not significantly different from measured values (at $P<0.05$). The various under- and overestimations by the model had no significant pattern across sites or treatments (at $P<0.05$) and are probably caused by heterogeneities or sites specific characteristics not captured by the model –given the fact that all process parameters were kept constant during all

validations. Modelled seasonal methane emissions did not differ significantly (at P<0.05) from measured seasonal methane emissions (Figure 2.6j) and had a coefficient of variation of only 8% with the measured emission and a Pearson correlation coefficient of 0.95, while emissions varied up to 2 orders of magnitude.

2.4 Sensitivity analysis on model assumptions

During the development of a process-based model some assumptions are made on process descriptions. In this section, we evaluate the influence of different model assumptions mentioned in section two. The most important assumption of the described model is that the importance of rice plants on methane emissions is large enough to justify a distinction between a rhizosphere and a bulk soil compartment. This assumption was tested by reformulating the model with one compartment with a uniform distribution of carbon substrates, while keeping the total carbon release equal to the default model. Transport was spatially averaged by applying an average τ to Eq. 2.12. An average methane oxidation fraction was derived from the oxidation fraction of both compartments. The results are presented in Figure 2.7a,c,e. Seasonal methane emissions increase 20-52% if one compartment is used, while total carbon substrate relaese was taken the same in both models. Methane emissions increase especially in the middle of the season, when methane oxidation in the rhizosphere is the largest. This influence by ROL dynamics is taken away in the one-compartment model, leading to poorer methane emission predictions.

Indirect support for the distinction between a rhizosphere and a bulk soil was obtained by showing the contribution of the bulk soil and of the rhizosphere to the overall methane emission. The independent estimate of ebullition -taken as the emission from the bulk soil- can be used to validate the concepts of the model by comparison with measured ebullition data. Results of the model are shown in Figure 2.7b,d,f for the same experiments as presented in Figure 2.7a,c,e. Both modelled and measured ebullition have their highest contribution at the start and end of the season, when plant influence is small. Modelled ebullition contributed 15-22% to the total methane emission at treatments with inorganic fertiliser additions -with two examples in Figure 2.7b,d- which is a reasonable value if no extra organic fertilisers are added (Byrnes et al., 1995; Nouchi et al., 1994; Schütz et al., 1989b). With the addition of extra rice straw, ebullition contributed 32-53% to the total methane emission and was 39% in MA96 (Figure 2.7f). These estimates are also comparable to sites to which organic fertiliser was added (Denier van der Gon and Neue, 1995a; Wassmann et al., 1996a). Moreover, the overall conductance, which can be calculated from the compartment contributions and their respective transport time coefficients, shows the same trends and has the same order of magnitude as the conductance presented by Hosono and Nouchi (1997). Unfortunately, an exact comparison is not possible, as Hosono and Nouchi (1997) did not present the number of shoots at each sampling. These results show that the model can predict methane transport characteristics, and that the division into two compartments yields a reasonable methane transport description.

a   b

c   d

e   f

<u>Figure 2.7</u>:   Model sensitivity with (thin lines) and without (thick lines) the distinction of an explicit rhizosphere for a) Ma 96 control, c) LB 97 control and e) LB 97 with straw. In figures b, d and f, the modelled ebullition (thick lines) and modelled total methane emission (thin lines) are compared to data for total emission (pluses) and ebullition (triangles) for MA 96 control, LB 97 control and LB 97 with straw, respectively.

One of the most sensitive factors influencing methane emissions from rice paddies is the production of carbon substrates (Chapter 3). If no extra straw is added, the contribution

of soil organic matter mineralisation to total carbon substrate release varies from 45% at the low soil carbon site Jakenan to 68% at the high carbon site Los Baños. The remainder is either directly –via root exudation and root decomposition- or indirectly – via rice straw- derived from plants. Given the importance of soil mineralisation, it is unfortunate that no mineralisation model has been developed specifically for anaerobic conditions. In this study, the general model described by Yang (1996) was used as default in this study as the description is independent of aerobic or anaerobic conditions and because it uses the least number of parameters. Two other mineralisation models were used to test the effect of soil mineralisation description on methane emission predictions: 1) a two-pools model and 2) the CENTURY model (Parton et al., 1987), which was applied by Cao et al. (1995).

The two-pools model assumes that soil organic carbon consists of two pools, each with a constant relative decomposition rate. The two pools do not interact and the sum of the pools is equal to the total soil organic carbon content. With this two-pools model Eq. 2.3 & 2.4 simplify to:

$$P_{min} = C_{min} \cdot (F_{fast} \cdot K_{fast} \cdot e^{-K_{fast} \cdot time} + (1 - F_{fast}) \cdot K_{slow} \cdot e^{-K_{slow} \cdot time}) \qquad (2.15)$$

in which F_{fast} (-) is the fraction of the organic matter pool that is assigned to the fast pool and K_{fast} and K_{slow} are decomposition constants (s^{-1}) of the fast pool and the slow pool, respectively. These three parameters were all fitted (Figure 2.8a) to experimental data from soil incubation studies (Chapter 5): F_{fast}= 0.022 (-), K_{fast}= 1.21 10^{-5} (s^{-1}) and K_{slow}= 1.25 10^{-8} (s^{-1}).

The CENTURY model was developed for aerobic soils. Parameter values of this model can thus not be used directly for anaerobic conditions. To avoid too many fitted parameters, pool distribution ratios were used from the CENTURY model. The distribution of plant residue between metabolic and structural carbon pools was estimated from the ratio lignin/nitrogen (Eq. 2 in Parton et al. (1987)) using data for rice plant characteristics presented by Saini (1989). While maintaining the same ratio in litter decomposition constants, the plant decomposition constants were estimated from data on rice straw decomposition, mentioned above. Conversion ratios of decomposing organic matter to CO_2 and decomposition constants for the soil carbon pools corrected for texture -that is known to influence methane emissions but that is not part of the Yang (1996) model-, were obtained from Parton et al. (1987). Only one decomposition constant ($K_{d,passive\ pool}$) remained to be fitted. Fluctuating moisture effects are absent in a continuously flooded rice paddy soil. Temperature effects were described by a calibrated Q_{10} value to allow comparison with the default model. Finally the three initial soil carbon pool sizes had to be calibrated, with the constraint that their sum is equal to the total organic carbon amount. This leaves two pool fractions to be calibrated: $F_{passive\ pool}$ and $F_{slow\ pool}$. All four parameters were optimised simultaneously against experimental soil incubation data (Chapter 5) for the smallest mean square error and the smallest change in pool size fractions during the season (Figure 2.8a). This led to $K_{d,\ passive\ pool}$ = 0.7 10^{-9} (s^{-1}), Q_{10}=2.71, $F_{passive\ pool}$= 0.738 (-) and $F_{slow\ pool}$=0.122 (-).

a

b

c

d

e
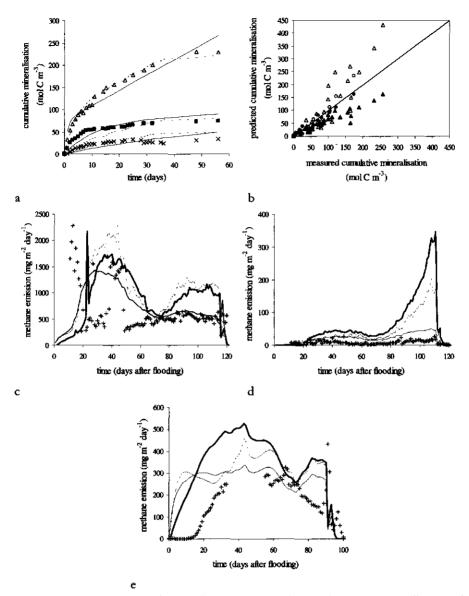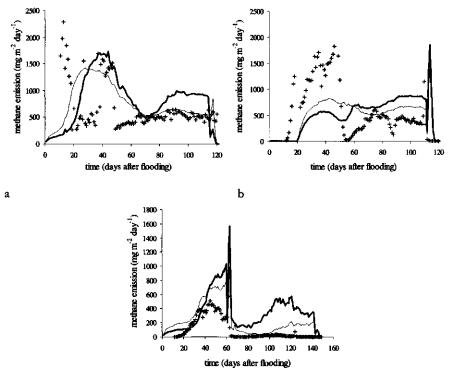
<u>Figure 2.8:</u>   Model sensitivity on soil organic matter mineralisation models. a) Calibration of
Parton et al. (1987) mineralisation model (dashes) and two-compartment model
(lines) with measured cumulative mineralisation in incubations of rice paddy soil
at 14 °C (crosses), 20 °C (filled squares) and 30°C (open triangles). b) Validation
of Parton et al. (1987) mineralisation model (closed symbols) and the two-
compartment model (open symbols) with independent data by Tsutsuki and
Ponnamperuma (1987) (triangles) and Inubushi et al. (1997) (circles). Influence
of Parton et al. (1987) mineralisation model (thick lines) and two-compartment
mineralisation model (dashes) compared to the default (thin lines) and measured
data (pluses) for c) MA 96 + straw, d) LB 97 +(NH$_4$)$_2$SO$_4$ and e) JK 96 control.

Both models could reasonably describe anaerobic soil mineralisation rates in rice paddy soils presented by Tsutsuki and Ponnamperuma (1987) and Inubushi et al. (1997), although the two-pools model overestimated mineralisation rates at high fertilisation (Figure 2.8b). With the two-pools model, methane emissions were 14-102% higher than for the default model (examples given in Figure 2.8c,d,e). The overestimation mainly occurs in the 2nd half of the season when predicted mineralisation rates began to deviate from measured mineralisation rates (Figure 2.8a). The modified CENTURY model is also less applicable than the default model, even though it was calibrated for anaerobic conditions. The deviations are hard to explain and may be coincidental or due to the fact that CENTURY was developed for long term predictions in aerobic systems. In absence of organic fertilisers the CENTURY model led to 13-270% higher methane emissions than for the default model (examples given in Figure 2.8d,e). With organic fertilisers, the CENTURY model performed similarly well as the default model (example given in Figure 2.8c), but still produced 18-28% higher emission estimates. Anaerobic mineralisation modelling deserves more attention.

a   b

c
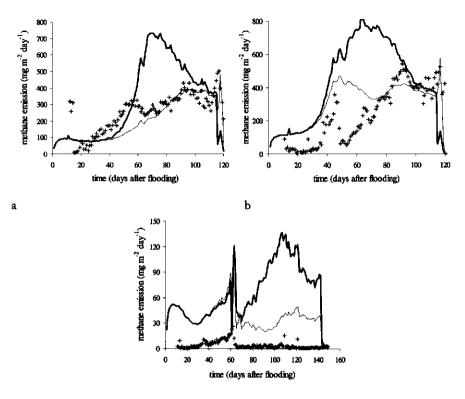
Figure 2.9:   Sensitivity of the model on the description of rice straw decomposition. A description with a constant relative decomposition rate for rice straw (thick lines) is compared to the default model (thin lines) and measured data (pluses) for a) MA 96 with straw, b) LB 97 with straw and c) BG 97 with straw.

Rice straw becomes an important source of carbon substrate if it is added as organic fertiliser, 50-62% of the total carbon release according to the model. In the model, it was assumed that organic fertilisers decompose according to Eq. 2.7. Normally, however, a constant relative decomposition rate, Eq. 2.6, for organic fertilisers is assumed. As a sensitivity analysis the model was run with a constant relative decomposition rate for organic fertilisers based on literature data, mentioned above, with incubation periods $\leq$ 120 days. This change in the model hardly affected the outcome if no organic fertilisers are added (results not shown). With the addition of organic fertilisers (Figure 2.9) the effects were larger and led to 9-17% higher emissions. Especially during the 2nd half of the season methane emissions were overestimated by the model with a constant relative decomposition rate. This can be explained by the fact that at that point in the season easily accessible carbon has been depleted, leading to decreased decomposition rates and thus to overestimations when a constant relative decomposition rate is used.

In various models (James, 1993; Grant, 1998; Segers and Kengen, 1998) competition between methane producing bacteria and other anaerobic bacteria is described by Michaelis-Menten kinetics. In this model, the competition was simplified to Eq. 2.10. Inclusion of Michaelis-Menten kinetics would only affect the competition with sulphate reducers, as nitrate and ferric iron reducers outcompete methanogens under all conditions. Sulphate reduction is only of minor importance for the seasonal electron balance (Chapter 5; Inubushi et al., 1984) and methane emissions are hardly affected even in an extreme scenario of outcompetition of methanogens by sulphate reducers (Chapter 3). The simplification of Eq. 2.10 is thus reasonable.

A more important assumption, as was already indicated in section 3, is that there is no reoxidation of electron acceptors in a flooded rhizosphere. This implicitly means that only methanotrophs and heterotrophic respiration consume the oxygen available in the rhizosphere. Unfortunately, our model cannot test this important assumption as the model does not distinguish gradients and because it is not possible to determine oxygen limited conversion rates with this model. The model of Segers (2000), however, takes into account diffusion and oxygen limitations. According to that model, reoxidation of electron acceptors is not important under oxygen limited circumstances. The assumption seems thus reasonable, although quantitative verification is not possible with the present model.

The final assumption in the model is that methane oxidation is linearly related to root activity, Eq. 2.8. This assumption was necessary due to a lack of quantitative data on changes in methane oxidation or ROL during the season. Only an average methane oxidation percentage could be calculated from the data. If the model is run with this average instead of an activity curve, the trends in methane emission are strongly influenced (Figure 2.10) and lead to major overestimations of methane emissions in the middle of the season, when root activity is highest. Seasonal methane emissions were 8-57% higher than for the default model. It is thus necessary to take into account the seasonal changes in methane oxidation, as is done in the default model. Root exudation and ROL are not only temporally dynamics but moreover depend on the rice cultivar. Unfortunately, there are no quantitative cultivar specific data, which limits the validation possibilities of the model for non-IR cultivars. More data are needed on these root activity characteristics.

a   b

c

<u>Figure 2.10</u>:   Sensitivity of the model on the description of methane oxidation. A description
                with a constant percentage of produced methane that is oxidized (thick lines) is
                compared to the default model (thin lines) and measured data (pluses) for a) MA
                94 control, b) MA 96 control and c) BG 97 control.

2.5 Concluding remarks

In this paper, a model for methane emission predictions from rice paddies at the field
scale level is described. Due to a lack of mechanistic knowledge, not all processes could
be described fully mechanistically. Therefore, the descriptions of most important system
properties were kept simple to achieve a well-balanced model, even though in some cases
more mechanistic knowledge is available. The model was validated, without fitting, with
data from independent field experiments at various sites in Asia. With only a few site
specific input parameters (Table 2.2), the seasonal dynamics in methane emissions could
be well described. Total seasonal methane emission was not significantly different from
measured seasonal emissions (at $P<0.05$), while the different conditions had led to
seasonal emissions differing over 2 orders of magnitude.

The sensitivity analysis also showed that the model assumptions were reasonable. The
most important assumption was the model simplification to distinguish two
compartments; a rhizosphere and a bulk soil compartment. The model performed worse
without such a division, showing the importance of heterogeneities introduced by the
plant, while -of the models refered to- only Arah and Stephen (1998) and Walter et al.

(1996) describe this heterogeneity, using a more physical approach. None of the models, however, include other heterogeneities, which probably had a major influence -in combination with site specific varaibilities- on the deviations between model and experiment. The sensitivity analysis also showed the importance of a proper quantitative description on anaerobic organic matter decomposition processes. Modelling these processes thus deserves more attention to improve future models, also because the empirical models mentioned in the introduction do not account for this soil process. Another important aspect of the model is the competition for substrate by alternative electron acceptors, which is -of the models refered to- only included in the model of James (1993). Neglect of this competition severely overestimates methane emissions at the start of the season especially in soils high in alternative electron acceptors, like Los Baños, for which this competition is important. A description of Eh independent of soil type will thus not suffice. In the model it was assumed and argumented that reoxidation of electron acceptors is not important, but it deserves more attention especially for soils high in alternative electron acceptors and for rainfed systems. The sensitivity analysis also showed that it is important to account for seasonal changes in methane oxidation, indicating that there is a need to understand this process. In the models of Huang et al. (1998) and Cao et al. (1995) a different oxidation dynamics was used, leading to an underestimation of methane emissions at the end of the season (results not shown).

From the model validation and sensitivity analysis we conclude that the assumptions made in this model are reasonable, because methane emissions are well predicted. The model can be used for larger scale applications for flooded rice paddies, because it makes use of general process relations and because it needs few site specific parameters. The site specific parameters can be obtained from general databases, facilitating application of the model. Caution is needed when the model is applied to rice cultivars for which the model was not parameterised.

Acknowledgements

Modelling methane emissions from rice paddies: Variability, uncertainty and sensitivity analysis of processes involved

P.M. van Bodegom[1,3], P.A. Leffelaar[1], A.J.M. Stams[2] and R. Wassmann[3,4]

[1] Lab. of Theoretical Production Ecology, Wageningen University (WU)
P.O. Box 430, 6700 AK Wageningen, The Netherlands
[2] Laboratory of Microbiology (WU), The Netherlands
[3] International Rice Research Institute, Los Baños, Philippines
[4] Fraunhofer Institute (IFU), Garmisch-Partenkirchen, Germany

**Modelling methane emissions from rice paddies: Variability, uncertainty and
sensitivity analysis of processes involved**

Abstract

Estimates of global methane emissions, to which rice cropping systems
contribute significantly, are uncertain. The variability and uncertainty of
variables governing emission rates and the sensitivity of emissions to these
variables determine the accuracy of methane emission estimates. A good tool for
quantification of sensitivities is a process-based model. This paper describes a
model that has been validated previously by experimental data. Variability and
uncertainty in processes and variables underlying methane emissions are
reviewed and the sensitivities of modelled methane emission estimates for
process variables are tested. The sensitivity analysis is carried out for two sites in
the Philippines at which methane emissions have been measured for several
years. The sensitivities of the model are compared to measured sensitivities,
both as a function of input parameters. The model sensitivity analysis shows that
the system is not sensitive to mechanisms of methane production or the
pathway of gas transport through the plant. Methane emissions are very
sensitive, however, to the description of substrate supply (both from the soil and
from organic fertilisers). Unfortunately, this description also represents a main
uncertainty. Uncertainty in methane emission estimates will thus remain large as
long as these processes are not well quantified.

3.1 Introduction

Methane is one of the principal greenhouse gases and accounts for 15-20% of the
radiative forcing added to the atmosphere (Houghton et al., 1996). Rice paddies
contribute for 9-30% to the global methane emissions (Houghton et al., 1996; Matthews
et al., 1991). Estimates of global methane emissions from rice paddies differ largely
depending on approaches, techniques and databases used for extrapolation. Lelieveld et
al. (1998) estimated 80 ± 50 Tg/yr using atmospheric chemistry models and tropospheric
methane distribution. Upscaling of field measurements generally indicate lower source
strengths, in the range of 50 ± 20 Tg/yr (Neue, 1997).
One of the principal causes for uncertainties in global estimates results from the large
intrinsic spatial and temporal variability in methane emissions. Over the past 15 years,
numerous field experiments identified magnitude, temporal pattern and controlling
factors of methane emissions from rice fields (this issue; Denier van der Gon and Neue,
1995a; Nouchi et al., 1994; Wassmann et al., 1996a). The large number of data that has
become available from these experiments is of great value for improved understanding of
the variability in methane emissions. The data show, among other things, that the
variability in methane emissions cannot be described by a simple relationship between
methane emissions and environmental variables (Walter et al., 1996). This is attributed to
the dynamic (diurnal and seasonal) and non-linear interactions between the processes
underlying methane emissions.
It is therefore beneficial to link the available data on methane emissions to knowledge of
the underlying processes, i.e. through a mathematical model. In recent years, a number of

models of methane emissions from rice fields have been published. Some models are empirical (Hosono and Nouchi, 1997; Huang et al., 1998), which can be problematic in view of the non-linear interactions and number of fitted parameters, leading to a loss in extrapolation reliability. Other models (Chapter 2; Arah and Stephen, 1998; Cao et al., 1995) are process-based models. They vary in the purposes for which they were developed and in the degree of mechanistic detail included.

Although most models can reproduce the patterns of methane emissions at one experimental site with reasonable accuracy, their potential for simulating emissions at other sites remains unknown. This potential depends on the variability and uncertainty of variables and processes on a process level and, in the next step, on the sensitivity of real systems and of models for those variable or uncertain processes.

The objectives of this paper are i) to review the variability and uncertainty in processes and variables underlying methane emissions, ii) to quantify the sensitivity of a model for such variability and to compare the model sensitivity with the real sensitivity where possible and iii) to determine the uncertainties in the range of methane emissions.
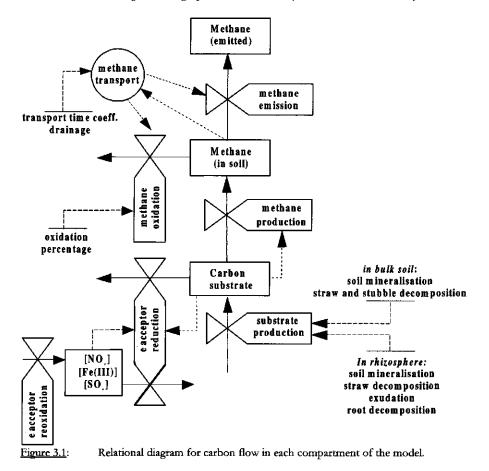
The sensitivity analysis is based on a process-based model, fully described below. Arguments for this model, validation with field experiments and analysis on model structure are in Chapter 2. Other process-based models that easily link parameters with measured entities could be used as well for such an analysis, and will be mentioned when relevant. For the model sensitivity analysis two sites, Maligaya (MA94) and Los Baños (LB97), both in the Philippines, were chosen to determine the responses to variable changes. At both sites methane emissions have been measured for several years (this issue; Metra-Corton et al., 1995; Wassmann et al., 1994; 1996a) and soil characteristics, management and temperature are known (Table 3.1). The analysis comprises two steps. First, a sensitivity analysis of methane emissions varying one single variable independently, is presented. The effects of a variable on emissions are analysed and compared to literature. Secondly, the relative sensitivity of modelled methane emissions for individual variable changes is determined for both sites. The accuracy to which the model is able to reproduce and predict encountered methane emissions at different experimental sites, can be assessed from a combination of the relative importance and information on uncertainty in variables.

Table 3.1:   Site characteristics of the case study experimental stations

	Los Baños (LB97)	Maligaya (MA94)
Soil organic carbon content (%)	1.86	1.21
Dithionite extractable iron (%)	2.27	1.15
Clay (%)	43	59
Silt (%)	44	33
Avg. seasonal temperature (°C)	26.5	29.6
Rice cultivar	IR72	IR72
yield (tons ha^{-1})	5.4	5.2
Fertiliser addition (kgha^{-1})	urea 150	urea 120, solophos 40, KCl 40

3.2 Model description

Methane emissions from rice fields are strongly influenced by the presence of the root system. The model incorporates this explicitly and distinguishes a rhizosphere and a bulk

soil compartment. The processes involved in emissions -described from the moment of flooding onwards- take place independently in both compartments (a flow diagram is given in Figure 3.1). In the mathematical description of the processes, it is attempted to combine simple process descriptions, while maintaining the most important characteristics of the processes. This is done to avoid excessively high data demand and to allow a future linkage to Geographic Information Systems for scenario analysis.

Figure 3.1: Relational diagram for carbon flow in each compartment of the model.

Dynamics of compartment contribution

The model calculates the extent of the rhizosphere compartment in time from actual root length density (RLD) (in m/m^3), which is empirically related to maximum root length density (RLD_{max}) (in m/m^3) based on data by Beyrouty et al (1988), Drenth et al. (1991), Kang et al. (1995), Slaton et al. (1990) and Teo et al. (1995):

$$RLD = \frac{RLD_{max}}{1+K \cdot e^{-rgr \cdot time'}} \qquad \qquad For\ RLD < RLD_{max}$$

$$RLD = \frac{RLD_{max}}{1+K \cdot e^{-rgr \cdot time'_{mor}}} \cdot e^{-k_{mor}(time' - time'_{mor})} \quad For\ RLD \geq RLD_{max} \qquad (3.1)$$

in which the *time'* is the relative time (time divided by the length of the growing season) and *rgr* (dimensionless relative growth rate), K $((RLD_{max}-RLD_{t=0})/RLD_{t=0})$, k_{mor} (dimensionless relative mortality rate of roots) and *time'$_{mor}$* (relative time at which roots start to die) are empirical constants (Table 3.2). The logarithm of RLD_{max} is empirically related to the logarithm of aboveground biomass, based on data by Drenth et al. (1991), Tanaka et al. (1995) and Teo et al. (1995).

From the actual root length density, the distance between roots (*root_dist*) (in m) is calculated, assuming that all roots exchange gases and that roots are randomly distributed through the puddled soil, by (based on Ogston, 1958):

$$root\_dist = \sqrt{\frac{\ln(2)}{\pi \cdot RLD}} \tag{3.2}$$

The fraction of the soil dominated by the rhizosphere (*F_rhizosphere*) is equal to:

$$F\_rhizosphere = \left(\frac{rhizo\_dist}{root\_dist}\right)^2 \tag{3.3}$$

in which *rhizo_dist* is the estimated extent of the rhizosphere around a single root (Table 3.2). *F_rhizosphere* can not become larger than one and is zero in the absence of plants. The fraction of the bulk soil is one minus *F_rhizosphere*. This description of the rhizosphere compartment is an extension of the model in Chapter 2 in which it was assumed that optimal plant growth occurred, so that almost all methane is emitted via the plant at RLD_{max}.

Table 3.2:   Model parameter values. For an explanation on the parameters, see main text.

parameter	Value	Unit	Reference
K	85.5	-	Chapter 2
rgr	13.3	-	Chapter 2
k_{mor}	1.53	-	Chapter 2
time$_{mor}$	0.6	-	Chapter 2
rhizo_dist	2.10^{-3}	m	Kirk et al., 1993
R_{min}	$1.25.10^{-4}$	$s^{-0.415}$	Chapter 2
S_{min}	0.585	-	Chapter 2
R_{fert}	$5.77.10^{-2}$	$s^{-0.623}$	Chapter 2
S_{fert}	0.377	-	Chapter 2
B_{exu}	$0.85.10^{-6}$	mol m^{-3} s^{-1}	Chapter 2
A_{exu}	$4.41.10^{-6}$	mol m^{-3} s^{-1}	Chapter 2
time$_{max}$	0.552	-	Chapter 2
σ	0.14	-	Chapter 2
$K_{d,root}$	$6.5.10^{-8}$	s^{-1}	Saini, 1989
$\tau_{rhizosphere}$	9.10^{3}	s	Chapter 2
τ_{bulk}	$1.08.10^{6}$	s	Chapter 2
B_{oxi}	0.10	-	Chapter 2
A_{oxi}	0.63	-	Chapter 2
$k_{reox}(FeS)$	$7.6.10^{-7}$	s^{-1}	Boudreau, 1996
$k_{reox}(Fe(II))$	$1.27.10^{-4}$	s^{-1}	Ahmad and Nye, 1990; Cappellen and Wang, 1996; Murase and Kimura, 1997
$k_{reox}(S^{2-})$	$5.60.10^{-6}$	s^{-1}	Ahmad and Nye, 1990; Cappellen and Wang, 1996; Murase and Kimura, 1997

Process dynamics within the compartments

In both compartments, carbon substrates are produced by anaerobic mineralisation, P_{min}, and fertiliser decomposition (from organic fertilisers and stubble incorporation), P_{fert}, both in mol C m^{-3} s^{-1}. The production rates are adapted from Yang (1996) assuming that substrates are consumed directly after release:

$$P_{min} = C_{min} \cdot (1 - S_{min}) \cdot K_{d_{min}} \cdot e^{-K_{d_{min}} \cdot time} \quad \text{and} \quad K_{d_{min}} = R_{min} \cdot time^{-S_{min}} \quad (3.4)$$

$$P_{fert} = C_{fert} \cdot (1 - S_{fert}) \cdot K_{d_{fert}} \cdot e^{-K_{d_{fert}} \cdot time} \quad \text{and} \quad K_{d_{fert}} = R_{fert} \cdot time^{-S_{fert}} \quad (3.5)$$

in which C_{min} is the soil organic carbon pool and C_{fert} is the amount of organic fertiliser added or stubble incorporated (both in mol C m^{-3}). R_{min} (in s^{Smin-1}), R_{fert} (in s$^{Sfert-1}$), S_{fert} (-) and S_{min} (-) are empirical parameters (Table 3.2).

In the rhizosphere additional substrates are provided by root exudation, P_{exu} (in molC m^{-3} s^{-1}), described by a gaussian curve:

$$P_{exu} = B_{exu} + A_{exu} \cdot \exp(-0.5 \cdot ((time' - time'_{max}) / \sigma)^2) \quad (3.6)$$

in which B_{exu} (baseline exudation), A_{exu} (maximum increase in exudation above the baseline), $time'_{max}$ (relative time of maximum exudation) and σ (spread of exudation in relative time) are empirical constants (Table 3.2). Root decomposition, P_{root}, described by a first order decay rate (in mol m^{-3} s^{-1}) also only occurs in the rhizosphere:

$$P_{root} = K_{d_{root}} \cdot (pool\ of\ dead\ roots) \quad (3.7)$$

in which $K_{d,root}$ is the relative decomposition constant for roots (Table 3.2) and pool of dead roots (in mol m^{-3}) changes in time under influence of root mortality and root decomposition.

All available substrate is consumed directly either by methanogens or by other anaerobic bacteria using alternative electron acceptors. Oxygen concentrations in the rhizosphere are low (Frenzel et al., 1992) and it is assumed that these concentrations are too low to affect methane production directly or to cause substantial electron acceptors reoxidation or aerobic respiration under flooded conditions. Therefore, NO$_3^-$ is the first electron acceptor to be reduced:

$$\frac{d[NO_3^-]}{dtime} = -v_{NO3} \cdot \sum P_x \quad (3.8a)$$

in which v_{NO3} is a stoichiometry factor for the carbon substrate needed to reduce NO$_3^-$ and $\sum P_x = P_{min} + P_{fert}$ or $\sum P_x = P_{min} + P_{fert} + P_{exu} + P_{root}$ for the bulk soil and rhizosphere, respectively. After NO$_3^-$, Fe(III) is reduced:

$$\frac{d[Fe(III)]}{dtime} = -v_{Fe} \cdot \sum P_x \quad (3.8b)$$

Methanogens and sulphate reducers are assumed to be completely outcompeted with respect to their carbon substrate by nitrate and iron reducing bacteria, but they compete - after NO$_3^-$ and Fe(III) disappearance- for available substrate. The competitive strength is proportional to [SO$_4^{2-}$] and normalised for [SO$_4^{2-}$]$_{t=0}$:

$$\frac{d[SO_4^{2-}]}{dtime} = -v_{SO4} \cdot \frac{[SO_4^{2-}]}{[SO_4^{2-}]_{t=0}} \cdot \sum P_x \quad (3.8c)$$

$$\frac{d[CH_4]}{dtime} = v_{CH4} \cdot \frac{[SO_4^{2-}]_{t=0} - [SO_4^{2-}]}{[SO_4^{2-}]_{t=0}} \cdot \sum P_x - CH_4\_transport\_rate \quad (3.9a)$$
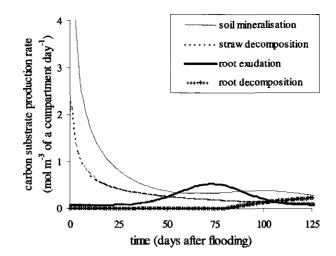
Figure 3.2:   Modelled change in contribution of different processes to carbon substrate
                production in MA94 during the season. In the rhizosphere all processes occur,
                while in the bulk soil compartment only soil mineralisation and straw
                decomposition occur.

It is generally found that the application of rice straw leads to higher methane emissions.
The available data on the effects of rice straw addition are summarised in Figure 3.3a,b.
Such data have been used to derive a logistic curve for the relative increase in methane
emissions versus straw application (Denier van der Gon and Neue, 1995a; Watanabe et
al., 1995b), but a mechanistic explanation for such a curve was not given. The model
(Figure 3.3c, default) produces a roughly linear increase from 0 to 10 tons of rice straw,
which means that a faster exhaustion of alternative electron acceptors (as explained
below), causing the site differences, only has a minor influence. Straw application will
also affect other processes than organic matter supply. These other effects contributed
considerably to the overall effects of straw application (Watanabe et al., 1998) and
include the influence of straw on rice crop performance. Nugroho et al. (1994; 1996;
1997) found positive biomass effects at low straw additions of 5 tons/ha, while Sass and
Fisher (1995) and Kludze and Delaune (1995a) reported rice biomass decreases at straw
additions of 11-22 tons/ha. The negative effects might be explained by an inhibition of
crop growth due to the accumulation of fermentative products (Bedford and Bouldin,
1994; Drenth et al., 1991) and nitrogen immobilisation. If we include effects on rice
biomass changes in the sensitivity analysis (Figure 3.3c, indirect) -simplified to a parabolic
curve with a maximum at 5 tons/ha and no change at 10 tons/ha- then modelled data are
still in the upper range of the experimental data (Figure 3.3b). This means that there are
clearly more adverse interactions between rice plant and straw than were accounted for,
especially if more than 10 tons straw/ha is applied. Possible other interactions are
changes in root oxygen release (see below), plant carbon supply or root morphology.
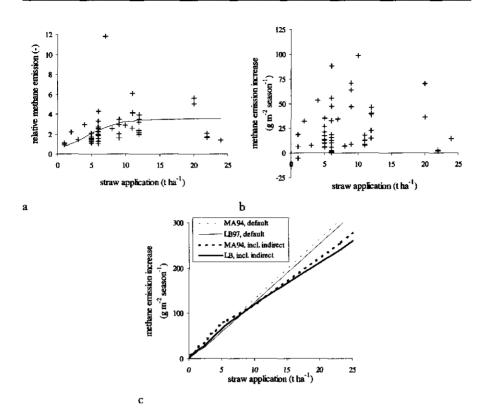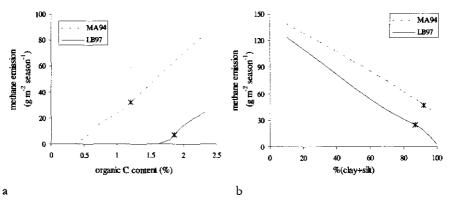
Figure 3.3:   Measured increase in seasonal methane emissions relative to controls without straw addition (a) and measured absolute increase in methane emissions (b). Data are from Denier van der Gon and Neue (1995a), Kimura et al. (1991,1993), Kludze and Delaune (1995a), Lindau and Bollich (1993), Minoda and Kimura (1994), Nouchi et al. (1994), Nugroho et al. (1994,1996,1997), Sass et al. (1991a), Sass and Fisher (1995), Schütz et al. (1989a), Watanabe et al. (1993,1994,1998) and Yagi and Minami (1990). Modelled effects of rice straw application on methane emissions (c) were calculated with and without ('default') the incorporation of an indirect effect of straw on rice yields.

The characteristics of the soil itself also influence the amount of methane emission. The important factors are 1) the amount of alternative electron acceptors, 2) the rate of transport within the soil (both treated below) and 3) the amount of available substrate (soil organic C content, Table 3.1; C_{min} in Eq. 3.4). The (hypothetical) influence of total soil organic matter contents is presented in Figure 3.4a by imposing different levels of this parameter. If all other parameters remain constant, the influence of this parameter on the model outcome is very large and depends on the amount of alternative electron acceptors present (explained below). The finding, however, may be directly related to the anaerobic mineralisation model itself, although several models seem to be equally valid based on the scarce data (Chapter 2). Anaerobic mineralisation processes are thus a very important uncertainty for predictive methane emission models.

Figure 3.4:   Influence of soil organic matter dynamics on seasonal methane emissions, via an imposed hypothetical variation in (a) total organic carbon content and (b) texture (via the protection of soil organic matter). Measured values in organic matter contents at the two sites are marked.

In some models (Huang et al., 1997; 1998), soil texture is also taken into account. Texture may affect diffusion of methane (which will be addressed below) or of carbon substrates. Diffusion limitations would ultimately lead to substrate accumulation, which has never been found in field studies. Soil texture, in particular clay particles, may also protect soil organic matter against breakdown (e.g. Hassink and Whitmore, 1997). Quantitative descriptions on the influence of increased protection on R_{min} and S_{min} are unknown. Therefore, this texture influence on methane emissions was tested with a different mineralisation model, which leads to a new Eq. 3.4 for soil organic matter mineralisation:

$$P_{min} = C_{min} \cdot (F_{fast} \cdot K_{fast} \cdot e^{-K_{fast} \cdot time} + (1 - F_{fast}) \cdot K_{slow} \cdot e^{-K_{slow} \cdot time}) \qquad (3.4')$$

in which F_{fast} is the fraction of the organic matter pool that is assigned to the fast pool (-) and K_{fast} and K_{slow} are the decomposition constants (s^{-1}) of the fast pool and the slow pool, respectively.

An increased protection will lead to a decrease in mineralisation rates for the slow pool. This effect of texture was estimated from Parton et al. (1987), assuming that the slow pool in the two compartment model is the same as the recalcitrant and lignin material pool in Parton et al. (1987):

$$K_{slow} = K_{default} \cdot (1 - 0.75 * (fraction_{clay+silt})) \qquad (3.12)$$

K_{fast} and $K_{default}$ were calibrated using texture and soil mineralisation data from anaerobic soil incubations (Chapter 2). K_{slow} for other textures can thus be calculated using Eq. 3.12 and means that the higher clay+silt content, the smaller K_{slow} becomes. This influence of texture via soil organic matter dynamics on methane emission estimates is very large, as presented in Figure 3.4b by imposing different percentage of (clay+silt). The trends in Figure 3.4a,b are similar to the ones found in a correlative study (Huang et al., 1997).

Methane production
Methanogens, the bacteria producing methane, mainly use acetate as a carbon substrate, but other substrates like H_2/CO_2 and formate contribute for 10-30% to methane

production (Achtnich et al., 1995b; Chin and Conrad, 1995; Rothfuss and Conrad, 1993). This contribution is less than the theoretical 33% valid for methanogenic systems (Gujer and Zehnder, 1983). Homoacetogens, converting H_2/CO_2 to acetate, might thus play a role in modifying the carbon flow. Besides the carbon substrate production, other conditions have to be fulfilled to produce methane.

The methanogens have to compete for the available substrates with other anaerobic bacteria, namely nitrate, manganese, ferric iron and sulfate reducers. Bacteria using organic electron acceptors (Lovley et al., 1996) do not seem important in mineral rice paddy soils (Chapter 5). The competition for carbon substrates in general follows thermodynamic rules: Nitrate reducers outcompete the other anaerobic bacteria for the substrates. In practice, nitrate reducers are of minor importance, however, because nitrate concentrations are low in rice soils. All nitrate is thus reduced within a few hours (Chapter 5; Achtnich et al., 1995a; Westermann and Ahring, 1987). Ferric iron reducers are also able to maintain acetate and H_2 concentrations below concentrations that can be metabolised by sulphate reducers or methanogens (Lovley and Phillips, 1987). These bacteria suppress sulphate reduction (Jakobsen et al., 1981) unless the amount of carbon substrate is not limiting (Lovley and Phillips, 1986; 1987). The thermodynamic characteristics of sulphate reduction are not very different from methane production. The affinity of sulphate reducers for H_2 is higher than the affinity of methanogens (Kristjansson et al., 1982) suppressing methanogens (Achtnich et al., 1995a). The differences in affinity for acetate are much smaller (Oude Elferink et al., 1994) and methane production and sulphate reduction can occur simultaneously (Achtnich et al., 1995b). Other anaerobic bacteria can influence methane production also through specific inhibitors such as NO, N_2O or H_2S. The inhibition by NO and N_2O occurs already at low concentrations (Balderston and Payne, 1976; Klüber and Conrad, 1998), while the effects of inhibition by sulphide are small (Kristjansson et al., 1982; Winfrey and Zeikus, 1977).

a   b
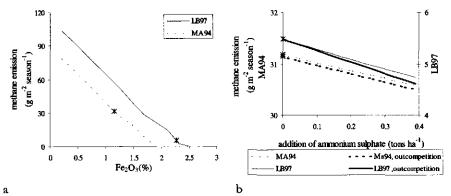
Figure 3.5:   Influence of initial ferric iron (a) and sulphate concentrations (b) on the modelled methane emissions. The influence of sulphate (b) was modelled with different model assumptions on the competition for carbon substrates. Measured values in sulphate contents at the two sites are marked. Note the different y-axes.
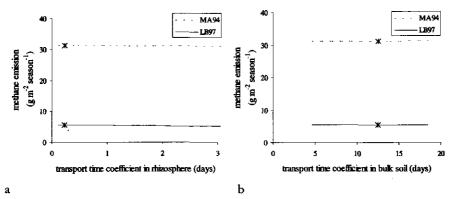
All these interactions were expressed in the model by an outcompetition of methanogens by nitrate and ferric iron reducers and a competition with sulphate reducers (Eq. 3.8, 3.9), which is a close approximation for the competition for acetate. The influences of initial ferric iron (determined by dithionite extractable iron, Table 3.1) and sulphate concentrations (mainly determined by fertilisation, i.e. ammonium sulphate) on methane emissions are presented in Figure 3.5. As in Figure 3.4, we impose a fictive variation of one soil parameter, for conditions of both field experiments. Iron reduction, the dominating reduction process in soils (Inubushi et al., 1984) inhibits methane production severely. At a given iron content, methane emissions are higher for the soil with the higher soil mineralisation (MA) (Figure 3.5a). Decreasing the anaerobic phase in rice soils, e.g. through dry seeding, decreases the period over which methane can be produced, while increasing the relative importance of iron reduction. With a large effect of iron on methane emission, one can also explain some very high Q_{10} values found for methane production (Segers, 1998). With an increase in temperature, soil mineralisation and thus methane production are stimulated not only directly, but alternative electron acceptors are depleted faster as well. If one corrects for this indirect effect, the temperature effects on methane production come in a normal range for biological processes. The effects of sulphate additions are much smaller. This is consistent with field data that show no methane emission reduction (Wassmann et al., 1993) or a reduction of 20-30% (Schütz et al., 1989a). If it is assumed that H_2 is the dominating substrate for methanogens, then sulphate reducers will also outcompete the methanogens. This alternative assumption in the model hardly changes the outcome (Figure 3.5b).

Some models (Cao et al., 1995) relate methane production to redox potential (Eh) and pH, which are in reality highly correlated (Tsutsuki and Ponnamperuma, 1987). Eh and pH do not seem good parameters for process-based models, as discussed elsewhere (Chapter 2). Only if pH<6.0, pH effects may occur. This might explain why urea application normally has no effect on methane emissions (Nugroho et al., 1994; Wassmann et al., 1993), while urea application decreased methane emissions in incubation experiments at application rates higher than 500 mg N/kg soil (Yang and Chang, 1998). Extreme salinity may also lead to a decreased methane production (Denier van der Gon and Neue, 1995b), but this is not accounted for in any model.

Methane transport

Produced methane is transported via aerobic interfaces, where methane oxidation takes place, to the atmosphere. There are four ways to transport methane: leaching, diffusion through the soil, transport via the plant and ebullition. High percolation rates reduce methane emissions significantly (Yagi et al., 1998) and will have to be considered in future models. Methane diffusion through the soil is a very slow process and hardly contributes to methane emissions (Rothfuss and Conrad, 1993; Schütz et al., 1989b). The diffusion of methane via the plant (in the rhizosphere compartment), which depends on root density, is the most important transport pathway to the atmosphere. On average, ebullition (in the bulk soil compartment) only contributes 10-20% to the seasonal methane emission (Byrnes et al., 1995; Nouchi et al., 1994; Schütz et al., 1989b). In case methane production is high at the start of the season (e.g. due to organic fertilisation), the seasonal contribution of ebullition can be up to 60% (Denier van der Gon and Neue,

1995a; Wassmann et al., 1996a). This difference can be understood from the conceptual ideas presented in the model.

Gas transport through rice plants is, contrary to other wetland plants, by diffusion and not by convection. In turn, methane production does not show a short term influence of photosynthetic activity (Denier van de Gon and Neue, 1995a; Wassmann et al., 1994), wind speed, humidity, light (Frenzel et al., 1992), transpiration (Byrnes et al., 1995) or radiation (Lee et al., 1981). Gases (both methane and oxygen) exchange with the soil at the tips of roots (Flessa and Fischer, 1992; Kumazawa, 1984), but quantitatively little is known about the fraction of the root surface that is active in gas exchange. The gases are transported via the aerenchyma of root and shoot (affected by the porosity) and exchange with the atmosphere through special micropores in the shoot (Nouchi and Mariko, 1993). For the quantitative understanding of the flow it is more important to know the largest resistance, which is probably at the root-shoot transition (Butterbach-Bahl et al., 1997). Quantitative data on this resistance are scarce, but probably this resistance will change during the season as root oxygen release (see below) and root morphology change during the season. The mechanism of transport through this transition is not known nor it is known if there is a transport interaction between tillers of one rice plant. The effects of those uncertainties might be small as the model showed hardly any influence of the transport time coefficient in the rhizosphere on seasonal methane emissions (Figure 3.6a). In this simulation it was assumed, however, that methane oxidation in the rhizosphere was independent of transport. In reality this may not be the case, as both processes are diffusion related. The influence of transport rates in the rhizosphere on methane oxidation is much larger in models that link these processes (e.g. Arah and Stephen, 1998).

a   b

Figure 3.6:   Influence of variation in modelled transport time coefficient of (a) the rhizosphere and (b) the bulk soil compartment on estimates of methane emissions. Default parameter values are marked.

The mechanisms of ebullition, gas transport via gas bubbles are even less understood. Qualitatively, one might think of a mechanism in which there is always an equilibrium between the concentration in the soil solution and partial pressure of the gas in a bubble (Watanabe and Kimura, 1995). If the concentration in the soil increases, gas will be captured in bubbles as the concentration in the soil solution is limited (depending on

temperature). If the pressure of the bubbles is larger than the combined pressure of overlying soil structure, root network and atmosphere, then bubble release will be triggered. From this conceptual idea, it can be understood why Mattson and Likens (1990) found influences of solar radiation, water temperature, air pressure and local water table on ebullition and why ebullition was hardly found at cloudy or rainy days (Nouchi et al., 1994). Quantitative models on this process are not known. Again the effects of these uncertainties in the mechanism on the prediction of seasonal methane emissions are small, as (hypothetical) changes in the transport time coefficient in the bulk soil (Figure 3.6b), e.g. caused by differences in soil texture or root density, hardly influence seasonal methane emission.

Transport time coefficients in bulk soil exceed those in the rhizosphere by several orders of magnitude (Table 3.2). From the combination of transport times per compartment and the seasonal changes in contribution of the compartments, the trends in conductance (Hosono and Nouchi, 1997) and in methane residence times (Kimura and Minami, 1995; Watanabe and Kimura, 1995) during the season can be calculated and understood.

The transport time coefficient hardly influences seasonal methane emissions (Figure 3.6), but it changes the variation of emissions within the season (results not shown). Diurnal patterns may be related to fluctuations in ebullition and root oxygen release (see below) (results not shown). Ebullition may be the main factor, because 1) the magnitude of the diurnal fluctuations is highest at the start of the season, when rice plants are small (Denier van der Gon and Neue, 1995a; Husin et al., 1995). 2) diurnal amplitudes are much higher in unvegetated plots than in vegetated plots (Nouchi et al., 1994) and 3) diurnal patterns of methane emissions are correlated with temperature (Sass et al., 1991b) and ebullition is triggered by temperature changes, while plant mediated transport is hardly influenced by temperature. The influence of temperature might also be indirect: At a higher temperature, methane production is stimulated, leading to an increase in methane concentration in the soil. This increased concentration might again trigger ebullition. Neue et al. (1997) identified methane concentration as a controlling factor for the diurnal patterns. If this indirect mechanism is indeed important, then some additional influence due to the plant might be expected, e.g. by diurnal changes in root exudation and root oxygen release. Unfortunately, there are no data available on these effects, but they may explain the differences in diurnal pattern between rice varieties found by Husin et al. (1995). As ebullition is not modelled mechanistically in methane emission models, quantification of the factors determining diurnal patterns remains difficult.

When floodwater recedes and the soil falls dry, all methane captured in the soil is released via the air-filled pores that are formed in the drying process (Denier van der Gon et al., 1996; Wassmann et al., 1994). The flush of methane is larger after a longer period of methane production, as more methane has been stored (Watanabe and Kimura, 1995). Similar effects occur by physical disturbances like cultural practices (Neue et al., 1997). Due to aerobic conditions developed by the disappearance of floodwater, the soil (and its electron acceptors) reoxidises as well, resulting in suppressed methane production after reflooding the soil. These negative effects on methane emissions are larger than the flushing effects if the period of drainage is long enough. Mid-season drainage has therefore become an effective mitigation option to decrease methane emissions. A good timing of (hypothetical) drainage is important to obtain an optimal result (Figure 3.7), whereas the number of dry periods appears to be less important (results not shown). The

modelled effects of drainage (Figure 3.7) are similar to what has been encountered experimentally (Sass et al., 1992; Nugroho et al., 1994; Yagi et al., 1996). The simplifications made in the model to describe reoxidation processes hardly influenced methane emission estimates, as can be seen from the small effects of neglecting FeS formation and oxidation (Figure 3.7).

a   b
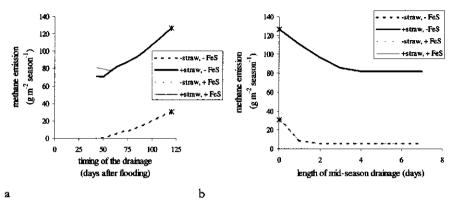
Figure 3.7:   Effects of (a) the timing of the mid-season drainage and (b) the length of a mid-season drainage, at 64 DAT, on top of a final drainage on modelled methane emissions, using the data set of MA94 only. Calculations were carried out with and without straw application and with and without a correction for the formation and oxidation of FeS. The situation with no intermediate drainage is marked.

Methane oxidation

At the aerobic interfaces, methane can be oxidised in the soil by methane oxidising bacteria, methanotrophs. There are two types of methane oxidising activity: high affinity (at low methane concentrations) and low affinity (at high methane concentrations) (Bender and Conrad, 1992). For the study of methane oxidation in wetlands, high affinity methane oxidation does not need to be considered (Segers, 1998). Low affinity methane oxidation may in principle occur anaerobically and aerobically. In the first case, methane oxidation may be coupled to nitrate, ferric iron or sulphate reduction. However, there is no evidence available that methane oxidation coupled to nitrate reduction occurs in wetlands. Nedwell and Watson (1995) could not show sulphate reduction to be coupled to methane oxidation in wetlands. Murase and Kimura (1994) and Miura et al. (1992) found a concurrence of a depletion of methane and an accumulation in ferrous iron in rice subsoil and interpreted this as a coupled ferric iron reduction/ methane oxidation. Other interpretations are however also possible. No enrichments or kinetics of anaerobic methane oxidisers in rice paddies are known.

If we restrict our considerations to aerobic methane oxidation, then two sites for oxidation can be distinguished: the rhizosphere and the soil-water interface. At the soil-water interface, methane oxidation is confined to 70-95% of the produced methane (e.g. Banker et al., 1995; Schütz et al., 1989b). This small range indicates that the presence or absence of the oxygen produced by algae does not have a large influence on methane oxidation. Oxidation at the soil-water interface is bypassed by ebullition.

The rhizosphere represents a far more dynamic system with many more uncertainties. Oxygen is released into the rhizosphere by root oxygen release (ROL), which is again influenced by root respiration and root transport resistances (treated above). The ROL changes diurnally (Satpathy et al., 1997), during the season (Satpathy et al., 1997), with cultivar (Wang et al., 1997; Kludze et al., 1994), with nutrient conditions (Kludze and Delaune, 1995a; 1995b) and with Eh (Kludze et al., 1993). Moreover, the estimate for ROL highly depends on the used methodology (Sorrell and Armstrong, 1994). The oxygen input is thus very variable and uncertain.

The released oxygen is not only used by the methanotrophs. Part of the oxygen is used for the chemical and bacterial reoxidation of reduced compounds and for heterotrophic respiration of low-molecular organic compounds (Ponnamperuma, 1972; Watson et al., 1997). The contribution (and its dynamics) of the different processes to oxygen consumption is not known, but it is known that methanotrophic activity is affected by salinity (Denier van der Gon and Neue, 1995b), NH_4^+ (Conrad and Rothfuss, 1991), elevated pH and $CaCO_3$ (King et al., 1990). Another complicating factor is that the aerobic zone moves through the soil (due to the combination of root growth and oxygen consumption). Bacterial activity will have to cope with this dynamics. This may result in growth of methanotrophs as the number of methanotrophs is higher in the rhizosphere than in the bulk soil (Gilbert and Frenzel, 1995; Kumaraswamy et al., 1997) and increases during the growing season (Gilbert and Frenzel, 1995; Watanabe et al., 1997). It also may result in a limited mortality as mortality rates of methanotrophs are low at small oxygen and methane availability (Roslev and King, 1994; Le Mer et al., 1996). Quantitative data on such adaptations are scarce. Finally, it is not certain whether methane oxidation takes place in the rhizosphere or in the roots of the rice plant (as methanotrophs were found inside the roots (Gilbert et al., 1998)). Apart from mechanistic uncertainties, there are several uncertainties in the measurement of methane oxidation, as discussed by Frenzel and Bosse (1996) and King (1996). All these uncertainties make the prediction of methane oxidation rates extremely difficult.
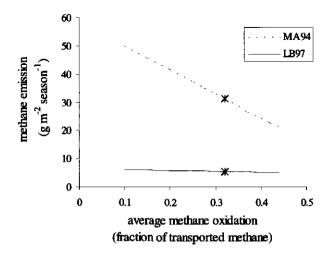
Figure 3.8:   Effects of a hypothetical change in average seasonal methane oxidation in the rhizosphere on methane emissions. Default parameter values are marked.

The effects of all these uncertainties on the estimation of methane emissions can be quite considerable as is shown by the model sensitivity of methane emissions to hypothetical variation of this estimate (Figure 3.8). This clearly needs further attention. The sensitivity on methane oxidation moreover depends on the time in the season that most methane release occurs.

Rice plant influence on the processes

The above analysis shows the major importance of rice plants for methane emissions, via its root system, exudation, oxygen release and root-shoot resistance. These effects have been integrated in correlative models between methane emissions and plant parameters, namely yield, total rice biomass, root density, plant height and shoot length. The results are however ambiguous. Watanabe et al. (1994) found a correlation between emission and shoot length, while Lindau et al. (1995) found no correlation between plant height and methane emission. Sass et al. (1990) correlated methane emission and aboveground biomass, while such a correlation was absent in the study of Watanabe et al. (1995a). Nouchi (1990) found a correlation between the number of tillers and methane emissions, while Denier van der Gon and Neue (1996) did not find such a correlation. The reason for these different results is that there are different influences of the plant on methane release (as explained above). Those influences will lead to non-linear results and will moreover change during the season and with different conditions. This model can investigate some of those influences. Other interactions can better be explained by a fully mechanistic approach, like the one presented by Arah and Stephen (1998). An example of an interaction that changes with the conditions is given in Figure 3.9. In the first scenario it is assumed that a constant aboveground biomass fraction equivalent to 30% of the yield (Table 3.1) is incorporated into the soil, which is a common, but unrealistic, assumption in global methane emission estimates. In such a scenario, the organic matter supply dominates methane emission changes, leading to an almost linear response with yield. In the second scenario it is assumed that the farmer incorporates the same amount of stubble (e.g. by cutting the rice at a certain constant height) independent of the yield obtained. In both scenarios the presence of rice plants stimulates methane emissions (by providing a substrate for methanogens), but the response is quite different for the two scenarios.

Plant variables do not only change during the season and with conditions, but also vary between varieties. Differences have been found in the root oxygen release (Kludze et al., 1994; Kludze and Delaune, 1995a; Wang et al., 1997), in gas permeability (Butterbach-Bahl et al., 1997) and root exudation (Kludze et al., 2000). This leads to large effects of rice varieties on methane emission (Husin et al., 1995; Lindau et al., 1995; Nugroho et al., 1997; Sass and Fisher, 1995; Watanabe et al., 1995a). The combined effects have been incorporated in the model of Huang et al. (1998) by an empirical variable, the variety index. Lumping the various effects in a single variable leads to a loss of a mechanistic basis and hence to a reduction of extrapolation beyond the range of calibration. The plant physiological differences in gas permeability (influencing both root oxygen release and methane transport) and root exudation (important in soils with a low carbon content) open possibilities for directed variety screening.
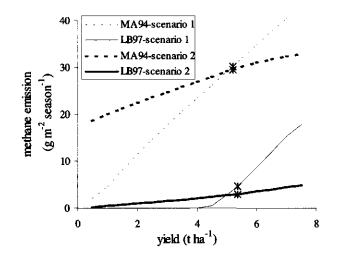
<u>Figure 3.9</u>:   Influence of yield differences on methane emission for two scenarios. The first
                 scenario assumes that the amount of stubble that is incorporated in the soil is
                 equal to 30% of the yield. The second scenario assumes that the amount of
                 stubble that is incorporated into the soil is 1500 kg/ha, independent of yield.
                 Measured yields at the two sites are marked.

3.4 Concluding remarks

Uncertainties and variability in the knowledge on underlying processes leading to methane emissions from rice cropping systems were reviewed. Sensitivity of these uncertainties and variabilities in processes on methane emissions were investigated with a process-based model. Model sensitivities were compared to system sensitivities, as far as these were known, i.e. for the effects of organic matter supply, drainage and sulphate additions. In those cases the model behaved similarly and with a similar sensitivity as the real systems. For situations for which only trends are known (for the transport characteristics and the contribution of different carbon substrates), the model also behaved similarly. The model thus fairly reproduces the real variability in methane emissions caused by the variability in underlying parameter values.

By plotting the relative change in methane emission versus the relative change of a variable within its plausible range, all model sensitivities can be compared (Figure 3.10). The figure shows great differences in sensitivities and a large variety of linear and non-linear responses. The responses were different for the two soils. Due to the high amount of reducible ferric iron in the Los Baños soil, this soil is more sensitive to variables influencing methane production (Figure 3.10b). In the Maligaya soil, variables influencing carbon substrate production and methane production are the most important variables as well, but methane oxidation is also a sensitive variable (Figure 3.10a). Other well-known uncertainties, like mechanisms of methane production or the pathway of gas transport through the plant do not seem to be important for the estimation of methane emissions.
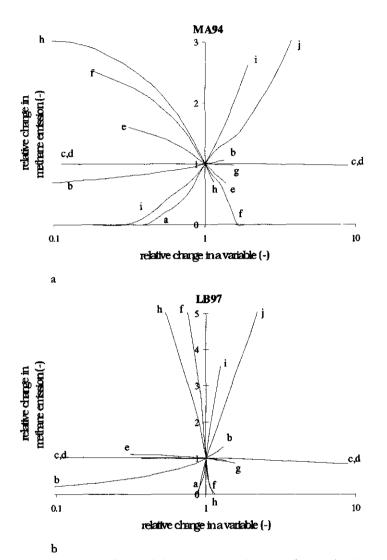
Figure 3.10: Sensitivity of modelled methane emissions to changes in the underlying parameters (both relative to site input parameter values) for (a) Maligaya and (b) Los Baños, Philippines. The tested parameters are: 'a' moment of drainage (relative to drainage at the end of the season), 'b' yield, 'c' and 'd' transport time coefficient in the rhizosphere and bulk soil compartment, respectively, 'e' percentage oxidation, 'f' iron content of the soil, 'g' application of $(NH_4)_2SO_4$ (relative to initial soil sulphate concentration), 'h' texture (influencing soil mineralisation), 'i' soil organic matter content and 'j' straw application. Note that the y-axis is linear and the x-axis is logarithmic.
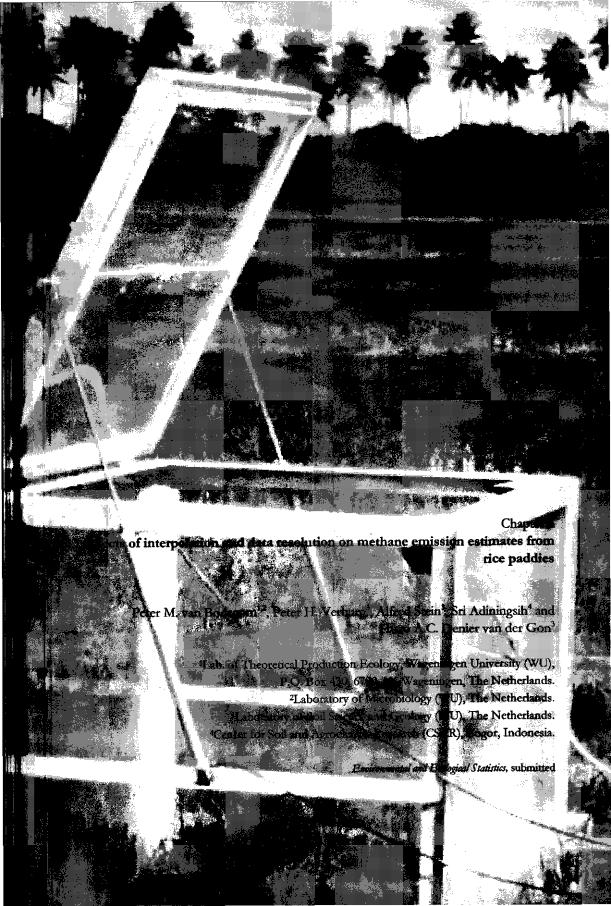
This analysis has two main implications. 1) The influence of straw application on soil-plant responses and the mechanisms of anaerobic soil organic matter mineralisation belong to the main uncertainties, and also strongly influence methane emissions (as is

indicated by the influence of texture, organic C soil and straw application). As long as these processes are not well understood, the predictability and extrapolation of modelled methane emissions will be limited at a field scale level and thus at a global scale level. The uncertainty in the range of methane emissions will thus remain large. 2) Methane emissions react non-linearly to variables describing the underlying processes, especially if interactions between underlying variables are taken into account (as can be seen from the different responses of the two soils). This means that global emission estimates based on average parameter values over large regions may deviate considerably from the real methane emission. For a better global prediction of methane emission, methodologies that account for spatial variability in sensitive parameters (like management and organic matter supply) will have to be developed.

Acknowledgements

Effects of interpolation and data resolution on methane emission estimates from rice paddies

Peter M. van Bodegom[1,2], Peter H. Verburg, Alfred Stein, Sri Adiningsih[4] and
Hugo A.C. Denier van der Gon[3]

[1]Lab. of Theoretical Production Ecology, Wageningen University (WU),
P.O. Box 430, 6700 AK Wageningen, The Netherlands.
[2]Laboratory of Microbiology (WU), The Netherlands.
[3]Laboratory of Soil Science and Geology (WU), The Netherlands.
[4]Center for Soil and Agroclimate Research (CSAR), Bogor, Indonesia.

Effects of interpolation and data resolution on methane emission estimates from rice paddies

Abstract

Rice paddies are an important source of the greenhouse gas methane. Global methane emissions estimates are however highly uncertain and do not account for effects of interpolation or data resolution errors. Such scaling effects were determined for the influence of soil properties in a case study of the island Java, Indonesia. The effects of different interpolation techniques, semivariograms and neighbour optimization were tested for soil properties by cross-validation. Interpolated organic carbon values were not significantly different from the original soil samples, but interpolated soil iron contents were. Interpolation led to a significant decrease in spatial heterogeneity in methane emissions. Soil properties were interpolated to derive data at different data resolutions. Mean and variance of soil properties were not significantly different for different data resolutions. Mean and variance of methane emissions at different data resolutions were however significantly different. These scaling effects were caused by the combination of interpolated data and a non-linear model. Correlations between soil properties smoothened some scaling effects. Real scaling effects will have been larger because small-scale variability was not accounted for. Scaling effects, including those caused by small-scale variability, will have to be considered to achieve unbiased global methane emissions estimates from rice paddies.

4.1 Introduction

Methane (CH_4) is an important greenhouse gas. The major sources of atmospheric CH_4 are known, but the contribution of these sources to the global CH_4 budget is highly uncertain. Rice paddies are among the important sources of atmospheric CH_4. Most estimates of global CH_4 emissions from rice paddies are multiplications of an average CH_4 emission rate by the length of the growing season and harvested area. Estimates of the global CH_4 source strength of rice paddies change frequently as new data become available or a different method is proposed. Recently published values are 117 ± 50 Tg/yr (Holzapfel-Pschorn and Seiler, 1986), 100 ± 40 Tg/yr (Aselmann and Crutzen, 1989), 100 ± 50 Tg/yr (Schütz et al., 1990), 42-82 Tg/yr (Bachelet and Neue, 1993), 60 ± 40 Tg/yr (Houghton et al., 1996), 50 ± 20 Tg/yr (Neue, 1997), 53 Tg/yr (Cao et al., 1998) and 80 ± 50 Tg/yr (Lelieveld et al., 1998), illustrating the large uncertainty. Since emissions from rice paddies cannot be directly measured at the national, continental or global scale, it is difficult - if not impossible- to judge which estimate is more realistic.

A major source of uncertainty is the large intrinsic variation in methane emission in time and space due to spatial variation in biophysical properties and agricultural management (e.g. Denier van der Gon and Neue, 1995a; Nouchi et al., 1994). Reducing the uncertainties is difficult because underlying processes leading to methane emissions are hard to quantify and because data characterising rice agricultural management or other necessary attributes are scarce.

An additional source of uncertainty is the methodology used to obtain global emissions, e.g. upscaling. As methane emissions cannot be measured at the global scale, or even at the national scale, suitable predictor variables have to be chosen to describe and explain variations in methane emissions if one uses an upscaling approach. At present, however, these predictor variables do not encompass local soil and management conditions, which are two factors that strongly influence methane emissions (Chapter 3). Attempts to account for local variations make use of large databases on land use and/or soil types with resolutions of 1°x1° (Bachelet and Neue, 1993) or 0.5°x0.5° (Cao et al., 1998). In these studies, effects of interpolation or data resolution errors were not accounted for. These so-called scaling effects are well-known to occur in erosion studies (e.g. Dunne et al., 1991) and may also be significant when upscaling methane emission to the global scale. Unfortunately, a thorough analysis of scales, at which all processes and data can be summarised properly to calculate global methane emissions, has not yet been made. Such optimal scales may well differ from the scale at which global databases are available.

The objective of this paper is to discuss possible scaling effects on methane emissions from rice paddies that arise from spatial variability in soil properties. Soil properties are chosen as a test case, because of their large influences on methane emission and because of data availability. The island of Java, Indonesia, is used as a case study, being an important rice growing area. Soil samples from rice fields of Java are collected and analysed on soil chemical and morphological properties by the Center for Soil and Agroclimate Research (CSAR). We focused on effects caused by i) choices made in interpolation of soil sampling data to land areas - interpolation effects - and ii) effects of different grid sizes for soil data and rice distributions on calculated methane emissions - data resolution effects. In principle, the methodology can be applied to any other area.

4.2 Materials and methods
4.2.1 Methane emission model description
The soil properties focused on are soil iron content (Fe) and soil organic carbon content (OC), because these two parameters are among the controlling variables for methane emissions from rice paddies (Chapter 3). A process-based model (Chapter 2) requires data on Fe and OC to calculate methane emissions. Two compartments, the rhizosphere and the bulk soil, are distinguished in this model. To simulate methane emissions the model contains simplified process-based descriptions of methane production, transport and oxidation for each compartment. Input parameter values used in the model were estimated from independent sources. The model was validated with experimental data collected in Asia (Chapter 2). Simulated seasonal methane emissions did not significantly differ from measured seasonal emissions (with a coefficient of variation of 8%). The model used in this paper was extended with a description for multiple drainage and for situations in which the rice yield was not optimal and for situations with a different rice variety (Chapter 3).

Besides data on soil properties, model inputs are rice variety and rice yield, inorganic and organic fertilizer input, length of the growing season and temperature. Since our objective was to study interpolation and data resolution effects of soil properties, weighted average values for input parameters other than soil properties were estimated and used (Table 4.1). Rice distribution data were based upon an integrated set (Verburg et al., 1999) collected from land use maps and agricultural statistics.

Table 4.1: Average or assumed values for controlling variables other than soil properties used to calculate CH_4 emissions with a process-based model.

Input parameter	Value	Source
Rice variety[a]	IR64	BPS, 1996
Rice yield	5.1 t/ha	BPS, 1995
NO_3 or SO_4 containing fertilizers [b]	34 kg/ha	BPS, 1994
Straw input	30% of the yield	Neue et al., 1990
Length of growing season	119 days	BPS, 1996
Temperature	26 °C	Verburg et al., 1999
Water management [c]	continuously flooded	

[a] This is the dominant rice variety on Java.

[b] Other inorganic fertilizers like urea do not directly influence CH_4 emission. The fertilization effect on rice production is included in the average yield.

[c] A significant part of the rice fields on Java is not continuously flooded (rainfed rice) but to clearly see the effects of spatial variation in soil properties this was neglected.

4.2.2 Interpolation effects

Quantification of spatial variability

Scaling effects arise if the spatial heterogeneity presented by point data (in this case soil samples) is not correctly integrated while scaling up to an area. Application of geostatistics, therefore, may spatially interpolate data using the autocorrelation of variability. This allows estimation of spatial characteristics by techniques from regionalized variable theory, by kriging. A semivariogram (Webster, 1985) was constructed for OC and Fe to quantify the relationship between the expected variance of two measurements and the distance separating the locations of the measurements, i.e. to quantify autocorrelation. Different variogram models (spherical, exponential, linear with sill and a gaussian model) were tested to fit the data. The best model for OC was a spherical model:

$$\gamma_s(h) = c_0 + a_s \cdot (\frac{3}{2} \cdot \frac{h}{r_s} - \frac{1}{2} \cdot (\frac{h}{r_s})^3) \qquad 0 < h < r_s$$
$$c_0 + a_s \qquad h > r_s \qquad (4.1)$$

where $\gamma_s(h)$ is the semivariogram and h is the distance (in km).

For Fe, the best model was an exponential model:

$$\gamma_e(h) = c_0 + a_e \cdot (1 - e^{-\frac{h}{r_e}}) \qquad h > 0 \qquad (4.2)$$

where $\gamma_e(h)$ is the semivariogram.

Soil parameter interpolation

Given a semivariogram model (and thus given autocorrelation) and a set of parameter estimates, interpolations to unsampled locations can be obtained through kriging. Ordinary kriging (Stein and Corsten, 1991) was employed optimizing the number of neighbours involved with a cross-validation procedure (Voltz and Webster, 1990). From the original dataset of 553 soil samples from different locations, 111 samples (20%) were randomly selected and put aside as a test set. The remaining 442 samples were used to

predict OC and Fe towards the test set. The predicted and measured values for the 111 samples were compared and analysed using 5 different statistical indices:

The mean error (*ME*) measures the bias of the prediction:

$$ME = \frac{1}{n} \sum_{i=1}^{n} \left\{ Z^*(x_i) - Z(x_i) \right\} \tag{4.3}$$

where $Z^*(x_i)$ is the predicted value and $Z(x_i)$ is the measured value. ME should be close to zero for unbiased methods.

The mean absolute error (*MAE*) is a measure of the total error of prediction:

$$MAE = \frac{1}{n} \sum_{i=1}^{n} \left| Z^*(x_i) - Z(x_i) \right| \tag{4.4}$$

MAE should be zero for a correct estimation.

The mean square error (*MSE*) combines both the precision and the bias of prediction:

$$MSE = \frac{1}{n} \sum_{i=1}^{n} \left\{ Z^*(x_i) - Z(x_i) \right\}^2 \tag{4.5}$$

MSE should be as small as possible.

The mean square deviation ratio R measures the goodness of fit of the prediction:

$$R = \frac{1}{n} \sum_{i=1}^{n} \left\{ Z^*(x_i) - Z(x_i) \right\}^2 / S_i^2 \tag{4.6}$$

where S_i^2 is the estimated variance for measured values of $Z(x_i)$. The better the estimate is on average, the closer is R to 1.

Finally, the correlation coefficient (ρ) was used:

$$\rho = \frac{\mathrm{cov}(Z^*(x), Z(x))}{S^*(x) \cdot S(x)} \tag{4.7}$$

where $cov(Z^*(x), Z(x))$ is the covariance between predicted and measured values, $S^*(x)$ is the estimated standard deviation of the predicted values and $S(x)$ is the estimated standard deviation of measured values.

The results for interpolation by ordinary kriging were compared with interpolation results obtained by inverse distance weighting (IDW). IDW does not use geostatistical information, but weighs the information as a function of distance (in this study a power 2 function was used). The number of neighbours involved in IDW was optimized by cross-validation in the same way as described above.

Methane emission interpolation

Methane emissions occur per definition over a certain area. The smallest area that could be distinguished in this study was 20x20 km, which is more detailed than the district level. This was the highest resolution for which spatial information on the model input parameters could be obtained. The effects of interpolation on spatially explicit estimates of methane emissions for Java were therefore analysed at this resolution (yielding 329 grids to describe Java).

Ordinary blockkriging - ordinary kriging applied and averaged for different positions within a block (Journel and Huijbregts, 1978) - was used as an interpolation technique for

OC and Fe, using all soil samples. As a sensitivity analysis alternative considerations were tested separately: i) Methane emissions were calculated using an exponential semivariogram for OC and a spherical semivariogram for Fe, instead of the optimal semivariograms. ii) Methane emissions were calculated using 12 neighbours in the kriging analysis instead of the optimal number. iii) For comparison of interpolation efficiency, methane emissions were calculated from arithmetic averages of OC and Fe in each grid (assuming that empty grids were not important rice areas and did not contribute to methane emissions). iv) Methane emissions were calculated by optimized ordinary blockkriging. The last was used as default in the remainder of the study.

4.2.3 Data resolution effects

Soil parameter data resolution

In addition to assumptions made for interpolation of soil samples to an area, data resolution is also important to the final results. Global methane emission estimates are generally based on emission factors multiplied with harvested area. Attempts to make spatial explicit estimates use coarse resolution data e.g. the FAO 1:5.000.000 soil map of the world (Bachelet and Neue, 1993). By contrast, the processes leading to methane emissions occur at very fine scales, e.g. the scale of a single root. Due to the complex process interactions involved in methane emissions, a non-linear response can be expected (Chapter 3). This means that a different outcome can be expected when calculating emissions first followed by averaging the results, than when averaging the data first followed by calculating emissions - as has been found for soil moisture deficits (Stein et al., 1991).

The effects of data resolution were tested in this study by choosing 20x20 km, 40x40 km, 100x100 km (which is similar to 1°x1°) and 'whole Java' (1021x322 km) as grids. The data for 20x20 km grids were calculated as mentioned above. In principle there are two upscaling procedures. In stepwise upscaling, data from the finer scale nearest by are used as input for interpolation – in this case ordinary blockkriging using the semivariograms for OC and Fe determined in Figure 4.1. This is a common upscaling procedure as only one finer scale has to be considered. However, in this study, the complete original soil sample set was used for interpolation at all data resolutions. This avoids that, at coarser data resolutions, semivariograms are extrapolated beyond the range accounted for. More important is that this procedure avoids that interpolation errors can accumulate at coarser data resolutions.

The statistical effects of data resolution were tested in two ways:

At each of the data resolutions (except for 'whole Java'), a cumulative probability density functions (pdf) was constructed for OC and Fe. These pdf's were compared to the cumulative pdf of the original 553 samples and tested for significant differences in variance (by a F-test) and in means of the underlying populations (by a student's t-test). This statistical analysis of the cumulative pdf's is not spatially explicit, as there are no spatially explicit measurements of methane emissions.

A somewhat better understanding of the spatial variance can be obtained when analysing the mean within-grid variance and the grid-means variances. In block kriging, interpolation is made to 100 locations within a grid, independent of the grid size. From these data the within-grid variance $(var \ (Z(x_j))$ can be calculated as:

$$\overline{\text{var}(Z(x_i))} = \frac{\sum\limits_{i=1}^{grids} \dfrac{\sum\limits_{j=1}^{100}(Z(x_{ij})-\overline{Z(x_i)})^2}{99}}{grids-1} \tag{4.8}$$

where *grids* is the number of grids at a certain data resolution.

The grid-means variance (*var(Z(x))*) is calculated as:

$$\text{var}(Z(x)) = \frac{\sum\limits_{i=1}^{grids}(Z(x_i)-Z(x))^2}{grids-1} \tag{4.9}$$

where *Z(x)* is the observed overall mean value.

Methane emission data resolution

Methane emissions were estimated for 20x20 km, 40x40 km, 100x100 km and 'whole Java' data resolutions by coupling for each grid block kriged OC and Fe to the model. This procedure did not allow the calculation of within-grid variances of methane emissions. Data resolution effects on methane emissions were therefore tested only on cumulative pdf's constructed at each data resolution. These pdf's were compared to the cumulative pdf based on the original 553 samples and tested for significant differences in variance (by a F-test) and in means of the underlying populations (by a student's t-test).

4.3 Results
4.3.1 Interpolation effects
Quantification of spatial variability

The spatial variability in both OC and Fe could be described by a significant semivariogram (Figure 4.1). For OC the estimated parameter values for the semivariogram are c_0=0.0948 %C^2, a_s=0.194 %C^2 and r_s = 35.5 km (r^2=0.97). If, as an alternative description, an exponential semivariogram was chosen for OC then the parameter values are c_0=0.0564, a_e=0.238 and r_e = 13.1 km (r^2=0.93). For Fe the estimated parameter values for the semivariogram c_0=0.399 %Fe^2, a_e=0.905 %Fe^2 and r_e = 12.9 km (r^2=0.87). If, as an alternative description, a spherical semivariogram was chosen for Fe then the parameter values are c_0=0.63, a_s=0.668 and r_s = 42.7 km (r^2=0.86). The best fitting semivariogram for each soil property is also displayed in Figure 4.1. The highly significant semivariograms show that autocorrelation is present even over these large distances considered.

The total distance considered in the analysis did not influence parameter estimation if the total distance was larger than 'r' nor did it influence the choice of a variogram model (Figure 4.1). Nugget variance (c_0) and sill variance (c_0+a) are higher for soil iron than for soil organic carbon, while average amount of soil iron and soil organic carbon are similar. The range of spatial dependence (the distance up to reaching the sill) is similar for soil organic carbon and soil iron. This surprises at first sight, because we expected a more local influence on soil organic carbon due to (highly variable) farmers' management. By contrast a larger spatial dependence was expected for soil iron, because that is thought to be dependent on parent material and thus on the geological circumstances. This suggests that field to field variation in farmers management could not be distinguished by this

dataset because of the large distances between sampling points. An alternative explanation is that field to field variation in OC is smaller than anticipated, e.g. because burning of crop residues after harvest and the absence of use of organic amendments have a levelling effect on OC variability.

a   b
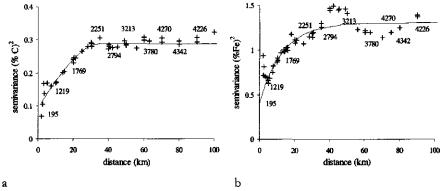
Figure 4.1:   Semivariogram of a) the soil organic carbon content and b) soil iron content. The number of data pairs at a distance is indicated as well.

Soil parameter interpolation

With the cross-validation procedure, the number of neighbours for ordinary kriging could be optimized for OC (Table 4.2) and Fe (Table 4.3). This optimal number of neighbours is related to the semivariogram – and thus on the dataset used - and more or less indicates the number of neighbours at a distance smaller than the range. The optimal number of neighbours for Fe is therefore only slightly higher than for OC.

Table 4.2:   Statistical indices for the cross-validation of soil organic carbon estimation by ordinary kriging with different numbers of neighbours accounted for. In between brackets the ranking is given (1 is best, 6 is worst). The average ranking is given in the bottom row.

	2	4	5	6	8	12
ME	0.001 (1)	-0.012 (2)	-0.013 (3)	-0.016 (6)	-0.014 (4)	-0.015 (5)
MAE	0.359 (5)	0.348 (4)	0.347 (3)	0.336 (1)	0.341 (2)	0.657 (6)
MSE	0.280 (5)	0.252 (3)	0.251 (2)	0.247 (1)	0.257 (4)	0.736 (6)
R	0.9910 (6)	0.9915 (4)	0.9916 (3)	0.9920 (1)	0.9917 (2)	0.9913 (5)
ρ	0.6531 (5)	0.6836 (3)	0.6843 (2)	0.6888 (1)	0.6744 (4)	0.3754 (6)
ranking	(4.4)	(3.2)	(2.6)	(2.0)	(3.2)	(5.6)

Also for the IDW procedure, an optimal number of neighbours could be distinguished by the cross-validation procedure for OC (Table 4.4) and Fe (Table 4.5). This optimal number differs from the number achieved for ordinary kriging as IDW employs a different weighing with distance.

Table 4.3:   Statistical indices for the cross-validation of soil iron content estimation by ordinary kriging with different numbers of neighbours accounted for. In between brackets the ranking is given (1 is best, 6 is worst). The average ranking is given in the bottom row.

	4	6	8	10	12	14
ME	-0.192 (5)	-0.194 (6)	-0.175 (2)	-0.168 (1)	-0.175 (3)	-0.178 (4)
MAE	0.813 (6)	0.795 (5)	0.781 (4)	0.779 (3)	0.772 (1)	0.776 (2)
MSE	1.277 (6)	1.229 (5)	1.211 (2)	1.222 (4)	1.213 (3)	1.210 (1)
R	1.020 (5)	1.022 (6)	1.016 (2)	1.014 (1)	1.017 (3)	1.018 (4)
ρ	0.4926 (6)	0.5045 (2)	0.5061 (1)	0.4954 (5)	0.4988 (4)	0.4989 (3)
ranking	(5.6)	(4.8)	(2.2)	(2.8)	(2.8)	(2.8)

Table 4.4:   Statistical indices for the cross-validation of soil organic carbon estimation by inverse distance weighting with different numbers of neighbours accounted for. In between brackets the ranking is given (1 is best, 6 is worst). The average ranking is given in the bottom row.

	2	4	6	8	10	12
ME	0.010 (1)	-0.013 (2)	-0.016 (3)	-0.018 (5)	-0.017 (4)	-0.147 (6)
MAE	0.368 (5)	0.361 (4)	0.352 (3)	0.347 (2)	0.343 (1)	0.676 (6)
MSE	0.294 (5)	0.278 (4)	0.268 (3)	0.267 (2)	0.264 (1)	0.815 (6)
R	0.9913 (5)	0.9916 (4)	0.9919 (3)	0.9922 (1)	0.9921 (2)	1.018 (6)
ρ	0.6424 (5)	0.6542 (4)	0.6649 (3)	0.6660 (2)	0.6691 (1)	0.4046 (6)
ranking	(4.2)	(3.6)	(3.0)	(2.4)	(1.8)	(6.0)

Table 4.5:   Statistical indices for the cross-validation of soil iron content estimation by inverse distance weighting with different numbers of neighbours accounted for. In between brackets the ranking is given (1 is best, 6 is worst). The average ranking is given in the bottom row.

	6	8	10	11	12	14
ME	-0.223 (6)	-0.216 (5)	-0.210 (2)	-0.208 (1)	-0.211 (3)	-0.212 (4)
MAE	0.838 (6)	0.830 (5)	0.827 (4)	0.822 (3)	0.819 (2)	0.818 (1)
MSE	1.318 (6)	1.304 (5)	1.299 (4)	1.286 (1)	1.287 (2)	1.291 (3)
R	1.030 (6)	1.028 (5)	1.026 (2)	1.025 (1)	1.027 (3)	1.028 (4)
ρ	0.4829 (4)	0.4849 (1)	0.4828 (5)	0.4835 (3)	0.4847 (2)	0.4827 (6)
ranking	(5.6)	(4.2)	(3.4)	(1.8)	(2.4)	(3.6)

To determine the performance of spatial interpolation, prediction towards the test set was also carried out by randomly selecting samples from the available data, i.e. without considering the neighbourhood. Both optimized interpolation methods perform better than these randomly selected samples (Table 4.6) for OC as might be expected for spatially correlated parameters. For Fe, IDW interpolation performed similarly as a random prediction. Spatial interpolation was thus not always better than a random selection for Fe. This is due to the high variance in the soil iron data (shown by the high MSE). This high variance was not accounted for in all interpolation procedures, leading

to high biases (high MAE). Ordinary kriging took best account of the spatial heterogeneity (Table 4.6), using the semivariogram, and will be used hereafter.

Table 4.6:   Statistical indices for the cross-validation of soil organic carbon and soil iron content estimation by a random selection, by optimized inverse distance weighting (with 10 and 12 neighbours for carbon and iron, respectively) and by optimized ordinary kriging (with 6 and 8 neighbours for carbon and iron, respectively). In between brackets the ranking is given (1 is best, 3 is worst). The average ranking is given in the bottom row.
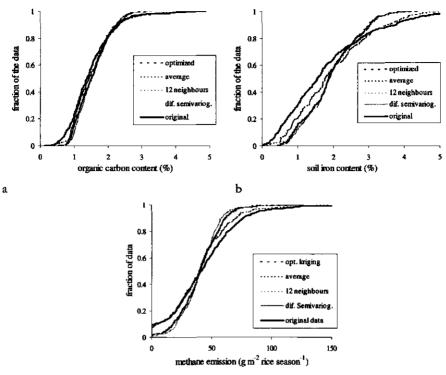
	Random	IDW	kriging	random	IDW	Kriging
	Soil organic carbon			Soil iron content		
ME	0.038 (3)	-0.018 (2)	-0.016 (1)	-0.117 (1)	-0.211 (3)	-0.174 (2)
MAE	0.910 (3)	0.343 (2)	0.336 (1)	1.287 (3)	0.819 (2)	0.781 (1)
MSE	1.278 (3)	0.264 (2)	0.247 (1)	2.635 (3)	1.287 (2)	1.211 (1)
R	0.9921 (2)	0.9922 (1)	0.9920 (3)	0.996 (1)	1.027 (3)	1.017 (2)
ρ	-0.069 (3)	0.669 (2)	0.689 (1)	-0.002 (3)	0.485 (2)	0.506 (1)
ranking	(2.8)	(1.8)	(1.4)	(2.2)	(2.4)	(1.4)

Methane emission interpolation

Interpolated OC and Fe values were used to predict methane emissions. Ordinary blockkriging was used as a kriging method to obtain area averaged values. The results for this analysis and for the sensitivity analysis are summarized in cumulative pdf for methane emissions (in g m^{-2} rice season^{-1}) in Figure 4.2c. For comparison, Figure 4.2 also contains the cumulative pdf of the original 553 samples. The underlying assumption is that the variance and distribution expressed in the pdf of the original data is representative for the real variance and distribution in methane emissions. The means of interpolated methane emissions were not significantly different from the emissions calculated from the original data (P<0.05). Mean methane emission could thus be described by interpolated soil properties. Spatial heterogeneity in methane emissions, however, was poorly described by interpolated soil properties, as is shown by the significant difference in a F-test (P<0.001) for all interpolation procedures.

This significant difference is caused by changes in OC (Figure 4.2a) or Fe (Figure 4.2b) by interpolation. The pdf of OC is not significantly affected by interpolation (P<0.01) as shown by t-tests and F-tests. The effects of interpolation on the estimation of Fe are much larger (Figure 4.2b) as might be expected from the poor cross validation results (Table 4.3). Both the variance and the mean of the underlying population were significantly different for all interpolated results compared to the original data, as shown by a F-test (P<0.001) and t-test (P<0.05), respectively. Changes in Fe values are thus probably the reason for the significant difference found for methane emission.

The sensitivity analysis showed no significant difference in either soil organic carbon or soil iron content between different interpolation procedures. The spatial heterogeneity in methane emissions was however significantly different for the different interpolation procedures (P<0.05).

a   b

c
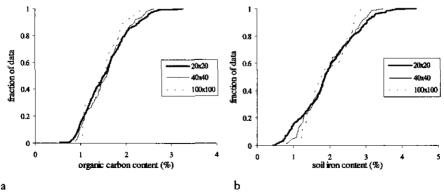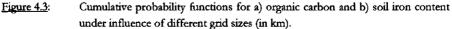
<u>Figure 4.2</u>:   Cumulative probability density functions (pdf's) for a) organic carbon, b) soil
                    iron content and c) methane emission under influence of different decisions
                    made for interpolation of soil properties.

4.3.2 Data resolution effects
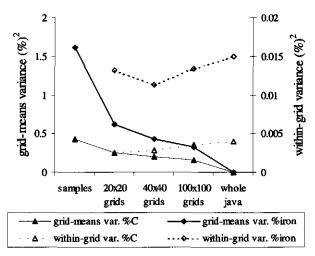
Soil parameter data resolution

Effects of data resolution on OC and Fe are summarized in cumulative pdfs (Figure 4.3).

a   b

<u>Figure 4.3</u>:   Cumulative probability functions for a) organic carbon and b) soil iron content
                    under influence of different grid sizes (in km).

Data resolution effects on these soil properties are very small. The variance and mean of the pdf's obtained for 20x20 km grid cells is not significantly different from the variance and mean for 40x40 or 100x100 grid cells (P<0.05), as shown by F-tests and t-tests.

<u>Figure 4.4</u>:   Development of the within-grid variance and the grid-means variance for organic carbon (%C) and soil iron content (%iron) as a function of data resolution. Note the different scales.

On the other hand, there are differences in the variances at different data resolutions, as is shown for the changes in within-grid variances and grid-means variances with data resolution (Figure 4.4). As grid sizes increase, the mean within-grid variance increases only slightly, indicating that the accuracy of the prediction in one particular grid slightly decreases with a coarser data resolution. The effects might have been small, because a constant (optimal) number of neighbours was considered at each data resolution. The effects on the variance of grid-means were much larger. About half of the variability in the soil property values was lost from the original samples to the first grid size due to interpolation (Figure 4.4). The large smoothening effect of interpolation might be another reason for the small changes in within-grid variances of the soil properties. Variance of grid-means decreases further with increasing size of the grids. Similar data resolution effects were found by Bouma et al. (1996) for nitrate leaching.

Methane emission data resolution

The blockkriged values for OC and Fe at the different grid sizes were used as input for the methane emission model. Calculated methane emissions (in $g\ m^{-2}$ rice season^{-1}) were used to construct a cumulative pdf at each data resolution (except for 'whole Java'). These pdf's were compared to the cumulative pdf of the original 553 samples (Figure 4.5) and tested for significant differences in variance (by a F-test) and in means of the underlying populations (by a student's t-test). Again, the variance at all data resolutions was significantly different from the variance described by the original data (P<0.001). Means of methane emissions at different data resolutions were only significantly different from emissions calculated from the original data at 100x100 km grids (P<0.05). The

mean of the pdf of methane emissions obtained for 20x20 km grid cells was not significantly different from the mean for 40x40 or 100x100 grid cells (P<0.05). Variances for 20x20 km grid cells were however significantly different from those for 40x40 and 100x100 grid cells (P<0.05), as shown by F-tests and t-tests.
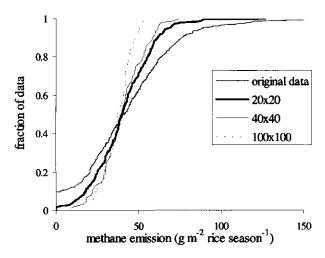
Figure 4.5:   Cumulative probability density functions (pdf) for methane emissions under influence of different data resolutions (in km) compared to a cumulative pdf based on model calculations of original data.

The spatial variance of methane emission estimates could not be analysed via the calculation of within-grid variances as was done for OC and Fe. The changes in methane emission estimates with data resolution can however be visualised spatially with a GIS representation (Figure 4.6). For that purpose, calculated methane emissions (in g m^{-2} rice season^{-1}) were multiplied with the total harvested area of rice in a grid and corrected for the total grid area to obtain methane emissions in g m^{-2} land year^{-1}. Total harvested areas for Java were constant for all data resolutions. Such a correction for harvested area does not affect the results of the statistical analysis shown above.
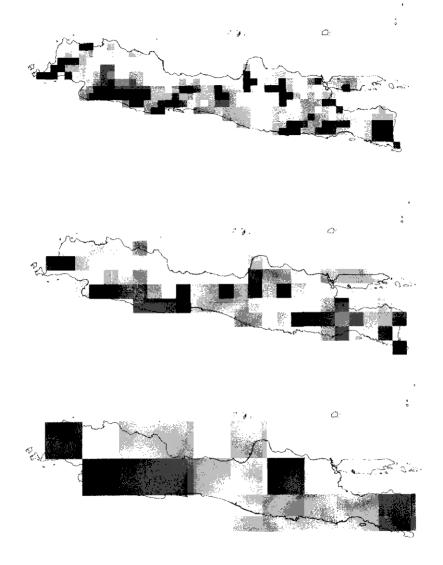
Figure 4.6 shows that there are clear changes in methane emission patterns with data resolution, even though the mean methane emission for Java does not change significantly with data resolution. So, information on the spatial variability of methane emissions is lost under influence of data resolution. However, the effects of interpolation on estimated methane emissions were larger - but harder to validate due to the lack of area averaged methane emission measurements - than the effects of data resolution.

4.4 Discussion
Methane emission estimates
The influence of upscaling soil samples to area averaged soil properties to calculate area averaged CH$_4$ emission estimates is summarised in Table 4.7. The CH$_4$ emission estimates presented in Table 4.7 do not present the actual CH$_4$ emission from rice fields on Java, because only spatial variability in soil properties was considered, taking average values for all other parameters.

methane emissions

g/m2/season

0 - 15		45 - 60		90 - 105	
15 - 30		60 - 75		105 - 120	
30 - 45		75 - 90		120 - 135	
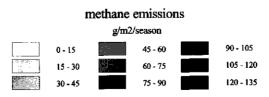
<u>Figure 4.6</u>: Effects of data resolution on the estimate of methane emissions, expressed in g CH_4 m^{-2} rice season^{-1}, for Java with a) 20x20 km grids, b) 40x40 km grids and c) 100x100 km grids

A realistic actual emission estimate should also consider other data sources, including other sources for soil data, as different data sources may change the outcome (unpublished results, van Bodegom et al.). Such an estimate should also account for spatial and temporal variability in e.g. climate, cropping areas, organic amendments and water management. In this study, those influences were intentionally not accounted for as it would obscure scaling effects under influence of variability in soil properties.

Table 4.7:   Emission estimates for Java using different methods.

	Methane emission (g m^{-2} rice season^{-1})		Emission Java (Tg)
	average	Standard deviation	Average
Original samples	43.21	28.95	-
Interpolation (20x20 grids):			
Other semivariogram	40.53	17.89	1.983
12 neighbours	40.35	15.79	1.985
Optimal kriging	40.51	17.97	1.983
Data resolution:			
20x20 grids	40.51	17.97	1.983
40x40 grids	40.44	13.89	2.027
100x100 grids	38.27	8.47	2.067
Whole Java	34.72	0	1.781

Scaling effects on soil properties were small. The effects of both interpolation and data resolution on OC were not significant. For Fe, only interpolation effects were significant and data resolution effects were not significant (compare Figures 4.2 and 4.3). For methane emissions, however, scaling effects were considerable. A significant effect of interpolation on variance could be shown (at $P<0.05$) and effects of data resolution on methane emissions were larger (up to 12%) than effects of data resolution for both OC and Fe (up to 3%). Variance of methane emissions calculated from the original soil samples was significantly different ($P<0.05$) for all interpolated methane emission estimates at all data resolutions. Moreover, mean methane emission calculated at 100x100 km grids (which is comparable to the grid size normally applied in upscaling of global methane emissions) was significantly different ($P<0.05$) from the mean methane emission calculated from the original data. Under influence of scaling effects, data resolution has a different influence on methane emissions in g m^{-2} rice season^{-1} than on total methane emission (in Tg), although the total amount of rice area was constant for all data resolutions. This is especially due to loss of information on spatial heterogeneities (Figures 4.5 and 4.6), through which high methane emissions are allocated to different sites with a different amount of rice area present at different data resolutions.

Interactions between model and data
Probably, these significant scaling effects are caused by the interaction between the interpolated data and the non-linear model. The original data represent point samples and had to be area averaged -interpolated- to allow regional estimation. Interpolation always implies some loss in accounted variability as is clearly shown in Figure 4.2 and Table 4.7. The effects of alternative assumptions in kriging were not significant and will

not be discussed further. The interpolated soil properties were coupled to a model, which also leads to a loss in accounted variability as models describe general trends only. Modelled methane emissions respond non-linearly to underlying soil properties. This response highly depends on the other conditions present (Chapter 3). In the case of Java, methane emissions are almost independent of soil organic carbon in the lower range and changes in soil iron content led to a more than linear change in methane emission (Figure 4.7). The extremes (e.g. hot spots) behave thus differently than the average, while spatial information on these extremes is lost by interpolation and modelling (Figure 4.6). This will automatically lead to scaling effects.

a   b
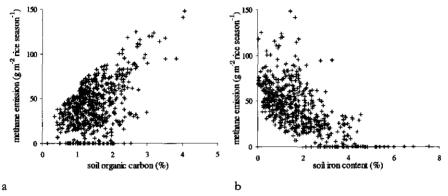
Figure 4.7:   Model estimation of methane emissions under influence of a) soil organic carbon and b) soil iron content

In spite of this, scaling effects on mean emissions were quite small. That is because mean methane emission estimates are influenced by an additional factor, i.e. the significant correlation ($P<0.006$) between soil iron content and organic carbon in the Java soil samples. It seems that this correlation counteracted the scaling effects due to interpolation and data resolution. Whether this applies for scaling effects in areas with soils from a completely different origin and/or different farmer's management remains to be seen. Scaling effects may be situation dependent and, more specifically depend on data distribution, correlations between data and relations between underlying processes that control the entity to be predicted (in our case CH_4 emission).

Small-scale variability
The initial scale of the analysis was determined by the distance between the soil samples and was much larger than the size of individual rice fields. Thus detailed scale variability in soil properties is not accounted for, but variability in methane emissions at detailed scales can be substantial. At the scale of individual rice plants, methane emissions showed a coefficient of variation (CV) of 44% (Denier van der Gon and Neue, 1996). However, this variability is most likely due to variation in plant properties and not soil properties, because all plants were grown in sieved, homogenized soils from the same field. At the scale of a single plot with the same management, soil property variability is an important variable that explains the observed variability with CV's typically ranging from 7-30% (Denier van der Gon and Neue, 1995a) with extremes up to 80%

(Wassmann et al., 1996b). Between farms in the same area, management can be different which may lead to additional variabilities at that scale. Such field to field variation in methane emission from rice paddies was found by Khalil et al. (1998b) in China, a country with many different rice cropping and organic carbon management patterns even at the local scale. So, variability will be present below the scale of our analysis and therefore not all variability could be captured in our study. This might explain the significant differences between interpolated soil properties and the original soil samples, independent of the assumptions made in the interpolation. Since only interpolated data could be used for further analysis, small-scale variability could not be accounted for in the determination of scaling effects. The full scaling effects of methane emissions may thus have been underestimated.

However, on Java, farmers' management might have levelled off small-scale variability (see section 3.1). The unexplained (smaller-scale) variability for OC and Fe was only about 30% of the total variance and the overall variability in OC and Fe could be accurately described by semivariograms. We do thus not expect small-scale variability to be dominant for Java.
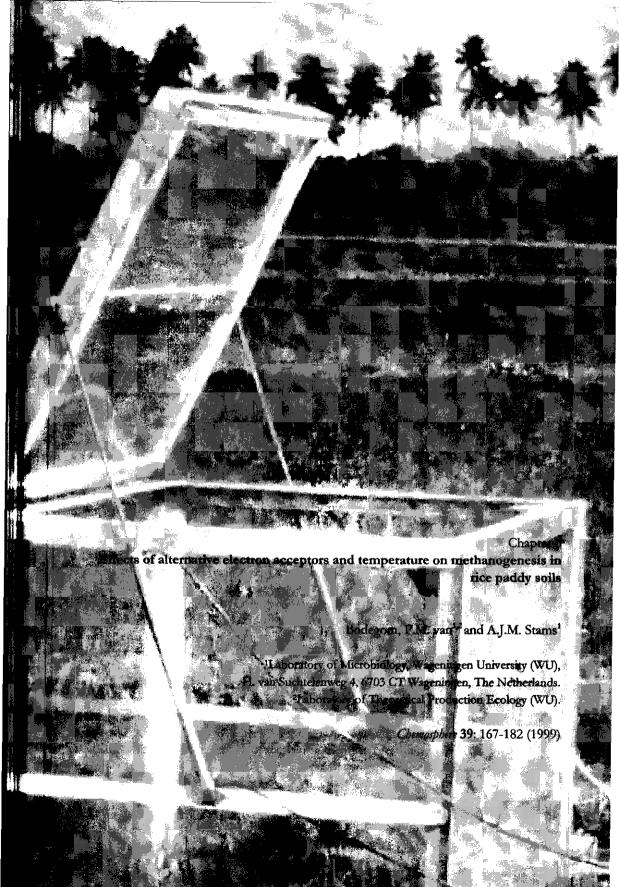
4.5 Conclusions

Clear scaling effects of interpolation and data resolution on means and variance of methane emissions were observed. These scaling effects were larger for methane emissions than for the underlying soil properties, OC and Fe, due to the non-linear model response to these properties. In this study the scaling effects were significant, but small, because soils on Java are relatively homogeneous and because correlations between soil properties smoothened some scaling effects. This coincidence makes Java suitable for upscaling of methane emissions from small scale to regional scale based on point data with a limited and acceptable increase in uncertainty in the final emission estimates.

Scaling effects may have been underestimated because small-scale variability was not accounted for, but in the case of Java this is not expected to change the findings dramatically. However, it is recommended that scaling effects on CH_4 emissions and on parameter values of underlying processes at scales below 20x20 km are also studied in the future to verify this. The combination of studies on scaling effects at small to regional scales in different rice growing countries with different parent material and/or rice agricultural practices may produce unbiased global methane emissions estimates from rice paddies.

Acknowledgements

Effects of alternative electron acceptors and temperature on methanogenesis in rice paddy soils

Bodegom, P.M. van[1,2] and A.J.M. Stams[1]

[1]Laboratory of Microbiology, Wageningen University (WU),
H. van Suchtelenweg 4, 6703 CT Wageningen, The Netherlands.
[2]Laboratory of Theoretical Production Ecology (WU).

between methanogens and bacteria that use alternative electron acceptors is a major uncertainty in the prediction of methane production.

The quantification of this competition is the objective of this paper. For this purpose, an incubation experiment was performed at different temperatures by measurement of the various electron donor and electron acceptor concentrations. From a comparison of the produced CO_2 and the CO_2 calculated from the reduction of all measured electron acceptors, it was possible to determine whether these inorganic electron acceptors are the most abundant electron acceptors in a rice paddy.

5.2 Materials and methods

Monitoring processes in the anoxic paddy soil

Soil was collected from the topsoil of paddy fields in Hangzhou (China). Twelve samples were mixed, air dried without grinding or sieving for 24 hours, transported to the Netherlands and stored for one week at 10°C. The moisture content of the soil was determined gravimetrically by oven-drying. It was 10% w/w and was thus low enough to avoid major changes in the soil during storage. Soil slurries were prepared in 1 litre serum bottles by mixing 250 ml sterilized distilled water with 100 g d.w. homogenized soil. The bottles were closed with butyl rubber stoppers. The bottles were repeatedly (6x) evacuated and flushed with N_2 gas to a final gas pressure of 150 kPa. The anoxic slurries were incubated in the dark in duplicate at three constant temperatures (14 ^{0}C, 20 ^{0}C and 30 ^{0}C). Additionally, a slurry with 3.75% v/v formaldehyde was prepared at each temperature to determine the abiotic release of CO_2. All bottles were continuously gently shaken to avoid concentration gradients in the soil slurries.

The changes in the slurries were monitored daily. Slurry samples of 1 ml were taken by N_2-flushed syringes for analysis of fatty acids, Fe^{2+}, NO_3^-, SO_4^{2-} and pH-H_2O. The samples were centrifuged for 5 min at 13,000 rpm and the supernatant was stored (after additional treatment, see below) at -20°C until analysis. For Fe^{2+} analysis, the soil pellet was resuspended in a 1M $CaCl_2$ solution and shaken for 1 hour to obtain the amount of adsorbed Fe^{2+}. After centrifuging the sample for 5 min at 13,000 rpm, this supernatant was collected and stored at -20°C until analysis. The headspace was sampled at the same time as the liquid phase with 1-ml syringes and analysed for CH_4, H_2 and CO_2. The monitoring frequency was decreased at the end of the experiment when changes were slower. The experiment was stopped when CH_4 production equalled CO_2 production.
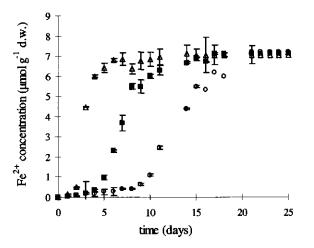
Analytical techniques
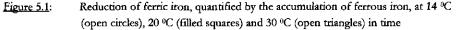
Formate and lactate were detected on an HPLC with an Ionpac AS6-SC column connected to a suppressed conductivity detector using 0.4 mM heptofluorbutyrate at 1 ml/min as an eluent. Acetate, propionate and butyrate were determined by gas chromatography, using a Chromosorb 101 column saturated with formic acid at 160°C, connected to a flame ionisation detector (FID). Prior to analysis the samples were diluted 1:1 with 1 M formic acid containing 1 mM isobutyric acid as internal standard. No other fatty acids appeared to be present in the soil slurries, because no other peaks were detected.

For Fe^{2+} analysis, both samples were stored after addition of the metol reductant solution (Walinga et al., 1995) to avoid reoxidation of Fe^{2+}, which might otherwise occur quickly after exposure to O_2. The Fe^{2+} in the liquid phase and the desorbed Fe^{2+} were analysed

colorimetrically with phenanthroline as reagents (Walinga et al., 1995). The absorbance was measured at a wavelength of 515 nm. Total Fe^{2+} is equal to the sum of Fe^{2+} in the two samples.

The supernatants for anion analysis were diluted 5:1 with a solution of 20 mM mannitol and 60 μM potassium bromide, as an internal standard. Inorganic anions were determined on an HPLC equipped with suppressed conductivity detection. Anions were separated on an Ionpac AS9-SC column using a 1.8 mM bicarbonate/1.7 mM carbonate eluent at 1 ml/min. Sulphide was determined as described by Trüper and Schlegel (1964). CH_4 was analysed by GC on a molecular sieve column at 70°C, coupled to a FID. H_2 was analysed on a molecular sieve column at 100°C coupled to a thermal conductivity detector (TCD). CO_2 was analysed on a Poropak Q column coupled to a TCD. The amounts of the different gases were quantified using standard curves obtained by injecting known amounts of gases.

Figure 5.1: Reduction of ferric iron, quantified by the accumulation of ferrous iron, at 14 °C (open circles), 20 °C (filled squares) and 30 °C (open triangles) in time

5.3 Results

In this incubation experiment we measured chemical species dynamics occurring under anaerobic conditions in a soil slurry at three temperatures (see Figures 5.1 to 5.3). During the anaerobic incubation NO_3^- was reduced first, followed by Fe^{3+} (Figure 5.1) and SO_4^{2-} (Figure 5.2). At the end of the incubation methane production (Figure 5.3) dominated. The reduction of NO_3^- is not shown separately, because under all conditions NO_3^- disappeared during the first day. During this period none of the other reduction processes started. The next reduction process, Fe^{3+}-reduction, was of quantitative importance. During this reduction process, CH_4 production and sulphate reduction contributed to less than 10% of the CO_2 production. The next step in the reduction sequence was not exclusive as SO_4^{2-}-reduction and CH_4-production occurred simultaneously, as can be seen from Figures 5.2 and 5.3. As long as sulphate was present, methane production rates were lower than when sulphate was absent. At the end of the incubation methane production was the dominating process in the slurry.
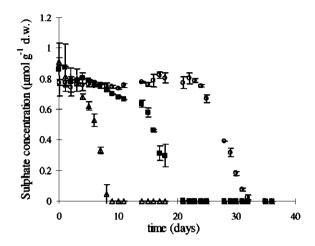
Figure 5.2:   Reduction of sulphate at 14 °C (open circles), 20 °C (filled squares) and 30 °C
              (open triangles) in time
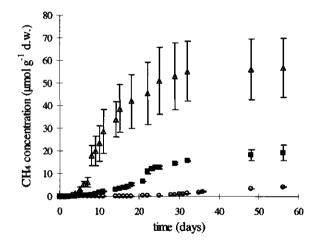
Figure 5.3:   Methane production at 14 °C (open circles), 20 °C (filled squares) and 30 °C
              (open triangles) in time

The incubation experiment was carried out at different temperatures. Therefore, it was possible to calculate the temperature dependence of the processes, which was expressed in a Q_{10} value. This parameter indicates the increase in reaction rate with a temperature increase of 10°C. The Q_{10} value of the processes was calculated from the slopes of the concentrations of the chemical species at different temperatures over time. For the calculation of this value only the phase in which the concerning process was dominant, was used. The rates of change at this phase at different temperatures were compared directly. This avoided that non-linear interactions due to the complex series of

degradation pathways and reduction sequences had major influences on the estimated values of Q_{10}.

The Q_{10} value for soil mineralisation (determined by CO_2 and CH_4 release) was 2.2, for iron reduction 2.4, for sulphate reduction 1.6, and for methane production 4.6. This means that, from 14 °C to 30 °C, methane formation rates increased 5.4 times as fast as sulphate reduction rates. The competitive-ness of the different microbial groups thus changed with temperature. We were only able to detect this temperature effect because acetate, which had accumulated during the first phase of the incubation, could be used at an accelerated rate at the onset of methanogenesis (Figure 5.4). If there had been no accumulation of acetate, the Q_{10} for methanogenesis would have been, per definition, equal to the Q_{10} of soil mineralisation.

a   b

c
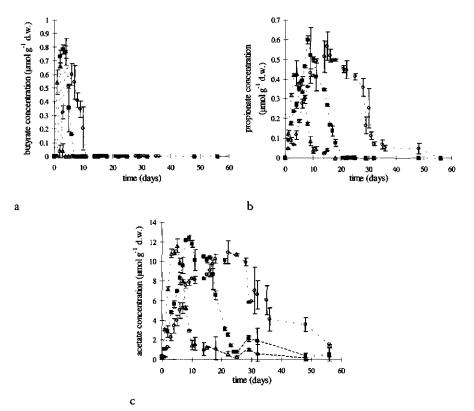
Figure 5.4:   Accumulation of intermediate fatty acids over time at 14 °C (open circles), 20 °C (filled squares) and 30 °C (open triangles) for (a) butyrate, (b) propionate and (c) acetate. Note the different scales at the y-axis.

To quantify the relative importance of the different electron acceptors, all reduced compounds were expressed in equivalents CO_2 (Figure 5.5). This is the amount of CO_2 produced by the metabolic reactions utilizing the measured electron acceptors and acetate as electron donor, assuming that acetate was the dominating electron donor. Figure 5.5 illustrates the reduction sequence discussed above.

The sum of all CO_2 equivalents was used to calculate a CO_2 balance to determine whether all important electron acceptors had been measured. For this purpose, the CO_2 equivalents calculated from the measured inorganic electron acceptor concentrations (indicated as 'total calculated CO_2 equivalents' in Figure 5.6) were compared to the net measured CO_2 (indicated as 'net measured CO_2 equivalents' in Figure 5.6). The net measured CO_2 production is the measured amount of released CO_2 corrected for abiotic CO_2 release (accounting for less than 1% to the total CO_2 release) and CO_2 released after accumulated intermediates (fatty acids and H_2) have decomposed. The slopes of the CO_2 accumulation curves decreased over time, indicating a decrease in mineralisation rates over time.
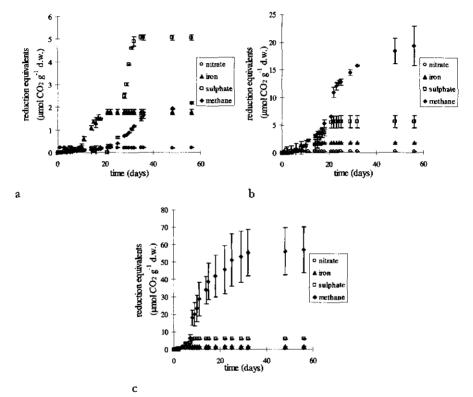
Figure 5.5:   Reduction sequence in the anaerobic rice paddy at (a) 14 °C, (b) 20 °C and (c) 30 °C over time. All reduced compounds were expressed in equivalents CO_2 to facilitate comparison of relative amounts

Comparison of the two series of data points in Figure 5.6 shows that almost all released CO_2 could be explained with the measured inorganic electron acceptors. At the start of the experiment a small difference between the two data series in Figure 5.6 occurred. This could mean that an alternative electron acceptor had not been accounted for. The difference between the two data series decreased over time.
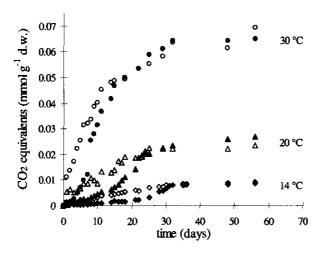
Figure 5.6:   Comparison of two methods of calculating cumulative CO_2 production for the incubation experiment. Filled symbols represent total calculated CO_2 equivalents and empty symbols represent net measured CO_2 equivalents. Each data point represents the average of two replicates

5.5 Discussion

Reduction sequence

In this incubation study, oxygen had been removed by flushing the bottles with N_2 gas. In reality, however, oxygen is the first compound to be reduced. Therefore, the effects of oxygen on methane production will also be discussed briefly based on published data. Methanogenic activity is inhibited in the presence of oxygen (Denier van der Gon and Neue, 1996). This is a combined effect of specific inhibition and competition for the electron donor. Aerobic heterotrophic bacteria are stimulated by the presence of oxygen and will compete for the available electron donor with methanogens and other anaerobic bacteria. Specific inhibition was shown in experiments carried out with pure methanogenic cultures (Fetzer and Conrad, 1993): Methane production was (partly) inhibited at oxygen concentrations higher than 0.05% O_2. Using a Henry's constant of 773 atm mol^{-1}l for O_2 at 25 °C, it can be calculated that this threshold level coincides with an oxygen concentration of 0.65 µM. As long as oxygen concentrations are above this level, methanogenesis will be completely suppressed. This effect is of importance, because such microaerophilic conditions can easily occur in a rice paddy (Frenzel et al., 1992). This low threshold concentration means, for instance, that methane production is restricted within the rhizosphere. Steep gradients of methane near the root surface could be the result of this.

Nitrate was the second compound to be reduced in our study. Nitrate reduction is however not of quantitative importance, because the pool size of nitrate was very small and all nitrate was reduced within a few hours. This is in accordance with data found for other soil systems (Achtnich et al., 1995a; Westermann and Ahring, 1987). Nitrate reduction will therefore be neglected in the further discussion of the results.

Fe^{3+}-reduction started some time after all nitrate had been reduced. This might indicate that Fe^{3+}-reduction was inhibited by an alternative electron acceptor that we did not measure or that the activity of the ferric-iron reducers had a small lag time as a consequence of the changed soil conditions during soil transport and storage. The Fe^{3+}-reduction was of quantitative importance and CH_4 production was suppressed almost completely during Fe^{3+}-reduction. Ferric-iron reducers are able to utilize acetate and H_2 concentrations far below levels that can be metabolised by methanogens or sulphate reducers (Lovley and Phillips, 1986; 1987). Only under conditions at which the amount of acetate and H_2 is not limiting, methanogenesis and ferric-iron reduction can occur simultaneously. Lovley and Phillips (1986) did not find a direct toxic effect of Fe^{3+} on methanogenesis and there are no inhibition effects of redox potential on methanogenesis (Fetzer and Conrad, 1993). Lovley and Phillips (1987) therefore concluded that competition for acetate and H_2 rather than a direct toxic effect of Fe^{3+} caused the suppression of methanogenesis. Michaelis-Menten kinetics for acetate could, however, not completely explain the extent of suppression of methanogenesis and sulphate reduction found in our study. This might indicate that at the start of the incubation, competition occurred for H_2 rather than for acetate. Roy et al. (1997) showed that at the start of an incubation of rice soil slurry the methanogenic population was dominated by hydrogenotrophic methanogens.

Sulphate reduction and methanogenesis occurred simultaneously, while methane production rates increased as sulphate concentrations decreased. This is in accordance with results of other studies (Achtnich et al., 1995b; Jakobsen et al., 1981; Westermann and Ahring, 1987). In general, a decrease in methanogenesis depends on environmental conditions. It has been found that direct toxic effects of sulphides were small (Kristjansson et al., 1982; Winfrey and Zeikus, 1977), and in this study soluble sulphide concentrations were below the detection limit, probably due to iron-sulphide precipitation. The low methane production in the presence of sulphate in the incubation experiment was probably caused by competition for organic carbon. Ratios of organic matter to sulphate have a large influence on the competition between sulphate reducers and methanogens (McCartney and Oleszkiewizc, 1993; Sinke et al., 1992). It has been found that if sulphate is in excess, sulphate reducers can outcompete methanogens for organic carbon (Schönheit et al., 1982; Visser et al., 1993), while at low sulphate concentrations different types of sulphate reducers compete for the available sulphate (Oude Elferink et al., 1994).

Temperature-dependent competition between methanogens and sulphate reducers

Competition between sulphate reducers and methanogens for electron donors was influenced by temperature. A comparison of the Q_{10} values for methanogenesis and sulphate reduction shows that CH_4 formation was favoured at higher temperatures. Westermann and Ahring (1987) also found higher Q_{10} values for methanogens than for sulphate reducers. The observed Q_{10} for methanogenesis is considerably different from a Q_{10} of 2, which is often expected for biological systems. Due to this high Q_{10} value for methanogenesis, not merely the conversion rates, but also the competitiveness of the microorganisms changed with temperature. A mechanistic explanation for this temperature effect is difficult, the more so as two different substrates, acetate and H_2, are involved. Based on the simplified schematic representation given in Figure 5.7, possible

explanations can be given. The basis of this figure is the competition for H_2 between sulphate reducers, methanogens and homoacetogens and the competition for acetate (which might partly be produced by homoacetogens) between methanogens and sulphate reducers. Syntrophic interactions between sulphate reducers and methanogens, e.g. the consumption of acetate that inhibits metabolic activities at high concentrations, are not expected as acetate concentrations were too low to be inhibiting (Fukuzaki et al., 1990). The temperature influence on the competition processes should therefore be understood to explain the difference in Q_{10} values.
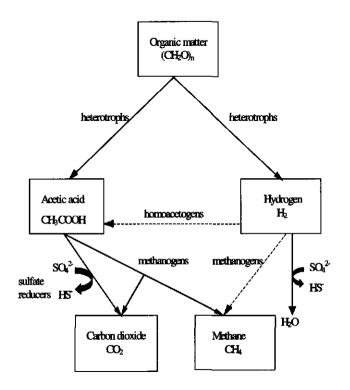
Figure 5.7: Schematic representation of the competition between sulphate reducers and methanogens for the available substrate

Sulphate reducers have a lower K_M value for H_2 than methanogens (Kristjansson et al., 1982), and can therefore maintain lower steady-state H_2 concentrations than methanogens (Achtnich et al., 1995a). In this study H_2 levels were usually below the detection limit, which was 25 ppmv. Achtnich et al. (1995b) showed that H_2 concentrations are higher if methane is produced from H_2. It is therefore unlikely that methanogens were able to win the competition for H_2 with sulphate reducers in our study. The conversion from H_2 to CH_4 in Figure 5.7 can thus be neglected.

The differences in K_M values for acetate between sulphate reducers and methanogens are much smaller. Schönheit et al. (1982) found that competition for acetate occurred

between 0.1 and 3 mM acetate. In situ concentrations of acetate are usually in this range (Achtnich et al., 1995b; Rothfuss and Conrad, 1993). In our incubation acetate levels varied from 0.5 to 3.5 mM. Active competition between sulphate reducers and methanogens for acetate therefore occurred in this incubation experiment, while the methanogens were outcompeted for H_2. Ueki et al. (1992) and Visser et al. (1993) found no acetoclastic sulphate reducers in some situations, while under the same conditions competition for H_2 took place between sulphate reducers and methanogens. In our soil system the temperature effects may be explained by a change in the competition for acetate with temperature, because the competition for H_2 was dominated by sulphate reducers at all temperatures.

Homoacetogens produce acetate from H_2, so this may affect the amounts of H_2 and acetate available for methanogenesis. In the absence of sulphate reducers, methanogens and homoacetogens compete for H_2. The amount of H_2 converted to acetate by homoacetogens varies between 7-70% (Chin and Conrad, 1995; Krumböck and Conrad, 1991; Rothfuss and Conrad, 1993), although the K_M for H_2 for homoacetogens is higher than for methanogens (Cord-Ruwisch and Ollivier, 1986; Cord-Ruwisch et al., 1988). This seems only possible if homoacetogens use H_2 mixotrophically (Dolfing, 1988; Schulz and Conrad, 1996). As a result more than 67% (valid for methanogenic systems (Gujer and Zehnder, 1983)) of the methane can be produced via acetate, namely 69-90%. This justifies a focus on fatty acids, of which acetate is the most abundant, in this study. The reasoning changes, however, if sulphate reducers are present. The K_M value for H_2 for homoacetogens is much higher than for sulphate reducers, and it has been found that homoacetogens are outcompeted completely in the presence of sulphate reducers in some situations (Cord-Ruwisch and Ollivier, 1986; Cord-Ruwisch et al., 1988). The homoacetogens are thus suppressed by sulphate reducers and will not be able to convert H_2 to acetate. Therefore homoacetogens could not have caused the observed temperature effect. The conversion from H_2 to acetate in Figure 5.7 can thus be neglected.

The high Q_{10} value of the methanogens may therefore be due to a competitive advantage of methanogens compared to sulphate reducers for acetate at increasing temperatures (bottom left in Figure 5.7). Such intrinsic temperature characteristics are known for pure methanogenic cultures (Schütz et al., 1990). These characteristics might be caused by either a larger increase in V_{max} or by a larger decrease in K_M for acetoclastic methanogens than for sulphate reducers with temperature. An increase in V_{max} can only be explained by an increase in the consumption capacity per unit biomass (Q_{max}), because it has been assumed that there was no net growth of methanogens during the incubation for reasons explained below. This also means that biomass is assumed to have been the same for all temperatures, because all samples came from the same slurry. How Q_{max} changes with temperature is not known. A somewhat higher temperature dependency of Q_{max} for methanogens than for other organisms might be expected, because the energy yield for methanogenesis is very low. Westermann et al. (1989) showed that K_M values for methanogens can change considerably with temperature. Chin and Conrad (1995) showed that the ΔG^0_T for acetoclastic methanogenesis became more negative with increasing temperatures. Based on theoretical considerations, one might therefore expect a decreasing K_M for acetoclastic methanogenesis with increasing temperatures. Based on the Van 't Hoff equation and the ΔH values given in (Thauer et al., 1977) sulphate

reducers are expected to have K_M values that will increase with increasing temperatures. Due to these possible differences in kinetic characteristics, methanogenesis may have gained importance as temperature increased. This might explain the observations.

It should also be noted that this temperature effect was found for different, but constant, temperature treatments. In environments with rapidly changing temperatures, all other factors being equal, organisms with the highest net growth rate and thus the best survival will win the competition. Cappenberg (1975) found that sulphate reducers won the competition at high organic carbon concentrations. At low organic carbon concentrations methanogenic biomass increased faster. In our study it was however assumed that there was no net growth of these bacteria. The effects of biomass growth will thus have been small.

The first argument for this assumption is that the time at which the limitations for methanogenic activity disappeared (indicated by an exponential increase in CH_4 concentrations) did not coincide with an accumulation of fatty acids. Fatty acids should, however, accumulate specifically in this period if methanogenic biomass had been limiting. Instead, the maximum fatty acid accumulation occurred earlier, around the onset of methanogenesis and sulphate reduction (Figure 5.7). This might indicate that the accumulation of fatty acids occurred due to the inhibition of these two processes by iron reducers.

Other arguments against net methanogenic growth as an important factor are: i) The transition from exponential accumulation of CH_4 to a linear accumulation of CH_4 occurred as soon as all SO_4^{2-} had disappeared (Figure 5.3). This indicates that the activity limitation was due to competition or inhibition by the alternative electron acceptors. ii) Already after one day, some very small amounts of CH_4 had been produced. Thus, the onset of CH_4 production apparently does not depend on growth and significant increase in numbers of methanogenic bacteria. iii) It was found by Mayer and Conrad (1990) that the number of viable methanogenic bacteria that was present in a dry and oxic paddy soil before submergence was as high as during active methanogenesis. iv) Schütz et al. (1989b) measured no change in the number of methanogens in a rice paddy soil during the growing season. v) The biomass of methanogens was not affected by storage under O_2 atmosphere (Fetzer et al., 1993; Mayer and Conrad, 1990; Peters and Conrad, 1995).

The non-limiting amounts of biomass might explain why the steady-state concentrations of acetate were too low to be detected. This also means that the turnover rates of acetate were very high and not limiting. The response of the microorganisms to temperature (for instance diurnal fluctuations) should in that case be the same as we suggest in this experiment. Further investigation is needed to determine whether this effect is indeed enough to explain diurnal fluctuations in methane emissions.

CO₂ balance

A CO_2 balance that was calculated from the measurements showed that the released CO_2 could be explained nicely with the measured inorganic electron acceptors. An alternative electron acceptor that was missed might have caused the difference between the curves at the start of the experiment. Such an alternative electron acceptor can be either manganese or an organic electron acceptor (Lovley et al., 1996). This means that, contrary to peat soil (Lovley et al., 1996), organic electron acceptors may not be important in rice paddies. Presumably, this is caused by the lower soil organic matter

levels in rice paddy soils than in peat. The initial difference between the curves decreased in time. A possible explanation for this effect is an underestimation of the total CO_2 production from increasing activity by homoacetogens, converting CO_2 to acetate. After all sulphate had disappeared from the system, homoacetogens might have been able to compete for the H_2.

a   b

c
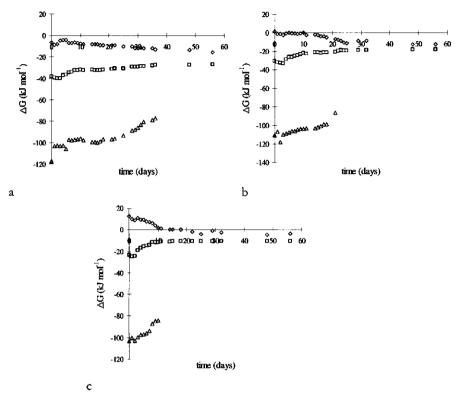
<u>Figure 5.8</u>:   Change in the Gibbs free energies (ΔG) for homoacetogens (diamonds), hydrogenotrophic methanogens (squares) and sulphate reducers (triangles) during the incubation at (a) 14 °C, (b) 20 °C and (c) 30 °C

Figure 5.8 shows that the Gibbs Free energy (ΔG) (based on ΔG^0 values obtained from Thauer et al. (1977), corrected for its temperature dependence by the Van 't Hoff equation) decreased for homoacetogens, while ΔG for methanogens and sulphate reducers increased (and sulphate concentrations decreased) in time. Conversion from CO_2 to acetate thus becomes more favourable over time. The resultant underestimation in CO_2 production might compensate for the underestimation in the calculated CO_2 released from the reduction processes, but this needs further investigation.

Figure 5.6 also revealed that mineralisation rates decreased in time. This is probably caused by a decrease in available carbon over time. Available carbon from aerobic mineralisation that had accumulated during the aerobic period, was released at the start of the experiment and induced the reduction processes. After a while, only less readily available carbon is mineralised. This also occurs in the field at the time of land

preparation. The change in mineralisation rates over time should therefore be taken into account when calculating methane emissions from initial methane production rates. The CO_2 release decreased further over time, because no further addition of organic matter occurred during the experiment. The change in soil mineralisation over time might provide an alternative explanation for the disappearance of the difference between the two curves in Figure 5.6. Less accessible carbon might not be described by the general formula $(CH_2O)_n$ that was assumed for the calculations. Consequently, less H_2 is produced causing an underestimation of the measured CO_2 equivalents.

5.6 Conclusions

It was shown that in anaerobic soil slurry from a rice paddy, first NO_3^- is reduced, followed by Fe^{3+} and SO_4^{2-} reduction and methane production. The first two steps in the reduction sequence were exclusive, while competition occurred between sulphate reducers and methanogens. The outcome of this competition was shown to be temperature-dependent, indicating that temperature not only influences conversion rates, but also the competitiveness of organisms. Most importantly, the CO_2 released could be explained with the measured inorganic electron acceptors, suggesting that organic electron acceptors do not seem to be important in rice paddies.

Acknowledgements

Microbial processes of CH$_4$ production in a rice paddy soil: model and experimental validation

Peter M. van Bodegom[1,2] and Johannes C.M. Scholten[3]

[1]Lab. of Theoretical Production Ecology, Wageningen University (WU),
P.O. Box 430, 6700 AK Wageningen, The Netherlands.
[2]Laboratory of Microbiology (WU), The Netherlands.
[3]Dep. of Biological Sciences, University of Warwick, Coventry, United Kingdom.

Microbial processes of CH$_4$ production in a rice paddy soil: model and experimental validation

Abstract

The importance of different anaerobic processes leading to CH$_4$ production in rice paddies is quantified by a combination of experiments and model. A mechanistic model is presented that describes competition for acetate and H$_2$/CO$_2$, inhibition effects and chemolithotrophic redox reactions. The model is calibrated with anaerobic incubation experiments with slurried rice soil, monitoring electron donors and electron acceptors influencing CH$_4$ production. Only the values for maximum conversion rates (V$_{max}$) for sulphate and iron reduction and CH$_4$ production are tuned. The model is validated with similar experiments in which extra electron donors or electron acceptors had been added. The differences between model estimates without kinetic parameter adjustments and experiment were not significant, showing that the model contains adequate process descriptions. The model is sensitive to the estimates of V$_{max}$, that are site dependent and to the description of substrate release, that drives all competition processes. For well-shaken systems, the model is less sensitive to chemolithotrophic reactions and inhibitions. Inhibition of sulphate reduction and methanogenesis during iron reduction can however explain acetate accumulation at the start of the incubations. Iron reduction itself is most probably retarded due to manganese reduction.

6.1 Introduction

In rice fields, small organic compounds become available by root exudation, root decay, organic fertiliser decomposition and soil organic matter mineralisation. Methane (CH$_4$) production is the terminal microbial process in anaerobic organic matter degradation in the absence of alternative electron acceptors like O$_2$, NO$_3^-$, Fe^{3+} and SO$_4^{2-}$. CH$_4$ production is suppressed directly or indirectly by the presence of alternative electron acceptors (e.g. Achtnich et al., 1995a; Jakobsen et al., 1981). This suppression seems to be caused by competition for common substrates, particularly H$_2$ and acetate, with microorganisms using alternative electron acceptors and by several direct inhibitions on CH$_4$ production caused by accumulated products of anaerobic respiring microorganisms. Quantification and significance of these processes for CH$_4$ production are a major uncertainty in CH$_4$ production prediction.

Due to complex interactions, it is difficult to obtain complete quantitative insight in all interactions by experiments alone, despite the fact that many experimental data are available. A combination of experimental data and a quantitative mechanistic model may lead to a better quantitative understanding of the interactions. In this paper, we present a new mechanistic model, calibrated and validated by experimental data. This model differs from other models in several important aspects: i) the model describes the conversions of frequently measured anaerobic alternative electron acceptors, in contrast to other models which summarise the alternative electron acceptors by one alternative electron acceptor (Segers and Kengen, 1998), neglect all alternative electron acceptors (Grant, 1998; Vavilin et al., 1994) or treat only SO$_4^{2-}$ (James, 1993; Lovley and Klug, 1986). ii) We

describe substrate competition by Michaelis-Menten rate expressions, which are more appropriate than first- or second-order rate expressions (used by Boudreau, 1996; van Cappellen and Wang, 1996) if different limitations occur in time or if saturation for a certain compound can occur. iii) In addition to competition effects, direct inhibitions due to alternative electron acceptors are introduced. These effects are usually neglected in competition descriptions (e.g. Gupta et al., 1994; James, 1993). iv) Contrary to e.g. Grant (1998) and James (1993), it is assumed that changes in microbial biomass are small. A constant biomass is taken, which simplifies model parameterisation and model extrapolation, because -scarce- data on mortality and growth of anaerobic bacteria are not needed. v) The model includes chemolithotrophic redox reactions. Omission of these reactions may cause overestimation of organic matter oxidation.

The objective of this paper is to obtain more quantitative insight in the significance of microbial interactions leading to CH_4 production in well-shaken incubation systems. A quantitative model is described, calibrated and validated by data from several incubation experiments. The model summarises mechanistic interactions between bacteria using alternative electron acceptors and CH_4 producing microorganisms. Transport descriptions are not included in the model, because it is applied to well-shaken systems only and the model cannot be used to predict field gradients (Hunter et al., 1998). Various aspects of the microbial interactions are discussed in more detail and quantified by model sensitivity analyses. These analyses also reveal gaps in knowledge.

6.2 Material and Methods
6.2.1 Model calibration
The model was calibrated using the experimental data of Chapter 5. In that study, soil slurries collected from rice paddies were incubated for 60 days at 14 $^{\circ}$C, 20 $^{\circ}$C and 30 $^{\circ}$C. CH_4 and CO_2 production, accumulation and degradation of intermediate fatty acids and changes in various electron acceptor concentrations were measured.

6.2.2 Incubation experiments for model validation
General experimental set-up
Soil was collected as described previously (Chapter 5). Soil slurries were prepared in 1 litre serum bottles by mixing 250 ml sterilised distilled water with 100 g d.w. homogenised soil. The bottles were closed with butyl rubber stoppers, were repeatedly (6x) evacuated and flushed with N_2 gas to a final pressure of 150 kPa. The anoxic soil slurries were incubated in the dark in triplicate at 20 $^{\circ}$C and 30 $^{\circ}$C, while shaken gently at 100 rpm. Additionally, slurries with 3.75% v/v formaldehyde were prepared in duplicate for each experiment to determine abiotic dynamics. All incubations were monitored daily for lactate, fatty acids, Fe(II), NO_3^-, NO_2^-, SO_3^{2-}, SO_4^{2-}, CH_4, H_2, NO, N_2O, CO_2, sulphide and pH-H_2O. Samples were taken as described previously (Chapter 5).

Short-term validation experiment with substrate additions
A validation incubation experiment was carried out for 20 days to test the effects of several substrate additions. The four treatments were the addition of 7.5 g/l rice straw (equivalent to 9 tons/ha) at day 3, addition of 15 mM acetate (below the inhibiting concentrations mentioned by Fukuzaki et al., 1990) at day 3, addition of 0.15 mmol H_2/l

(below the thermodynamically inhibiting concentrations) to the headspace at day 3, 5, 7, 9, 11 and 14 and a control treatment without additions.

Long-term validation experiment with sulphate addition
A validation experiment was carried out to test the effects of sulphate addition. Air-dried samples were incubated at 10 °C for 2 months, to decrease the amount of readily degradable carbon. Then, slurries were prepared and incubated for 60 days. In the first treatment 4 mM ammonium sulphate was added at day 0. The second treatment was a control without additions.

Short-term experiment on factors determining the lag phase for iron
Lag phases for iron reduction have been found to depend on temperature and pre-incubation conditions. It was hypothesised that an unmonitored electron acceptor, either humic acids or reducible manganese, caused this lag phase. Only the effects of reducible manganese were tested, because soil humic acid content was low. Soils incubated for 20 days were therefore monitored additionally for Mn(II). Both adsorbed and dissolved Mn(II) were extracted as described for Fe(II) in Chapter 5.

Analytical techniques
Lactate, fatty acids, Fe(II), NO_3^-, NO_2^-, SO_3^{2-}, SO_4^{2-}, CH_4, H_2, NO, N_2O, CO_2, sulphide and pH-H_2O were analysed as described in Chapter 5. No other low molecular weight organic acids could be detected in the soil slurries. In the short-term incubation on factors determining the lag phase for iron, reducible iron and reducible manganese were analysed by Inductively Coupled Plasma Atomic Emission Spectrometer (ICP-AES).

6.2.3 Model description
The model -summarised in Figure 6.1- describes the different microbial processes involved in anaerobic organic matter degradation in well-shaken soil slurries.

Substrate release
Basis of the model is the production of acetate and H_2/CO_2. These substrates are produced by soil organic matter mineralisation and by the decomposition of complex organic substances. This can be summarised by:

$$(CH_2O)_n + \frac{1}{3}nH_2O \rightarrow \frac{1}{3}nCH_3COOH + \frac{1}{3}nCO_2 + \frac{2}{3}nH_2 \tag{6.1}$$
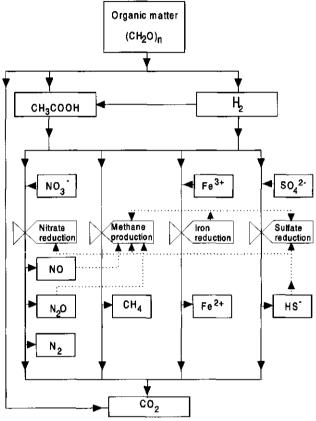
This reaction rate changes in time, because of decreases in easily accessible carbon. For a system that starts at the introduction of anaerobiosis (e.g. by the preparation of a rice paddy field after a dry fallow period), the reaction rate P_{min} can be described by (Yang, 1996):
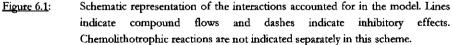
$$P_{min} = C_{min} \cdot (1 - S) \cdot K_d \cdot e^{-K_d \cdot time} \tag{6.2}$$

Where C_{min} is the -constant- soil carbon content (mol C m⁻³ water) and K_d is the relative decomposition rate, given by:

$$K_d = R \cdot time^{-S} \tag{6.3}$$

Where R (time^{S-1}) and S (-) are empirical parameters. More details about the parameters and parameter value determinations are described in Chapter 2. Rice straw decomposition is described by a similar set of equations, changing C_{min} into the amount of rice straw carbon. Substrate production from other sources, like root exudation, is not explicitly modelled, because such sources were absent in the calibration and validation experiments.

<u>Figure 6.1</u>:   Schematic representation of the interactions accounted for in the model. Lines indicate compound flows and dashes indicate inhibitory effects. Chemolithotrophic reactions are not indicated separately in this scheme.

Substrate competition

In the presence of alternative electron acceptors, methanogens have to compete for acetate and H_2 with anaerobically respiring microorganisms using NO_3^-, SO_4^{2-} and Fe(III) as electron acceptors. This competition is described by substrate conversion rates (V: mol m^{-3} water s^{-1}). For methanogens (m_i), substrate conversion is described by Michaelis-Menten kinetics:

$$V_{m_i} = Q_{\max,m_i} \cdot B_{m_i} \cdot \frac{[substrate]}{K_{M,m_i} + [substrate]} \tag{6.4}$$

where B is the microbial biomass (mol biomass m⁻³ water), Q_{max} is the specific microbial activity (mol mol⁻¹ biomass s⁻¹) and $K_{M,mi}$ is the affinity constant (mol m⁻³ water) while i is H₂ (hydrogenotrophic methanogens) and acetate (aceticlastic methanogens), respectively. The substrate conversion rates for the other anaerobic microorganisms ('e_i') is summarised by double Michaelis-Menten kinetics:

$$V_{e_i} = Q_{max,e_i} \cdot B_{e_i} \cdot \frac{[e^- donor]}{K_{M,d_i} + [e^- donor]} \cdot \frac{[e^- acc]}{K_{M,a_i} + [e^- acc]} \tag{6.5}$$

where $K_{M,d}$ and $K_{M,a}$ are the affinity constants (mol m⁻³ water) for the electron donor (e^- donor) and electron acceptor (e^- acc), respectively. Acetate and H₂ are electron donors and NO₃⁻, NO, N₂O, reducible iron and SO₄²⁻ are included as electron acceptors. All K_M values are summarised in Table 6.1. For iron the total reducible iron concentration is used and not the Fe(III) in the solution, thus assuming that ferric iron dissolution is not the rate-limiting step. Concentrations of gaseous compounds (NO, N₂O, CO₂, CH₄) are corrected for the equilibrium with the gas phase by Henry's law.

Microbial biomass changes are not included in the model. Arguments for a constant biomass for methanogens and bacteria using alternative electron acceptors are given elsewhere (Chapter 5; Asakawa et al., 1998; Segers and Kengen, 1998). The constant microbial biomass allows a simplification of Eq. (6.4)-(6.5):

$$Q_{max} \cdot B = V_{max} \tag{6.6}$$

where V_{max} is a potential conversion rate (mol m⁻³ water s⁻¹).

It is assumed that K_M values are independent of temperature, although both thermodynamic considerations (Chapter 5) and experimental data (Westermann et al., 1989) falsify this assumption. There are however not enough quantitative data to describe such changes with temperature. Temperature influence on V_{max} values is described using a Q_{10} value, indicating the increase in reaction rates at a temperature increase of 10 °C:

$$V_{max}(T) = V_{max}(T_{ref}) \cdot Q_{10}^{\frac{(T-T_{ref})}{10}} \tag{6.7}$$

where T_{ref} is the reference temperature, which is 30°C in this study.

In Table 6.1 the V_{max} values at the reference temperature are indicated for the microbial processes. This table presents the total V_{max}, which is the sum of conversions via acetate and via H₂. To avoid too many degrees of freedom in the model calibration, it is assumed that V_{max}(via H₂) = V_{max}(via acetate), because there are not enough published data that allow a further specification. Only for CH₄ production it is assumed that V_{max}(via acetate) is twice the value of V_{max}(via H₂). This assumption allows 70-80% of the CH₄ to be produced via acetate (compared to a theoretical 67%) (Chin and Conrad, 1995; Rothfuss and Conrad, 1993). Due to homoacetogenesis, a H₂/CO₂ to acetate conversion that mainly occurs after sulphate depletion (Chapter 5), aceticlastic methanogenesis is more important than hydrogenotrophic methanogenesis. By correcting the methanogenic V_{max} in this way, it is not necessary model homoacetogenesis explicitly. The competition outcome is completely determined by differences in V_{max} values, affinity constants and reactant concentrations.

Table 6.1:   Kinetic microbiological parameters used in this study at reference temperature - 30°C.

Reaction	K_M electron donors (mol m^{-3} H$_2$O)		K_M electron acceptor (mol m^{-3} H$_2$O)	$V_{max\ (total)}$ (mol ε acc m^{-3} H$_2$O s^{-1})
	acetate	H$_2$		
nitrate reduction	0.09 [1]	0.1*10^{-3} [6]	0.42 [12] (NO$_3$)	1.2 * 10^{-4} [15]
	0.09 [2]	0.1*10^{-3} [6]	5.93 [2] (NO)	8.6* 10^{-5} [2]
	0.09 [1]	0.1*10^{-3} [6]	5.93 [1] (N$_2$O)	8.6 * 10^{-5} [1]
iron reduction	0.23 [3]	0.22*10^{-3} [7]	61 [13] (Fe^{3+})	5.0 * 10^{-4} [*]
sulphate reduction	0.79 [4]	2.87*10^{-3} [8]	0.23 [14] (SO$_4$$^{2-}$)	0.8 * 10^{-5} [*]
methanogenesis	2.56 [5]	13.3*10^{-3} [9]	n.a.	2.0 * 10^{-5} [*]
Denitrification/ HS$^-$ oxidation	1.68 [10] (HS$^-$)		1.75 [10] (NO$_3$$^-$)	6.8 * 10^{-5} [16]
Denitrification/ iron oxidation	0.9 [11] (Fe^{2+})		3.6 [1] (NO$_3$$^-$)	1.1 * 10^{-5} [17]

product inhibition	Threshold concentration (mol m^{-3} H$_2$O)	Maximum concentration (mol m^{-3} H$_2$O)
HS$^-$ inhibition on NO$_3$$^-$ reduction	0.65 [18]	10 [18]
HS$^-$ inhibition on SO$_4$$^{2-}$ reduction	3.75 [19]	27.2 [19]
HS$^-$ inhibition on methanogenesis	3.46 [20]	13.7 [20]
N$_2$O inhibition on methanogenesis	6.3 * 10^{-2} [21]	0.21 [21]
NO inhibition on methanogenesis	1.8 * 10^{-3} [21]	0.01 [21]

[1]   Leffelaar and Wessel, 1988

[2]   Assumed to be equal to (1)

[3]   No data, estimated between K_M(SO$_4$) and K_M(NO$_3$) by thermodynamics (Conrad, 1996)

[4]   Brandis-Heep et al., 1983; Middleton and Lawrence,1977; Visser et al., 1996

[5]   Jetten et al., 1990; Powell et al., 1983; Zehnder et al., 1980

[6]   No data, estimated from thermodynamics using Conrad (1996)

[7]   Klüber and Conrad, 1993

[8]   Kristjansson et al., 1982; Lupton and Zeikus, 1984; Robinson and Tiedje, 1984

[9]   Kristjansson et al., 1982; Lupton and Zeikus, 1984; Robinson and Tiedje, 1984; Zehnder and Wuhrmann, 1977

[10]   Estimated from Brunet and Garcia-Gil, 1996

[11]   Estimated from Straub et al., 1996

[12]   Klemendtsson et al., 1977; Leffelaar and Wessel, 1988; Murray et al., 1989

[13]   Estimated from Achtnich et al., 1995a; Lovley and Phillips, 1986; Roy et al., 1998

[14]   Brandis-Heep et al., 1983; Ingvorsen et al., 1984; Middleton and Lawrence, 1977

[15]   Brunet and Garcia-Gil, 1996; Leffelaar and Wessel, 1988; Sweerts et al., 1990

[16]   Estimated from Bak and Pfennig, 1991; Brunet and Garcia-Gil, 1996

[17]   Estimated from Benz et al., 1998; Straub et al., 1996

[18]   Brunet and Garcia-Gil, 1996; Sørensen et al., 1980

[19]   McCartney and Oleskiewicz, 1993; Okabe et al., 1995; Visser et al., 1996

[20]   McCartney and Oleskiewicz, 1993; Visser et al., 1996; Winfrey and Zeikus, 1977

[21]   Balderston and Payne, 1976; Klüber and Conrad, 1998

[*]   Calibrated in this study

Chemolithotrophic redox conversions

Electron acceptor kinetics is complicated by the occurrence of chemolithotrophic redox conversions, occuring when inorganic compounds act as electron donor. Such conversions are included, but only two conversions occurring in freshwater systems could be quantified:

Coupled nitrate reduction to N_2/sulphide oxidation to sulphate (e.g. Dannenberg et al., 1992) is included and described by the following substrate conversion rate description:

$$V = V_{max} \frac{[HS^-]}{K_{M,HS} + [HS^-]} \cdot \frac{[NO_3^-]}{K_{M,NO_3} + [NO_3^-]} \tag{6.8}$$

Additionally, coupled nitrate reduction to N_2/iron oxidation to ferric iron (e.g. Straub et al., 1996) is described by the following description:

$$V = V_{max} \frac{[Fe^{2+}]}{K_{M,Fe} + [Fe^{2+}]} \cdot \frac{[NO_3^-]}{K_{M,NO_3} + [NO_3^-]} \tag{6.9}$$

The experiments were initiated under anaerobic conditions. Therefore, aerobic respiration and electron acceptor reoxidation by oxygen are not included in the model. The absence of aerobic respiration and the absence of transport limit the possibilities of above-mentioned chemolithotrophic conversions due to the lack of oxidised substrates.

Lag time and inhibition during iron reduction

In a previous study we observed a lag phase of a few days before iron reduction started (Chapter 5). Other incubation experiments (Achtnich et al., 1995a; Ratering and Conrad, 1998; Roy et al., 1997) also showed a slow start of iron reduction. This lag time cannot be explained from competition with nitrate reducers (results not shown). We therefore apply a fully empirical lag time for iron reduction as a function of temperature, based on experimental data (Chapter 5).

Sulphate reduction and CH_4 production were severely inhibited during iron reduction (Ratering and Conrad, 1998; Roy et al., 1997). Neither substrate competition (Ratering and Conrad, 1998) nor redox effects (Chapter 2; Ratering and Conrad, 1998) could explain this inhibition. Therefore, we postulate an empirical direct inhibition by iron on sulphate reduction and CH_4 production. This inhibition is described by a constant threshold reducible iron concentration above which no sulphate reduction or CH_4 production occurs.
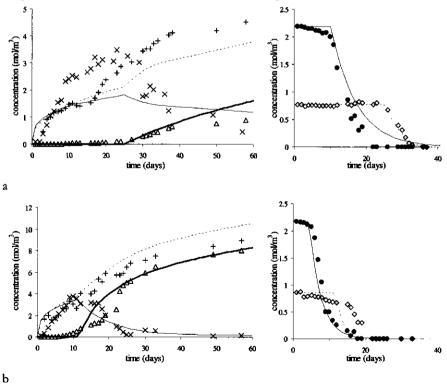
Direct inhibitions
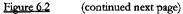
Direct inhibitions are inhibitory effects on CH_4 production caused by intermediates produced by anaerobic respiring microorganisms This inhibition is described by two parameters, a threshold concentration of toxic intermediates below which no inhibition occurs and a maximum concentration above which complete inhibition occurs.

Inhibition increases linearly in between these concentrations. Inhibition of CH_4 production by sulphide, NO and N_2O, inhibition of sulphate reduction by sulphide and inhibition of nitrate reduction by sulphide are included (Table 1). Inhibition of N_2O on iron reduction may occur (Klüber and Conrad, 1998), but cannot be quantified. Inhibitions by SO_3^{2-} and NO_2^- are not included either, because these compounds were never detected experimentally. Data for half-saturation constants for inhibition were not always available, but results are not affected if such description is used when available (results not shown).

6.3 Results

6.3.1 Model calibration

Anaerobic incubation of slurried paddy soil led to a sequential reduction of electron acceptors (Figure 6.2). Nitrate was reduced first (data not shown), followed by iron. After these reduction processes, sulphate reduction and methane production started simultaneously, although low rates of sulphate reduction and methane production were already measured during nitrate reduction and iron reduction. At the end of the incubation, only methanogens were consumed acetate and H_2/CO_2 and methanogenesis was solely controlled by substrate production rates. The sequence proceeded faster at higher temperatures (Figure 6.2). Model calculations also showed an overlapping reduction sequence and were not significantly different from experimental results at each temperature (at P<0.05) $-r^2 > 0.90$ for all electron acceptors.

a

b

Figure 6.2   (continued next page)

c
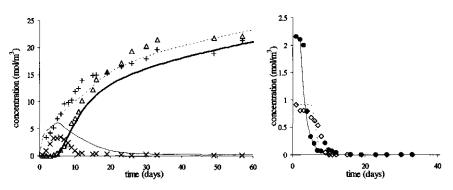
Figure 6.2:   Comparison of experiment (symbols) and model (lines) for the calibration of a
                   long term incubation experiment with rice paddy soil at (a) 14°C, (b) 20°C and
                   (c) 30 °C. Indicated are CH₄ (open triangles and thick lines), CO₂ (pluses and
                   dashed lines) and acetate (crosses and thin lines) in the left figures and sulfate
                   (open diamonds and dashed lines) and reducible iron (closed circles and thin
                   lines) in the right figures. Note the different scales.

The combined reduction processes caused a CO_2 release (Figure 6.2), which was
corrected for abiotic CO_2 release and CO_2 release coupled to propionate and butyrate
accumulation, because these processes were not modelled explicitly. At the start of the
incubation a lot of H_2, acetate and CO_2 was released. Not all released H_2 and acetate was
consumed immediately and accumulated. Acetate disappeared when methane production
was the dominating process. H_2 was already below the detection limit, 10Pa, after 4 days
(data not shown). The model calculates a high mineralisation rate of readily accessible
carbon at the start of the incubation. The resulting CO_2 release is not significantly
different (at P<0.05) from measured CO_2 at any temperature with $r^2=0.96$. Acetate
accumulation was approached only qualitatively. The quantity was significantly different
from measured acetate concentrations (at P<0.05). Acetate accumulation is difficult to
predict, because it equals the difference between soil mineralisation and soil reduction
rates. The accumulation is very sensitive to small deviations in these descriptions, while
especially soil mineralisation is difficult to predict.

6.3.2 Model validation
Two model validation experiments were carried out to test the model applicability. Both
validation experiments were performed with the same soil. Calibrated V_{max} values were
used in the model, because soil storage does not affect microbial numbers (Mayer and
Conrad, 1990).

Short-term validation experiment with substrate additions
The reduction sequence was accelerated -lag phases of CH_4 production were reduced- by
substrate additions (shown for 20°C in Figure 6.3. Trends are similar at 30°C). Modelled
CO_2 release increase under influence of substrate addition was not significantly different
(at P<0.05) from the measurements, while no microbial parameter value had been
changed. Substrate release was least increased in the H_2 treatment and most in the acetate

treatment as is shown by the changes in CO_2 and CH_4 in time (Figure 6.3). The increase in available substrate also increased CH_4 release rates. Measured and modelled CH_4 production rates were not significantly different (at $P<0.05$) for the control, straw addition and H_2 addition. In case of acetate addition (Figure 6.3d), the model significantly underestimated (at $P<0.05$) acetate consumption rates and the concomitant release of CH_4.

a   b

c   d
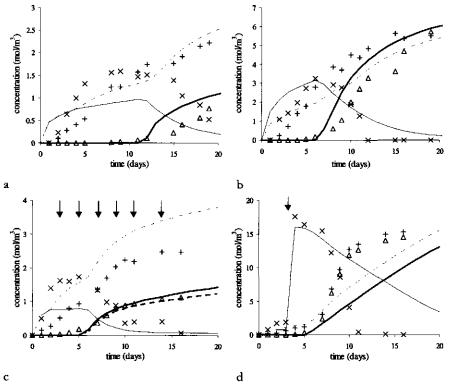
Figure 6.3:   Comparison of model and experiment for the short term validation experiment at 20°C for (a) control, (b) addition of rice straw, (c) repeated addition of H_2, indicated by arrows and (d) addition of 15 mM acetate, indicated by an arrow. Symbols are as indicated in Figure 6.2.

Long-term validation experiment with sulphate addition

Sulphate was added in the 2nd model validation experiment. Methanogenesis was only partly inhibited by sulphate addition (Figure 6.4). Modelled initiation and release of CH_4 under influence of sulphate additions was not significantly different from the measurements (at $P<0.05$), although modelled methane production rates in Figure 6.4d were lower than measured. The model significantly underestimated sulphate reduction rates after $t=20$ days if sulphate was added. Sulphate reduction rates were not significantly different in the control (at $P<0.05$).

In all incubations of Figure 6.4, organic substrate release -shown by the release of CO_2 and CH_4- was much lower than in the calibration experiment (Figure 6.2). The model

corrected for the loss of easily accessible carbon during storage and CO_2 release was not significantly different from measured values, at $P<0.05$, although modelled CO_2 release rates were in all cases slightly higher than measured values.

a   b

c   d
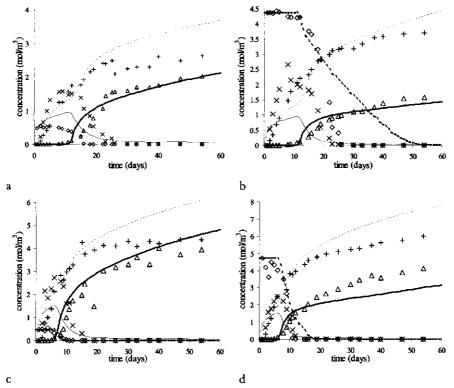
Figure 6.4:   Comparison of model and measured data for the long term validation experiment for (a) control at 20°C (b) addition of 4 mM sulphate at 20°C, (c) control at 30°C and (d) addition of 4 mM sulphate at 30°C. Symbols are as indicated in Figure 6.2.

Short-term experiment on factors determining the lag phase for iron

The model includes an empirical temperature dependent description for the lag time for iron reduction. This lag phase cannot have been caused by substrate limitation, because substrate concentrations were high during the first few days nor can it be explained by direct inhibition, because N_2O and NO had disappeared one day after all nitrate had been consumed. The lag phase dependence on temperature (Chapter 5), on preincubation redox conditions (Ratering and Conrad, 1998) and an unexplained CO_2 release in the period before iron reduction (Chapter 5) suggest the influence of a more competitive electron acceptor, like reducible manganese. The results of a short-term incubation experiment on the initiation of iron reduction (Figure 6.5) show that iron reduction only started after almost all manganese had been reduced. This suggests that the lag phase is indeed caused by manganese reduction.
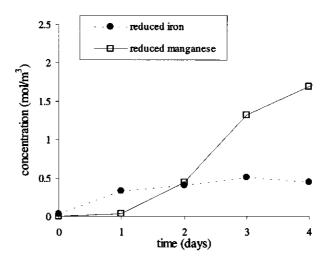
Figure 6.5:   Sequence of iron reduction and manganese reduction in the short term
               validation experiment at 20°C

6.4 Discussion
6.4.1 Calibration of the model
Model and experiment performance were not significantly different, except for acetate accumulation, while most kinetic microbial parameters (Table 6.1) resembled average values from published data that were kept constant in all simulations. Temperature effects were described by Q_{10} values, based on values obtained previously (Chapter 5) for nitrate, sulphate and iron reduction and CH_4 production and a Q_{10} of 2 for other processes. Only V_{max} for sulphate and iron reduction and for CH_4 production were calibrated, because V_{max} is system dependent as it includes a measure of microbial biomass and activity, which again depend on site history and soil adsorption characteristics. V_{max} values for other processes were not calibrated, because there were not enough experimental data to justify this. Calibrated V_{max} values are all in the range of values derived from published data. The V_{max} for iron reducers is similar to the V_{max} calculated from Achtnich et al. (1995a), Lovley and Phillips (1986, 1987, 1988) and Roy et al. (1997) assuming that acetate was not rate limiting. The same applies for the modelled V_{max} for sulphate reducers (Crill and Martens, 1986; Lovley and Phillips, 1987; Roy et al., 1997) and for methanogens (Crill and Martens, 1986; Sass et al., 1990; Sigren et al., 1997).

Because of the system dependence of V_{max} values, it is important to know the sensitivity of the processes for these estimates. CH_4 production rates are enhanced by 40% during CH_4 production initiation if V_{max} of CH_4 production is doubled (Figure 6.6a), causing a concomitant decrease in acetate and increase in CO_2 concentrations. At the same time, sulphate reduction rates decrease slightly at low sulphate concentrations, when the competitiveness of sulphate reducers is negatively affected (results not shown). A correct estimation of V_{max} is thus important, while V_{max} values are not always available. This limits the general applicability of the model. Estimation of V_{max} from direct estimates of microbial numbers is difficult, because such estimates are affected by similar errors.

Another issue is the distribution of V_{max} for methanogenesis. Aceticlastic methanogenesis V_{max} was assumed to be twice as high as the hydrogenotrophic methanogenesis V_{max} to account implicitly for homoacetogenesis in the CH_4 production phase. On the other hand, hydrogenotrophic methanogens are more active than aceticlastic methanogens at the start of the rice-growing season (Roy et al., 1997). If V_{max} of hydrogenotrophic and aceticlastic methanogenesis are taken equal, then CH_4 production rates decrease 8% (Figure 6.6b), while sulphate and iron reduction rates increase less than 2% (results not shown). Methanogens are less competitive for H_2 than for acetate (Achtnich et al., 1995b; Jakobsen et al., 1981; Lovley and Phillips, 1987), while H_2 conversion is given more importance in this analysis. It is thus important to account for homoacetogenesis and for community dynamics within a functional group. This further complicates the estimation of V_{max} values.

The redox sequence in the incubations was well predicted at various temperatures with only the calibration of V_{max} values. The redox sequence was incompletely separated in both model and experiment, while a complete separation would be predicted based upon thermodynamically determined affinity constants. The additional influence of potential conversion rates, direct inhibitions and lag times, however, induced sequence overlap.
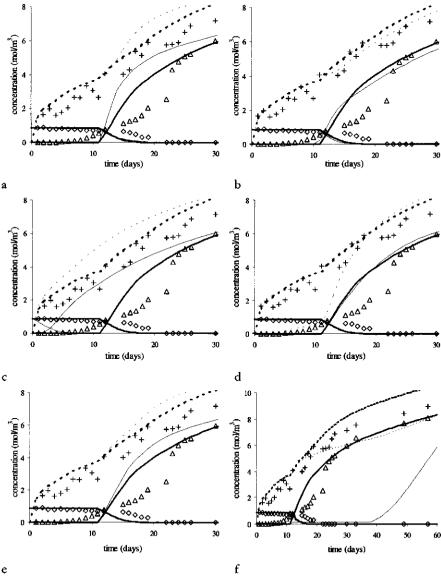
The combination of a high V_{max} and a very high affinity for both acetate and H_2 gave the nitrate reducers a large competitive advantage over bacteria using other electron acceptors (Table 6.1). In addition, NO but not N_2O concentrations were high enough - maximally $7 \ 10^{-3}$ mol m^{-3}- to inhibit methane production during the first 2 days. This might be important in N-fertilised rice paddy fields.

Iron reducers had a higher V_{max} and higher affinity for both acetate and H_2 than sulphate reducers and methanogens, which gave them a competitive advantage. Effects of inhibition on CH_4 production and sulphate reduction during iron reduction, however, also played a significant role. Acetate (and H_2) concentrations were too high to limit sulphate reduction initiation and if no empirical inhibition is included, then sulphate reduction and CH_4 production are initiated immediately, which is much faster than experimentally found (Figure 6.6c). This again leads to a faster release of CO_2. The inhibition could be predicted well by a single threshold concentration for reducible iron, independent of temperature and substrate (Figures 6.3 and 6.4). This suggests indeed a direct inhibition, even though such effect has not been described and even though the mechanism for such inhibition is unknown. An effect of redox potential seems improbable, since this has been falsified for methanogens (Fetzer and Conrad, 1993) and a redox potential effect on sulphate reducers is not known. The inhibition is an important cause for the ineffective acetate consumption and concomitant measured acetate accumulation.

One hypothesis to explain the apparent inhibition is the simultaneous occurrence of sulphate reduction and sulphide reoxidation coupled to iron reduction. If such explanation is true, anaerobic methane oxidation coupled to iron reduction should occur as well, although this process has never been proven. Other chemolithotrophic reactions seem not important in well-shaken systems. If the V_{max} for the other chemolithotrophic reactions -coupled nitrate reduction/sulphide oxidation and coupled nitrate reduction/iron oxidation- is put to zero, nothing changes in the model outcome (results not shown). In field situations, where various reduced and oxidised substances become

available by transport, such reactions might however be important. More research is needed to eludicate the role of chemolithotrophic reactions.

CO_2 release was also well captured by the model. However, if substrate release is simplified to the release of only acetate - attributing all V_{max} to the V_{max} for acetate conversion and assuming that all H_2/CO_2 is transformed by homoacetogens- then CO_2 release is retarded and acetate accumulation overestimated. Initiation and rate of methane production is however hardly influenced (Figure 6.6d), because carbon substrate is not limiting methane production initiation.

a

b

c

d

e   f

Figure 6.6   (continued next page)

g
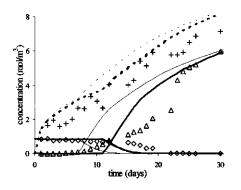
Figure 6.6:   Model sensitivity analysis at 20°C for the experimental results of the calibration
              experiment and modelled results of the default model (thick) and of the
              sensitivity analysis (thin) for CH_4 (triangles), CO_2 (pluses) and sulphate
              (diamonds) for (a) double V_{max} values for CH_4 production, (b) equal V_{max} for
              hydrogenotrophic and aceticlastic methanogenesis, (c) no inhibition of sulphate
              reduction and methane production by reducible iron, (d) without introducing
              H_2, (e) introducing K_M values for CH_4 production as a function of temperature,
              (f) use of sulfide inhibition parameters on methane production based on
              Cappenberg (1974) -note the different scales- and (g) no introduction of a lag
              phase for iron reduction.

Temperature effects were also described well by the model. This means that the
microbial community can react instantaneously to changes in temperature (without
having to grow or induce enzymes). This information might be important to understand
day and night rhythms in CH_4 emissions, found regularly in field studies (e.g. Sass et al.,
1991b; Schütz et al., 1989a; Yagi et al., 1996). It was assumed that substrate affinity was
constant with temperature. For methanogens it was however shown that at 20°C the K_M
for both acetate and H_2 is higher than at the reference temperature of 30°C (Westermann
et al., 1989). Such higher affinity for methanogens (maintaining constant K_M values for
other microbial processes, by a lack of quantitative data) increases CH_4 production rates
by 21% during the initiation phase and methanogens compete more effectively with
sulphate reducers (Figure 6.6e). After sulphate is depleted, CH_4 production rates are
limited by substrate production rates and become equal to default rates. The quantitative
influence of temperature on K_M values needs thus more consideration and might have to
be determined separately for various functional groups and e.g. for fast growing and slow
growing acetate consuming methanogens.

6.4.2 Model validation
Short-term validation experiment with substrate additions

The first validation experiment tested the model with different carbon substrate regimes -
forced by the addition of straw, H_2 and acetate. This is an important validation, because
organic substrate release drives the reduction sequence, providing the necessary
electrons. The model could describe both the increase in CH_4 release rates -expected
from Michaelis-Menten kinetics- and the decrease in the lag phase for CH_4 production

and sulphate reduction without changing any microbial kinetic parameter value. Similar effects of substrate additions on the initiation of sulphate reduction and CH_4 production have been found by others (Achtnich et al., 1995b; Roy et al., 1997) and can be explained by the combination of a less severe competition for substrates and a faster depletion of alternative electron acceptors. These effects of substrate availability are very large and suggest that a proper description of substrate availability is more important for CH_4 production explanation than kinetic microbiological parameters.

The only situation for which the model was significantly different (at $P<0.05$) from the experimental results, was for acetate addition. A possible explanation is that the V_{max} for CH_4 production was not fine-tuned well enough, while the system was more sensitive to this value than in other cases, because other limitations were absent in this case. Another explanation is that growth of methanogenic biomass occurred in this special case, thus causing an increase in V_{max}. Especially the biomass of *methanosarcina*, a fast growing acetate consuming methanogen, might have increased in this period. This complication is not important for field situations, because acetate never accumulates to such high concentrations and the model could describe the effects of acetate accumulation under influence of high rice straw additions.

Long-term validation experiment with sulphate addition

Model validation with sulphate additions is an important test, because sulphate reducers are kinetically the most comparable competitors to methanogens. CH_4 production was only partly inhibited during sulphate reduction, showing that sulphate reducers are not able to outcompete the methanogens. Inhibiting sulphide concentrations were never reached. Only if methane production inhibition is described by the sulphide values of Cappenberg (1975), then methane production is inhibited for 38 days (Figure 6.6f), which is much larger than in reality.

The model underestimation of sulphate reduction at high sulphate levels might imply that growth of sulphate reducers could be important if sulphate concentrations are increased above concentrations naturally found in the field. Such situations might occur in rice paddies if inorganic fertilisers containing sulphate are applied.

The experiment also showed that organic substrate release was reduced by a factor 4-5 by storage. Model predictions for this decreased release were not significantly different from measured values, but to fully account for losses during storage the model should be expanded with a more detailed description of soil mineralisation.

Short-term experiment on factors determining the lag phase for iron

The results of Figure 6.5 suggest that manganese reduction might explain the empirical lag time for iron reduction introduced in the model to describe the late start of iron reducers. Iron reduction, sulphate reduction and CH_4 production start about 4 days earlier than experimentally found if no lag phase is introduced (Figure 6.6g). This again leads to an overestimation of CO_2 in the early phase. A lag phase is thus necessary to describe the redox sequence. A mechanistic description of this lag phase is not yet possible, because kinetic parameters for manganese reduction are highly uncertain. This limits the applicability of the model because, if manganese reduction causes the lag phase, the lag phase will be dependent on reducible manganese concentrations and substrate release rates and thus upon soil type.

6.5 Conclusions

Combination of model and experiments showed the quantitative importance of different microbial interactions leading to CH_4 production in well-shaken systems. The mechanistic model was calibrated with incubation experiments at different temperatures by tuning only the V_{max} values for sulphate and iron reduction and for CH_4 production. The model thus balances mechanistic detail and available information well. Model results agreed with the validation experiments without the adjustment of any kinetic parameter.

The competition for acetate and H_2/CO_2 is the most important factor determining methane production. The model is therefore very sensitive to the description of substrate release. Competition outcome is partly determined by differences in V_{max} values, which are system dependent. The V_{max} should be estimated separately for H_2 and acetate, as can be determined in experiments with labelled acetate and bicarbonate. This limits model applicability.

On the other hand, the model showed that chemolithotrophic reactions and direct inhibitions of NO, N_2O and S^{2-} are not important in these well-shaken systems. The inhibition of sulphate reduction and methanogenesis during iron reduction explains acetate accumulation, but the mechanisms are unknown. The retardation of iron reduction is probably caused by the -uncertain- manganese reduction. A final gap in knowledge is the temperature dependence of affinity constants, while this has a clear influence on the outcome.

Diffusive gas transport through flooded rice systems

[1]P.M. van Bodegom, [2]T. Groot, [3]B. van den Hout, [1]P.A. Leffelaar and [1]J. Goudriaan

[1]Lab. of Theoretical Production Ecology, Wageningen University (WU),
P.O. Box 430, 6700 AK Wageningen, The Netherlands.
[2]Laboratory of Microbiology (WU), The Netherlands.
[3]Department of Molecular and Laser Physics, Catholic University Nijmegen, The Netherlands.

Diffusive gas transport through flooded rice systems

Abstract

In this paper a fully mechanistic model based on diffusion equations for gas transport in a flooded rice system is presented. The model has transport descriptions for various compartments in the water saturated soil and within the plant. Plant parameters were estimated from published data and experiments independent of the validation experiment. An independent experiment is described in which the diffusion coefficient of sulfurhexafluoride (SF_6) in water saturated soil was determined. The model was validated by experiments in which transport of SF_6 through soil and plant was monitored continuously by photoacoustics. The independent default settings could reasonably predict gas release dynamics in the soil-plant system. Calculated transmissivities and concentration gradients under the default settings show that transport within the soil was the most limiting step in this system, which explains why most gases are released via plant mediated transport. The root-shoot interface represents the major resistance for gas transport within the plant. A sensitivity analysis of the model showed that gas transport in such a system is highly sensitive to the estimation of the diffusion coefficient of SF_6 and to the root distribution with depth. This can be understood from the calculated transmissivities. The model is less sensitive to changes in the resistance at the root-shoot interface and in the root fraction active in gas exchange. The model may be helpful in understanding diel patterns found for greenhouse gas emissions.

7.1 Introduction

Rice is one of the most important crops in the world. From 1951 to 1990 the harvested area of rice increased from 104 to146 million ha (IRRI, 1991). Rice is cultivated under a wide variety of climatic, soil and hydrological conditions. Temporary or continuous flooding accounts for 86% of the global rice production (Neue and Roger, 1994). Under these flooded conditions, gas transport is hampered and oxygen depletion develops quickly. Rice plants adapt to this situation by the development of aerenchyma, both in roots and in shoots.

Gas transport through rice plants occurs, contrary to many other wetland plants (Allen, 1997), only by diffusion and not by convection (Groot et al., 2000). Gases exchange via diffusion between the water-saturated soil and the root. This exchange mainly occurs at the root tip and through openings around lateral roots (van Noordwijk and Brouwer, 1993; Flessa and Fischer, 1992). Both in roots and shoots, gases diffuse via the gas phase through aerenchyma (Ando et al., 1983). At the root-shoot interface, both aerenchyma systems are separated by a region of porous plant material (Groot et al., 2000), that reduces gas diffusion between root and shoot (Butterbach-Bahl et al., 1997). The gases exchange with the atmosphere either at the stomata or at special micropores (Nouchi and Mariko, 1993).

All kinds of gases are transported by this plant transport system, for instance plant produced ethene (Lee et al., 1981) and oxygen (Jackson and Armstrong, 1999). The oxygen transport to the roots and into the soil is very important for the plant to create

microaerophilic conditions in the rhizosphere to detoxify anaerobically produced compounds (Kumazawa, 1984) and to allow proper root respiration. Gases produced in the anaerobic soil travel to the atmosphere via this plant mediated transport. Examples are the exchange of N_2, CO_2, N_2O and CH_4. Except for N_2, these gases are important greenhouse gases. Up to 90% of the methane emissions from rice paddies occurs via this plant mediated transport (Nouchi et al., 1994; Schütz et al., 1989b).
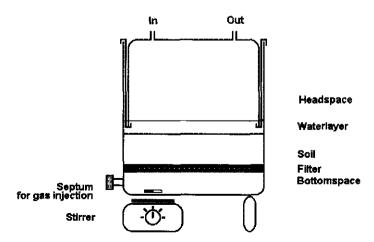
It is thus important to quantify the mechanisms of gas transport in the anaerobic plant-soil system. Various models have been published on oxygen transport within one root (Armstrong and Beckett, 1987; Luxmoore et al., 1970a). Plant mediated transport of methane from rice paddies has been described by one fitted overall conductance value (Hosono and Nouchi, 1997). The diffusion of gaseous compounds into the rhizosphere starting at the root surface was modelled by Newman and Watson (1977) and Darrah (1991a,b). A combination of all these concepts into one mechanistic model for gas transport through the various compartments in a water saturated soil-plant system does not seem to exist, however.

Therefore, this paper describes a mechanistic model on gas transport through a water saturated soil-plant system. In the model, various plant compartments and soil layers are distinguished to compare the transmissivities of each compartment. The analysis of model behaviour enables us to better understand and quantify the rate limiting steps in gas transport, which is helpful for the estimation of greenhouse gas emissions and for plant physiological applications. The model was validated by experiments in which the transport of the inert trace gas sulfurhexafluoride (SF_6) was monitored and quantified. SF_6 can be measured very sensitively and at high time resolutions by photoacoustics. This technique was therefore used in this study.

7.2 Materials and methods
Determination of the SF_6 diffusion coefficient in soil

For SF_6 the diffusion coefficient in water and soils was unknown (Langø et al., 1996). We therefore determined the diffusion coefficient ourselves. The set-up is depicted in Figure 7.1.

Figure 7.1:   Set-up for the determination of the diffusion coefficient of SF_6 in water
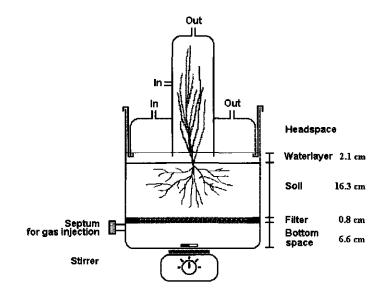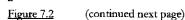
A known amount of pure SF_6 was injected into a stirred bottom compartment containing water. From there it diffused into the soil-water compartment through a P_1-filter with a porosity of 28% and pores of 100-160 μm, permeable to water and dissolved products but not to gas bubbles. The soil-water compartment contained a few centimeters of water saturated soil topped with a water layer. The thickness of each layer was measured by a micrometer. The water was maintained at a constant level with a syphon connected to a communicating vessel. Water saturated N_2 gas flowing through the headspace with a rate of 1 liter/h carried SF_6 to the detector. A nafion tube to trap water and a 10 ml KOH column to trap CO_2 were installed in front of the detector.

The experiment was carried out twice with two different soil layer thicknesses. In the first experiment, the water saturated soil was 2.55 centimeter thick and had 1.10 cm water on top. In the second experiment a column with 1.09 cm water saturated soil and 0.33 cm water op top was used. The diffusion coefficient for SF_6 could be calculated from these two experiments (see section 7.3.2).

Model validation

For model validation a similar set-up was used as described above for the determination of the diffusion coefficient of SF_6 in water and soil, but this time the column contained a soil-rice plant system. Rice (*Oryza sativa L.*) cultivar IR 72, a short-duration, photoperiod-insensitive high yielding modern cultivar developed by IRRI, was used. Rice seeds germinated on petri dishes were double planted into a 17-centimeter deep mixture of rice paddy soil collected in the Philippines supplemented with Dutch river clay containing a low amount of organic matter. Plant spacing was 12.5 cm from the walls and 20 cm between plants. The plants were grown in a greenhouse in the Netherlands with a constant temperature of 26 °C and a 12 h dark-12 h light regime. After two weeks, the seedlings were thinned to one plant per spot in order to obtain uniform plant density.

a

Figure 7.2   (continued next page)

b
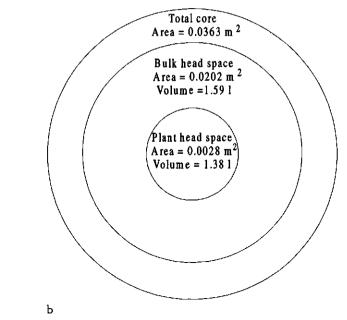
Figure 7.2:   Set-up for the model validation experiment a) side-view and b) top-view

The first validation experiment started 90 days after germination and the second experiment started 103 days after germination. At the day the experiment started, an undisturbed plant-soil core was taken from the container in the greenhouse (to avoid wall growth). The core was installed into the set-up shown in Figure 7.2 and had a soil moisture content of 0.57 m^3 water m^{-3} soil. During the validation experiment, the plant was kept in a 12 h dark-12 h light regime and a constant temperature of 22 °C. Aluminium was attached around the core to obtain good light exposure at all sides of the plant.

Two milliliter pure SF_6 was injected into the stirred bottom compartment containing water. From there it diffused through a P_1-filter, the soil and via the plant into the headspace. The water level was maintained at a constant level with a syphon. Water saturated air with a flow rate of 1 l/h was used as a carrier gas. CO_2 and H_2O traps were installed in front of the detector. SF_6 emission was monitored for 23 days and 16 days, respectively. In this paper we present data from gas released via plant mediated transport.

CO$_2$-laser based trace gas detection
SF_6 concentrations were quantified by on-line CO_2-laser based trace gas detection. A CO_2-laser has typically 90 laser lines in the infrared (wavelength 9-11 µm) region of the electromagnetic spectrum. All gases possessing high absorption strength combined with a characteristic absorption profile in the CO_2-laser region can easily be detected by photoacoustics. The gas flow to be analysed is guided through a detection cell through which a laser beam is directed. By comparing the signals at different laser lines, the gas response can be separated from other interfering signals. When the laser irradiates the gas, the molecules may absorb photons and get excited into a higher rotational-vibrational state. This excitation energy is converted into kinetic energy of the molecules,

i.e. heat. In our case the molecules are periodically exited with a CO_2-laser in the infrared wavelength region by modulating the laser beam with a mechanical chopper at about 1 kHz. In the confined volume of the cell this causes a sound wave well detectable by a microphone. The CO_2 laser has a gas discharge tube of 40 cm long. The generated photoacoustic wave increases linearly with the incoming laser power. For this reason the low noise photoacoustic cell is placed inside the laser cavity. To enhance the photoacoustic signal further, the detection cell is designed as an acoustic resonator, matching the chopper frequency. The electric signal coming from the microphone is fed into a lock-in amplifier to improve the signal-to-noise ratio and to filter out acoustical noise picked up by the microphone.

SF_6 gas has a strong rotational-vibrational Q-band of the v_3 vibration at 947.9 cm^{-1}. At atmospheric pressure a large number of rotational lines of this band overlap with the CO_2-laserline at 947.74 cm^{-1} resulting in an absorption strength of 0.85 Torr^{-1} cm^{-1} (Cox and Gnauck, 1980). Our CO_2-laser photoacoustic cell is able to detect SF_6 concentrations down to 5 pptv.

Determination of plant characteristics

During the growth of the rice plants in the greenhouse, the dates at which a tiller formed was recorded and the tiller itself was labelled. Root length density was measured in rice plants grown in the same batch as the plants used in the model validation experiment. An undisturbed soil-plant core of 16 cm thick was harvested in the same week the validation experiment started. The whole core was frozen for a week at −20 °C. The frozen soil core was sawn into 4 equally thick horizontal layers. Roots were washed and stored at 4 °C in 17% acetic acid solution. Root length per soil layer was determined in duplicate by a Comair Root Length Scanner, type HDH.

7.3 Model
7.3.1 Model description
Transport

The basis of the model is the diffusion of gas (either in the gas phase or dissolved in water) through different compartments present in a soil-plant system. These compartments are the bottom space and filter of our experimental set-up, the soil, the stagnant water layer on top of the soil, the headspace and plant roots and plant shoots. In the model, the soil is divided into N layers of equal thickness. Transport through convective flows is neglected as convective flows contribute little to the total water and solute transport in rice systems (Denier van der Gon and van Breemen, 1993; de Willigen and van Noordwijk, 1994). The diffusive gas flows (*Flow$_{i,j}$*) across an interface (in mol/s) can be described with:

$$Flow_{i,j} = \kappa_{i,j} \cdot ([C_j] - [C_i]) \tag{7.1}$$

in which $\kappa_{i,j}$ is the transmissivity of the interface between i and j (in m^3 water s^{-1} or m^3 gas s^{-1} depending on the medium). $\kappa_{i,j}$ is a transport parameter through a porous medium that combines diffusion coefficients and medium properties (explained below). [C] is the concentration in a compartment and is expressed in the same volumetric medium units as the transmissivity and corrected for porosity, if necessary. The concentrations in the headspace, roots and shoots are expressed in the gas phase, as this is the dominant

transporting medium for these compartments. The concentrations are corrected by root porosity and shoot porosity, respectively. Root porosity depends on rice variety (Colmer et al., 1998), stage in the growing season (van Noordwijk and Brouwer, 1993) and the environment. In a more reduced environment more aerenchyma is formed (Ota, 1970). In the model, an average value of 0.295 m^3 air m^{-3} root is used, which is an average from data presented in Armstrong et al. (1991), Barber et al. (1962), Butterbach-Bahl et al. (1997), Colmer et al. (1998), Jensen et al. (1969), Kludze and Delaune (1995a,b), Kludze et al. (1993) and Luxmoore et al. (1970a). Shoot porosity is estimated at 0.39 m^3 air m^{-3} shoot (Jensen et al., 1969; Butterbach-Bahl et al., 1997). In the soil, the dominant transport is via the water phase and is corrected via θ, the water filled porosity (in m^3 water m^{-3} soil).

If compartments i and j have different media, then $\kappa_{i,j}$ is expressed in m^3 water s^{-1} and the concentration in the medium with the gas phase is corrected for the gas solubility by the Ostwald coefficient (α), which is calculated at the reference temperature from Langø et al. (1996). Temperature dependence is calculated from the empirical equation and its values given by Wilhelm et al. (1977).

Because $Flow_{i,j}$ (Eq. 7.1) in rice paddies is determined by diffusion, $\kappa_{i,j}$ can be calculated in analogy to Fick's law:

$$\kappa_{i,j} = \frac{A_{i,j} \cdot D_{i,j}}{z_{i,j}} \tag{7.2a}$$

in which $A_{i,j}$ is the total cross section area at the interface (in m^2), $D_{i,j}$ is the diffusion coefficient (in $m^2 s^{-1}$; the exact formulation and dimensions are described by Eq. 7.3a) and $z_{i,j}$ is the diffusion distance (in m). This formulation applies to the transmissivity of the bottom space-filter interface ($\kappa_{b,f}$) with $z_{b,f}$ equal to half the filter thickness and $D_{b,f}$ equal to the effective diffusion coefficient in the filter (D_f) treated in Eq. 7.3b. This formulation is allowed, because the bottom space is continuously stirred and does not limit transport. The interface between soil layers ($\kappa_{s,s}$) can be treated similarly, with $z_{s,s}$ as the soil layer thickness and $D_{s,s}$ equal to the diffusion coefficient in soil (D_s), treated in Eq. 7.3a. The transmissivity of the water-headspace interface ($\kappa_{w,h}$) has $z_{w,h}$ of half the water layer thickness and $D_{w,h}$ equal to the diffusion coefficient of SF_6 in water (D_w, in m^2 water s^{-1}). Finally, the transmissivity between soil and roots ($\kappa_{s,r(x)}$) can also be treated this way with $z_{s,r(x)}$ half the distance between roots and $D_{s,r}$ the soil diffusion coefficient (D_s). Subscript x indicates the layer number. The formulation of $A_{s,r(x)}$ is treated below (Eq. 7.8).

If the interface extends over two different media, then a weighted average of characteristics of both media is accounted for in $\kappa_{i,j}$:

$$\kappa_{i,j} = \frac{A_{i,j}}{z_i / D_i + z_j / D_j} \tag{7.2b}$$

Such a formulation applies to the transmissivity between filter and soil ($\kappa_{f,s}$) (with z_f is half the filter thickness and z_s is half the soil layer thickness) and to the transmissivity between soil and water layer ($\kappa_{s,w}$) (with z_w is half the water layer height).

The transmissivity between roots in different soil layers ($\kappa_{r,r}$) accounts for different root cross section areas ($A_{r(x)}$) in different layers, explained further in Eq. 7.11 (layer numbers are indicated with subscripts x and $x+1$, respectively):

$$\kappa_{r,r} = \frac{D_a}{z_r \cdot \left(\dfrac{1}{A_{r(x)}} + \dfrac{1}{A_{r(x+1)}} \right)} \tag{7.2c}$$

in which z_r is the half the root length of an individual root in a layer (Eq. 7.10) and D_a is the diffusion coefficient of SF_6 in air (in m^2 gas s^{-1}). The total root length of an individual root in a layer equals the soil layer thickness divided by root tortuosity (described by Eq. 7.9).

While gases can diffuse normally through the plant via root aerenchyma and shoot aerenchyma, gas transport is retarded at two interfaces -the interfaces root-shoot and shoot-headspace. Tissue porosity is severely reduced at the root-shoot interface, imposing an additional resistance and at the shoot-headspace the stomata or micropores introduce an additional resistance to diffusion.

The transmissivity of the root-shoot interface ($\kappa_{r,t}$) is described analogous to serially connected resistances:

$$\kappa_{r,t} = \frac{1}{\dfrac{1}{\omega_{r,t} \cdot A_t} + \dfrac{z_r}{D_a \cdot A_{r(1)} \cdot \varepsilon_{r(1)}} + \dfrac{z_t}{D_a \cdot A_t \cdot \varepsilon_t}} \tag{7.2d}$$

in which $\omega_{r,t}$ is the conductance for the root-shoot interface (in m^3 gas m^{-2} tiller s^{-1}), z_t is half the diffusion distance in a tiller (quantified below), A_t is the tiller cross section area (Eq. 7.13), ε_r is root porosity and ε_t is tiller porosity (both quantified above). The conductance at the root-shoot interface seems an important limitation for gas transport through rice plants (Butterbach-Bahl et al., 1997). Various experiments were designed to estimate this conductance. The conductance was highly variable and was significantly affected by methodology, tiller position and tiller age (Groot et al., 2000). The model uses an average value for root-shoot conductance of $2.04.10^{-6}$ m^3 gas m^{-2} tiller s^{-1} (Groot et al., 2000) as a default value.

The transmissivity for the shoot-headspace interface ($\kappa_{t,h}$) is described with:

$$\kappa_{t,h} = \frac{1}{\dfrac{1}{\omega_{t,h} \cdot A_s \cdot LAI \cdot \varepsilon_t} + \dfrac{z_t}{D_a \cdot A_t \cdot \varepsilon_t}} \tag{7.2e}$$

in which $\omega_{t,h}$ is the micropore conductance through which methane is known to be released from a rice plant (Nouchi and Mariko, 1993) and A_s is the soil surface (m^2 soil). For simplicity the micropore conductance is given the same value as the stomata conductance, which varies between 0.003 and 0.02 m gas s^{-1} (Penning de Vries et al., 1989). In the model a value of 0.007 is used. LAI is the leaf area index (m^2 plant m^{-2} soil), which equals 4 for a well-developed rice plant canopy (Penning de Vries et al., 1989).

Diffusion coefficients
All transport characteristics have now been described except for D_f and D_s. Both are complicated by the influence of tortuosities -the increase in pathway due to soil structure- and water and gas porosities. D_s is described by:

$$D_s = \frac{\varepsilon \cdot D_a \cdot \tau_a}{\alpha} + \theta \cdot D_w \cdot \tau_w \tag{7.3a}$$

in which D_i is in m^3 water m^{-1} soil s^{-1}, ε is the gas filled porosity (in m^3 gas m^{-3} soil), τ_a is the tortuosity of gas filled pores (in m soil m^{-1} gas) and τ_w is the tortuosity of water filled pores (in m soil m^{-1} water). Tortuosities are described according to Campbell (1985):

$$\tau_a = \alpha \cdot \varepsilon^{(\beta-1)} \tag{7.4a}$$

$$\tau_w = \alpha \cdot \theta^{(\beta-1)} \tag{7.4b}$$

in which α and β are dimensionless empirical parameters, equal to 0.9 and 2.3, respectively (Campbell, 1985).

The filter is water saturated and has a water content (θ_f) of 0.28 m^3 water m^{-3} filter. The tortuosity, τ_f is however unknown and was determined according to a method described below. This leads for the diffusion coefficient in the filter, D_f, to:

$$D_f = \tau_f \cdot \theta_f \cdot D_w \tag{7.3b}$$

If a bulk concentration instead of a concentration in one of the phases is used in combination with an effective diffusion coefficient, as is done in Stephen et al. (1998), then a change in transport rates is predicted upon a change in total porosity or upon other discontinuities, whereas real concentrations and thus real transport do not change.

Plant characteristics
The plant influences several transport parameters: $z_{s,r(x)}$, the diffusion distance between roots, $\kappa_{r,r}$ the transmissivity between roots in different soil layers, $\kappa_{r,s}$ the transmissivity of the root-shoot interface and $\kappa_{s,h}$ the transmissivity at the shoot-headspace interface. All these parameters are dynamic parameters and depend on root biomass: $z_{s,r(x)}$ is influenced directly by the number of roots, $\kappa_{r,r}$ via $A_{r(i)}$ and z_r. $\kappa_{r,s}$ and $\kappa_{s,h}$ are influenced via the dynamic parameters A_s and z_s.

Diffusion distance between soil and roots ($z_{s,r(x)}$)
The diffusion distance between soil and roots is equal to half the distance between two roots. This distance depends on the root length density in a specific layer. Assuming that roots in a layer can be approached by randomly distributed infinite lines (assuming an infinitely small root radius), the average $z_{s,r}$ in soil layer x is (derived from Ogston, 1958):

$$z_{s,r(x)} = \sqrt{\frac{-\ln(0.5)}{\pi \cdot RLD_x}} \tag{7.5}$$

in which RLD_x is the root length density in layer x (in m m^{-3} soil) and is calculated from:

$$RLD_x = average\_RLD \cdot rel\_RLD_x \tag{7.6}$$

in which *average_RLD* (in m m^{-3} soil) is the total average root length density over the soil profile at time t. This variable is calculated from Eq. 3.1. *rel_RLD$_x$* is a dimensionless empirical factor that equals the root length density in soil layer x divided by the total average root length density present at time t. To estimate *rel_RLD$_x$* it is assumed that root lengths decrease exponentially with depth. The slope and intercept of the depth profile change during the growing season due to root growth into deeper layers. *rel_RLD$_x$* is given by:

$$rel\_RLD_x = (a_1 + b_1 \cdot t) \cdot e^{-(a_2 + b_2 \cdot t) \cdot \frac{x}{N}} \tag{7.7}$$

in which t is time after transplanting the rice crop (in s) and a_1, a_2, b_1 and b_2 are empirical parameters to describe the exponential function and are estimated from root length density data by Beyrouty et al. (1988), Kang et al. (1994), Slaton et al. (1990) and Teo et al. (1995) shown in Figure 7.3a. a_1, a_2, b_1 and b_2 are equal to 4.63 (-), 5.09 (-), -4.16 10^{-7} (s^{-1}) and -5.87 10^{-7} (s^{-1}), respectively, according to a minimum mean square error with observed data. The fit with $r^2=0.62$ was not significantly different from observed data, according to a student's t-test (P<0.05).

The estimates for rel_RLD_x were compared to the measured root length density of the plant used in the first validation experiment (harvested 102 days after transplanting). The results (Table 7.1) are similar and only estimated values for rel_RLD_x are used in the remaining part of the paper.

Table 7.1: Measured and modelled root length density distribution with soil depth. The total root length density (RLD_x in m m^{-3}) in a soil layer and the relative root length density in a soil layer (rel_RLD_x, dimensionless) are shown.

	measured RLD_x	measured rel_RLD_x	modelled rel_RLD_x
0-4 cm	$1.72.10^5$	1.45	1.54
4-8 cm	$1.45.10^5$	1.23	1.19
8-12 cm	$9.7.10^4$	0.820	0.922
12-16 cm	$5.9.10^4$	0.499	0.713

Root characteristics, $A_{s,r(x)}$, $A_{r(x)}$ and z_r

The soil-root cross section area over which diffusion takes place, $A_{s,r(x)}$, is given by:

$$A_{s,r(x)} = F_{exch} \cdot number\ of\ roots_x \cdot 2 \cdot \pi \cdot R_{root} \cdot root\ length \tag{7.8}$$

in which F_{exch} is the fraction of the root surface active in gas exchange. Gas exchange mainly occurs around the root tip of primary roots and along lateral roots (Flessa and Fisher, 1992). Tanaka et al. (1995) found that on average 83-90% of the total root length constituted of lateral roots and Yamauchi et al. (1987) found a contribution of 96%. It is estimated that the root tip forms 5.4% of the primary root, based on the observation that 94.6% of an individual primary root is aerenchymous and the fact that root tips are not aerenchymous (Beyrouty et al., 1988). Based on these observations F_{exch} will vary between 0.84 and 0.96. For the model, 0.90 is chosen as a default value.

root length is the average individual root length in a layer (in m) and is estimated, assuming that roots are small chimneys that cross a soil layer with a certain tortuosity, as:

$$root\ length = \frac{soil\ layer\ thickness}{\tau_r} \tag{7.9}$$

in which τ_r is the root tortuosity, which is estimated at 0.56 m soil m^{-1} root using Denier van der Gon and Neue (1996). From the *root length*, one can calculate z_r as:

$$z_r = \frac{root\ length}{2} \tag{7.10}$$

The root cross section area over which diffusion takes place, $A_{r(x)}$, is given by:

$$A_{r(x)} = number\ of\ roots_x \cdot \pi \cdot (R_{root})^2 \tag{7.11}$$

in which R_{root} is the root radius of a single root, calculated to be on average $0.28\ 10^{-3}$ m, based on a root radius for primary roots of 0.9-1.5 mm (Yu et al., 1995) and a lateral root radius of 0.1 mm, calculated from Drenth et al. (1991). The *number of roots* in a layer x is a function of RLD_x and is thus a dynamic parameter:

$$number\ of\ roots_x = \frac{RLD_x \cdot soil\ layer\ thickness \cdot A_s}{root\ length} \tag{7.12}$$

Tiller characteristics, A_t and z_t
The shoot cross section area over which diffusion takes place, A_t, is given, analogous to the root cross section area, by:

$$A_t = number\_of\_tillers \cdot \pi \cdot (R_{tiller})^2 \tag{7.13}$$

in which R_{tiller} is the tiller radius, which was measured for rice plants of the same rice variety by Groot et al. (2000) and for which the average value of $3.2\ 10^{-3}$ m is used as default in the model. The *number_of_tillers* is a function of time and was monitored while growing rice plants in the growing chamber. The growth curve of the number of tillers was fit using a universal logistic growth curve:
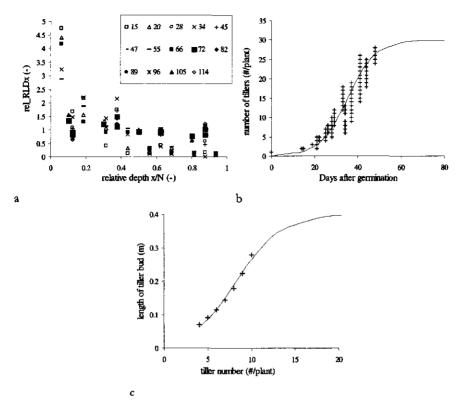
$$number\_of\_tillers = \frac{maximum\ number}{1 + K_{til\_no} \cdot e^{-rgr_{til\_no} \cdot t}} \tag{7.14}$$
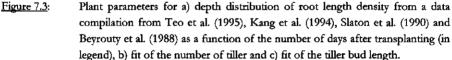
in which *maximum number* is the maximum possible number of tillers and is estimated at 31 (#/plant), similar to data of Watanabe and Kimura (1995). K_{til_no} ((maximum tiller number-number of tillers$_{t=0}$)/number of tillers$_{t=0}$) and rgr_{til_no} (relative growth rate of number of tillers) were fitted to our tiller number observations (Figure 7.3b) at 31 and 1.5 10^{-6} s^{-1}, respectively.
The diffusion length through the tiller, z_t, is half the distance from the root-shoot interface to the micropores. The micropores are located around the top gap between the epidermis of the culm and leaf sheath (Nouchi and Mariko, 1993). z_t can thus be assumed to be half the length of a tiller bud. This length depends on the time of tiller emergence. The later the emergence, the longer the tiller. The time it takes for a tiller to become fully developed is equal to the time needed to form two new tillers (Hanada, 1995). Neglecting this growing period, the average tiller bud length only depends on the number of tillers. The average tiller bud length was fit by a universal logistic growth curve:

$$tiller\ bud\ length = \frac{maximum\ length}{1 + K_{til\_length} \cdot e^{-rgr_{til\_length} \cdot tiller\ number}} \tag{7.15}$$

in which *maximum length* is the maximum possible length of a tiller bud, estimated at 0.40 m (personal observation). K_{til_length} ((maximum length-tiller bud length$_{t=0}$)/tiller bud length$_{t=0}$) and rgr_{til_length} (relative growth rate) were fit at 26.1 and 0.394 tiller number^{-1}, respectively. A comparison with observed data is given in Figure 7.3c.

a

b

c

Figure 7.3: Plant parameters for a) depth distribution of root length density from a data compilation from Teo et al. (1995), Kang et al. (1994), Slaton et al. (1990) and Beyrouty et al. (1988) as a function of the number of days after transplanting (in legend), b) fit of the number of tiller and c) fit of the tiller bud length.

A carbon balance is included in the computer model and never showed relative deviations >10^{-6}. Time steps in the model are determined by the characteristic time of the fastest flow, which is the flow in root and shoot (see section 7.4.1). The calculation of the amount of gas released in time is used for model validation.

7.3.2 Estimation of SF$_6$ diffusion coefficients

The prediction of SF$_6$ gas transport was limited by two unknown parameters, τ_f and the D_w for SF$_6$. Both parameters were estimated simultaneously by a measurement set-up without a plant, described in section 7.2. For both experiments an effective diffusion coefficient (D_{eff}) can be related to the transport characteristics according to:

$$\frac{total\,thickness}{D_{eff}} = \frac{filter\,thickness}{D_w \cdot \theta_f \cdot \tau_f} + \frac{soil\,thickness}{\dfrac{\varepsilon \cdot D_a \cdot \tau_a}{\alpha} + \theta \cdot D_w \cdot \tau_w} + \frac{water\,thickness}{D_w} \quad (7.16)$$

All thicknesses were measured (in m), θ was measured (0.57 m^3 water m^{-3} soil) and τ_a, τ_w, θ_f and α were known. D_{eff} was estimated numerically with Eq. 7.1, 7.2a, 7.3 and 7.4, while assigning the same constant D_{eff} to each compartment. The soil and water thickness were different in the two experimental replicates, yielding two D_{eff} values. The

two unknown parameters, τ_f and D_w, could be solved analytically in combination with Eq. 7.16 by substitution. This resulted in a SF_6 diffusion coefficient in water of $1.31 \cdot 10^{-9}$ m^2 s^{-1} (at T=303 K) and a τ_f of 2.78 m filter m^{-1} water. The results of the two experiments and the modelled SF_6 release using the calculated τ_f and D_w are shown in Figure 7.4.

a   b
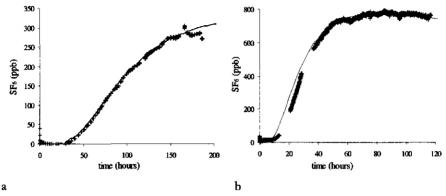
<u>Figure 7.4</u>:   Fit of diffusion coefficient to measured concentrations of SF_6 for a) the first experiment and b) the second experiment

Temperature dependence of D_w is calculated with a Q_{10} value. The Q_{10} value is given the value of 1.31, analogous to Segers (2000), after comparison with the temperature dependence of common atmospheric gases. The diffusion coefficient of SF_6 in air at any temperature is calculated from the binary diffusion coefficients using the formulations and parameter values given in Hirschfelder et al. (1964).

7.4 Results
7.4.1 Model validation
With the determination of the diffusion coefficients, all parameters to describe the soil-plant system are known. The average transmissivities for the different compartments for the first model validation experiment are presented in Figure 7.5. The transmissivities for the root compartment (except for the upper root layer that includes the root-shoot interface) and the shoot compartment are much higher than transmissivities of other compartments. The transmissivities show that diffusion through the rice plant is not the rate-limiting step, as was suggested already by Lee et al. (1981) and Armstrong and Gaynard (1976). The combined transmissivities for the soil-root interface, root and shoot compartments are also higher than the transmissivity for the soil compartment itself. In addition, concentration gradients within the soil are much smaller than between soil and root (results not shown). This explains why most of the gas produced in the soil (e.g. methane) is emitted via plant mediated transport -given that the root system is well developed- (e.g. Schütz et al., 1989b). The transmissivity and the concentration gradients for the soil compartment are by far the smallest and thus the rate-limiting step in gas transport through the soil-plant system. The transmissivity for the soil-root transport is the second rate-limiting step. This shows, in accordance with the suggestion of Jackson and Armstrong (1999), that the root surface represents a major gas transport resistance.

Transport limitations due to diffusion in soil and water are more severe than those at the water-air interface. It thus seems improbable that measurement techniques, e.g. using closed chambers for greenhouse gas emission measurements, will lead to major changes in measured gas release rates.
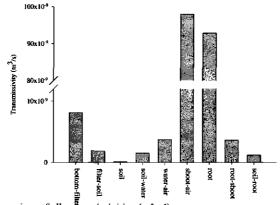
Figure 7.5: Overview of all transmissivities (m^3 s^{-1})

The results of the validation experiments are shown in Figure 7.6. SF_6 follows a pattern similar to the diffusion experiments without a rice plant. The model predicts the gas transport through the soil-plant system with reasonable accuracy without fitting any parameter and using only default settings. If the plant presence is neglected, diffusion rates are severely underestimated, because the plant mediated transport pathway is blocked (data not shown). Inclusion of the characteristics of the plant system is thus necessary for the prediction of gas flows. On the other hand, gas transport rates are only slightly increased (data not shown) if it is assumed that conductivity through the plant is infinite and thus the gas is released into the atmosphere as soon as it enters the plant. These results can be understood from the transmissivities shown in Figure 7.5.

Measured gas concentrations in Figure 7.6a show distinct spikes. An increase in SF_6 concentrations occurred within two hours after the light was turned on and a downward spike was found after the light was turned off. Equilibrium was obtained within few hours and the SF_6 signal represents real emission values while equilibrium was present. Similar spikes occurred when the temperature was increased artificially by 5 °C, excluding direct effects of light radiation (data not shown).

In the second validation experiment the flow inlet had been moved to the bottom of the headspace. This resulted in an immediate mixing of the air within the headspace and avoided spike formation (Figure 7.6b). This indicates that the spikes were not caused by changes in the diffusion coefficient or solubility with temperature, but that probably the headspace compartment had not been mixed properly in the first validation experiment, even though there had been a continuous flow. It seems that at a temperature increase, mixing with the lower part of the compartment increased, leading to a release of accumulated SF_6. At the moment the light was turned off and temperature decreased, mixing decreased as well and a new equilibrium was formed after some time.

a   b
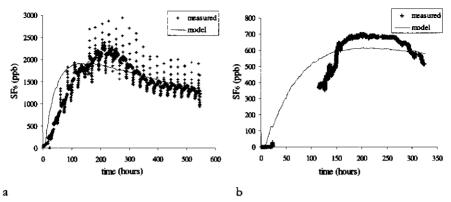
Figure 7.6:   Measured and modelled changes in SF₆ concentrations in time in a) the first
                validation experiment and b) the second validation experiment. Modelled
                concentrations were calculated with the default settings of the model

In both validation experiments, the measured SF_6 signal started to increase later than the modelled SF_6 release. This might have been caused by the way of injecting SF_6. Gaseous SF_6 had been added to the bottom space and the gas dissolved by stirring. The temporary presence of small gas bubbles underneath the filter may have retarded gas diffusion.

7.4.2 Model sensitivity analysis

The model presented in this paper describes gas transport in a soil-plant system as mechanistically as possible. It can predict SF_6 release reasonably well without fitting any experiment specific parameter. Some plant parameters were estimated from a general expression including the time after germinating in combination with the total aboveground biomass. Other plant parameters were derived from published data. Soil transport characteristics were estimated either from published data or from experiments independent of the validation experiments. Even though no parameter fitting was performed, it is important to understand the sensitivity of gas transport to the various parameters, because many parameter values are variable or uncertain. Only parameters influencing transport processes with low conductances will affect SF_6 release. From Figure 7.5 it follows that SF_6 release is hardly sensitive to processes within tillers and roots. These processes were therefore not studied in our sensitivity analysis. We focussed on effects of the exchange surface of the roots, the diffusion coefficient of SF_6 in water, the conductance at the root-shoot interface and the effects of different distributions of RLD_x. The latter is of importance for the determination of $\kappa_{s,r(x)}$. All variables were varied one at a time within the range estimated from experiments and published data. For comparison, we used data from the first validation experiment, because this experiment had a uninterrupted measurement series.

Effects of the root fraction permeable to gas, F_{exch}
Only lateral roots and root tips contribute to gas exchange at the root surface. The influence of increasing F_{exch} -which is almost equivalent to the sensitivity for a variation in root radius- is small (Figure 7.7a) and one might as well assume that the complete root surface is active in gas exchange. The total root surface is largely determined by the

lateral roots (leading to a default setting for F_{exch} of 0.90). Only if F_{exch} is decreased below 0.8 -thus assuming that there are only primary roots in the system- then the systems response is modified without improving the transport description. Such low F_{exch} values are, however, not likely to be encountered in nature. The system is not sensitive to F_{exch} if F_{exch} is kept in a reasonable range.

a   b

c   d
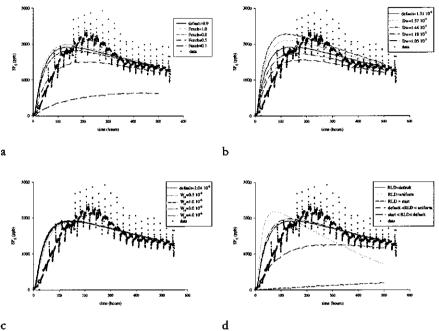
<u>Figure 7.7:</u>   Sensitivity analysis of the model. The sensitivity were tested against measured values for a) the fraction of the root surface active in gas exchange (F_{exch}), b) estimation of the diffusion coefficient of SF_6 in water at T=303 K (D_w), c) different estimates for the conductivity at the root-shoot interface of the rice plant ($\omega_{r,t}$) and d) different root distributions. Two extremes, a uniform distribution with depth and a root distribution with depth as it is at the start of the season and their intermediates were tested.

Effects of diffusion coefficient of SF_6 in water, $D_{w,SF6}$
The effects of a change of plus and minus 5 and 10% in the default estimate of $1.31\ 10^{-9}$ $m^2\ s^{-1}$ for $D_{w,SF6}$ are much larger and major differences in the systems response are found (Figure 7.7b). This can be understood from Figure 7.5, which shows that the transport through the soil is the rate-limiting step. An increase in $D_{w,SF6}$ overestimates transport during large periods of the incubation. A decrease in $D_{w,SF6}$ describes the response slightly better at the start, but poorer than the default settings in the central period of the incubation. It seems not unreasonable that $D_{w,SF6}$ was overestimated if one considers that $D_{a,SF6}$ was $1.01\ 10^{-5}$ at 303 K and that D_w is about 10^{-4} times D_a. There is thus a need for better experiments to determine $D_{w,SF6}$.

Under influence of temperature changes, D_w can easily change by 5 or 10%. Such changes lead to large changes in gas emission patterns (although less than estimated by the conductance predictions of Hosono and Nouchi (1997)) and may contribute considerably to the diel emissions patterns found e.g. for methane emissions (e.g. Nouchi et al., 1994).

Effects of the root-shoot conductance, $\omega_{r,t}$

Although the low conductance at the root-shoot interface is by far the most important resistance for plant transport within the plant and one of the lower transmissivities in the complete soil-plant system, the effects of a change in $\omega_{r,t}$ are small (Figure 7.7c). The values for $\omega_{r,t}$ were varied within the range encountered in experiments (Groot et al. (2000)), but the system was almost insensitive to these changes.

On the other hand, if there had been no transport limitation, like $\omega_{r,o}$ within the plant, then gas concentrations within the plant would have been similar to ambient concentrations. Methane concentrations within the plant are, however, much higher than ambient concentrations (Byrd et al., 2000).

Effects of root length distribution with depth, rel_RLD_x

An average fitted rel_RLD_x was used in the model. This distribution was estimated from published data and tested for our validation experiment (Table 7.1). The differences with measured distributions were small but, given the plasticity of root distributions and the transport limitation induced by the transport between soil and root, the sensitivity for rel_RLD_x was tested. The influence of different assumptions for rel_RLD_x on measured gas release rates was very large (Figure 7.7d). Hardly any SF_6 is released at a root distribution that occurs at the start of the season (keeping the same total average RLD over the profile). With a uniform rel_RLD_x, SF_6 release is increased, especially at the start of the incubation. This shows -as expected based on the transmissivities in Figure 7.5- that the bottom layers are the most important layers for the gas transport to provide a fast shortcut to plant mediated transport. The differences in measured and predicted rel_RLD_x for the bottom layers (Table 7.1), may thus have led to the differences in measured and predicted SF_6 release. Due to the plasticity of rel_RLD_x it will be very hard to make a fully accurate prediction of the dynamics in gas release rates from soil-plant systems.

7.5 Conclusions

In this paper we present a fully mechanistic model based on diffusion equations for the gas transport in a soil-plant system of flooded rice. The model combines transport descriptions within the soil with those within the plant and is more comprehensive than other published transport models. Model parameters were estimated from published data and experiments from the validation experiment. These default settings could reasonably predict gas release dynamics in a soil-plant system. Deviations between model and measurement are most probably caused by the chosen root distribution with depth, as was shown by the sensitivity analysis. Calculated transmissivities and concentration gradients under the default settings show that transport within the soil is the most limiting step in this system, which explains why most gases will be released via plant mediated transport. The low transmissivity in the soil also explains why the system is

highly sensitive to changes in the estimation of $D_{w,SF6}$. This may however change if a different rel_RLD_x is chosen. At a rel_RLD_x that occurs at the start of the season, the low number of roots at the bottom layers limit transport from the bottom space, as shown by the sensitivity analysis. The root-shoot interface represents the major resistance for gas transport within the plant.

This mechanistic model helps to understand the importance of plant mediated transport, but may also provide insight in other features of gas transport in flooded plant-soil systems. At in situ conditions, the distance between the site of gas production and roots is much smaller than in our experimental system. The limiting factor for gas transport, $D_{w,SF6}$, is sensitive to temperature changes. This fact, in combination with the shorter diffusion distances, might provide a -partial- explanation for diel patterns found for greenhouse gas emissions.

Acknowledgements

Methane oxidation in the rice rhizosphere: Competition for oxygen

[1,2]Peter van Bodegom, [2]Fons Stams, [1]Liesbeth Mollema, [1]Sara Boeke and [1]Peter Leffelaar

[1] Lab. of Theoretical Production Ecology, Wageningen University (WU),
P.O. Box 430, 6700 AK Wageningen, The Netherlands.
[2] Laboratory of Microbiology (WU), The Netherlands.

Methane oxidation in the rice rhizosphere; Competition for oxygen

Abstract

A mechanistic approach is presented to understand oxidation of the greenhouse gas methane in the rice rhizosphere of flooded paddies. Methane oxidation involves the conversion of methane and oxygen to CO_2 and water by obligate methanotrophic bacteria. In flooded rice paddies these methanotrophs compete for available O_2 with other types of bacteria. Soil incubation studies and Most Probable Number (MPN) counts of oxygen consumers show that microbial oxygen consumption rates are dominated by heterotrophic and methanotrophic respiration. MPN counts of methanotrophs show large spatial and temporal variability. The most abundant methanotrophs (*Methylocystis sp.*) and heterotrophs (*Pseudomonas sp.* and *Rhodococcus sp.*) were isolated and characterised. Growth dynamics of these species at carbon and oxygen limitations are presented. Theoretical calculations based on measured growth dynamics show that methanotrophs are only able to outcompete heterotrophs at low oxygen concentrations (frequently <5 µM). The oxygen concentration at which methanotrophs win the competition with heterotrophs is not dependent on methane concentration, but it is highly affected by organic carbon concentrations in the paddy soil. Methane oxidation is severely inhibited at high acetate concentrations. This is in accordance with competition experiments between *Pseudomonas sp.* and *Methylocystis sp.* carried out at different oxygen and carbon concentrations. We hypothesise that methane oxidation mainly occurs at microaerophilic, low acetate conditions and thus not very close to the root surface. Acetate and oxygen concentrations in the rice rhizosphere are in the critical range for methane oxidation and a high variability in methane oxidation rates is thus expected.

8.1 Introduction

Rice paddies are an important source of the greenhouse gas methane (Houghton et al., 1996). The magnitude of methane emission from rice paddies reflects the balance between methanogenesis and methanotrophy. Methane oxidation occurs at anaerobic/aerobic interfaces with available oxygen and methane: the soil-water interface and the rice rhizosphere. At the soil-water interface methane oxidation efficiencies are fairly constant at 70-95% of the transported methane (Banker et al., 1995; Epp and Chanton, 1993; Gilbert and Frenzel, 1995; Schütz et al., 1989b). Estimates of methane oxidation in the rice rhizosphere are much more variable. They range 7-90% of the transported methane (Denier van der Gon and Neue, 1996; Epp and Chanton, 1993; Gilbert and Frenzel, 1995; Holzapfel-Pschorn et al., 1985; Sass et al., 1992) and still vary from 7-52% if only data obtained from specific inhibitor studies are included. A better mechanistic understanding of rice rhizospheric methane oxidation is important for a good prediction of methane emissions from rice paddies.

Obligate methanotrophic microorganisms carry out methane oxidation. In freshwater wetlands, high affinity methanotrophy (Bender and Conrad, 1992) does not have to be considered (Segers, 1998) and neither does anaerobic methane oxidation (Chapter 3).

Nitrifiers are also of little importance to methane oxidation in the rice rhizosphere (Bodelier and Frenzel, 1999). Methanotrophic activity is thus determined by oxygen and methane concentrations. Methanotrophs are the most important methane sink in the rice rhizosphere and there is thus no competition for methane. However, an intensive competition for oxygen occurs. Quantification of the competition for oxygen forms the basis for a better understanding of methane oxidation rates. Important oxygen sinks are plant respiration, chemical oxidation and microbial oxidation.

This paper quantifies oxygen sinks in rice paddies. Isolation and characterisation of the most abundant microbial oxygen consumers in this system are described. Their growth kinetics in relation to oxygen and carbon substrate concentrations is studied. Competition experiments for oxygen between these organisms and theoretical considerations of competition for oxygen are presented. This should result in a better mechanistic understanding of methane oxidation in the rice rhizosphere.

8.2 Materials and Methods
8.2.1 Sinks for oxygen in a rice paddy soil
Overall oxidation rates

Ten soil slurries were prepared in 120-ml bottles by mixing 25 g air dried rice paddy Maahas soil from the Philippines (Wassmann et al., 1998) with 25 ml water. The bottles were closed with butyl stoppers and incubated anaerobically for 2 months at 30°C while shaken at 120 rpm to obtain a fully reduced soil. After 2 months, samples were taken for analysis of inorganic anions and Fe^{2+}. Reoxidation of nitrogen, iron and sulphurous compounds was measured in duplicate in bottles opened for 8 hours, 1 day, 2 days and 4 days, respectively and in a control that was not opened at all. Samples for inorganic anions and Fe^{2+} were taken daily. The same experiment was carried out at 15 and 20°C.

Aerobic microbial communities

A soil slurry was prepared from air-dried rice paddy Maahas soil from the Philippines. The slurry was left to stabilise for 1 week at 30°C while shaking at 120 rpm. Dilution series down to 10^{-10}/g d.w. soil with a step size of a factor 3 were prepared in triplicate in 120-ml bottles with 25 ml sterile Nitrate Mineral Salts (NMS) medium (Whittenbury et al., 1970) and closed with butyl stoppers. Series were prepared at 20% O_2/ 80% N_2 with 30 mM acetate, at 1% O_2/ 99% N_2 with 30 mM acetate and at 1% O_2/ 19% CO_2/ 80% H_2 with 1 mM acetate. For each series, treatments with different additional electron donors were prepared by adding 240 mM Fe^{2+}, 30 mM $S_2O_3^{2-}$ -which is more stabile than H_2S- 30 mM NH_4^+, 10% CH_4 in the gas phase and no additional donor, respectively. A control without soil was included for each treatment. Optical density (O.D.) -measured routinely photospectrometrically at 660 nm- and the consumption of electron donors and electron acceptors were monitored weekly for ten weeks. Positive growth was assumed if a significant decrease in the additional electron donor concentration (or in acetate concentration in case no additional electron donor was added) was determined.

For iron oxidation, tubes with gel-stabilised gradients (Emerson and Moyer, 1997) were prepared with and without soil inoculation. After 4 weeks, the tubes were frozen and cut into small bands. Each band was analysed for Fe^{2+} and O_2 after thawing.

Microbial oxygen consumption rates

Enrichments from the highest dilution with growth on acetate, Fe^{2+}, $S_2O_3^{2-}$, NH_4^+ and CH_4 at 1% O_2 and 1 mM acetate were used to quantify the potential activity of microbial oxygen consumption. The total number of bacteria in these enrichments was counted using a Bürker-Türk counting cell. 10 ml of the enrichment was added to 25 ml freshly made sterile NMS medium in a 120 ml bottle with 1% O_2 in N_2 and additional 30 mM acetate, 240 mM Fe^{2+}, 30 mM $S_2O_3^{2-}$, 30 mM NH_4^+ or 10% CH_4, respectively. Bottles were incubated in the dark at 30°C shaking at 120 rpm. Oxygen concentrations in the gas phase were monitored daily for two weeks.

8.2.2 Culture isolation and characterisation

Microorganisms were isolated from the highest dilution from the MPN counts (section 8.2.1). The heterotrophs and the methanotrophs from the highest dilution with growth were enriched in NMS-medium with acetate and CH_4 as sole C-source, respectively. By a combination of inoculation and selection on liquid NMS media and NMS media in highly purified agar, microorganisms were isolated from the enrichments.

Cell morphology of isolated heterotrophs, strains *HET-1* and *HET-2*, was analysed in liquid NMS-medium and acetate as sole C-source by microscopy. Colony morphology was analysed by growth on NMS-medium in agar with acetate as sole C-source. Gram stain reaction and the presence of cytochrome oxidase were tested (Krieg, 1984). The use of acetate, ethanol, glucose, citrate, lactose and fumarate as sole C-source by the organisms in liquid aerobic NMS medium at 30°C was tested. The decomposition of urea, arginine, lysine, ornithine and tryptophane in liquid aerobic NMS-medium at 30°C was also tested. The denitrifying capacity, reduction of sulphurous compounds and the fermentation of glucose, mannitol, inositol, sorbitol, rhamnose, sucrose, melibiose and arabinose at anaerobic conditions were tested in liquid NMS-medium at 30°C. The denitrifying capacity was also tested in solid agar with NMS-medium at 30°C. The growth temperature response on 30 mM acetate in liquid NMS-medium was tested at 10, 20, 30, 37 and 45°C. rDNA of the heterotrophic strains on agar plates was amplified in a PCR-reaction with the universal 16 S rDNA primers 27F and 1492R. The size of the PCR-product was tested on an agarose gel and purified using the QIAquick purification kit. Amplified 16S rDNA was sequenced with the Big Dye Terminator Cycle Sequencing kit (Perkin Elmer). The 1st isolate was sequenced with the 342F primer, the 2nd isolate with the 500F primer. After the sequencing reaction, DNA was precipitated with the isopropanol precipitation reaction (Perkin Elmer) to remove the Big Dye Terminator. The sequencing products were analysed with an ABI310 Genetic Analyzer (Perkin Elmer).

Cell morphology of a methanotrophic isolate, strain *MOX-1*, was analysed in liquid NMS-medium with a 30% CH_4 headspace by phase contrast microscopy. Colony morphology was analysed by growth on NMS-medium in agar with a 30% CH_4 headspace as sole C-source. Gram stain reaction (Krieg, 1984) was tested. Transmission Electron Microscopy (TEM) was used for the characterisation of flagellae, plasmatic membranes and intracellular storage compounds.

8.2.3 Determination of growth kinetics

MPN counts for methane oxidation in the rhizosphere

Rice plants were grown in soil with 15 cm spacing and a large area around the plants to avoid wall effects. Soil samples were taken at four moments during the growing season. At each moment, soil cores were taken at different distances from the main plant (Figure 8.1). Material from the top 2 cm was discarded to avoid interference of methanotrophs accumulated at the soil-water interface. The samples were mixed, diluted in triplicate in 120-ml bottles with 25 ml sterile NMS medium in dilution series down to 10^{-10}/g d.w. soil with a step size of a factor 3 and closed with butyl stoppers. A headspace with air was enriched by 30% CH_4. All samples were incubated at 30°C in the dark without shaking for 5 months. Every 30 days (and at time zero), samples for CH_4 were taken.
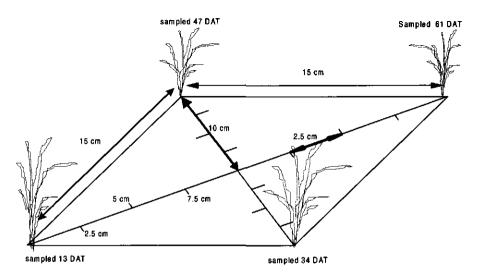
Figure 8.1:   Set-up for soil sampling the Most Probable Number of methanotrophs at different moments during the season and at different distances from the main stem of the plant. A rice plant is located at each corner.

Pure culture experiments

Monod substrate half-saturation constants for microbial growth (K_s in mol/l) and the maximum specific growth rate (μ_{max} in h^{-1}) (further explained in section 8.3) were determined for the isolated heterotrophs and for the methanotroph. Chemostats were found to be inadequate for this purpose due to the extremely low, steady constant oxygen concentrations needed. Instead, use was made of batch experiments in which oxygen and carbon concentrations were monitored at least once a day. The organisms were pregrown at low oxygen concentrations to simulate rhizospheric conditions. This was necessary because kinetic properties depend on the growth conditions (Kightley et al., 1995). Sterile 120-ml bottles with 25 ml NMS medium and closed with butyl stoppers were inoculated with organisms in the logarithmic growth stage. For each species, 8-10 bottles with various initial oxygen and carbon concentrations -one was limiting and the other in excess- were incubated in the dark at 30°C. Concentrations were chosen based

on results of preliminary experiments and on published data. Heterotrophs were grown with acetate and methanotrophs with methane as sole C-source. Samples were taken at anaerobic conditions with syringes flushed in N_2 medium containing sodium dithionite and analysed for oxygen, acetate or methane. Bacterial numbers were analysed routinely by O.D. measurements. A species-specific relationship between O.D. and bacterial numbers was obtained by relating O.D. to Bürker-Türk counting cell measurements. Kinetic parameters were fitted by minimising the Mean Square Error between calculated and measured specific growth rates at different limiting substrate concentrations.

BOM experiments

The μ_{max} for strain HET-2 was validated polarographically with a Clark-type oxygen electrode (Biological Oxygen Monitor (BOM)) mounted in a thermostatically-controlled and continuously stirred vessel at 25°C. The vessel was closed except for a small hole through which substrate and culture additions could be made. The oxygen electrode was calibrated with an oxygen-saturated suspension. The vessel contained 3 ml oxygen saturated sterile NMS-medium with abundant acetate (20 mM). A 100 μl microbial suspension, with a known cell density was added to the vessel. Cells had been pregrown at 25°C and were harvested in the logarithmic growth stage. Oxygen consumption upon addition of substrate was recorded continuously during 30 minutes and corrected for endogenous respiration. The relative oxygen consumption rate was determined from the exponential decrease in oxygen concentration in time. μ_{max} was calculated from relative oxygen consumption rate assuming a yield of 0.375 mol C_B/mol C_S (section 8.3) and an average size of 1.87 10^{-13} g C/cell (Bratbak, 1985).

8.2.4 Competition for oxygen between microorganisms

Competition experiments

Competition for oxygen between strain HET-1 and strain MOX-1 was determined in batch experiments. Equal numbers of bacteria as determined from measurements with the Bürker-Türk counting cells were added to 25 ml sterile NMS medium in 120-ml bottles containing N_2-gas. Different amounts of carbon sources, CH_4 and acetate, and oxygen were added to these bottles. Incubations were made with initial concentrations of 2, 5 and 10 mmol CH_4/l gas and of 0.5 and 2-4 mmol O_2/l gas. The bottles were incubated at 30°C, while shaken continuously at 120 rpm. Concentrations of O_2, CH_4 and acetate were monitored at least once a day until one of the substrates was depleted. Samples were taken at anaerobic conditions with syringes flushed in N_2 medium containing sodium dithionite and analysed for oxygen, acetate, methane and O.D.. The (six) experiments were carried out in 4-6 replicates.

Theoretical description of competition

The outcome of the competition between heterotrophs and methanotrophs can also be predicted theoretically from the measured kinetic parameters. These theoretical calculations are presented in section 8.3.

8.2.5 Chemical analyses

All samples were centrifuged (after extraction, if any) for 5 min at 13,000 rpm and the supernatant was analysed. Acetate was determined by gas chromatography, using a Chromosorb 101 column saturated with formic acid at 160°C, connected to a flame ionisation detector (FID). Prior to analysis the samples were diluted 1:1 with 1 M formic acid containing 1 mM isobutyric acid as internal standard. Fe^{2+} in water and in a 50:1 0.5 M HCl extraction were analysed colorimetrically with phenanthroline as reagents (Walinga et al., 1995). The absorbance was measured at a wavelength of 515 nm on a photospectrometer. NH_4^+ concentrations were analysed colorimetrically with a glutamate assay (Kun and Kearney, 1974). Samples for inorganic anions were diluted 5:1 with a solution of 20 mM mannitol and 60 μM potassium bromide, as an internal standard, and analysed on a HPLC equipped with suppressed conductivity detection. Anions were separated on an Ionpac AS9-SC column using a 1.8 mM bicarbonate/1.7 mM carbonate eluent at 1 ml/min. CH_4 was analysed by GC on a molecular sieve column at 70°C, coupled to a FID. O_2 was analysed on a molecular sieve column at 100°C coupled to a thermal conductivity detector (TCD). The amounts of CH_4 and O_2 were quantified using standard curves obtained by injecting known amounts of gases.

8.3 Theoretical calculations on competition

In case of a dynamic microbial population, as is the case in the rice rhizosphere, a straight forward method to calculate microbial biomass kinetics is the application of a double Monod equation, assuming that there are no other inhibitory effects:

$$\mu = \mu_{max} \frac{[O_2]}{K_{s,O_2} + [O_2]} \cdot \frac{[C]}{K_{s,C} + [C]} \tag{8.1}$$

in which μ is the specific or relative growth rate (s^{-1}), μ_{max} is the maximum specific growth rate (s^{-1}), $K_{s,O2}$ and $K_{s,C}$ are the Monod substrate half-saturation constants for oxygen and carbon (mol/l), respectively and *[C]* is the concentration of the carbon substrate, all referring to the water phase (mol/l). Specific growth rates reach μ_{max} values if neither oxygen nor carbon is limiting growth. Substrate half-saturation constants are the concentrations of a limiting substrate at which half of the maximum specific growth rate is obtained, if other substrates are not limiting.

Eq. 8.1 can be used to determine the results of competition between heterotrophs and methanotrophs, using *[C]* is [CH_4] for methanotrophs and *[C]* is [CH_3COOH] for heterotrophs. We describe this outcome of short-term competition for oxygen between heterotrophs and methanotrophs by a critical oxygen concentration, *[$O_{2,crit}$]*. It is assumed that competition only takes place for oxygen and that, except for this substrate competition, there are no other interactions. *[$O_{2,crit,g}$]* is defined as the oxygen concentration at which the specific growth rates (subscript *g*) of heterotrophs (subscript *h*) and methanotrophs (subscript *m*) are equal. Assuming that carbon substrates are not limiting and using Eq. 8.1, *[$O_{2,crit,g}$]* is:

$$[O_{2,crit,g}] = \frac{\mu_{max,m} \cdot K_{s,O_2,h} - \mu_{max,h} \cdot K_{s,O_2,m}}{\mu_{max,h} - \mu_{max,m}} \tag{8.2}$$

More general, with limiting carbon substrates:

$$[O_{2,crit,g}] = \frac{\mu_{max,m} \cdot \dfrac{[CH_4]}{K_{s,C,m}+[CH_4]} \cdot K_{s,O_2,h} - \mu_{max,h} \cdot \dfrac{[CH_3COOH]}{K_{s,C,h}+[CH_3COOH]} \cdot K_{s,O_2,m}}{\mu_{max,h} \cdot \dfrac{[CH_3COOH]}{K_{s,C,h}+[CH_3COOH]} - \mu_{max,m} \cdot \dfrac{[CH_4]}{K_{s,C,m}+[CH_4]}} \quad (8.3)$$

However, it is not μ, but the absolute consumption rates of the substrate for which competition takes place that determines the results of competition. Neglecting the consumption for maintenance purposes (because maintenance costs were implicitly accounted for in our experimental set-up), the consumption rate (V in mol $l^{-1}s^{-1}$) is related to μ by:

$$V = \frac{\mu \cdot B}{Y} \quad (8.4)$$

in which B is the bacterial carbon (mol C_B/l) and Y is the apparent yield (mol C_B/mol C_S, with subscript s referring to 'substrate'). Analogously to the critical oxygen concentration for growth, a critical oxygen concentration for consumption, $[O_{2,crit,c}]$, can be defined at which both microbial groups consume equal amounts of oxygen:

$$[O_{2,crit,c}] = \frac{\mu_{max,m} \cdot B_m \cdot Y_h \cdot \dfrac{[CH_4]}{K_{s,C,m}+[CH_4]} \cdot K_{s,O_2,h} - \mu_{max,h} \cdot B_h \cdot Y_m \cdot \dfrac{[CH_3COOH]}{K_{s,C,h}+[CH_3COOH]} \cdot K_{s,O_2,m}}{\mu_{max,h} \cdot B_h \cdot Y_m \cdot \dfrac{[CH_3COOH]}{K_{s,C,h}+[CH_3COOH]} - \mu_{max,m} \cdot B_m \cdot Y_h \cdot \dfrac{[CH_4]}{K_{s,C,m}+[CH_4]}} \quad (8.5)$$

To win the short-term competition, it is thus not only necessary to have good growth kinetics, but also to have enough biomass and a good yield. For this study Y_m is estimated at average at 0.296 ± 0.078 mol C_B/mol C_S (Buchholz et al., 1995; Dedysh et al., 1998; Jørgensen, 1985; Jørgensen and Degn, 1983; Harwood and Pirt, 1972; Nagai et al., 1973; Sipkema et al., 1998) and Y_h as 0.375 ± 0.039 mol C_B/mol C_S (Gerritse et al., 1992; Pirt, 1965; Tros et al., 1996). Bacterial carbon is calculated from microbial numbers. It is assumed that methanotrophic numbers in the rhizosphere equal 10^8/g d.w. (section 8.4.3) and heterotrophic numbers equal 10^9/g d.w. (section 8.4.2). An average amount of $1.87 \cdot 10^{-13}$ g C/cell (Bratbak, 1985) is assumed for the heterotrophs. The amount of carbon in methanotrophs is decreased proportionally to their smaller size (calculated from the calibration curve of O.D. versus bacterial numbers (section 8.4.3)).

8.4 Results and discussion
8.4.1 Sinks for oxygen in a rice paddy soil
Overall oxidation rates
If oxygen was allowed into the bottles with soil slurries, a fast increase in oxidised products (NO_3^- and SO_4^{2-}) and a decrease of Fe^{2+} occurred. First order rate constants in day^{-1} were derived from the oxidation states (Table 8.1). Iron was oxidised much faster than sulphurous compounds as could be expected from thermodynamics. NH_4^+ was oxidised at a much lower rate and also much slower than found elsewhere (Table 8.1). This might be due to a limitation of NH_4^+, which concentrations were very low in our soil (data not shown). A first order rate approach might not have been valid for this situation. The rate constants calculated at 15°C and 20°C were only slightly smaller (<10%) than those at 30°C (data not shown), indicating that the oxidation rates were mainly influenced by chemical and not by microbial reactions.

Table 8.1:   Rate constants of oxygen consumption (in day⁻¹) for overall oxidation (as
               determined in a soil slurry experiment at 30 °C) and for microbial reoxidation (as
               determined from microbial enrichments). A comparison with published data on
               overall oxidation is given. (n.d.= not determined, n.s.=not significant)

	overall oxidation	microbial oxidation	overall published
nitrogen	0.023	0.015	18.6 [1,2]
iron	15	n.s.	41.5 [2,3,4,5]
sulphur	0.78	0.045	0.77 [2,4,5]
methane	n.d.	0.17	
acetate	n.d.	1.8	

[1]Soetaert et al., 1996; [2]van Cappellen and Wang, 1996; [3]Ahmad and Nye, 1990; [4]Murase and
Kimura, 1997; [5]Ratering and Conrad, 1998

Aerobic microbial communities

The results of the MPN counts at aerobic conditions are shown in Table 8.2. The
number of bacteria found at 20% O_2 was significantly different ($P<0.05$) and orders of
magnitude larger than at 1% O_2 after 10 weeks of incubation. This might imply that 10
weeks is not enough to estimate the population size able to grow at 1% O_2 (details in
section 8.4.3). The population sizes estimated at 1% O_2 and 1 and 30 mM acetate,
respectively, were not significantly different, indicating that the oxidation of compounds
other than acetate was mainly carried out by autotrophic organisms.

Table 8.2:   Most Probable Number (MPN) estimates for various conditions in number of
               bacteria/g d.w. soil after stabilisation of the number and at most after 10 weeks
               of incubation at 30 °C.

Bacterial group	MPN at 1% O_2 1 mM acetate	MPN at 1% O_2 30 mM acetate	MPN at 20% O_2 30 mM acetate
Heterotrophs	3.10^5	10^6	10^9
Methanotrophs	10^7	3.10^6	10^7
NH_4^+ oxidisers	10^3	0	3.10^5
$S_2O_3^{2-}$ oxidisers	3.10^5	10^5	10^6
Fe^{2+} oxidisers	0	0	0

Heterotrophs and methanotrophs were the most abundant groups at all conditions
(Table 8.2). All other microbial groups seemed to play only a minor role in the
consumption of oxygen in the rice rhizosphere. Conditions for both heterotrophs and
methanotrophs are good in the rice rhizosphere. Methane concentrations are high due to
anaerobic conditions, while oxygen diffuses into the soil, yielding good conditions for
methanotrophs. Heterotrophs can make use of diverse carbon sources, of which various
fatty acids and especially acetate are abundant in rice soils (e.g. Chin and Conrad, 1995;
Chapter 5) and near decaying rice roots (Conrad and Klose, 1999). Their potential
growth rates are high (see section 8.4.3) and some heterotrophs can denitrify at anaerobic
conditions. This combination explains why numbers of heterotrophic bacteria are high in
rice soil (this study; Gilbert and Frenzel, 1998; Watanabe et al., 1979).
Ammonia oxidation can take place by nitrifiers and by methanotrophs (which have some
affinity for ammonia). At 20% O_2, methane oxidation was more important than the total

ammonia oxidation, which might indicate that nitrifiers were less abundant than methanotrophs, in agreement with results found by others (Bodelier and Frenzel, 1999; Kumaraswany et al., 1997). At low oxygen concentrations, hardly any ammonia oxidation was found. At 1% O_2 mainly heterotrophic respiration was found. Probably, the difference in respiration rates between acetate and ammonia oxidation was not due to the lower affinity of ammonia oxidisers, but due to the higher number of heterotrophs outcompeting ammonia oxidisers (Bodelier and Laanbroek, 1997) and scavenging most of the available oxygen. This also means that ammonia oxidisers will play only a minor role in the rice rhizosphere, because at the low oxygen concentrations, they will be outcompeted by the heterotrophs and the contribution of ammonia oxidisers to methane oxidation seems negligible (Bodelier and Frenzel, 1999). Moreover, NH_4^+ concentrations in the rice rhizosphere are usually less than 0.5 mM (Bodelier and Frenzel, 1999; Gilbert and Frenzel, 1998), further limiting the role of ammonia oxidation.

Thiosulphate oxidisers were found to be present at all conditions (and in similar numbers as found by Stubner et al. (1998)), but they were present in lower numbers than the methanotrophs and heterotrophs. The MPN counts at low oxygen and low acetate concentrations (Table 8.2) indicate that thiosulphate was mainly oxidised autotrophically. Many colonies were formed on purified agar with thiosulphate and without acetate (data not shown).

Contrary to other reports (Emerson and Moyer, 1997; Emerson et al., 1999), no iron oxidation (different from chemical oxidation) could be detected in the MPN counts, neither with nor without acetate addition. Even in gradient tubes, no differences in oxygen and iron profiles between inoculated and sterile tubes could be detected (data not shown). Chemical iron oxidation proceeded much faster than microbial oxidation. Microbial iron oxidation can thus be neglected compared to chemical oxidation.

Microbial oxygen consumption rates

Oxygen consumption by enrichments was, similar to overall oxidation rates, expressed by first order rate constants (Table 8.1). Rate constants for ammonia, thiosulphate and ferrous iron were much smaller than those found for chemical oxidation. Nitrifiers have a low potential growth rate (Hunik et al., 1994), which might explain the low rate constant found for NH_4^+ oxidation. Microbial thiosulphate oxidation was also much lower than the overall oxidation, which is in contrast to what has been found by Stubner et al. (1998). Thus, the contribution of chemical and microbial processes to thiosulphate oxidation cannot be given. No microbial iron oxidation was found in the enrichments.

Based on the rate constants, heterotrophic respiration and methanotrophic respiration seem the most important microbial sinks of oxygen. Oxidation rates expressed as an initial activity per bacterium showed similar results (data not shown).
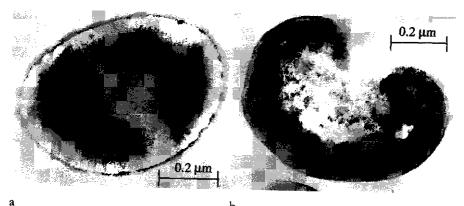

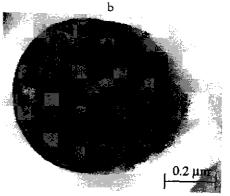### 8.4.2 Culture isolation and characterisation

Based on the first experiments, the two most important oxygen consuming microbial groups, the heterotrophs and methanotrophs, were selected for further experiments. Heterotrophs and methanotrophs from the highest dilution with growth were enriched and isolated in NMS-medium with acetate and CH_4 as sole C-source, respectively.

Two species of heterotrophic microorganisms were isolated. Strain *HET-1* is a gram negative, oxidase positive, motile straight rod of 0.8-1.0 by 1.4-1.8 μm. It forms small colonies with a smooth, white and viscous appearance on plates. The organism grows on NMS medium with nitrate as sole nitrogen source and acetate, ethanol, glucose, citrate, lactose or fumarate as sole C-source at 30 °C. The organism can also decompose urea, arginine, lysine, ornithine and tryptophane at 30 °C. At anaerobic conditions, the organism can denitrify nitrate (both in liquid and agar NMS media), but it cannot grow fermentatively or by the reduction of sulphurous compounds. The organism is able to grow at 10-37 °C and does not grow at 45 °C. A comparison of the partial 16S DNA analysis of the isolate with the GenBank showed as the highest score 99% association with various strains of *Pseudomonas stutzeri*, which is in accordance with the physiological characteristics (Krieg, 1984). Below, the isolate will be referred to as *Pseudomonas strain HET-1*.

Strain *HET-2* is a gram positive, oxidase negative, non-motile straight rod, sometimes occurring in pairs and measuring 0.8-1.0 by 1.1-1.4 μm. On plates, it forms small colonies with a red, viscous appearance, a rough edge and branches. The organism grows on NMS medium with nitrate as sole nitrogen source and acetate, ethanol, glucose, citrate or fumarate as sole C-source. Lactose does not support growth. The organism can also decompose arginine, lysine and ornithine, but not tryptophane and urea at 30 °C. At anaerobic conditions, the organism cannot denitrify or reduce sulphurous compounds and it cannot grow fermentatively. However, it appears to be able to grow at microaerophilic conditions, because it can grow several centimeters below an agar surface. The organism grows between 10 and 37 °C, but does not grow at 45 °C. A comparison of the partial 16S DNA analysis of the isolate with the GenBank showed as the highest score 99% association to *Rhodococcus erythropolis* and *Rhodococcus erythreus*. The physiological characteristics are in accordance with those of *Rhodococcus* (Goodfellow and Minnikin, 1991; Krieg, 1984). Below it will be referred to as *Rhodococcus HET-2*.

One methanotrophic strain that grows in NMS medium with methane as sole C-source and nitrate as sole N-source was isolated from the highest dilution with methanotrophic growth. The organism is a non-motile, gram negative organism with a coccoid and reniform appearance. It has no flagellae, as can be seen on the negatively stained preparation (Figure 8.2a). The average size is 0.4-0.6 by 0.7-1.0 μm. On plates, it forms small round, smooth and butyrous colonies with white/light yellowish appearance. The growth in liquid media is evenly dispersed and the organisms are routinely grown at 30 °C. Cells have a few layers of paired internal membranes located along the cytoplasmatic membrane. The membranes are mostly stacked, but sometimes there are spaces between the membranes. Based on these observations (Figure 8.2b), the membranes were identified as Type II membranes (Davies and Whittenbury, 1971). Polyphosphate accumulates in the cytosol (Figure 8.2c). Based on this morphology, the organism was tentatively identified as *Methylocystis* (using Bowman et al., 1993) and will be called *Methylocystis MOX-1* in this paper. A domination of a type II methanotroph in the MPN counts is also expected based on the dynamics in a rice paddy. Type II organisms are better survivors at dry conditions and can utilise lower oxygen (Amaral and Knowles, 1995) and nitrogen concentrations than type I methanotrophs (Graham et al., 1993). Type II outcompete type I methanotrophs at high methane concentrations (Graham et al., 1993). This expectation is in accordance with other studies that isolated type II

Methylosinus species (Bowman et al., 1993; Dianou and Adachi, 1999) and Methylocystis species (Takeda, 1988) from rice paddies. Type II methanotrophs prevailed in rice paddies (le Mer et al., 1996; Henckel et al., 1999). In rice roots, type II methanotrophs were also the dominating methane oxidisers (Calhoun and King, 1998) and Gilbert et al. (1998) isolated only type II methanotrophs from rice roots.

a   b
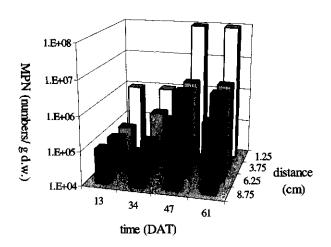
c

Figure 8.2: Transmission Electron Microscope preparations of the methanotrophic isolate showing a) a negatively stained preparation for flagellae determination, b) cytoplasmic membranes and c) accumulation of polyphosphate inside the cell.

8.4.3 Determination of kinetic parameters

MPN counts for methane oxidation in the rhizosphere

The spatial and temporal growth dynamics of methanotrophs was investigated by MPN counts. Methanotrophic numbers increased during the growing season and decreased with distance from the main stem (Figure 8.3). This is directly related to the availability of oxygen. More oxygen becomes available in time due to root growth and its root oxygen release. Oxygen availability is less at a larger distance from the main rice stem, because of lower root densities at larger distances. This shows that oxygen availability, and not methane availability, is limiting growth of methanotrophs. The number of methanotrophs was therefore larger in the rhizosphere than in the bulk soil, in

accordance with data presented by others (e.g. de Bont et al., 1978; Gilbert and Frenzel, 1995; 1998).

Figure 8.3:   Most Probable Number of methanotrophs at different moments during the growing season (given in Days After Transplanting (DAT)) and at different distances from the main stem of the plant.

Concomitantly with the number of methanotrophs, a significant change in maximum methane oxidation rate was found both in time and with distance from the main rice stem (data not shown). Methane oxidation was thus related to methanotrophic growth. In this experiment, higher numbers of methanotrophs were found than reported by others (10^4-4.10^6/g d.w.) using incubation periods varying between 3 and 8 weeks (Bodelier and Frenzel, 1999; Bosse and Frenzel, 1997; Espiritu et al., 1997; Gilbert and Frenzel, 1995; Joulian et al., 1997). The number of methanotrophs obtained after 5 months were similar to those after 4 months. MPN counts after 5 months were, however, on average one order of magnitude higher than those obtained after 2 months of incubation (data not shown), although spatial and temporal differences were large. The total number of methanotrophs can thus be underestimated using a 2 months incubation period.

Pure culture experiments

The dynamics in MPN counts implies that growth kinetics has to be included to allow a good understanding of the microbial competition for oxygen. Microbial growth in the batch experiments was assessed by O.D. measurements. The O.D. was linearly related to the number of microorganisms, measured with the Bürker-Türk counting cells (Figure 8.4). Specific growth rates obtained from the bacterial number dynamics were related to the average limiting substrate concentration during the sampling interval (Figure 8.5). The Monod substrate half-saturation constants for microbial growth (K_s in mol/l) and the maximum specific growth rate (μ_{max} in h^{-1}) were fitted for each microorganism and

each limiting substrate combination by minimising the Mean Square Error between experimental data and fit (Tables 8.3 and 8.4). The R^2 of the fit was in all cases >0.65 and modelled and measured μ values were not significantly different (P<0.05), although there is some scatter in the data because a continuous process was monitored in a discontinuous batch experiment. The μ_{max} values determined with different limiting substrates were similar (Tables 8.3 and 8.4).
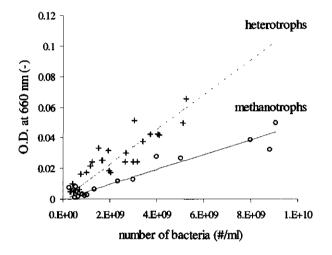
Figure 8.4: Calibration of the Optical Density (O.D.) measurements with the direct counts of bacterial numbers using the Bürker-Türk counting cells for methanotrophs and heterotrophs.

The K_s values determined in these batch experiments are comparable with values presented by others (Tables 8.3 and 8.4), although variability among published values is large (see section 8.4.4). μ_{max} values determined in this batch experiment are lower than average published values, especially the μ_{max} of methanotrophs is at the lower end of the measured values. μ_{max} values might have been decreased, because the microorganisms have been enriched, isolated and routinely grown at low oxygen concentrations to mimic rice rhizosphere conditions.

BOM experiments
The μ_{max} for *Rhodococcus HET-2* was validated by BOM experiments at acetate limiting conditions. The μ_{max} calculated from this experiment was 0.12±0.03 h^{-1}, which is consistent with the values measured in the batch experiments. The μ_{max} is thus comparable for all experimental conditions.
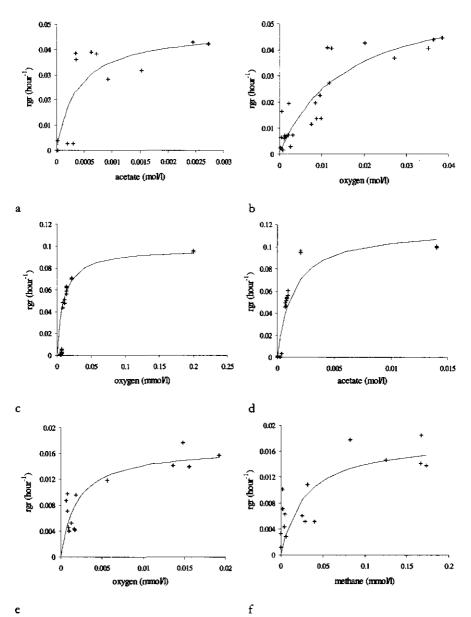
Figure 8.5:   Relative growth rates μ (rgr) of a-b) *Pseudomonas HET-1*, c-d) *Rhodococcus HET-2* and e-f) *Methylocystis MOX-1* at oxygen and carbon limited conditions, respectively. Note the different scales.

<u>Table 8.3</u>: Monod half-saturation constants for microbial growth (K_s in mol/l water) for oxygen (O_2) and acetate (Ac) and the maximum specific growth rate (μ_{max} in h^{-1}) for heterotrophic pure cultures.

|	$K_{s,O2}$ (in M)	$K_{s,Ac}$ (in M)	μ_{max} (in h^{-1})
Pseudomonas HET-1 C-limited	n.d.	0.36 10^{-3}	0.054
Pseudomonas HET-1 O$_2$-limited	15 10^{-6}	n.d.	0.062
Rhodococcus HET-2 B.O.M.	n.d.	n.d.	0.12
Rhodococcus HET-2 C-limited	n.d.	1.3 10^{-3}	0.12
Rhodococcus HET-2 O$_2$-limited	9.0 10^{-6}	n.d.	0.098
Published pure cultures	9.4 10^{-6} [1,2,3,4,6,7]	0.58 10^{-3} [8,9,11]	0.23 [1,2,5,9,10]

[1]Bodelier and Laanbroek, 1997; [2]Gerritse and Gottschal, 1993; [3]Sipkema et al., 1998; [4]Krooneman et al., 1996; [5]Robertson and Kuenen, 1984; [6]Geraats et al., 1990; [7]Sharma and Ahlert, 1977; [8]Gerritse et al, 1992; [9]Tros et al., 1996; [10]Iwahori et al., 1995; [11]Blackall et al., 1991

<u>Table 8.4</u>: Monod half-saturation constants for microbial growth (K_s in mol/l water) for oxygen (O_2) and methane (CH_4) and the maximum specific growth rate (μ_{max} in h^{-1}) for methanotrophic pure cultures.

	$K_{s,O2}$ (in M)	$K_{s,CH4}$ (in M)	μ_{max} (in h^{-1})
Methylocystis MOX-1 C-limited	n.d.	28 10^{-6}	0.018
Methylocystis MOX-1 O$_2$-limited	1.9 10^{-6}	n.d.	0.017
Published pure cultures	6.7 10^{-6} [1,2,3,5]	29 10^{-6} [2,4,5,7,8]	0.12 [2,3,5,6,7,8]
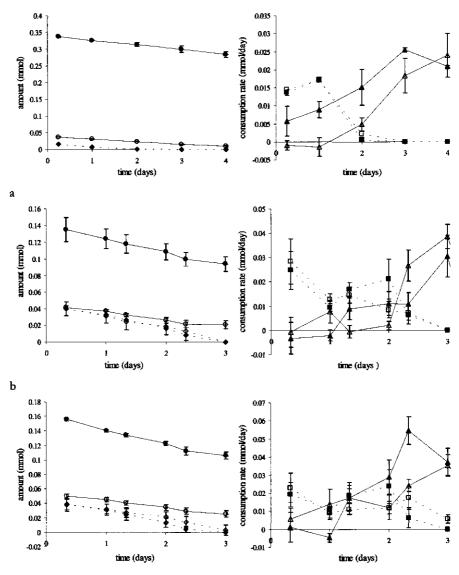
[1]Jørgensen, 1985; [2]Harwood and Pirt, 1972; [3]Gerritse and Gottschal, 1993; [4]O'Neill and Wilkinson, 1977; [5]Nagai et al., 1973; [6]Amaral and Knowles, 1995; [7]Graham et al., 1993; [8]Sipkema et al., 1998

8.4.4 Competition for oxygen between methanotrophs and heterotrophs
Competition experiments
The batch experiments showed a lower $K_{s,O2}$ and μ_{max} for methanotrophs, compared to the heterotrophic cultures. Based on these characteristics it is expected that methanotrophs will only win the competition for oxygen with the heterotrophs at very low oxygen concentrations. This hypothesis was tested in competition experiments with equal numbers of *Methylocystis MOX-1* and *Pseudomonas HET-1* at different methane concentrations and low (around $K_{s,O2}$ for both organisms, expecting the most severe competition) and high oxygen concentrations.
In all competition experiments, methane consumption rates increased after competition for oxygen had stopped and all acetate was consumed (Figure 8.6). This increase is partly due to growth of the methanotrophs, which leads to increased biomass that can consume methane. However, the absence of competition for oxygen after all acetate was consumed is probably more important. At high oxygen concentrations, methane consumption rates already increased before all acetate was depleted -due to less severe competition for oxygen. At low oxygen concentrations methane consumption was suppressed for a longer period and to lower acetate concentrations. Only at both high methane concentrations and low oxygen concentrations, methane consumption rates increased earlier (Figure 8.6c). Competition for oxygen was thus limiting methane oxidation rates.

a

b

c

Figure 8.6:   Competition for oxygen between methanotrophs and heterotrophs at initially a)
                2 mmol CH_4/l gas, b) 5 mmol CH_4/l gas and c) 10 mmol CH_4/l gas and at
                initial concentrations of 0.5 mmol O_2/l gas (open symbols) and 2-4 mmol O_2/l
                gas (closed symbols). Indicated are the amount of oxygen (circles) and of acetate
                (diamonds) and the consumption rates of methane (triangles) and of acetate
                (squares). Note the different scales.

Acetate consumption rates were higher than methane consumption rates, as long as
acetate was present. Acetate consumption rates were only slightly suppressed at high
methane concentrations. *Pseudomonas HET-1* is thus a better competitor than *Methylocystis*

MOX-1, which is reflected in the μ_{max} values of the organisms. An exception occurred at non-limiting carbon concentrations in combination with low oxygen concentrations when *Methylocystis MOX-1* had higher consumption rates (Figure 8.6c). In that case, the Monod equation predicts that the $K_{s,O2}$ value determines the outcome of the competition. The ratio of acetate consumption rate to methane consumption rate was indeed found to be significantly -at $P<0.05$- correlated to oxygen concentration (data not shown). It is expected that significant methane oxidation can only occur in the rice rhizosphere at low oxygen and high methane concentrations.

Theoretical description of competition
The Monod parameters obtained in the batch experiments (section 8.4.3) were used to calculate the critical oxygen concentrations at which specific growth rates for each microbial group were equal (Eq. 8.3). A negative oxygen concentration was calculated for the competition between *Rhodococcus HET-2* and *Methylocystis MOX-1* at non-limiting carbon concentrations, which indicates that *Rhodococcus HET-2* outcompetes *Methylocystis MOX-1* at all oxygen concentrations at these conditions. This is caused by the much higher μ_{max} for *Rhodococcus HET-2*. A $[O_{2,crit,g}]$ of 3.8 μM was calculated for the competition between *Pseudomonas HET-1* and *Methylocystis MOX-1* at non-limiting carbon concentrations. At lower oxygen concentrations, the methanotroph obtained higher specific growth rates, while the opposite was true for higher oxygen concentrations.

The results for $[O_{2,crit,g}]$ at methane concentrations from 0 μM to saturation and acetate concentrations from 0-1 mM are shown in Figure 8.7a,b. $[O_{2,crit,g}]$ was in general not very sensitive to the methane concentration. Only at very low methane concentrations, $[O_{2,crit,g}]$ decreased. A $[O_{2,crit,g}]$ of 20 μM or higher was calculated for most acetate concentrations (5-30 μM) in rice paddies in the methanogenic phase (Achtnich et al., 1995b; Frenzel et al., 1999). Such oxygen concentrations are regularly found in the rice rhizosphere (Frenzel et al., 1992; Gilbert and Frenzel, 1995; 1998; Revsbech et al., 1999), implying that specific growth rates of methanotrophs can be similar to those of heterotrophs, although μ_{max} for the heterotrophs was much higher (Tables 8.3 and 8.4). At low acetate concentrations, $[O_{2,crit,g}]$ was slightly lower for the competition with *Pseudomonas HET-1* than for *Rhodococcus HET-2*, because of the lower $K_{s,C}$ for *Pseudomonas HET-1*. At high acetate concentrations, $[O_{2,crit,g}]$ was higher for the competition with *Pseudomonas HET-1* than with *Rhodococcus HET-2*, because of the lower μ_{max} of *Pseudomonas HET-1*. Only at oxygen concentrations lower than $[O_{2,crit,g}]$, methanotrophs had a higher μ than heterotrophs.

$[O_{2,crit,c}]$ dynamics as a function of methane and acetate (Eq. 8.5) for a situation of equal biomass were similar to the situation calculated in Figure 8.7a,b and had only slightly higher values (data not shown). These slightly higher values are caused by the (slightly) lower yield values for methanotrophs. In correspondence with the competition experiments (section 8.4.4), growth of methanotrophs was strongly suppressed at high acetate concentrations. The oxygen concentrations in the competition experiments were regularly higher than $[O_{2,crit,c}]$ which explains why acetate consumption rates were higher than methane consumption rates in the competition experiments. Only at low oxygen concentrations and non-limiting carbon concentrations, for which a $[O_{2,crit,c}]$ of 6 μM was calculated in competition with *Pseudomonas HET-1*, the consumption rates of the methanotrophs were higher.

The situation changed dramatically when actual biomass estimates were used to calculate $[O_{2,crit,c}]$. With non-limiting carbon concentrations, a negative $[O_{2,crit,c}]$ was calculated, indicating that methanotrophs were outcompeted by the heterotrophs at all oxygen concentrations. At acetate limiting conditions (and no methane limitation) the $[O_{2,crit,c}]$ became positive at acetate concentrations lower than 53 and 56 µM for *Pseudomonas HET-1* and *Rhodococcus HET-2*, respectively. Again, methane concentrations hardly had any influence on $[O_{2,crit,c}]$ as shown in Figure 8.7c,d. Biomass estimates are thus of major importance for the estimation of competition outcomes.

a   b

c   d
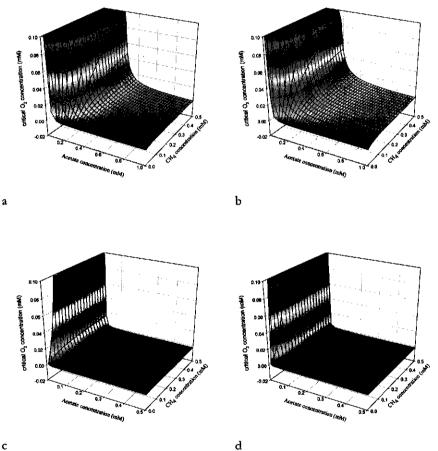
Figure 8.7:   Critical oxygen concentration for competition between *Methylocystis MOX-1* and heterotrophs- *Pseudomonas HET-1* (b,d) and *Rhodococcus HET-2* (a,c)- for a,b) specific growth rates and c,d) consumption rates.

All parameters to calculate $[O_{2,crit,c}]$ are more or less uncertain. The estimates of μ_{max} and K_s are not very precise, given their dynamic nature and experimental errors. The coefficients of variation in these parameters were estimated from published data referred

to in Tables 8.3 and 8.4. Standard deviations for yield are given in section 8.3 and it was estimated that the coefficient of variation in B is 50%. A Monte Carlo approach (Keesman and van Straten, 1990) of 1000 runs varying all parameters within the ranges given by their coefficients of variation and assuming an acetate concentration of 50 μM and non-limiting methane concentrations was carried out. The overall $[O_{2,crit,c}]$ was 3 ± 7 μM (default 0.13 μM) for competition with *Pseudomonas HET-1*. In 42% of the combinations, methanotrophs were outcompeted by *Pseudomonas HET-1* and $[O_{2,crit,c}]$ of the remaining combinations was 7 ± 8 μM. This analysis shows that, even though variability in the parameters is large, the range of $[O_{2,crit,c}]$ estimates is limited. The conclusions drawn for the default settings can thus be applied more generally.

8.5 Concluding remarks

In this study the competition for oxygen between methanotrophs and other oxygen sinks was determined. Incubation studies showed that microbial oxygen consumption was dominated by heterotrophic and methanotrophic respiration. Besides these microbial oxygen sinks, chemical iron oxidation was important. The most abundant methanotrophs and heterotrophs were isolated and growth kinetic parameters were determined. Based on the determined parameters -in combination with kinetic data by others- the competition between heterotrophs and methanotrophs was quantified experimentally and theoretically.

A basic assumption in this study is that methane oxidation rates are limited by oxygen. Such a limitation appeared to be present in the MPN counts of the methanotrophs and is in accordance with other studies (Bosse and Frenzel, 1997; Calhoun and King, 1997; King, 1996). The theoretical calculations showed indeed that methane concentrations hardly limited methanotrophic consumption rates. Another assumption is that the data for the most abundant microorganisms can be extrapolated to overall methane oxidation kinetics. The fact that the determined affinity constants were similar to average affinity constants presented by others supports that this extrapolation might be correct.
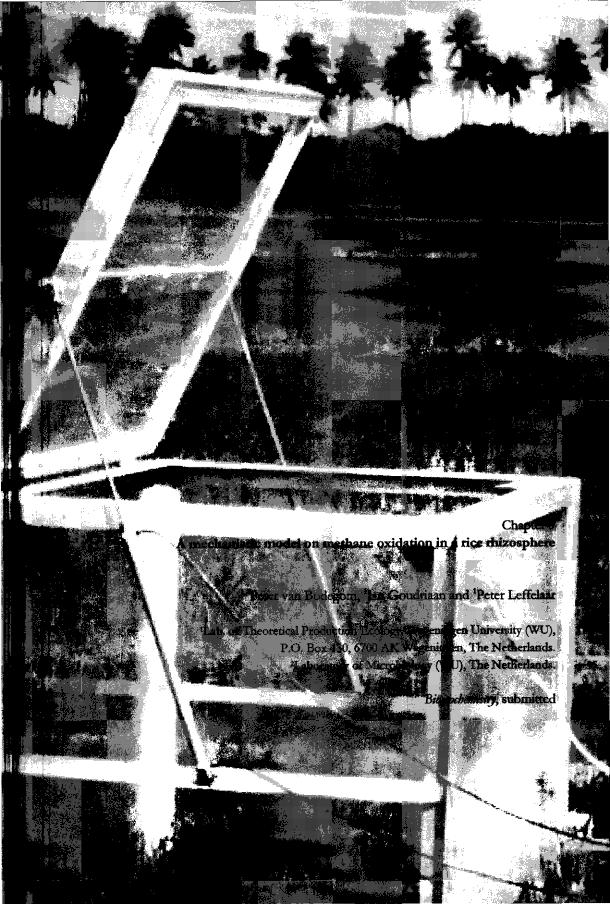
Both competition experiments and theoretical calculations on competition showed that methanotrophs outcompeted heterotrophs only at low oxygen concentrations, due to their lower $K_{s,O2}$. At higher oxygen concentrations, except at very low acetate concentrations, methanotrophs were outcompeted, mainly due to their lower μ_{max}. Based on these observations and the presence of easily accessible carbon substrate in rice fields, it is expected that methane oxidation rates at the root surface will be very low, except if oxygen availability is not limiting methane oxidation rates at the root surface. Methanotrophs have been found at the rice root surface (Bosse and Frenzel, 1997; Calhoun and King, 1998) and inside the rice root (Gilbert et al., 1998; Watanabe et al., 1997), but they were less abundant on the root than in the rhizosphere (Gilbert and Frenzel, 1998). Probably, heterotrophs will consume most oxygen close to the root surface, while methanotrophs will be active a bit further away from the root surface at lower oxygen concentrations. Methane oxidation efficiency at the soil-water surface is probably higher than in the rhizosphere, because of the lower acetate concentration in the bulk soil in combination with the longer residence time of methane in the microaerophilic zone.

The necessity of low oxygen and low acetate concentrations was accentuated when actual biomass estimates were included. Heterotrophic biomass was higher than

methanotrophic biomass. Methane oxidation was further restricted to areas with low oxygen and low acetate concentrations. Methane oxidation will thus only occur at microaerophilic conditions. The large influence of microbial biomass on the competition outcome shows that prediction of methane oxidation rates will be difficult, unless actual biomass is measured. Predictions of biomass dynamics have limited accuracy as long as quantitative general information on microbial biomass maintenance and survival strategies, as presented for methanotrophs by Roslev and King (1994; 1995) are scarce.

The high variability of in-situ microbial biomass and substrate concentrations found in the rice rhizosphere, in combination with the sensitivity of the outcome of competition for these variables, indicates that the high variability found in rhizospheric methane oxidation rates might be real. Methane oxidation will be most effective at low oxygen and low acetate concentrations. Insight in microbial biomass dynamics limits a more precise prediction of its dynamics.

A mechanistic model on methane oxidation in a rice rhizosphere

Peter van Bodegom, Jan Goudriaan and [1]Peter Leffelaar

Lab. of Theoretical Production Ecology, Wageningen University (WU),
P.O. Box 430, 6700 AK Wageningen, The Netherlands.
[1]Laboratory of Microbiology (WU), The Netherlands.

A mechanistic model on methane oxidation in a rice rhizosphere

Abstract

In this paper, a mechanistic model is presented on the processes leading to methane oxidation in rice rhizosphere. The model is driven by oxygen release from a rice root into an anaerobic rice soil. Oxygen is consumed by heterotrophic and methanotrophic respiration, described by double Monod kinetics, and by chemical iron oxidation, described by a second order reaction. Production of substrates for these reactions -ferrous iron, acetate and methane- are described by an exponential time dependent organic matter mineralisation in combination with modified Michaelis Menten kinetics for the competition for acetate and CO_2/H_2. Compounds diffuse between the rhizosphere, root and atmosphere. An extra diffusion resistance between the rice root and shoot is included as well as active transport across the root surface for root exudation and plant nutrient uptake. Iron adsorption is described dependent on pH. The model predicts root oxygen release, compound gradients and compound concentrations in a rice rhizosphere well. Also methane oxidation estimates are comparable to experimental estimates. A sensitivity analysis showed however that methane oxidation is highly dependent on model initialisation and parameterisation. Equilibrium is not obtained within the period that a single root influences a soil microsite. The equilibrium is moreover dependent upon the diffusion resistance across the root surface. Methane oxidation depends thus on root growth dynamics and is therefore highly variable in space and time. Methane oxidation dynamics appears differently whether it is expressed per methane produced or per methane lost by emission or oxidation. This difference is caused by the non-equilibrium conditions that result in a large change in methane storage. A general prediction of methane oxidation is very difficult given the high variability and the lack of knowledge to allow prediction of this variability.

9.1 Introduction

Rice paddies are suspected to contribute substantially to the increasing atmospheric methane concentration. Methane emission reflects the balance between methane production and oxidation. Methane oxidation in rice paddies occurs at the soil-water interface and in the rhizosphere, where both oxygen and methane are available. Methane oxidation rates in the rhizosphere are highly variable and plant mediated transport is the dominant methane emission pathway (Schütz et al., 1989b). A better mechanistic understanding of rice rhizospheric methane oxidation is thus important for a good prediction of global methane emissions.

Various processes determine rhizospheric methane oxidation (schematically represented in Figure 9.1). Methane is produced at anaerobic sites in a rice paddy by methanogens, which compete for carbon substrates with microorganisms that use alternative electron acceptors of which iron oxides are the most important (Chapter 5; Inubushi et al., 1984). Carbon substrates become available via soil organic matter mineralisation, root decomposition and root exudation (Chapter 2). Root exudates diffuse towards the

anaerobic sites. Methane diffuses towards the root surface and is released into the atmosphere through aerenchyma channels present in rice roots and shoots (Nouchi and Mariko, 1993). Oxygen diffuses through the same aerenchyma channels into the soil - root oxygen release- while part of the oxygen is already consumed in the roots by root respiration (Ando et al., 1983). Methane oxidation can occur at sites where methane and oxygen concentration profiles overlap. Methanotrophs have to compete for the available oxygen with other processes, of which heterotrophic respiration and chemical iron oxidation are most important (Chapter 8). Chemical iron oxidation again depends on adsorbed iron and pH (Kirk et al., 1990) and thus on CO_2 production and plant nutrient uptake.
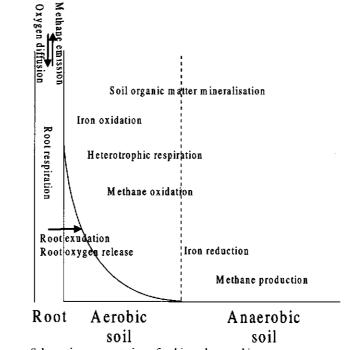
Figure 9.1:   Schematic representation of a rhizosphere and its processes

Various models have been developed for some of the processes mentioned above. Some process-based methane emission models describe organic substrate production and methane production (e.g. Cao et al., 1995), but do not consider competition with alternative electron acceptors (Arah and Stephen, 1998; Cao et al., 1995; Walter et al., 1996). Cao et al. (1995) treats methane oxidation as a fraction of methane production and Walter et al. (1996) assumes no oxygen limitation on methane oxidation. A kinetic model describing methane oxidation in rice paddies (Cai and Yan, 1999) neither assumes oxygen limitation of methane oxidation nor includes methane production. Grant (1999) and Ridgwell et al. (1999) presented methane oxidation models that can only be used in aerobic soils without plants and are therefore not suitable for rice paddies. Armstrong and Beckett (1987) presented a mechanistic model on oxygen dynamics within an aerenchymous root, but included no rhizospheric oxygen dynamics. Available

rhizosphere models describe iron dynamics (Jones et al., 1996; Kirk, 1993) or dynamics of heterotrophic respiration (Darrah, 1991a,b; Newman and Watson, 1977), but no methane oxidation. The most comprehensive rhizosphere model that can be used to estimate methane oxidation is described by Segers (2000), that was developed for wetland plants. Parameterisation of wetland dynamics is very complicated and Segers (2000) therefore simplified electron acceptor dynamics, soil organic matter mineralisation, heterotrophic respiration and root gas transport. This makes the model of Segers (2000) less suitable for a mechanistic understanding of methane oxidation dynamics.

None of the described models are thus directly suitable for a mechanistic description of methane oxidation in rice rhizosphere. In this paper we describe a mechanistic model on methane oxidation in rice rhizosphere using available information on all underlying processes shown in Figure 9.1. Model predictions are compared with other models and with in-situ measurements. A model sensitivity analysis is presented to determine the variability in modelled methane oxidation as a function of the underlying processes and to improve the mechanistic understanding of methane oxidation in a rice rhizosphere.

9.2 Model description

The mechanistic model describes the kinetics of aerobic oxidation of the most important electron donors and the diffusion of those electron donors from a rice root surface and their release within a rice rhizosphere. Transport within the rhizosphere and the release of gaseous compounds via the root to the atmosphere is described. Methane oxidation in a rice rhizosphere system can be simulated mechanistically with this combination of kinetics and transport.

Aerobic oxidation

Methane oxidation in rice rhizosphere is oxygen limited (Chapter 8). It is therefore of prime importance to estimate the dynamics of oxygen consumption processes properly. Although denitrifiers can outcompete rice plants for nitrate (Reddy and Patrick, 1986), denitrification is a minor soil sink of reducing equivalents because nitrate concentrations are low and denitrification is negligible in unfertilised rice paddies (Arth et al, 1998). Nitrifying bacteria are outcompeted by plant roots and heterotrophs at limiting amounts of ammonia (Reddy et al., 1989; Verhagen et al., 1995). Sulphur oxidisers have been found in rice rhizosphere (Stubner et al., 1998) and sulphate concentrations are significantly higher in rice rhizosphere in comparison with the bulk soil (Dannenberg and Conrad, 1999; Wind et al., 1995), but sulphur oxidation rates are lower than other oxidation rates (Chapter 8). The most important oxygen sinks in a rice rhizosphere are therefore chemical iron oxidation (Eq. 9.1), microbial methane oxidation (Eq. 9.3) and microbial heterotrophic respiration (Eq. 9.4) (Chapter 8).

$$4Fe^{2+} + O_2 + 10H_2O \text{->} 4Fe(OH)_3 + 8H^+ \tag{9.1}$$

Iron oxidation rate, R_{Feox} (mol m^{-3} water s^{-1}), is given by (Ahmad and Nye, 1990):

$$R_{Feox} = k \cdot [Fe_s^{2+}] \cdot [O_2] \tag{9.2}$$

in which k is the iron oxidation constant ($0.344.10^{-3}$ m^3 mol^{-1} s^{-1}, according to Ahmad and Nye (1990)), subscript s reflects that iron is adsorbed to clay particles. [...] represents a compound concentration in the water phase (mol m^{-3}) and is corrected for the

solubility in the gas phase, if appropriate. Similarly to Kirk et al. (1990), only fast iron oxidation is considered in this study. 0.25 moles of O_2 are consumed during the oxidation of one mol of ferrous iron.

Heterotrophic respiration is simplified to oxidation of acetate, because acetate is the most important organic acid in rice soils (e.g. Chin and Conrad, 1995; Sigren et al., 1997) and around decaying rice roots (Conrad and Klose, 1999).

$$CH_4 + (2-\alpha_m)O_2 \rightarrow (1-\alpha_m)CO_2 + (2-\alpha_m)H_2O + \alpha_m<CH_2O>_m \tag{9.3}$$

$$CH_3COO^- + H^+ + 2(1-\alpha_h)O_2 \rightarrow 2(1-\alpha_h)CO_2 + 2(1-\alpha_h)H_2O + 2\alpha_h<CH_2O>_h \tag{9.4}$$

in which $<CH_2O>$ represents a simplified description of microbial biomass. α is a reaction coefficient which is numerically equal to the microbial yield Y (in mol microbial carbon per mol carbon consumed) and is estimated from a data compilation (Chapter 8). Subscript $_m$ indicates methanotrophs and subscript $_h$ indicates heterotrophs. Microbial growth is taken proportional to biomass and the specific growth rate μ (s^{-1}) is expressed by Double Monod kinetics as:

$$\mu_i = \mu_{\max,i} \frac{[O_2]}{K_{sO2_i} + [O_2]} \cdot \frac{[C_i]}{K_{sC_i} + [C_i]} \tag{9.5}$$

in which μ_{max} is the maximum specific growth rate (s^{-1}), K_s is the affinity constant for a compound (mol m^{-3}) (values from a data compilation (Chapter 8)) and C_i stands for methane or acetate for methanotrophs or heterotrophs, respectively. Total microbial oxygen consumption is not only influenced by growth, but also by maintenance and growth independent microbial decay. These processes are usually neglected in experiments in which kinetic parameters are measured and are thus implicitly incorporated into these parameters. This allows to define microbial oxygen consumption rate, $R_{O2,i}$ (mol O_2 m^{-3} water s^{-1}), as:

$$R_{O2_i} = \mu_i \cdot B_i \cdot \frac{v_i - \alpha_i}{\alpha_i} \tag{9.6}$$

in which B is the microbial biomass (mol C m^{-3}) and v is a stoichiometry coefficient, which is 2 and 1 for methanotrophs and heterotrophs, respectively. Microbial carbon substrate consumption, R_{C_i} (mol C m^{-3} water s^{-1}), is calculated analogously as:

$$R_{C_i} = \frac{\mu_i \cdot B_i}{\eta_i \cdot \alpha_i} \tag{9.7}$$

in which η a stoichiometry coefficient for the number of moles C in the substrate (1 and 2 for methanotrophs and heterotrophs, respectively). The fraction of consumed carbon substrate that is not incorporated into biomass is oxidised to CO_2.

Production of electron donors

Within a rice rhizosphere, production and consumption of carbon substrates and ferrous iron can occur simultaneously. The production of acetate and CO_2/H_2 is driven by soil organic matter mineralisation, P_{min} (in mol C m^{-3} s^{-1}), neglecting root decay and the decomposition of organic fertilisers, and is described by Yang (1996):

$$P_{\min} = C_{\min} \cdot (1 - S_{\min}) \cdot K_{d_{\min}} \cdot e^{-K_{d_{\min}} \cdot time\_season} \tag{9.8}$$

in which C_{min} is the soil organic carbon pool (mol C m^{-3}) and:

$$K_{d_{min}} = R_{min} \cdot time\_season^{-S_{min}} \tag{9.9}$$

R_{min} ($s^{S_{min}-1}$) is the relative decomposition rate at *time_season*=1 and S_{min} (-) represents the rate of change of $K_{d,min}$. R_{min} and S_{min} have been determined experimentally (Chapter 2). *time_season* is the time after flooding the soil (s) and is taken 40 days after transplanting in the default settings, because at that point a reasonable rice root system has been developed.

Methane is produced from acetate and from CO_2/H_2. Methanogens have to compete for these substrates with heterotrophs and ferric iron reducing bacteria that also use acetate and CO_2/H_2:

$$CH_3COO^- + H^+ \to CO_2 + CH_4 \tag{9.10}$$

$$CO_2 + 4H_2 \to 2H_2O + CH_4 \tag{9.11}$$

$$8\ Fe(OH)_3 + CH_3COO^- + 17H^+ \to 8\ Fe^{2+} + 2CO_2 + 22H_2O \tag{9.12}$$

$$2Fe(OH)_3 + H_2 + 4H^+ \to 2Fe^{2+} + 6H_2O \tag{9.13}$$

Both methane production, $R_{CH4,p}$ and ferric iron reduction, $R_{Fered,p}$ are inhibited in the presence of oxygen. Moreover, methane production seems to be inhibited directly in the presence of reducible ferric iron (Chapter 6). Microbial biomass dynamics seems not important for methane production (subscript $_p$) and ferric iron reduction (subscript $_t$). Both rates can thus be described by a modified Michaelis Menten kinetics:

$$R_{CH4\,j} = V_{max_{j_p}} \cdot \frac{[e^- donor_j]}{K_{M,j_p} + [e^- donor_j]} \cdot \frac{1}{1 + K_{i,O2_p} \cdot [O_2]} \cdot \frac{1}{1 + K_{i,Fe} \cdot [Fe_s^{3+}]} \tag{9.14}$$

$$R_{Fered\,j} = V_{max_{j_f}} \cdot \frac{[e^- donor_j]}{K_{M,j_f} + [e^- donor_j]} \cdot \frac{[Fe_s^{3+}]}{K_{M,Fe} + [Fe_s^{3+}]} \cdot \frac{1}{1 + K_{i,O2_f} \cdot [O_2]} \tag{9.15}$$

in which the e^- $donor_j$ is either H_2 or acetate and the maximum conversion rate $Vmax_{H2,p}$ equals $7.6\ 10^{-6}$ mol $m^{-3}s^{-1}$, $Vmax_{Ac,p}$ equals $3.8\ 10^{-6}$ mol $m^{-3}s^{-1}$ $Vmax_{H2,f}$ and $Vmax_{Ac,f}$ equal $1.2\ 10^{-4}$ mol $m^{-3}s^{-1}$ (Chapter 6). The affinity constant $Km_{H2,p}$ is $13.3\ 10^{-3}$ mol m^{-3}, $Km_{Ac,p}$ is 2.56 mol m^{-3}, $Km_{H2,f}$ is $0.22\ 10^{-3}$ mol m^{-3} $Km_{Ac,f}$ is 0.23 mol m^{-3} and Km_{Fe} is 61 mol m^{-3} (Chapter 6). The inhibition constant $K_{i,O2}$ (defined similarly in Arah and Stephen (1998)) for methane production is estimated at 47 m^3 mol^{-1} (from Fetzer and Conrad, 1993; Nedwell and Watson, 1995). $K_{i,O2}$ for ferric iron reduction will be smaller and is chosen at $2/3$ of the value for methane production. $K_{i,Fe}$ is taken at 8.3 m^3 mol^{-1} total reducible iron (Chapter 6). The ferric iron concentration has a subscript $_s$ to indicate that Fe^{3+} is precipitated as $Fe(OH)_3$ and dissolved and reduced by microbes, leading to a release of ferrous iron into the soil solution.

Root compound conversions

The important process within a root that influences methane oxidation is root respiration, $R_{n,p}$ (mol O_2 cm^{-3} root s^{-1}), which is described according to Luxmoore (1970a), neglecting the influence of assimilates on root respiration:

$$R_{resp} = resp_{max} \cdot \frac{(O_2)_{root}}{K_{resp} + (O_2)_{root}} \tag{9.16}$$

in which $(O_2)_{root}$ is the concentration in a root (mol m^{-3} gas), $Resp_{max}$ is the maximum rate of root respiration ($3.23.10^{-9}$ mol cm^{-3} root s^{-1} for rice (Luxmoore, 1970b)) and K_{resp} (6.42

mol m^{-3} gas for rice roots (Luxmoore, 1970b)) is the oxygen concentration at which respiration is half $Resp_{max}$. Root respiration is assumed to occur across the whole root length, which is assumed to be 0.22 m (Armstrong et al., 1991; Kludze and Delaune, 1995). CO_2 is produced by root respiration.

All biological reactions are presumed to proceed with a temperature dependence that can be described by a Q_{10} value, which is the relative increase in reaction rates at a temperature increase of 10°C, of 2 (Atlas and Barta, 1987).

Iron adsorption

Iron transport in rice rhizosphere is complex and highly depends on pH dependent solubility. All ferric iron is immobile -indicated as $[Fe^{3+}{}_s]$- precipitated as $Fe(OH)_3$, neglecting other iron precipitates and is produced by iron oxidation and decreased by iron reduction. Ferrous iron is present in two forms: $[Fe^{2+}]$ -mobile in the soil solution and produced by iron reduction- and $[Fe^{2+}{}_s]$ -immobile, adsorbed to clay particles and consumed by iron oxidation. The equilibrium, which is assumed to occur almost instantaneously, between $[Fe^{2+}]$ and $[Fe^{2+}{}_s]$ is given by (Kirk et al., 1990):

$$[Fe^{2+}] = \left(\frac{\{Fe_s^{2+}\} + \{Fe_s^{3+}\}}{a} \right)^{1/m} \cdot \left(\frac{\{Fe_s^{2+}\}}{\{Fe_s^{2+}\} + \{Fe_s^{3+}\}} \right)^{1/n} \tag{9.17}$$

in which {.} represents a concentration expressed in mol kg^{-1} soil, a and m are Freundlich isotherm parameters (0.032 kg^{-1} mol$^{1 \cdot m}$ m^{3m} and 0.57, respectively (calculated from Ahmad and Nye (1990)). n describes the pH dependence of Fe^{2+} adsorption on partially oxidised soil (Kirk et al., 1990):

$$n = n_A \cdot e^{-n_B \cdot pH} \tag{9.18}$$

in which n_A is 30 and n_B is 0.9 pH^{-1} (Kirk et al., 1990). The pH is determined by the soil acidity, $[HS]$ (mol m^{-3} water) and the soil buffer capacity b_{HS} (39.6 mol m^{-3} water pH^{-1}, calculated from Kirk et al. (1990)) (Nye, 1972):

$$\frac{dpH}{dt} = -\frac{1}{b_{HS}} \cdot \frac{d[HS]}{dt} \tag{9.19}$$

Temporal change in [HS] is determined by the production of acidity (in this study iron oxidation), consumption of acidity (in this study iron reduction) and transport of the most dominant base pairs in a soil layer l, H^+-H_2O and H_2CO_3-HCO_3^-:

$$\frac{dHS}{dt}_l = (Flow_{H_{l-1}^+} - Flow_{H_l^+}) - (Flow_{HCO3_{l-1}^-} - Flow_{HCO3_l^-})$$
$$+ \lambda \cdot R_{FeOx} \cdot V_{w_l} - \lambda \cdot R_{Fered} \cdot V_{w_l} \tag{9.20}$$

in which λ is a stoichiometry constant depicting the number of H^+ transferred per iron and $V_{w,l}$ is the water volume (m^3) in soil layer l. Transport is described by flow rates from layer l to layer $l+1$ (Eq. 9.21) and layer 1 is located closest to the root.

Concentrations and flows of H^+ are calculated by combining Eq. 9.19, 9.20, 9.21 and an active root release of H^+ to balance nitrogen uptake (next section). Concentrations and flows of HCO_3^-, $Flow_{HCO3}$, are calculated from concentrations and flows of total CO_2 available in a soil layer (which is $CO_2(l)$ + $CO_2(g)$ + $H_2CO_3(l)$ + $HCO_3^-(l)$, neglecting CO_3^{2-} because pH<8). Total CO_2 is produced by soil mineralisation, methane production, iron reduction, root respiration and respiration coupled to methane and acetate oxidation (all

treated above). Total CO_2 is distributed among water and gas phase as a function of pH in each soil layer l according to chemical equilibria for dissolution of CO_2 (pK_1=1.406), hydration of CO_2 to H_2CO_3 (pK_2=2.616) and the acid-base reaction of H_2CO_3 to HCO_3^- (pK_a=3.76) (Garrels and Christ, 1965; Kerns, 1960). Produced total CO_2 is transported through the system via diffusion through water and gas phase.

Transport

All reactions described above can occur at different distances, r, from the root. In the model, a cylindrical geometry of 20 layers around a root has been incorporated. The thickness of the layers increases linearly with distance from the root, as the steepest gradients will occur closest to the root. The first soil layer has the same thickness as the root radius, r_{root} (m), which was estimated at 0.37 10^{-3} m from primary root data (Drenth et al., 1991).

Under influence of all reactions, gradients develop between compartments and diffusive flows occur. In the model, convective flows are neglected, because these flows contribute little to total water and solute transport in rice systems (Denier van der Gon and van Breemen, 1993; de Willigen and van Noordwijk, 1994). It is also assumed that the contribution of gas bubbles to transport is negligible at the short distances considered in the model. Adsorption of organic acids on iron oxides is also neglected, contrary to the model of Jones et al. (1996). The diffusive flow (mol s^{-1}) out of soil layer l to layer $l+1$ for all mobile compounds, M (O_2, CH_4, acetate, H_2, CO_2, HCO_3^-, H_2CO_3, Fe^{2+} and H^+), can thus be described by:

$$Flow_{M\,l} = D_{eff_M} \cdot A_l \cdot \frac{\partial [M]}{\partial r} \qquad (9.21)$$

in which D_{eff_M} is the effective diffusion coefficient (m^3 water m^{-1} soil s^{-1}) and A_l is the cross section area (m^2 soil) between soil layer l and layer $l+1$. $D_{eff,M}$ is given by:

$$D_{eff_M} = \frac{D_{A_M} \cdot \tau_B \cdot \varepsilon^{\tau_A}}{\alpha_M} + D_{W_M} \cdot \tau_B \cdot \theta^{\tau_A} \qquad (9.22)$$

in which ε is the gas filled porosity (m^3 gas m^{-3} soil), θ is the water filled porosity (m^3 water m^{-3} soil), α_M is the Ostwald coefficient (m^3 gas m^{-3} water) and is taken from Wilhelm et al. (1977) for all M that can occur in the gas phase. τ_B and τ_A determine soil tortuosity -path length extension- and have values of 0.9 and 2.3, respectively (Campbell, 1985). $D_{A,M}$ is the diffusion coefficient of compound M in air (m^2 gas s^{-1}) and is calculated against N_2 as a function of temperature according to theory by Hirschfelder et al. (1964). $D_{W,M}$ is the diffusion coefficient of a compound M in water (m^2 water s^{-1}) (CH_4: 2.22 10^{-9} m^2 s^{-1} (Jähne et al., 1987), O_2: 2.99 10^{-9} m^{2}s^{-1} (Langø et al., 1996), H_2: 5.34 10^{-9} m^{2}s^{-1} (Langø et al., 1996), HCO_3^- and H_2CO_3: 1.40 10^{-9} m^{2}s^{-1} (Nye, 1972), CO_2: 2.22 10^{-9} m^{2}s^{-1} (Langø et al., 1996), Fe^{2+}: 0.707 10^{-9} m^{2}s^{-1} (O'Connor et al., 1971), H^+: 8.4 10^{-9} m^{2}s^{-1} (Nye, 1972), acetate: 0.672 10^{-9} m^{2}s^{-1} (Darrah, 1991a) all at 30 °C). Temperature dependence of $D_{W,M}$ is described by a Q_{10} value of 1.31 (Segers, 2000).

Besides various soil layers, a root compartment and an atmospheric compartment are distinguished. The root and atmospheric compartments are dominated by the gas phase and exchange between these compartments is given by:

$$Flow_{M^{'}_{air-root}} = \omega_{r,l} \cdot A_l \cdot \#_r \cdot ((M^{'}_{air}) - (M^{'}_{root})) \qquad (9.23)$$

in which (M') is the concentration of a volatile compound M' (O_2, CH_4, CO_2, H_2) in the gas phase (mol m^{-3} gas), $\omega_{r,t}$ is the conductance at the rice root-shoot interface (estimated at 2.04 10^{-6} m^3 gas m^{-2} tiller s^{-1}, Groot et al. (2000)), A_t is the cross section area of a tiller (estimated to be 3.2.10^{-5} m^2) and #$_r$ is the number of roots per tiller (estimated to be 22 (Colmer et al., 1998; Harada and Yamazaki, 1993)). (M'$_{root}$) is corrected for root porosity. $\omega_{r,t}$ is by far the most important limiting factor for gas transport in a rice plant (Chapter 7) and therefore other factors were neglected. This also implies that (M'$_{root}$) can be assumed to be homogeneous and that root respiration does not have to be solved spatially explicitly (this contrary to Armstrong and Beckett (1987)), because exchange between roots and atmosphere is about 45 times slower than mixing within a root. This also allows the assumption that exchange sites between root and soil (mainly at root tips and root hairs (Flessa and Fischer, 1992)) are homogeneously spread across the root surface. In addition, it is assumed that compound exchange between soil and root is not limited by root access. The root surface itself does not introduce an additional resistance, analogous to the situation at a leaf surface, where the limited area of the stomata does not introduce an extra resistance for transport (Monteith and Unsworth, 1990). This leads to:

$$Flow_{M'root-soil} = \frac{1}{\dfrac{r_{root} \cdot \alpha_C}{D_{AM} \cdot A_{root} \cdot \varepsilon_{root}} + \dfrac{r_{root}}{D_{WM} \cdot A_{root} \cdot (1-\varepsilon_{root})} + \dfrac{0.5 \cdot r_1}{D_{eff_M} \cdot A_{0.5}}} \cdot ([M']_1 - \alpha_C \cdot (M'_{root})) \quad (9.24)$$

in which A_{root} is the root surface available for gas exchange (m^2) assuming an active root length available for exchange of 0.075 m (Armstrong, 1971b), ε_{root} is the root porosity to convert $D_{A,M}$ to a root surface (estimated from a data compilation at 0.295 m^3 gas m^{-3} root (Chapter 7)), $A_{0.5}$ is the soil cross section area halfway the first soil layer (m^2) and r_1 is the thickness of the first soil layer (m).

Root oxygen release can also be calculated with Eq. 9.24, because biochemically and photo-synthetically produced oxygen are not of importance in rice (Ando et al., 1983). If oxygen gradients within the root are important, then the model will underestimate root oxygen release, because oxygen concentrations at the root cortex is above the average root oxygen concentration (Armstrong and Beckett, 1987).

Root exudation, assumed to be either acetate -shown to be a major constituent of root exudates (Dannenberg and Conrad, 1999)- or converted instantaneously into acetate (Dannenberg and Conrad, 1999), cannot be described by diffusion equations, because exudation is partly an active process, e.g. to allow phosphate uptake:

$$Flow_{Ch,root-soil} = E \cdot A_{root} \quad (9.25)$$

in which E is the root exudation rate (estimated at 9.6.10^{-10} mol m^{-2} root s^{-1} (Hoffland et al., 1989; Delhaize et al., 1993), which is similar to data presented by Lu et al. (1999) for default root radius and root length.

For H$^+$ diffusion across the root surface an eq. similar to Eq. 9.24 is used, using an apoplast pH of 6.5 (Mattsson et al., 1998):

$$Flow_{H+root-soil} = \frac{1}{\dfrac{r_{root}}{(1-\varepsilon_{root}) \cdot A_{root} \cdot D_{W_{H+}}} + \dfrac{0.5 \cdot r_1}{D_{W_{H+}} \cdot \tau_B \cdot \theta^{\tau_A} \cdot A_{0.5}}} \cdot ([H^+]_1 - [H^+_{root}]) \quad (9.26)$$

In addition an active root release of H$^+$ to balance plant uptake of ammonia is included. As default, a nitrogen uptake of 5 kg N ha^{-1} day^{-1} is assumed.

Boundary and initial conditions

The atmosphere represents one system boundary (for which the exchange is dealt with above). The 2nd boundary occurs at the interface between rhizosphere and bulk soil. It is assumed that net exchange at this boundary is zero. This can be interpreted as equilibrium between bulk soil and outer soil layer or that the outer soil layer meets the outer layer of a proximate root.

The amount of a compound M in a compartment is calculated from the production and consumption rates (corrected for compartment volume) and flows into and out of the compartment. The concentration of compound M is calculated from the amount M and compartment volume. The model simulation starts with an anaerobic soil that comes under influence of an oxygen releasing root at time zero. Dissolved methane is assumed to be 0.35 mol m^{-3} water (Rothfuss and Conrad, 1993; 1998) and initial acetate concentration is estimated at 0.05 mol m^{-3} from anaerobic soil in equilibrium (Chin and Conrad, 1995; Rothfuss and Conrad, 1993). All iron is assumed to be reduced and is estimated from the total reducible iron content, on average 180 μmol g d.w.$^{-1}$ (Yao and Conrad, 1999). Total dissolved CO_2 is estimated to be 6 mol m^{-3} (Conrad et al., 1986). Soil pH is chosen to be initially 6.7 (Ponnamperuma, 1972). Initial microbial biomass of heterotrophs and methanotrophs is estimated from biomass data presented for anaerobic bulk soil in rice paddies (Chapter 8; Gilbert and Frenzel, 1998; Kumaraswamy et al., 1997). Gaseous concentrations in the root are assumed to be in equilibrium with the atmosphere. The model was run to simulate 48 hours. This is about the maximum united period that a microsite is under influence of oxygen release from a single rice root (Flessa and Fischer, 1992). A carbon balance was included in the model and never showed relative deviations $>10^{-6}$.
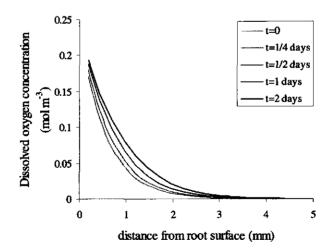
9.3 Results

Model performance

Figure 9.2: Development of oxygen gradients in a rice rhizosphere after introduction of a rice root at an anaerobic microsite at t=0.

The driving force of the model is diffusive transport of oxygen from the atmosphere into the anaerobic soil. Part of the oxygen did not reach the soil, but was consumed in the roots, 4.11 μmol cm^{-2} root surface day^{-1}. Root oxygen release (ROL) was one of the diffusive flows calculated by the model and decreased in time (under influence of increasing soil oxygen concentrations) from 2.7 μmol cm^{-2} root day^{-1} to 1.8 μmol cm^{-2} root day^{-1}. The combination of root respiration, ROL and oxygen exchange with the atmosphere led within two hours to stable root oxygen concentrations of 2.37 mol m^{-3} gas (5.7% v/v).

Under influence of ROL, oxygen was introduced into an initially anaerobic rhizosphere and an oxygen gradient was established within few minutes. Most of the oxygen was consumed directly (total oxygen consumption, which is treated below, was more than 99% of the ROL), but rhizospheric oxygen consumption never fully equalled ROL. This led to slightly increasing oxygen concentrations in time without obtaining stable gradients (Figure 9.2). No oxygen was present beyond 3 mm from the root surface.

a   b

c
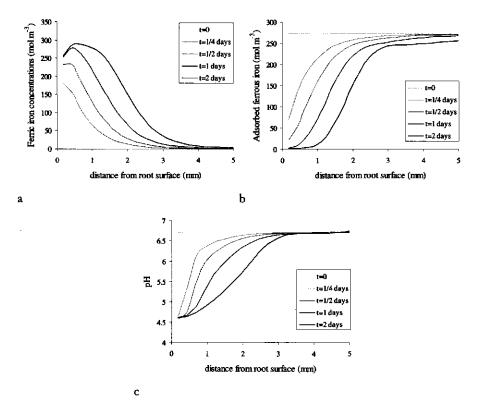
Figure 9.3:   Development of gradients for a) total ferric iron, b) adsorbed ferrous iron and c) pH in a rice rhizosphere after introduction of a rice root at an anaerobic microsite at $t=0$.

The introduction of oxygen into the rhizosphere triggered many oxidative processes. Ferric iron concentration increased (Figure 9.3a) and ferrous iron concentration decreased (Figure 9.3b) instantaneously near the root surface, but the maximum ferric

iron concentration moved away from the root surface in time. Around one 1 mm from the root surface, the ferric iron accumulated to concentrations that were higher than the initial total iron concentration. The pH decreased 2 units near the root surface under influence of iron oxidation (Figure 9.3c). Iron reduction had a minor counteracting influence on the pH decrease, because iron reduction rates were on average 25 times lower than iron oxidation rates. Maximum iron reduction rates occurred around 2 mm from the root surface, while the maximum iron oxidation rates occurred at 0.5 mm from the root surface (Figure 9.4c). Neither active (via nutrient uptake) nor passive (via carbon dioxide diffusion) flows of H^+ across the root surface had a big influence on the soil pH: Neglect of both flows caused an additional pH decrease in the soil layer closest to the root of 0.17 unit.

a   b

                    c
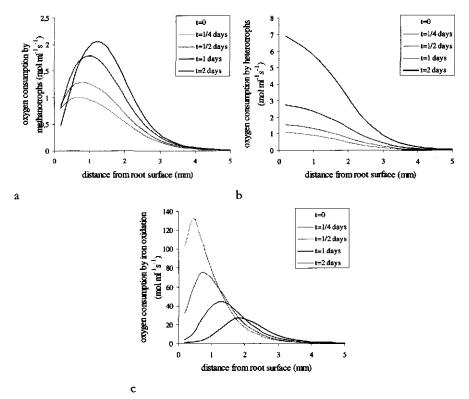
Figure 9.4:   Competition for oxygen: Oxygen consumption rates by a) methanotrophs, b) heterotrophs and c) iron oxidation in a rice rhizosphere after introduction of a rice root at an anaerobic microsite at t=0.

Iron oxidation was the most important oxidative process in the rice rhizosphere and accounted initially for 97% of the consumed oxygen. Iron oxidation rates decreased in time under influence of a decrease in available reduced iron (Figure 9.3b, ferrous iron concentration in the soil solution was negligibly small) and accounted for 80% of the oxygen consumption after two days of root influence. Methanotrophic and heterotrophic respiration increased in time, both relatively and absolutely. Heterotrophs were the

initialisation (taken from average anaerobic conditions). A sensitivity analysis, changing each parameter independently -which is correct because each parameter is independent- was carried out to determine the dependency of the fraction of lost methane via methane oxidation (Figure 9.6).
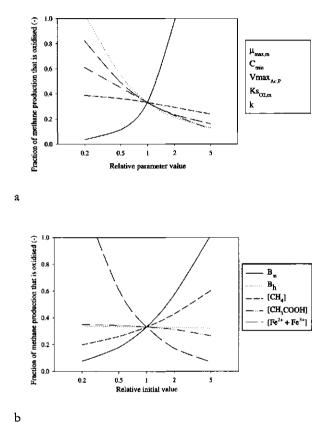

a

b

<u>Figure 9.7</u>:   Sensitivity of the model expressed as the fraction of methane production that is oxidised under influence of a) model parameter values and b) model initialisation. Parameters are as in Figure 6.

Methane oxidation was mainly limited by oxygen. The sensitivity of methane oxidation on methane production (influenced by C_{min} and $Vmax_{Ac,P}$) and on initial methane concentrations was less than the sensitivity on parameters influencing competition for oxygen. The highest sensitivity was obtained for parameters influencing the competition for oxygen between methanotrophs and chemical iron oxidation. Methanotrophs had a better competitive ability at a higher initial biomass (B_m), higher maximum relative growth rate ($\mu_{max,m}$) and a higher affinity for oxygen (lower $Ks_{O2,m}$) and if chemical oxidation proceeded slower, i.e. at a lower k and at lower total iron concentrations ($[Fe^{2+} + Fe^{3+}]$). Heterotrophs had much less effect on methane oxidation as shown by the hardly any sensitivity for B_h and $[CH_3COOH]$. The sensitivity for root exudation and kinetic parameters of the heterotrophs was even less (results not shown). This can be explained

from the smaller competitive ability of heterotrophs compared to chemical iron oxidation. Soil oxygen concentrations were mainly determined by the oxygen consumption processes in the soil. The conductivity of the root-shoot barrier (ω_{rs}) and root respiration hardly influenced ROL (due to efficient exchange with the atmosphere) and thus hardly influenced methane oxidation (results not shown).

Although methane oxidation is usually estimated from a difference in methane emissions with and without addition of specific inhibitors on methane oxidation, and is thus directly related to the methane oxidation fraction presented in Figure 9.6, these estimates are usually related to methane production. This procedure neglects the large changes - also in comparison to methane production rates- in soil methane storage in proximity of a rice root. Because this may have major implications for the interpretation of methane oxidation rates, a sensitivity analysis on methane oxidation as a fraction of methane production was performed (Figure 9.7).

In general, the sensitivities in Figure 9.7 were similar to those in Figure 9.6, with a few exceptions. The sensitivity for C_{min} was much higher; a high C_{min} resulted in high methane production compared to total soil methane storage and led to a seemingly lower efficiency of methane oxidation. A similar reasoning can be followed for $Vmax_{Ac,P}$, which showed a negative relationship with methane oxidation fraction, whereas it had a slightly positive relation in Figure 9.6. The positive relationship in Figure 9.6 was caused by the inhibition of a higher $Vmax_{Ac,P}$ on iron recycling, thus increasing the competitive ability of methanotrophs. Also the initial [CH$_4$] shows a reverse relationship with methane oxidation in Figure 9.7 compared to Figure 9.6. A high initial [CH$_4$] decreased the contribution of produced methane to oxidised methane and increased thus the apparent methane oxidation fraction. In some conditions the methane oxidation fraction increased even above one, showing that care has to be taken when calculating a methane oxidation fraction.
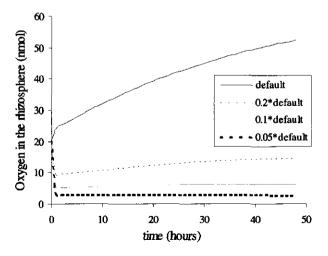

Figure 9.8:   Oxygen amounts in the rice rhizosphere in time as a function of conductivity over the soil-root interface, relative to its default description.

The sensitivity analysis showed that the methane oxidation fraction is highly sensitive and non-linearly influenced by model parameterisation and initialisation, which makes methane oxidation hard to predict. Not only methane oxidation, but also the steady state for oxygen is influenced by the model parameterisation. At default conditions, oxygen amounts in the rice rhizosphere tended to increase in time. Decreasing the transport conductivity across the root-soil interface led however to decreasing oxygen in the rice rhizosphere (Figure 9.8, initialised with oxygen concentrations above zero to allow comparison). Decreasing oxygen concentrations in the rice rhizosphere have been predicted by Kirk (1993) and might well have been caused by his choice on transport conductivity across the root-soil interface (which value was unfortunately not documented).

9.4 Discussion
Model limitations
Like all models, the model presented in this paper has several limitations. It is important to understand these limitations to interpret model performance. Microbial aerobic dynamics was limited to one methanotrophic species and one heterotrophic species, whereas many organisms interact in a rice rhizosphere. Arguments for excluding nitrification and sulphur oxidation are given in section 2, but one can still argue that one representative of a microbial group cannot mimic a complete microbial population. The affinity constants were however averages taken from published values and were similar to affinity constants found for dominant microorganisms isolated from a rice paddy (Chapter 8). The maximum relative growth rates were also average published values and might thus represent average conditions. Bodelier et al. (2000) showed however that methanotrophic activity in rice paddies might be increased significantly by nitrogen fertilisation. Such interactions are not explicitly accounted for in the model and need more research as the sensitivity analysis showed that $\mu_{max,m}$ had a large influence on the fraction of methane oxidised. Many of the parameter values for other processes, like iron oxidation, methane production and soil mineralisation, are variable or uncertain. For these parameter values a sensitivity analysis has been carried out and the influence could be quantified, although the variability in parameter values limits the application of the model for prediction purposes.

Besides in the rice rhizosphere, methanotrophs (Bosse and Frenzel, 1997; Gilbert and Frenzel, 1998) and heterotrophs (Watanabe et al., 1979) have also been found at the rice root surface. These are not explicitly accounted for by the model, but the first soil layer is so thin (1/4* root diameter) that it can be assumed that this soil layer represents the root surface as these will be hard to distinguish experimentally. Methanotrophs have also been found inside the rice root (Bosse and Frenzel, 1997; Gilbert et al., 1998). The activity of the microorganisms inside the root is however not known and their possible influence on total methane oxidation could therefore not be quantified. Given the short residence time of methane inside the root and the dominant gas phase within the root their influence will however probably be small.

A more important limitation of the model seems that a homogeneous cylindrical geometry around the active part of a primary root has been used. An alternative spherical geometry around each root tip (of the primary and the laterals roots) does not represent reality either, because such geometry would need the assumption of a full sphere around

a tip, while in reality each tip is in exchange with the other parts of the root. Application of a spherical geometry did not lead to different results for the methane oxidation fraction (results not shown), although the gradients within the soil were steeper, because of the faster volume change with distance from the root surface. The reason for the comparable results for different geometries is that the exchange across the root surface and within the root are not the limiting factors for methane oxidation.

A final limitation of the model is that root growth dynamics was not accounted for explicitly. None of the models mentioned in the introduction of the paper include root growth dynamics. This dynamics may however be important because of the absence of a steady state within the period over which a root is influencing a certain microsite. The implications of this limitation are therefore explored later on.

Model performance

There are no mechanistic models on methane oxidation in a rhizosphere, except for the model of Segers (2000), and there are no in situ measurements on methane oxidation in the rhizosphere, but model outcomes can be compared with various measurements and model estimates for different parts of the model.

The model was driven by ROL into a rice rhizosphere. Unfortunately, many measurements of ROL expressed ROL per plant or per gram root, which would necessitate additional conversion with additional uncertainty. Those data were therefore excluded from comparison. Armstrong (1969) measured 4.2-6.8, Armstrong (1971a) 1.9-3.6 and Colmer et al. (1998) 0.8-1.5 μmol cm^{-2} root day^{-1} in rice. These measurements are all in the same range as the ROL calculated by the model. Our calculated root respiration of 4.1 μmol cm^{-2} root day^{-1} is similar to 3.0-4.2 (Armstrong, 1971a) and 2.1-2.5 μmol cm^{-2} root day^{-1} (Armstrong, 1971b). The ratio of root respiration and ROL can also be compared with measurements. Ueckert et al. (1990) showed that ROL was increased by a factor 2.6 when root respiration was inhibited, which means that root respiration is 1.6* ROL. In our model we obtain an estimate of 1.52-2.28*ROL. Root respiration had little influence on ROL as was shown in our sensitivity analysis, although root respiration was higher than ROL. This is in accordance with Colmer et al. (1998) who state root respiration rates are not a major factor determining the pattern of ROL along roots. Root oxygen concentrations are the resultant of root respiration, gas exchange with the atmosphere and ROL. Our modelled oxygen concentration of 5.7% v/v is comparable with 2-14% v/v (Raalte, 1940) and 0.4-10.4% v/v (Revsbech et al., 1999). Modelled root cortex oxygen concentrations (Armstrong and Beckett, 1987) vary between 0-20% v/v depending on root length and diffusion characteristics.

Oxygen release into the anaerobic soil led to oxygen gradients, which did not proceed further than 3 mm from the root surface. Armstrong (1970) modelled an extent of 2.3-2.9 mm for rice roots and Kirk (1993) also modelled 3 mm. Modelled oxygen concentrations varied from 0-190 μM with an average of 60 μM. These concentrations are comparable to those experimentally found by Frenzel et al. (1992) 10-115 μM, Gilbert and Frenzel (1998) 10-152 μM and Revsbech et al. (1999) 0-96 μM.

The introduction of oxygen triggered iron oxidation, leading to ferrous iron depletion and an accumulation of immobile ferric iron near the root surface. Kirk (1993) modeled similar distributions. Ferric iron accumulated to concentrations higher than the initial values. This is in accordance with measurements of Conlin and Crowder (1989) and

Wang and Peverly (1999). Such metal accumulation might either intensify toxicity or might be beneficial for micronutrient uptake. A steep pH gradient of 2 units established near the root surface under influence of acidity produced by iron oxidation, which was not balanced by acid consumption by iron reduction, similar to what was modelled by Kirk (1993). Measurements indicate variable gradients of 1-2.5 units (Begg et al., 1994), 0.6 units (Gilbert and Frenzel, 1998) and 0.2 units (Revsbech et al., 1999).

Methanotrophs and heterotrophs have to compete for oxygen with chemical iron oxidation, that dominated oxygen consumption. Reddy et al (1980) also found that at first oxygen consumption is dominated by chemical iron oxidation and that only thereafter both chemical and microbial oxidation reactions occur. Howeler and Bouldin (1971) found a somewhat lower contribution of iron oxidation, 50%, to total oxygen consumption in swamp soils. Swamp soils are however in general much richer in organic carbon than rice paddy soils. A higher contribution of heterotrophic respiration can therefore by expected for swamp soils. Watson et al. (1997) found in peat soils that 89-94.2% of the microbial respiration is via heterotrophic respiration. We found a 75% contribution of heterotrophic respiration to microbial respiration for rice paddies.

Oxygen consumption by methanotrophs in combination with methane release to the atmosphere and methane production led to changes in methane gradients. Methane production was only inhibited in the first 1.5 mm from the root surface in the rice rhizosphere. In the remaining aerobic rhizosphere, methane production was almost similar to the methane production under anaerobic conditions. The methane gradient in the rhizosphere was mainly determined by methane release to the atmosphere and was highly similar to the gradients measured by Gilbert and Frenzel (1998). In the rice root, methane concentrations were, with 140 ppm, much higher than background atmospheric concentrations. The authors are not aware of rhizospheric acetate data to compare the model estimates with. This is a pity, because other models on rhizospheric organic carbon predict similar (Jones et al., 1996), slightly higher (Newman and Watson, 1977) or much higher (Darrah, 1991a,b) carbon concentrations and all show decreasing organic carbon concentrations with distance from the root. This different trend from our model (Figure 9.5a) is explained by the fact that all other models were developed for aerobic systems, which do not have a large change in consumption efficiency with distance from the root surface.

Given the proper model performance on the individual processes, the model can be used to calculate methane oxidation rates and compare those values with measured values of methane oxidation. However, such a comparison may be difficult, because of the many different methods used to measure methane oxidation. Even methane oxidation estimates with specific inhibitors, which yield the most accurate estimates of methane oxidation, vary from 4% (Denier van der Gon and Neue, 1996) to 52% (Epp and Chanton, 1993). Bodelier et al. (2000) recently showed that methane oxidation is highly dependent on nitrogen fertilisation. The sensitivity analysis of the model showed that high variabilities are probably not experimental artefacts, but reality. Methanotrophic biomass estimates in the rice rhizosphere can differ more than an order of magnitude, standard deviations in various estimates of the maximum specific growth rates of the methanotrophs ($\mu_{max,m}$) and the methanotrophic constant for oxygen ($Ks_{O2,m}$) are more than 50% (Chapter 8) and methane concentrations in rice paddies have a spatial variability of more than 300% (Rothfuss and Conrad, 1998). Such differences in

environmental conditions change modelled methane oxidation fractions by more than 250% as shown by the sensitivity analysis, even though only one parameter was changed at a time. A sensitivity analysis carried out by Segers (2000) also showed that methane oxidation fractions could vary between 0-100%.

On average, the model predicts a methane oxidation of 8.5% of the total amount of methane lost and 33% if expressed as a fraction of methane production. This is much smaller than the model estimates of Watson et al. (1997). It is however similar to a measured average methane oxidation of 29-34% of methane produced (Banker et al., 1995; Bosse and Frenzel, 1998; Denier van der Gon and Neue, 1996).

A direct comparison with measured values is however difficult, because the calculated methane oxidation fraction depends on the definition. Both definitions are used simultaneously, while this is not correct given the large change in methane storage due to methane released to the atmosphere. The dissynchronisation of methane production and methane oxidation makes that the definitions represent highly different situations. Without correction for changes in methane storage, the calculated methane oxidation fraction marks an upper boundary (33% in the default simulation), representing a situation in which the losses of methane in the rhizosphere are quickly refilled by methane produced in the surrounding anaerobic soil. Such situations may occur in soils with low root length densities. In such situations, a diffusive flow instead of an equilibrium should be considered across the outer boundary of the rhizosphere. Such a diffusive flow did not change the value of the simulated methane oxidation fraction (results not shown). On the other hand, methane oxidation as a fraction of total methane loss (8.5%) represents a lower boundary for methane oxidation and is only representative for a complete plant if the distance between primary roots is equal or closer than 10 mm everywhere in the soil. Depending on the root length density the overall average for rhizospheric methane oxidation calculated by the model is thus 8.5-33% and that is similar to published values obtained by the use of specific inhibitors.

Rice rhizosphere dynamics

The model showed two important things: i) The fraction of methane that is oxidised highly depends on model initialisation and other variable parameters. ii) There is no steady state within the period that a single root influences a soil microsite, because the growing root passes too quickly. The consumption of oxygen by chemical iron oxidation and microbial respiration is always smaller than ROL. As soon as a root tip reaches an anaerobic microsite, oxygen concentrations will increase according to the default simulation. Results with decreased conductivity across the root-soil interface (Figure 9.8) show a different situation. Under influence of root growth, the positions of exudate and oxygen release change however continuously in time. After an oxygen releasing period, the microsite becomes anaerobic within a few hours (results not shown), because root growth rates are with 1-2 cm day^{-1} much higher than the few mm diffusion per day in water. Aerobic conditions develop again when a new root arrives at the microsite. The length of the period in between depends on the root length density. This means that the rice soil is a dynamic system and that the rice rhizosphere is not a static, steady state environment.

Methane oxidation is a.o. highly influenced by the initial microbial biomass, and especially by methanotrophic biomass. Given the temporal dynamics in a rice

rhizosphere, it seems that this biomass will mainly be determined by the extent to which methanotrophs are able to survive anaerobic periods. There is not much information available on this subject, although it seems that methanotrophs can survive anaerobic conditions for long periods (Roslev and King, 1994; 1995). The model predicts that methanotrophic biomass increases to maximally 800% of its initial value within two days (the maximum heterotrophic biomass was less than 400% of its initial value). Experimentally, methanotrophic numbers in the rhizosphere have been found to be up to 2 orders of magnitude higher than in the bulk soil (Chapter 8; Gilbert and Frenzel 1998; Kumaraswamy et al., 1997). Methanotrophic biomass has also been found to increase during the season (Chapter 8). These increases are probably due to the combination of a good survival and rapid growth if oxygen is available. Methanotrophic biomass and methane oxidation will thus depend on the history of the microsite. A better prediction of methane oxidation will be possible if more quantitative information on adaptation and survival capacities of methanotrophs and heterotrophs becomes available. In time, not only microbial biomass may change, but also the concentrations of acetate, methane and ferrous iron will change. The turnover time for root exudates is less than ¼ day. Consumption is larger than the production of carbon substrates and ferrous iron. Depending on root growth dynamics and root length densities, the carbon substrates or ferrous iron may thus become limiting, influencing the methane oxidation fraction. Moreover, the effects described above will depend on whether a root tip or lateral roots are considered. Methane oxidation will thus be highly variable, both spatially and temporarily and will depend on the history of the microsite.

9.5 Conclusions

This paper presents an extensive integrative mechanistic model on the processes leading to methane oxidation in rice rhizosphere. Modelled predictions on processes, a.o. root oxygen release, and modelled compound distributions were similar to what has been found experimentally. The introduction of a growing root into a reduced soil microsite leads to a fast increase in oxygen concentrations near the root, accumulation of ferrous iron, pH decrease and depletion of acetate and methane near the root surface. Estimates of methane oxidation depend on the definition used. Methane oxidation as a fraction of methane produced was comparable (33%) to experimental estimates, but should only be applied in soil with low root densities. The fraction methane lost via oxidation, which is a more appropriate measure in soils with normal or high root length densities, was much lower (8.5%). A sensitivity analysis showed that methane oxidation depends on model initialisation and parameterisation and that it is especially sensitive to parameters influencing the competition between methanotrophs and chemical iron oxidation. Other processes, e.g. methane production or heterotrophic respiration, have much less influence. Methane oxidation depends thus on root growth dynamics and will be highly spatially and temporarily variable, which makes a general prediction of methane oxidation difficult.

Acknowledgements

General discussion

This thesis describes the development of a model on methane emissions from rice paddies that can be coupled to a Geographical Information System (GIS) to estimate regional emissions. Such a model should be process-based, to allow extrapolation, and should need only few input parameters, to allow the estimation of emissions at a regional scale using commonly available databases. In this chapter I will evaluate to which extend these objectives have been realised. Three issues will be discussed: i) The extend to which the field scale model could predict methane emissions from rice paddies with few input parameters (also in comparison with earlier developed field scale models), ii) The validity of the process-based field scale model by a comparison between process descriptions in the field scale model and outcomes of developed mechanistic models on these processes, iii) The possibilities for upscaling by a combination of model and databases.

10.1 Emission predictions with a field scale model

Several models on methane emissions from rice paddies were published the last few years. Some of these models were highly empirical (Hosono and Nouchi, 1997; Huang et al., 1998), others were process-based (Arah and Stephen, 1998; Cao et al., 1995; Khalil et al., 1998a). The advantage of empirical models is that they need only few input parameters. Results of empirical models are however difficult to extrapolate beyond the area for which they were developed, which is problematic in view of the upscaling objective. Some process-based models (Arah and Stephen, 1998; Khalil et al., 1998a) need site specific parameters, like on methane production potential and plant transport characteristics. This makes these models not suitable for upscaling, although their process-based descriptions are proper. The model of Cao et al. (1995) is process-based and needs only few parameters, which makes this model potentially suitable for upscaling. Some of the descriptions in this model however do not seem proper in view of recent process information (discussed below). Therefore, it was chosen to develop a new process-based field scale model on methane emissions from rice paddies (Chapter 2).

None of the models, including the model presented in this thesis, is suitable to predict diurnal variation -high in the afternoon and low during the night- in methane emissions. The processes leading to diurnal variations are complicated and only partly understood. Diurnal variations depend in many cases on temperature (Chanton et al., 1997; Wang et al., 1999) and are much larger early in the season (Satpathy et al., 1997) and in unvegetated than in vegetated paddies (Byrnes et al., 1995). This suggests a major influence of ebullition on diurnal variations. Ebullition is not treated explicitly in any of the models. Diurnal variations will therefore not be considered in this discussion. Neither can the model be used for predictions of emissions from ratoon crops, a rice crop produced by regrowth of previously harvested rice, which is produced in e.g. Texas. The new model (Chapters 2 and 3) uses process information to simplify the process description making one crucial assumption, which is the division between a rhizosphere and a bulk soil compartment. This approach led to a process-based model that needs only few parameters and which is thus potentially suitable for upscaling. The model was validated with field methane emission data by closed chambers -which do not seem to

bias emission estimates- and showed a standard deviation of less than 10% compared to the measurements (Chapter 2; Figure 10.1c).

For the methane emissions from 6 treatments at 2 sites in the Philippines (Figure 10.1a,b), the model presented in this thesis performed better than the two other published models that can be used with few parameters, both for the daily and the seasonal dynamics. The other models were originally not parameterised for the Philippines, but for Italy (Cao et al., 1995) and Texas, USA (Huang et al., 1998), respectively. The model of Huang et al. (1998) performs better than the model of Cao et al. (1995) -that was reprogrammed- for almost all treatments. The model of Huang et al. (1998) which was developed for soils low in soil organic carbon, underestimates methane emissions in most treatments, because soil mineralisation was neglected. On the other hand, the model of Cao et al. (1995) is almost fully determined by soil mineralisation and is hardly influenced by site specific conditions. Both Cao et al. (1995) and Huang et al. (1998) neglect the influence of alternative electron acceptors and overestimate methane emissions at Los Baños, that is high in reducible iron. From these comparisons, the development of a new process-based model that needs few input parameters (like the model of this thesis) seems thus justified. A more complete comparison with sites from all over the world is however necessary to provide a conclusive answer.

a   b
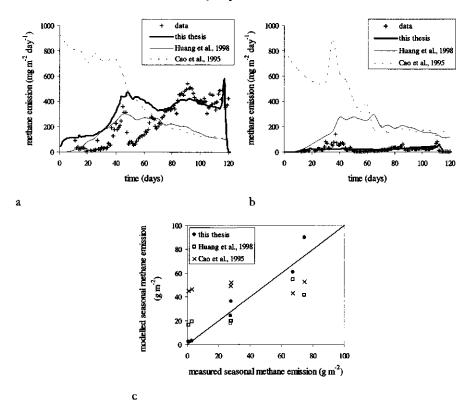

c

Figure 10.1:   Methane emission measurements and predictions using different models for different sites in the Philippines; a) Maligaya wet season 1996, b) Los Baños wet season 1997 and c) seasonal methane emissions.

10.2 Validity of the field scale model

Methane production

In the field scale model, two major simplifications on the description of methane production were made. i) It was assumed that produced carbon substrates were directly used by microorganisms reducing nitrate, sulfate, ferric iron or producing methane without intermediate accumulation. ii) It was assumed that the microbial reduction sequence followed strictly the redox sequence and thus that microorganisms outcompeted each other.

The mechanistic methane production model (Chapter 6) combines available knowledge on the processes leading to methane production under anaerobic conditions. Microbial competition for common substrates -acetic acid, H_2 and some inorganic electron donors- is described by Michaelis-Menten kinetics. This implies that actual substrate concentrations are calculated and used in the model. In addition, some other microbial interactions that are only partly understood, like product inhibitions and lag times, are accounted for as mechanistically as possible.

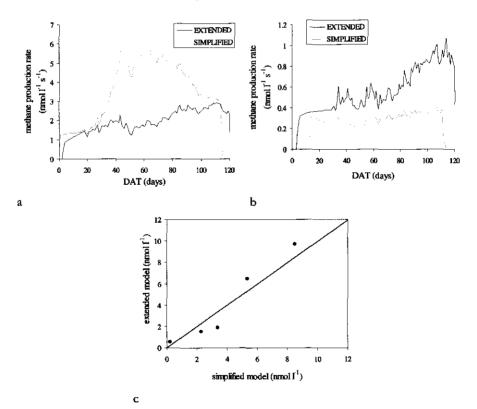a   b

c

Figure 10.2:   Comparison between field scale –simplified- model and extended mechanistic model estimates on methane production for a) seasonal dynamics at Maligaya, wet season 1996 at the control treatment, b) seasonal dynamics at Los Baños, wet season 1997 at the control treatment and c) seasonal methane production.

Methane estimates for both models were compared for all validation treatments discussed in Chapter 3. Two examples are shown in Figure 10.2a,b. At the Maligaya site with relatively low reducible iron, the simplified model simulates higher methane production rates than the extended model, except at the beginning and the end of the season. At that point, the reducible iron is below its inhibiting concentrations and all available substrate is directly converted into methane. In the extended model, not all available substrate can be consumed directly, because of limited production rates. The competitive ability of the methanogens compared to the iron reducing bacteria increases during the season. This leads to a steady increase in methane production rates during the season. A similar pattern is found for the extended model for Los Baños, whereas the simplified model predicts less methane production than the extended model. At Los Baños, the reducible iron concentrations are high. The simplified model predicts no methane production at the start of the season and very small production rates at other moments due to the simplified description for competition. Depending on the ratio of substrate availability to reducible iron, either the neglect of substrate accumulation or the outcompetition effects dominate the deviation between the estimates of the extended and simplified model. The largest differences between the two production estimates coincided with the highest differences between predicted and measured methane emissions (Chapter 2; Figure 10.1). Methane production on a seasonal basis for both models is quite related, which is important to know because seasonal estimates are used for upscaling purposes.

Besides a validation of the simplified model, the mechanistic model can also be used to identify gaps in knowledge. There is a lack of quantitative knowledge on the temperature dependence of affinity constants, on manganese reduction kinetics, on the use of inorganic compounds as electron donors and on the inhibition of sulphate reduction and methane production during iron reduction. Humic acid reduction does not seem important in rice paddy soils, but might become more important in organically fertilised rice paddies. Coupling of thermodynamics with kinetic descriptions might improve some of the uncertainties. Introduction of different microbial species, like homoacetogens and the distinction between *Methanosarcina* and *Methanosaeta*, might further improve the understanding but would make it completely impossible to apply the model for upscaling. These uncertainties on methane production have a strong influence during the first part of the season. To understand the dynamics of methane emissions in this period, a better quantitative understanding of the processes leading to methane production is needed.

Methanogens have also been found at the root surface, as recently described by Grosskopf et al. (1998). These methanogens might have different kinetic characteristics than methanogens in the soil slurry (Conrad et al., 2000). At the rice root surface aerobic conditions prevail, which will inhibit methanogens directly (Nedwell and Watson, 1995). This inhibition was not accounted for in the model. Due to the presence of oxygen, part of the acetate will be consumed during heterotrophic aerobic respiration (Chapter 9), which is much faster than the anaerobic consumption of acetate. This was neither accounted for in the model. This might have led to an overestimation of substrate accumulation in the rice rhizosphere. The methane production model can thus not be directly used for predictions near the root surface.

A high spatial variability -as explained above for the root surface- occurs at many other microsites within the rice paddy, e.g. around soil cracks or soil aggregates. This variability limits, in combination with non-linear relations, the prediction possibilities of methane production for a complete rice paddy.

A prerequisite for a good model on methane production is that the production of carbon is well described. The influence of different descriptions for soil organic matter mineralisation is considerable (Chapter 2). A model specifically developed for anaerobic conditions does not exist, but such a model might improve the predictions. Such model should at least account for different mineralisation rates as affected by different dominating electron acceptors (D'Angelo and Reddy, 1999; McLatchley and Reddy, 1998) and should distinguish various hydrolysis and mineralisation steps (Vavilin et al., 1996). The mineralisation model presented in this thesis seems to be the best description available (Chapter 2).

Besides gaps in knowledge, there is also a deficiency in quantitative data. The V_{max} for acetic acid and H_2 of nitrate reduction, ferric iron reduction, sulphate reduction and methanogenesis in principle have to be estimated for each situation separately. The differences in V_{max} estimates and the consequences of these differences can be considerable (Chapter 6), but will, by definition, be unknown during upscaling. It is encouraging, that the mechanistic model with average estimates for V_{max} values gave similar seasonal methane production values to the simplified model (Figure 10.2c). This might be different in a situation with high organic fertiliser applications, when V_{max} values will probably be higher (Wassmann et al., 1998). This may lead to a methane emission underestimation at high applications, when using the mechanistic model. It can be argued that methane emissions are underestimated if carbon substrate concentrations at the end of the growing season are still considerable.

Methane transport

Methane transport is described in the field scale model by a mean residence time, which is constant throughout the season, multiplied by the methane concentration in a compartment (Chapter 2). The mean residence time was different for each compartment and was much larger for the bulk soil than for the rhizosphere. The residence times were estimated from published data as 2.5 hours for the rhizosphere and 12.5 days for the bulk soil. The development of a mechanistic model on gas transport through a flooded soil-plant system (Chapter 7) allows a mechanistic validation of estimated residence times.

The mean compound residence time in the rhizosphere can be estimated from the sum of the ratios of compartment volume over compartment conductance for rice shoot, rice root and rhizospheric soil. The volume of the rice shoot depends on the number of tillers, tiller length and tiller radius. The volume of the rice root depends on the root radius, root length and number of roots and the volume of the rhizospheric soil depends additionally on the distance between the roots. The conductances in shoot and root depend on the diffusion coefficient in air and on the conductance over stomata and the root-shoot interface, respectively. The conductance in the rhizospheric soil depends on the soil diffusion coefficient. All these parameters can be calculated from the equations given in Chapter 7. Results are shown in Figure 10.3.

The average residence in the rhizosphere is 5.1 hours and this difference with the imposed residence time in the field scale model can be neglected on a seasonal scale. Contrary to the estimate in the field scale model, the mechanistic model shows large dynamics during the season. This dynamics is mainly caused by changes in the residence time in the rhizospheric soil, which also in absolute terms is the dominant contributor to the residence time in the rhizosphere compartment. The residence time in rhizospheric soil is mainly determined by the distance between the roots, which is again a function of the root length density. The root length density is different at different soil depths, at different times of the growing season and depends moreover on the rice cultivar. In the field scale model differences in soil depth were neglected for arguments given in Chapter 2. Due to non-linear relationships between root length density and root distance, these soil depth differences might lead to a refinement of components that contribute to the overall residence time in the rhizosphere, but will probably not change overall dynamics.
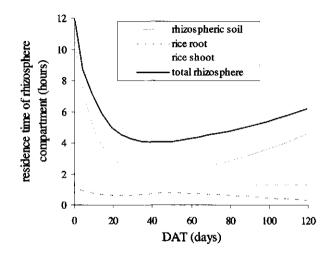

Figure 10.3:   Calculated residence time in the total rhizospheric compartment based upon individual residence time for the rhizospheric soil, rice root and rice shoot as a function of the time in the growing season.

Temporal changes in root length will have more influence. Both the temporal change in root length and the total root length density that is obtained depends on many variables, such as site, fertiliser use and rice cultivar (Slaton et al., 1990; Tanaka et al., 1995). Quantification and prediction of the effects of these factors is difficult. In this thesis all data on this subject were averaged and only data from high yielding rice varieties were used. Prediction of these changes will however be important for mechanistic modelling of methane emissions from rice paddies under different conditions and different rice varieties, especially because of the influence of root distance on methane oxidation (treated below). Rice varieties will not only influence root length density, but also root exudation, root respiration, root transport conductivity and root oxygen release. The results of Figure 10.3 show that although variability in root conductance are up to a factor 5, this will only lead to a doubling of the rhizospheric residence time. For a seasonal estimate of methane emissions, this factor is therefore less important. Root

respiration is also only of minor importance (on methane oxidation) as shown below. Root oxygen release is also highly cultivar dependent (Satpathy et al., 1998) and affects methane oxidation. Root exudation, an important carbon source for methane production in soil low in organic carbon, is another factor causing large differences in methane emissions from different rice varieties as mentioned in Chapter 3. These factors need to be known before mechanistic modelling of methane emissions from rice paddies can be applied for different rice cultivars in upscaling.

The residence time of methane in the bulk soil can also be estimated from the theory presented in Chapter 7. The total residence time in the bulk soil is the sum of the residence times in the soil and in the water layer on top of the soil. These residence times are again determined by the layer thickness and the diffusion coefficient of methane in water. If an average soil depth of 10 cm -which is half the average thickness of a rice paddy- and a flooding layer of 2 cm is applied, then a residence time of 122 days is calculated. This is much higher than the 12.5 days for measured average residence time.

The main reason for the difference between calculated and measured residence times is that the dominant pathway in the bulk soil is not diffusion, but ebullition (Chapter 2). Ebullition is a complex process that depends among others on methane concentration, soil bulk density, soil structure and the production of other gases. Ebullition is usually neglected in field scale models, while it is an important pathway for methane. Ebullition is only implicitly accounted for in the field scale model presented in this thesis. If ebullition is accounted for, then it is taken as a function of saturated methane concentrations (Arah and Kirk, 2000; Grant, 1998). The most comprehensive description is presented by Segers (2000), but even that description is, necessarily, partly empirical. If methane transport is to be described mechanistically, then a model on ebullition needs to be developed.

Methane oxidation

The field scale model describes methane oxidation as a bell-shaped, time dependent fraction of methane production. The parameter values for the gaussian function were based on an average estimated methane oxidation fraction of 33% and estimated root oxygen release dynamics throughout the season. The average methane oxidation fraction was only based on measurements using specific inhibitors, because indirect methods to measure methane oxidation highly overestimated methane oxidation (Chapter 2; King, 1996). Root oxygen release will drive methane oxidation in the rhizosphere, because methane oxidation in the rice rhizosphere is oxygen limited (Chapter 8, Bosse and Frenzel, 1997). Root oxygen release was estimated from root exudation data -which is highest when the root is most active-, because root oxygen release and root exudation appear to be coupled via changes in membrane permeability (Setter et al., 1989). One function of root oxygen release is to detoxify reduced products like Fe^{2+}, H_2S and organic acids, which is needed most when the root is most active. Circumstantial evidence is found from the fact that the root oxidative power – which unfortunately cannot be used directly to estimated root oxygen release (Ando et al., 1983)- had a similar seasonal dynamics as the imposed gaussian curve (Satpathy et al., 1997).

The mechanistic model (Chapter 9) does not impose any direct relationship between methane production and methane oxidation. Instead, the important aerobic and anaerobic chemical and microbial interactions occurring in the rice rhizosphere were

accounted for. Using all these interactions, the competition for oxygen between methanotrophs and other oxygen sinks -heterotrophic respiration, chemical iron oxidation and root respiration- was calculated. Calculated methane oxidation rates were compared with methane lost from the rhizosphere during the same period (caused by methane emission and methane oxidation) and to the actual methane production rate during the same period.

Mechanistic estimates of methane oxidation were calculated by running the mechanistic oxidation model (Chapter 9) for one day at different times during the growing season (Figure 10.4). Initial concentrations of acetic acid, ferrous iron, ferric iron and methane were estimated from a coupled model of the mechanistic methane production model (Chapter 6) and the field scale model (Chapter 2) and by running this coupled model as a function of the growing season. Mineralisation rates were directly estimated from the time of the growing season (Chapter 2). Root exudation rates were varied during the season according to the gaussian curve introduced above. Initial methanotrophic and heterotrophic biomass were estimated as a function of the growing season from Most Probable Number counts (Chapter 8).
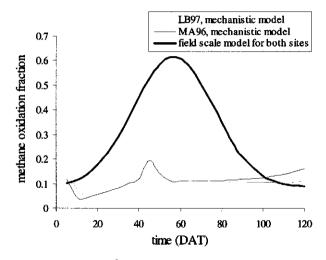
Figure 10.4:   Comparison between field scale model and mechanistic model estimates on methane oxidation.

Both estimates for methane oxidation peak in the middle of the growing season. The small peak found for the mechanistic model occurs probably at different moments during the season for different roots and will smooth to a gaussian type of curve. Calculated methane oxidation is slightly site dependent, which is mainly due to a difference in alternative electron donors. At the start of the season, the mechanistic model calculates higher methane oxidation fractions, but this difference can be neglected because methane production rates are very low at that point. There is however a major difference in the absolute methane oxidation fraction calculated for both models. This difference may have several reasons:

i) The lower estimate for the mechanistic model may partly be due to the low calculated methane concentrations in the rice rhizosphere. These concentrations were far below

saturation and might be caused by the continuous methane release from the rhizosphere in the field scale model, whereas in reality methane will only be released close to lateral roots or root tips. Actual methane concentrations and therefore methane oxidation rates, will thus be underestimated.

ii) Methane oxidation is usually estimated from a difference in methane emission when using specific inhibitors. Methane oxidation as a fraction of the methane lost was therefore used for comparison with the field scale model. In most reports, including those used for estimation in the field scale model, calculated methane oxidation is directly related to methane production. This is not strictly correct because changes in methane storage are neglected in this approach. Changes in methane storage in the rice rhizosphere -and thus between the two calculations for methane oxidation- can be enormous (Chapter 9), because roots provide an efficient pathway for methane to escape to the atmosphere. This might have major implications for the interpretation of methane oxidation rates, so far never considered.

iii) Recycling in rice rhizosphere of electron acceptors, like ferrous iron and sulphides, is neglected in the field scale model, while it was shown (Chapter 9) that reoxidation of ferrous iron in the rice rhizosphere is important. Sulphur recycling in the rice rhizosphere might explain the influence of sulphate fertilisation on methane emissions from rice paddies (Denier van der Gon et al., 2000). This neglect overestimates methane oxidation and experiments with stabile isotopes might help to quantify these processes. Recent methane oxidation measurements indicate that methane oxidation is probably closer to 10-30% (Bodelier et al., 2000) than 10-60%, as used in the field scale model. The neglect of alternative electron acceptor recycling and overestimation of methane oxidation is mechanistically speaking wrong. Overall methane emissions are however not influenced by these errors, because this neglect only has an influence within the electron acceptor input of the electron balance (Segers, 1999). For the electron balance, and thus for methane emissions, it does not matter whether electrons are recycled via methane or via iron. In both cases the overall reaction equation can become the same:

$$CH_3COOH \rightarrow CH_4 + CO_2$$
$$\underline{CH_4 + 2O_2 \rightarrow CO_2 + 2H_2O} +$$
$$CH_3COOH + 2O_2 \rightarrow 2CO_2 + 2H_2O$$

and

$$16H^+ + CH_3COOH + 8Fe(OH)_3 \rightarrow 8Fe^{2+} + 2CO_2 + 22H_2O$$
$$\underline{4Fe^{2+} + O_2 + 10H_2O \rightarrow 4Fe(OH)_3 + 8H^+} +$$
$$CH_3COOH + 2O_2 \rightarrow 2CO_2 + 2H_2O$$

The application of a mechanistic model for methane oxidation does not necessarily mean that methane oxidation can be predicted well. There are still several additional factors that need to be considered and that are only partly known. Measurement of root oxygen release, the driving factor for methane oxidation is difficult and uncertain (Sorrell and Armstrong, 1994). Anaerobic methane oxidation is thermodynamically possible, but never proved to occur, and was therefore not included. It is also known that methanotrophs and heterotrophs are present at the root surface (Bosse and Frenzel,

1997; Gilbert and Frenzel, 1998). These are not explicitly accounted for by the model, but the first soil layer is so thin (1/4* root diameter) that it can be assumed that this soil layer represents the root surface. Methanotrophs have also been found inside the root (Bosse and Frenzel, 1997; Gilbert et al., 1998) and even on or in the leaves (unpublished results). The number of microorganisms inside the plant and their activity are not known and their possible influence on total methane oxidation could therefore not be quantified. Given the short residence time of methane inside the plant (Chapter 7), their influence will probably be small. The influence of other uncertain parameters like root respiration, root exudation and root conductance were also shown to be small (Chapter 9). More important is the uncertainty in kinetic parameters of the methanotrophs and chemical iron oxidation. Changing the -highly uncertain- rate constant for chemical iron oxidation, k, leads to a more than proportional change in methane oxidation rates. The influence of $\mu_{max,m}$ is even larger (Chapter 9), while the standard deviation in $\mu_{max,m}$ amounts 50% (Chapter 8), depending on conditions and on the methanotrophic species chosen. Recent results of Bodelier et al. (2000) showed that the growth of methanotrophs is ammonia limited. Fertilisation with urea will increase $\mu_{max,m}$ and thus methane oxidation. After ammonia has been taken up by the rice plant, methane oxidation will decrease again. The survival of microorganisms in adverse conditions is another limiting factor. Quantification of these effects deserves high priority and limits the application of mechanistic insights for upscaling.

Finally, a major limitation for the use of the mechanistic model to estimate methane oxidation at the field scale or higher scales, is -as shown before for the processes of methane production and methane transport- the parameterisation. The influence of various initial parameters on methane oxidation estimates is large (Chapter 9) because no steady state gradients are established within a short time frame. Estimation of these parameter values is difficult due to the spatial and temporal variability of the processes, driven by root growth dynamics, which is hard to estimate (as shown above). Besides the large spatial and temporal dynamics of concentrations of methane and acetate (Rothfuss and Conrad, 1998) and acetate, the dynamics of methanotroph biomass is important (Chapter 9). This dynamics is not only influenced by $\mu_{max,m}$, but also by the survival of methanotrophs under anaerobic conditions. The influence of different descriptions for survival, adaptation and maintenance is large (results not shown). Unfortunatley, these processes are poorly understood (Roslev and King 1994; 1995). It might also be questioned whether a Double Monod description is appropriate in all circumstances.

The influence of temporal variability is shown in Figure 10.5. It was assumed that microbial mortality did not occur. In Figure 10.5, the mechanistic model was adapted to a spherical geometry. The simulation starts at a soil microsite in exchange with a root tip. While the root grows at a rate of 1 cm day^{-1} (Wopereis et al., 1995) different conditions occur at this microsite. After the root tip of 1-2 cm (Armstrong, 1971a; Kumazawa, 1984), an anaerobic root zone passes. Then, the soil comes into contact with the oxygen releasing lateral roots, that are around 7 cm from the apex (Armstrong, 1971a). In the meantime, the concentrations of acetate and methane changed due to anaerobic processes and as a result the methane oxidation at the lateral roots is higher than at the root tip. These results can however not be generalised, because of the many non-linear interactions. All together it can be concluded that, due to the complications, a

mechanistic model on methane oxidation will be very difficult to apply in upscaling studies.
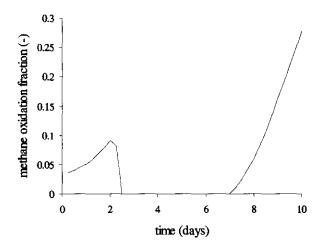
Figure 10.5: Temporal dynamics in methane oxidation around a single rice root under influence of root growth using the mechanistic model on methane oxidation with a spherical geometry.

10.3 Upscaling possibilities for methane emissions

Although there are considerable differences between mechanistic process descriptions and the corresponding descriptions in the field scale model, the predicted seasonal methane emissions for the field scale model had only a deviation of 7% compared with measured emissions. Given the large uncertainty in global methane emissions, 20-100 Tg CH_4 yr^{-1}, the field scale model is not limiting the accuracy of global methane emissions.

A model that predicts emissions with only few input parameters available in regional databases is, however, not the only necessity in upscaling. Other factors are the estimation of input parameters, data handling and data resolution. Although it was tried to keep the number of input parameter to the minimum, some crucial parameters are difficult to estimate. This applies for instance to the amount of reducible iron, which has to be estimated from extracted iron. Data on the relationship between reducible and extractable iron are scarce. Another example is the straw management of farmers, which has a large influence on methane emissions (Denier van der Gon et al., 2000), while it is not included in agricultural databases. Not all data are available at the same data resolution, while some data are only available as point data. This makes data interpolation necessary and induces errors (Chapter 4). Data resolution is also of importance. Most estimates assume a homogeneous methane emission within each country, while resolution effects might occur due to non-linear relations between methane emissions and underlying parameters in combination with the high spatial and temporal variability in underlying parameters. This was shown for the case study of Java (Chapter 4; Denier van der Gon et al., 2000). In an analysis for the case study of Java (van Bodegom et al., 2000) it was shown that the uncertainties introduced by estimating methane emissions from a model were much smaller (7%) than uncertainties due to data interpolation

(32%), use of different data sources (48%), or data resolution (9%). In this analysis only data effects under influence of soil information were included. If all data variability (e.g. of variability in yield, harvest index or water and nutrient management) would have been included, the effects might have been even larger.

The presence of these scaling effects means that data availability and not model uncertainty is the limiting factor in upscaling of methane emissions from rice paddies to regional scales. Many of the data issues are not accounted for in upscaling studies, which might partly explain the large uncertainty in the global estimates. Only with more detailed databases might an unbiased estimate of methane emissions from rice paddies be possible. As long as this information is not available it will be hard to obtain less uncertain emission estimates by the application of upscaling alone.

10.4 Conclusions

Comparison between mechanistic process models and simplified descriptions in the field scale model showed some deviations between the different descriptions. Still, mechanistic models or a combination of these mechanistic models are not suitable for application in upscaling. Some processes, like ebullition and microbial dynamics, are poorly understood and limit application. Even if all processes can be quantified, the unknown spatial and temporal variability of the parameters will still limit the application. A simplified process-based field scale model will therefore have to be used for upscaling. The process-based model presented in this thesis is suitable for that purpose, although the incorporation of alternative electron acceptor recycling combined with a downward adjustment of methane oxidation would be advisable. The field scale model presented in this thesis compares favourably with other field scale models, although for a generalisation of the results, more validation sites are necessary. The deviation in seasonal methane emissions was 7% for 6 sites in the Philippines.

With this small model deviation the objectives mentioned in the introduction of this thesis are met. This does not mean that upscaling for methane emissions from rice paddies can be applied successfully. Several problems can be mentioned; i) Essential data on the spatial distribution of variables, like water, nutrient and cultivar management are not available, ii) High heterogeneity in combination with the non-linear relations induces scaling errors, which can be considerable when applying large scale databases. With detailed databases and geostatistical tools, the heterogeneity can be accounted for, but this estimate will be regionally specific, iii) Validation is seriously hampered by the lack of independent data at a regional scale. Validation by downscaling techniques could in principle be possible but is severely hampered by data on atmospheric CH_4 mixing ratios (Houweling, 2000). Upscaling of methane emissions from rice paddies remains thus a major scientific challenge.

Samenvatting

van Bodegom, P.M., 2000. Methaanemissies uit rijstvelden; experimenten en modellering. Proefschrift Wageningen Universiteit, Wageningen.

Inleiding

Dit proefschrift behandelt modelontwikkeling en experimenten uitgevoerd om methaanemissies uit rijstvelden te begrijpen en te voorspellen. De methaanconcentratie in de atmosfeer is de afgelopen eeuw verdubbeld en draagt daarmee ongeveer 20% bij aan het versterkte broeikaseffect. Dit versterkte broeikaseffect kan niet alleen mondiale opwarming veroorzaken, maar kan ook weerspatronen veranderen en kan leiden tot meer extreme weerstypen, zoals stormen, overstromingen en droogtes. Rijstvelden veroorzaken ruim 10% van de mondiale methaanemissies en zijn hiermee een belangrijke anthropogene bron van methaanemissies. De huidige schatting is erg onzeker. Een betere mondiale schatting van methaanemissies uit rijstvelden zou kunnen helpen om het nut van technologieën die moeten leiden tot minder methaanuitstoot te evalueren. Bovendien zou een betere schatting voor rijstvelden de onzekerheid in de schattingen van andere methaanbronnen kunnen verminderen. De doelen van dit proefschrift zijn i) de ontwikkeling van een procesmatig veldschaalmodel dat kan worden gekoppeld aan een geografisch informatiesysteem (GIS) om regionale methaanemissies uit rijstvelden te berekenen en te voorspellen en ii) de processen die leiden tot methaanemissies uit rijstvelden te begrijpen en te kwantificeren door experimenten uit te voeren en modellen te ontwikkelen.

Een procesmatig veldschaalmodel

De temporele en spatiële variatie in gemeten methaanemissies is vaak groot en slecht begrepen. Bovendien zijn de processen die leiden tot methaanemissies vaak niet-lineair. Empirische en correlatieve modellen hebben om deze redenen maar een beperkte toepasbaarheid en extrapoleerbaarheid. Het ontwikkelde veldschaalmodel is daarom op de onderliggende processen gebaseerd. Echter, een koppeling aan een GIS vereist ook dat het aantal noodzakelijke inputparameters tot een minimum wordt beperkt en bovendien dat de inputparameters algemeen beschikbaar zijn. Om dit te bereiken, zijn de processen die leiden tot methaanemissies -hieronder uitgebreider behandeld- vereenvoudigd. Een cruciale stap in de vereenvoudiging was de verdeling van rijstgrond in een rhizosfeer -grond onder directe invloed van plantenwortels- en een bulkgrond zonder invloed van planten. Deze onderverdeling maakte vereenvoudiging van de procesbeschrijvingen mogelijk.

Het veldschaalmodel is gevalideerd met onafhankelijke veldmetingen van methaanemissies uit rijstvelden in de Filipijnen, China en Indonesië. Het model was goed in staat om zowel de dynamiek in methaanemissies als de totale seizoensemissies te voorspellen met slechts enkele inputparameters en is behalve voor verschillende lokaties ook getest voor verschillende seizoenen en voor verschillende toevoegingen van meststoffen. De standaarddeviatie ten opzichte van de metingen was minder dan 10% en was daarmee nauwkeuriger dan andere modellen. Een gevoeligheidsanalyse van het model toonde aan dat de modelaannames redelijk waren en dat het expliciet

onderscheiden van de rhizosfeer noodzakelijk was voor een goede voorspelling van methaanemissies.

De nauwkeurigheid van het veldschaalmodel werd bepaald door de variabiliteit en onnauwkeurigheid van de processen die leiden tot methaanemissies in combinatie met de gevoeligheid van emissies voor die onderliggende processen. Het veldschaalmodel was niet zo gevoelig voor de manier waarop methaanproduktie of methaantransport werd beschreven. Het was echter wel heel gevoelig voor de beschrijving van het vrijkomen van substraat voor methaanproduktie. De hoeveelheid substraat die vrijkomt was echter slecht bekend. De gekozen beschrijving voor het vrijkomen van substraat lijkt een belangrijke reden voor de nauwkeuriger schattingen van methaanemissies door het gepresenteerde veldschaalmodel ten opzichte van andere modellen.

Het proces van methaanproduktie

In een zuurstofloze grond worden, in plaats van zuurstof, alternatieve electron acceptoren gereduceerd. Incubatie-experimenten met bodemslurries uit rijstvelden toonden aan dat eerst nitraat werd gereduceerd, gevolgd door ijzer- en sulfaatreductie en methaanproduktie. Er trad vooral substraatcompetitie -voor acetaat en H_2/CO_2- op tussen sulfaatreducerende en methaanproducerende microorganismen. Alle processen verliepen sneller bij hogere temperatuur, maar de mate waarin verschilde per proces. Methaanproducerende microorganismen kwamen in een competitief voordeel bij hogere temperaturen. Dit zou verklaard kunnen worden door een verandering in affiniteit voor acetaat met temperatuur. Incubatie-experimenten toonden tevens aan dat organische electron acceptoren niet van belang zijn in rijstvelden.

Op basis van deze en aanvullende experimenten, waarin extra electronacceptoren of electrondonoren waren toegevoegd, is een mechanistisch model ontwikkeld dat de competitie voor substraat, maar ook inhibitie-effecten en chemolithotrofe redox reacties -reacties zonder koolstofbron- analyseerde. In het model werden de maximale omzettingssnelheden gecalibreerd met incubatie-experimenten. Alle andere parameterwaarden werden uit gepubliceerde gegevens afgeleid. Het model werd gevalideerd met incubatie-experimenten waarin extra electron donoren of electron acceptoren waren toegevoegd. De verschillen tussen model en experiment waren niet significant en er werd geconcludeerd dat het model adequate procesbeschrijvingen had. Een gevoeligheidsanalyse van het model toonde aan dat het model gevoelig was voor schattingen voor de maximale omzettingssnelheid en voor beschrijvingen voor het vrijkomen van substraat, hetgeen de gevoeligheid van het veldschaalmodel hiervoor verklaart. Inhibitie van methaanproduktie en sulfaatreductie door ijzer gaf een verklaring voor de ophoping van acetaat aan het begin van incubaties.

Het proces van gastransport

Eenmaal geproduceerd methaan diffundeert via de bodem en de plant naar de atmosfeer. De snelheid waarmee dit gebeurt is onderzocht met experimenten waarbij het transport van het inerte gas SF_6 werd gevolgd door gronden met en zonder rijstplanten d.m.v. fotoacoustische detectietechnieken. Deze experimenten werden gebruikt om een mechanistisch diffusiemodel voor gastransport door een overstroomd rijstsysteem te valideren. De benodigde parameterwaarden voor dit model werden geschat op basis van gepubliceerde gegevens en uit experimenten die onafhankelijk van de validatie-

experimenten werden uitgevoerd. Het diffusieverloop van SF_6 kon redelijk goed worden voorspeld door het mechanistische model. Het model toonde duidelijk aan dat diffusie door de bodem de limiterende factor is in het gastransport door het bodem-plant systeem, wat verklaart waarom veel methaan via de rijsplant wordt geëmiteerd. Binnen de plant was de overgang tussen wortel en spruit de meest limiterende factor voor gastransport. De snelheid van gastransport werd vooral bepaald door de diffusiecoëfficient en door de wortelverdeling over de diepte.

Het proces van methaanoxidatie
Voordat methaan de atmosfeer bereikt, kan het geoxideerd -geconsumeerd- worden in zuurstofbevattende lagen van de bodem. De toplaag van de grond en de waterlaag erop is zuurstofhoudend. Van deze laag is de methaanoxidatie vrij goed bekend. De rijst rhizosfeer is ook zo'n zuurstofbevattende zone. Methaanoxidatieschattingen voor deze zone zijn echter heel variabel. Verschillende experimenten en beschouwingen hebben aangetoond dat methaanoxidatie in de rhizosfeer zuurstofgelimiteerd is. Daarom zijn bodemincubatie-experimenten uitgevoerd en zijn tellingen van zuurstofconsumerende bacteriën verricht. De aantallen methaanoxiderende bacteriën waren zowel temporeel als spatieel sterk variabel. Deze experimenten hebben ook aangetoond dat chemische ijzeroxidatie, microbiële heterotrofe respiratie en microbiële methaanoxidatie de belangrijkste zuurstofconsumerende processen waren in de rijstrhizosfeer. De meest talrijke heterotrofe en methanotrofe bacteriën zijn geïsoleerd en gekarakteriseerd. De groei van deze bacteriën onder koolstof- en zuurstoflimitaties is gekwantificeerd. Bovendien zijn competitie-experimenten tussen heterotrofen en methanotrofen uitgevoerd onder verschillende methaan- en zuurstoflimitaties. Deze experimenten toonden aan dat methaanoxidatie het alleen wint van heterotrofe respiratie bij lage zuurstof- en acetaatconcentraties.

Op basis van de experimenten werd gehypothetiseerd dat methaanoxidatie niet heel dicht bij de rijstwortel zal plaatsvinden, omdat de methanotrofen dichterbij de wortel de competitie zouden verliezen van de heterotrofen. Om dit verder te onderzoeken, is er een mechanistisch model van de rijstrhizosfeer ontwikkeld. Dit model bevatte zowel reacties die leiden tot de produktie van acetaat, methaan en gereduceerd ijzer als reacties waarbij deze stoffen door zuurstofconsumptie worden geoxideerd. Daarnaast was er een pH-afhankelijke ijzeradsorptie in het model opgenomen en werd het diffuse transport van verschillende stoffen door de rhizosfeer en de rijstplant beschreven. Dit model kon goed de zuurstofafgifte door de rijstwortel voorspellen, alsmede concentraties van verschillende stoffen in de rhizosfeer. Dit model bevestigde de hypothese dat methaanoxidatie iets verder van de wortel af zal plaatsvinden. Methaanoxidatie- schattingen waren lager dan veelal gepresenteerd en waren bovendien sterk afhankelijk van de opgegeven condities. Die condities betroffen vooral de zuurstofconcentratie en andere parameters die de competitie tussen methaanoxidatie en chemische ijzeroxidatie beïnvloeden. Daarnaast bleek dat er geen evenwicht in de rhizosfeer kan worden bereikt in de korte periode dat een wortel een bepaalde plek in een bodem beïnvloedt, aannemende dat alleen de worteltop zuurstof uitscheidt en dat de worteltop zich door wortelgroei door de bodem verplaatst. Door wortelgroei ontstond een dynamisch systeem dat leidde tot een grote variabiliteit in methaanoxidatie. Dit betekende tevens dat

methaanoxidatieschattingen anders waren als ze werden uitgedrukt per eenheid methaan <u>verdwenen</u> uit de rhizosfeer dan wel per eenheid methaan <u>geproduceerd</u> in de rhizosfeer.

Bruikbaarheid van het veldschaalmodel

De mechanistische studies hebben de dynamiek van het systeem aangetoond en hebben bijgedragen aan een beter begrip van de onderliggende processen. Dit begrip kon gebruikt worden om de vereenvoudigingen in het veldschaal model te evalueren. In het veldschaalmodel was aangenomen dat substraat direct werd geconsumeerd en dat de volgorde van de reductie bepaald werd door de redoxsequentie. Die vereenvoudigingen leidden tot een overschatting van methaanproduktie als er relatief veel substraat was en tot een onderschatting als er veel alternatieve electron acceptoren waren. De verschillen waren over het algemeen echter vrij gering. In het veldschaalmodel werd aangenomen dat methaan binnen enkele uren vanuit de rhizosfeer in de atmosfeer kwam. Dit werd bevestigd door het mechanistische transportmodel. In de bulkgrond werd het transport bepaald door transport van gasbellen dat helaas niet onderzocht kon worden met een diffusiemodel, waardoor er geen vergelijking gemaakt kon worden. Tenslotte konden de methaanoxidatieschattingen met elkaar worden vergeleken. Volgens het mechanistische rhizosfeer model werd er minder methaan geoxideerd dan in het veldschaalmodel werd aangenomen. Daar staat echter tegenover dat in het veldschaalmodel de recycling van alternatieve electron acceptoren was genegeerd. Deze verwaarlozingen heffen elkaar op, omdat ze binnen de electronenbalans tegen elkaar wegvallen. Al met al was het veldschaalmodel in staat om met weinig inputparameters methaanemissies zeer redelijk te voorspellen.

Het veldschaalmodel is dus in principe geschikt om in combinatie met GIS regionale methaanemissies te schatten. Om tot regionale emissieschattingen te komen, moest echter ook voldaan worden aan een aantal andere voorwaarden. De inputparameters moesten goed afgeschat kunnen worden. Dat was niet voor alle inputparameters altijd het geval. Daarnaast leidde de noodzaak van data-interpolatie tot fouten. Deze foutenbron kon beperkt worden door een juiste interpolatietechniek en semivariogram te kiezen. Het verlies aan informatie over heterogeniteit leidde echter alsnog tot schaaleffecten in schattingen van regionale methaanemissies in een case study voor het eiland Java. Schaaleffecten traden ook op als grovere dataresoluties werden gekozen. Dergelijke schaaleffecten worden regelmatig genegeerd in opschalingsstudies en kunnen leiden tot onnauwkeurige emissieschattingen. In opschalingsstudies zal, mede door het beschikbaar gekomen veldschaalmodel, niet langer modelkwaliteit maar de beschikbaarheid van goede data limiterend zijn voor het tot stand komen van goede regionale methaanemissieschattingen.

References

Acharya C.N. (1935). Studies on the anaerobic decomposition of plant materials. III. Comparison of the course of decomposition of rice straw under anaerobic, aerobic and partially aerobic conditions. *Biochem. J.* 29: 1116-1120

Achtnich C., F. Bak and R. Conrad (1995a). Competition for electron donors among nitrate reducers, ferric iron reducers, sulfate reducers and methanogens in anoxic paddy soil. *Biol. Fertil. soils* 19: 65-72

Achtnich C., A. Schuhmann, T. Wind and R. Conrad (1995b). Role of interspecies H_2 transfer to sulfate and ferric iron-reducing bacteria in acetate consumption in anoxic paddy soil. *FEMS Microbiol. Ecol.* 16: 61-70

Ahmad A.R. and P.H. Nye (1990). Coupled diffusion and oxidation of ferrous iron in soils. I. Kinetics of oxygenation of ferrous iron in soil suspension. *J. Soil Sci.* 41: 395-409

Allen L.H. Jr. (1997). Mechanisms and rates of O_2 transfer to and through submerged rhizozomes and roots via aerenchyma. *Soil Crop Sci. Soc. Florida Proc.* 56: 41-54

Amaral J.A. and R. Knowles (1995). Growth of methanotrophs in methane and oxygen counter gradients. *FEMS Microbiol. Lett.* 126: 215-220

Ando T., S. Yoshida and I. Nishiyama (1983). Nature of oxidizing power of rice roots. *Plant Soil* 72: 57-71

Arah J.R.M. and G.J.D. Kirk (2000). Modelling rice-plant mediated methane emission. *Nutr. Cycl. Agroecosys.* (in press)

Arah J.R.M. and K.D. Stephen (1998). A model of the processes leading to methane emission from peatland. *Atmos. Env.* 32: 3257-3264

Armstrong W. (1969). Rhizosphere oxidation in rice: an analysis of intervarietal differences in oxygen flux from the roots. *Physiol. Plant.* 22: 296-303

Armstrong W. (1970). Rhizosphere oxidation in rice and other species: a mathematical model based on the oxygen flux component. *Physiol. Plant.* 23: 623-630

Armstrong W. (1971a). Radial oxygen losses from intact rice roots as affected by distance from the apex, respiration and waterlogging. *Physiol. Plant.* 25: 192-197

Armstrong W. (1971b). Oxygen diffusion from the roots of rice grown under non-waterlogged conditions. *Physiol. Plant.* 24: 242-247

Armstrong W. and P.M. Beckett (1987). Internal aeration and the development of stelar anoxia in submerged roots. A multishelled mathematical model combining axial diffusion of oxygen in the cortex with radial losses to the stele, the wall layers and the rhizosphere. *New. Phytol.* 105: 221-245

Armstrong W. and T.J. Gaynard (1976). The critical oxygen pressures for respiration in intact plants. *Physiol. Plant.* 37: 200-206

Armstrong W., P.M. Beckett, S.H.F.W. Justin and S. Lythe (1991). Modelling and other aspects of root aeration by diffusion. In: *Plant life under oxygen deprivation. Ecology, Physiology and Biochemistry.* M.B. Jackson, D.D. Davies and H. Lambers (Eds), SPB Academic Publishers, The Hague, Netherlands, p. 267-282

Arth I., P. Frenzel and R. Conrad (1998). Denitrification coupled to nitrification in the rhizosphere of rice. *Soil Biol. Biochem.* 30: 509-515

Asakawa S., M. Akagawa-Matsushita, Y. Koga and K. Hayano (1998). Communities of methanogenic bacteria in paddy field soils with long-term application of organic matter. *Soil Biol. Biochem.* 30: 299-303

Aselmann I. and P. Crutzen (1989). Global distribution of natural freshwater wetlands and rice paddies: Their net primary productivity, seasonality and possible methane emissions. *J. Atmos. Chem.* 8: 307-358

Atlas R.M. and R. Barta (1987). *Microbial Ecology: Fundamentals and applications.* Benjamin/Cummings, CA

Bachelet D. and H.U. Neue (1993). Methane emissions from wetland rice areas of Asia. *Chemosphere* 26: 219-237

Bak F. and N. Pfennig (1991). Microbial sulfate reduction in littoral sediment in Lake Constance. *FEMS Microbiol. Ecol.* 85: 31-42

Balderston W.L. and W.J. Payne (1976). Inhibition of methanogenesis in salt marsh sediments and whole-cell suspensions of methanogenic bacteria by nitrogen oxides. *Appl. Env. Microbiol.* 32: 264-269

Banker B.C., H.K. Kludze, D.P. Alford, R.D. Delaune and C.W. Lindau (1995). Methane sources and sinks in paddy rice soils: relationship to emissions. *Agr. Ecosys. Env.* 53: 243-251

Barber D.A., M. Ebert and N.T.S. Evans (1962). The movement of ^{15}O through barley and rice plants. *J. Exp. Bot.* 13: 397-403

Bedford B.L. and D.R. Bouldin (1994). Response to the paper 'on the difficulties of measuring oxygen release by root systems of wetland plants', by B.K. Sorrell and W. Armstrong. *J. Ecol.* 82: 185-186

Begg C.B.M., G.J.D. Kirk, A.F. Mackenzie and H.U. Neue (1994). Root-induced iron oxidation and pH changes in the lowland rice rhizosphere. *New Phytol.* 128: 469-477

Bender M. and R. Conrad (1992). Kinetics of methane oxidation in oxic soils exposed to ambient air and or high CH_4 mixing ratios. *FEMS Microbiol. Ecol.* 101: 261-270

Benz M., A. Brune and B. Schink (1998). Anaerobic and aerobic oxidation of ferrous iron at neutral pH by chemoheterotrophic nitrate-reducing bacteria. *Arch. Microbiol.* 169: 159-165

Beyrouty C.A., B.R. Wells, R.J. Norman, J.N. Marvel and J.A. Pillow (1988). Root growth dynamics of a rice cultivar grown at two locations. *Agron. J.* 80: 1001-1004

Biro Pusat Statistik (BPS) (1994). *Struktur ongkos usaha tani padi dan palawija (Cost structure of farms paddy and palawija).* BPS, Jakarta, Indonesia

Biro Pusat Statistik (BPS) (1995). *Survei partanian - produksi tanaman padi di Indonesia 1994 (Agricultural survey - production of paddy in Indonesia 1994).* BPS, Jakarta, Indonesia

Biro Pusat Statistik (BPS) (1996). *Survei luas tanaman padi dengan pendekatan rumah tangga di Jawa 1996.* BPS, Jakarta, Indonesia

Blackall L.L., V. Tandoi and D. Jenkins (1991). Continuous culture studies with *Nocardia amarae* from activated sludge and their implications for Nocardia foaming control. *Res. J. WPCF* 63: 44-50

Bodegom P.M. van, P.H. Verburg and H.A.C. Denier van der Gon (2000). Upscaling methane emissions from rice paddies: problems and possibilities. *Global Change Biol.* (submitted)

Bodelier P.L.E. and H.J. Laanbroek (1997). Oxygen uptake kinetics of *Pseudomonas chlororaphis* grown in glucose- or glutamate-limited continuous cultures. *Arch.Microbiol.* 167:392-395

Bodelier P.L.E. and P. Frenzel (1999). Contribution of methanotrophic and nitrifying bacteria to CH_4 and NH_4^+ oxidation in the rhizosphere of rice plants as determined by new methods of discrimination. *Appl. Env. Microbiol.* 65: 1826-1833

Bodelier P., P. Roslev, T. Henckel and P. Frenzel (2000). Stimulation by ammonium-based fertilizers of methane oxidation in soil around rice roots. *Nature* 403: 421-424

Bont J.A.M. de, K.K. Lee and D.F. Bouldin (1978). Bacterial oxidation of methane in a rice paddy. *Ecol. Bull.* 26: 91-96

Bosse U. and P. Frenzel (1997). Activity and distribution of methane-oxidizing bacteria in flooded rice soil microcosms and in rice plants (*Oryza sativa*). *Appl. Env. Microbiol.* 63: 1199-1207

Bosse U. and P. Frenzel (1998). Methane emissions from rice microcosms: The balance of production, accumulation and oxidation. *Biogeochemistry* 41: 199-214

Boudreau B.P. (1996). A method-of-lines code for carbon and nutrient diagenesis in aquatic sediments. *Computers Geosci.* 22: 479-496

Bouma J., H.W.G. Booltink and P.A. Finke (1996). Use of soil survey data for modeling solute transport in the Vadose zone. *J. Env. Qual.* 25: 519-526

Bowman J.P., L.I. Sly, P.D. Nichols and A.C. Hayward (1993). Revised taxonomy of the methanotrophs: description of Methylobacter gen. nov., emendation of Methylococcus, validation of Methylosinus and Methylocystis species and a proposal that the family Methylococcaceae includes only the group I methanotrophs. *Int. J. Syst. Bact.* 43: 735-753

Brandis-Heep A., N.A. Gebhardt, R.K. Thauer, F. Widdel and N. Pfennig (1983). Anaerobic acetate oxidation to CO_2 by *Desulfobacter postgatei*. 1. Demonstration of all enzymes required for the operation of the citric acid cycle. *Arch. Microbiol.* 136: 222-229

Bratbak G. (1985). Bacterial biovolume and biomass estimations. *Appl. Env. Microbiol.* 49: 1488-1493

Brunet R.C. and Garcia-Gil L.J. (1996). Sulfide-induced dissimilatory nitrate reduction to ammonia in anaerobic freshwater sediments. *FEMS Microbiol. Ecol.* 21: 131-138

Buchholz L.A., J.V. Klump, M.L.P. Collins, C.A. Brantner and C.C. Remsen (1995). Activity of methanotrophic bacteria in Green Bay sediments. *FEMS Microbiol. Ecol.* 16: 1-8

Buendia L.V., R. Wassmann, R.S. Lantin, H.U. Neue, A.M. Javellana, C.S. Bueno, N. Nocon, A. Umali and L.A. Lubigan (2000). A five-year study of methane emissions from rice fields in Los Baños (Philippines). *Nutrient Cycl. Agroecosys.* (in press)

Butterbach-Bahl K. (1992). *Mechanismen der Produktion und Emission von Methan in Reisfeldern: Abhängigkeit von Felddüngung und angebauter Varietät*. Diss. Techn Uni. München. Schriftenreihe des Fraunhofer Institut für Atmosphärische Umweltforschung Bd 14. Wiss Verl. Mauraun, Frankfurt

Butterbach-Bahl K., H. Papen and H. Rennenberg (1997). Impact of gas transport through rice cultivars on methane emission from rice paddy fields. *Plant Cell Environ.* 20: 1175-1183

Byrd, G.T., F.M. Fisher and R.L. Sass (2000). Relationships between methane production and emission to lacunal methane concentrations in rice. *Global Biogeochem. Cycl.* 14: 73-83

Byrnes B.H., E.R. Austin and B.K. Tays (1995). Methane emissions from flooded rice soils and plants under controlled conditions. *Soil Biol. Biochem.* 27: 331-339

Cabrera M.L. (1993). Modeling the flush of nitrogen mineralization caused by drying and rewetting soils. *Soil Sci. Soc. Am. J.* 57: 63-66

Cai Z.and X. Yan (1999). Kinetic model for methane oxidation by paddy soil as affected by temperature, moisture and N addition. *Soil Biol. Biochem.* 31: 715-725

Calhoun A. and G.M. King (1997). Regulation of root-associated methanotrophy by oxygen availibility in the rhizosphere of two aquatic macrophytes. *Appl. Env. Microbiol.* 63: 3051-3058

Calhoun A. and G.M. King (1998). Characterization of root-associated methanotrophs from three freshwater macrophytes: *Pontederia cordata, Sparganium eurycarpum* and *Sagittaria latifolia. Appl. Env. Microbiol.* 64: 1099-1105

Campbell G.S. (1985). *Soil physics with basic transport models for soil-plant systems.* Developments in Soil Science 14, Elsevier, Amsterdam, The Netherlands

Cao M., J.B. Dent and O.W. Heal (1995). Modeling methane emissions from rice paddies. *Global Biogeochem. Cycl.* 9: 183-195

Cao M., K. Gregson and S. Marshall (1998). Global methane emission from wetlands and its sensitivity to climate change. *Atmos. Env.* 32: 3293-3299

Cappellen P. van and Y. Wang (1996). Cycling of iron and manganese in surface sediments: a general theory for the coupled transport and reaction of carbon, oxygen, nitrogen, sulfur, iron and manganese. *Am. J. Sci.* 296: 197-213

Cappenberg Th.E. (1975). A study of mixed continuous cultures of sulfate-reducing and methane-producing bacteria. *Micr. Ecol.* 2: 60-72

Chanton J.P., G.J. Whiting, N.E. Blair, C.W. Lindau and P.K. Bollich (1997). Methane emission from rice: stable isotopes, diurnal variations and CO_2 exchange. *Global Biogeochem. Cycl.* 11: 15-27

Chin K. and R. Conrad (1995). Intermediary metabolism in methanogenic paddy soil and the influence of temperature. *FEMS Microbiol. Ecol.* 18: 85-102

Cicerone R.J. and R.S. Oremland (1988). Biogeochemical aspects of atmospheric methane. *Global Biogeochem. Cycl.* 2: 299-327

Colmer T.D., M.R. Gibberd, A. Wiengweera and T.K. Tinh (1998). The barrier to radial oxygen loss from roots of rice (*Oryza sativa* L.) is induced by growth in stagnant solution. *J. Exp. Bot.* 49: 1431-1436

Conlin T.S.S. and A.A. Crowder (1989). Location of radial oxygen loss and zones of potential iron uptake in a grass and two nongrass emergent species. *Can J. Bot.* 67: 712-722

Conrad R. (1993). Mechanisms controlling methane emission from wetland rice fields. In: *Biogeochemistry of global change. Radiatively active trace gases.* R.S. Oremland (Ed), Chapman & Hall, New York, p. 317-335

Conrad R. (1996). Soil microorganisms as controllers of atmospheric trace gases (H_2, CO, CH_4, OCS, N_2O, and NO). *Microbiol. Rev.* 60: 609-640

Conrad R. and M. Klose (1999). Anaerobic conversion of carbon dioxide to methane, acetate and propionate on washed rice roots. *FEMS Microbiol. Ecol.* 30: 147-155

Conrad R. and Rothfuss F. (1991). Methane oxidation in the soil surface layer of a flooded rice field and the effect of ammonium. *Biol. Fertil. Soils* 12: 28-32

Conrad R., B. Schink and T.J. Phelps (1986). Thermodynamics of H_2-consuming and H_2-producing metabolic reactions in diverse methanogenic environments under in situ conditions. *FEMS Microbiol. Ecol.* 38: 353-360

Conrad R., F. Bak, H.J. Seitz, B. Thebrath, H.P. Mayer and H. Schütz (1989a). Hydrogen turnover by psychrotrophic homoacetogenic and mesophilic bacteria in anoxic paddy soil and lake sediment. *FEMS Microbiol. Ecol.* 62: 285-294

Conrad R., H.P. Mayer and M. Wüst (1989b). Temporal change of gas metabolism by hydrogen-syntrophic methanogenic bacterial associations in anoxic paddy soil. *FEMS Microbiol. Ecol.* 62: 265-274

Conrad R., M. Klose and P. Claus (2000). Phosphate inhibits acetotrophic methanogenesis on rice roots. *Appl. Env. Microbiol.* 66: 828-831

Cord-Ruwisch R. and B. Ollivier (1986). Interspecific hydrogen transfer during methanol degradation by *Sporomusa acidovorans* and hydrogenophilic anaerobes. *Arch. Microbiol.* 144: 163-165

Cord-Ruwisch R., H-J. Seitz and R. Conrad (1988). The capacity of hydrogenotrophic anaerobic bacteria to compete for traces of hydrogen depends on the redox potential of the terminal electron acceptor. *Arch. Microbiol.* 149: 350-357

Cox D.M. and A. Gnauck (1980). Continuous-wave CO_2 laser spectroscopy of SF_6, WF_6 and UF_6. *J. Mol. Spectroscopy* 81: 207-215

Crill P.M. and Martens C.S. (1986). Methane production from bicarbonate and acetate in an anoxic marine sediment. *Geochim. Cosmochim. Acta* 50: 2089-2097

D'Angelo E.M. and K.R. Reddy (1999). Regulators of heterotrophic microbial potentials in wetland soils. *Soil Biol. Biochem.* 31: 815-830

Dannenberg S. and R. Conrad (1999). Effect of rice plants on methane production and rhizospheric metabolism in paddy soil. *Biogeochemistry* 45: 53-71

Dannenberg S., M. Kroder, W. Dilling and H. Cypionka (1992). Oxidation of H_2, organic compounds and inorganic sulfur compounds coupled to reduction of O_2 or nitrate by sulfate-reducing bacteria. *Arch. Microbiol.* 158: 93-99

Darrah P.R. (1991a). Models of the rhizosphere. I. microbial population dynamics around a root releasing soluble and insoluble carbon. *Plant Soil* 133: 187-199

Darrah P.R. (1991b). Models of the rhizosphere. II. A quasi three-dimensional simulation of the microbial population dynamics around a growing root releasing soluble exudates. *Plant Soil* 138: 147-158

David C.C. and K. Otsuka (1994). *Modern rice technology and income distribution in Asia.* IRRI, Manilla, Philippines

Davies S.L. and R. Whittenbury (1970). Fine structure of methane and other hydrocarbon-utilizing bacteria. *J. Gen. Microbiol.* 61: 227-232

Dedysh S.N., N.S. Panikov and J.M. Tiedje (1998). Acidophilic methanotrophic communities from Sphagnum peat bogs. *Appl. Env. Microbiol.* 64: 922-929

Delhaize E., P.R. Ryan and P.J. Randall (1993). Aluminium tolerance in wheat (*Triticum aestivum* L.). II. Aluminium-stimulated excretion of malic acid from root apices. *Plant Physiol.* 103: 695-702

Denier van der Gon H.A.C. and N. van Breemen (1993). Diffusion-controlled transport of methane from soil to atmosphere as mediated by rice plants. *Biogeochemistry* 21: 177-190

Denier van der Gon H.A.C. and H.U. Neue (1995a). Influence of organic matter incorporation on the methane emission from a wetland rice field. *Global Biogeochem. Cycl.* 9: 11-22

Denier van der Gon H.A.C. and H.U. Neue (1995b). Methane emission from a wetland rice field as affected by salinity. *Plant Soil* 170: 307-313

Denier van der Gon H.A.C. and Neue H.U. (1996). Oxidation of methane in the rhizosphere of rice plants. *Biol. Fertil. Soils* 22: 359-366

Denier van der Gon H.A.C., N. van Breemen, H.U. Neue, R.S. Lantin, J.B. Aduna, M.C.R. Alberto and R. Wassmann (1996). Release of entrapped methane from wetland rice fields upon soil drying. *Global Biogeochem. Cycl.* 10: 1-7

Denier van der Gon H.A.C., P. van Bodegom, S. Houweling, P. Verburg and N. van Breemen (2000). Combining upscaling and downscaling of methane emissions from rice fields: methodologies and preliminary results. *Nutr. Cycl. Agroecosys.* (in press)

Devai I. and R.D. Delaune (1996). Light hydrocarbon production in freshwater marsh soil as influenced by soil redox conditions. *Water Air Soil Poll.* 88: 39-46

Dianou D. and K. Adachi (1999). Characterization of methanotrophic bacteria isolated from a subtropical paddy field. *FEMS Microbiol. Lett.* 173: 163-173

Dolfing J. (1988). Acetogenenis. In: *Biology of anaerobic microorganisms.* A.J.B. Zehnder (Ed), John Wiley and Sons, New York, USA, p. 417-468

Drenth H., H.F.M. ten Berge and F.W. Meijboom (1991). Effects of growth medium on porosity and branching of rice roots (*Oryza Sativa* L.). In: *Simulation and systems analysis for rice production (SARP).* F.W.T. Penning de Vries, H.H. van Laar and M.J. Kropff (Eds), Pudoc, Wageningen, The Netherlands, p. 162-175

Dunne T., W.H. Zhang and B.F. Aubry (1991). Effects of rainfall, vegetation, and microtopography on infiltration and runoff. *Water Resources Res.* 27: 2271-2285

Emerson D. and C. Moyer (1997). Isolation and characterization of novel iron-oxidizing bacteria that grow at circumneutral pH. *Appl. Env. Microbiol.* 63: 4784-4792

Emerson D., J.V. Weiss and J.P. Megonigal (1999). Iron-oxidizing bacteria are associated with ferric hydroxide precipitates (Fe-plaque) on the roots of wetland plants. *Appl. Env. Microbiol.* 65: 2758-2761

Epp M.A. and J.P. Chanton (1993). Rhizospheric methane oxidation determined via the methyl fluoride inhibition technique. *J.Geophys. Res.* 98: 18413-18422

Espiritu B.M., K. Adachi and T. Senboku (1997). Effect of application of rice straw and cellulose on methane emission and biological nitrogen fixation in a subtropical paddy field. III. Populations of methane-oxidizing bacteria in soil and rice rhizosphere. *Soil Sci. Plant Nutr.* 43: 729-734

Fetzer S. and R. Conrad (1993). Effect of redox potential on methanogenesis by *Methanosarcina barkeri. Arch. Microbiol.* 160: 108-113

Fetzer S., F. Bak and R. Conrad (1993). Sensitivity of methanogenic bacteria from paddy soil to oxygen and desiccation. *FEMS Microbiol. Ecol.* 12: 107-115

Flessa H. and Fischer W.R. (1992). Plant-induced changes in the redox potentials of rice rhizospheres. *Plant Soil* 143: 55-60

Frenzel P. and U. Bosse (1996). Methyl fluoride, an inhibitor of methane oxidation and methane production. *FEMS Microbiol. Ecol.* 21: 25-36

Frenzel P., B. Thebrath and R. Conrad (1990). Oxidation of methane in the oxic surface layer of a deep lake sediment (Lake Constance). *FEMS Microbiol. Ecol.* 73: 149-158

Frenzel P., F. Rothfuss and R. Conrad (1992). Oxygen profiles and methane turnover in a flooded rice microcosm. *Biol. Fertil. Soils* 14: 84-89

Frenzel P., U. Bosse and P.H. Janssen (1999). Rice roots and methanogenesis in a paddy soil: ferric iron as an alternative electron acceptor in the rooted soil. *Soil Biol. Biochem.* 31: 421-430

Fukuzaki S., N. Nishio and S. Nagai (1990). Kinetics of the methanogenic fermentation of acetate. *Appl. Env. Microbiol.* 56: 3158-3163

Garrels R.M. and C.L. Christ (1965). Solutions, minerals and equilibria. *Harper & Row, New York, USA*

Geraats S.G.M., C.M. Hooijmans, E.W.J. van Niel, L.A. Robertson, J.J. Heijnen, K.C.A.M. Luyben and J.G. Kuenen (1990). The use of a metabolically structured model in the study of growth, nitrification and denitrification by *Thiosphaera pantotropha. Biotechn. Bioeng.* 36: 921-930

Gerritse J. and J.C. Gottschal (1993). Two-membered mixed cultures of methanogenic and aerobic bacteria in O_2-limited chemostats. *J. Gen. Microbiol.* 139: 1853-1860

Gerritse J., F. Schut and J.C. Gottschal (1992). Modelling of mixed chemostat cultures of an aerobic bacterium, *Comamonas testosteroni*, and an anaerobic bacterium, *Veillonella alcalescens*: Comparison with experimental data. *Appl. Env. Microbiol.* 58: 1466-1476

Gilbert B. and P. Frenzel (1995). Methanotrophic bacteria in the rhizosphere of rice microcosms and their effect on porewater methane concentration and methane emission. *Biol. Fertil. Soils* 20: 93-100

Gilbert B. and P. Frenzel (1998). Rice roots and CH_4 oxidation: the activity of bacteria, their distribution and the microenvironment. *Soil Biol. Biochem.* 30: 1903-1916

Gilbert B., B. Aßmus, A. Hartmann and P. Frenzel (1998). In situ localization of two methanotrophic strains in the rhizosphere of rice plants. *FEMS Microbiol. Ecol.* 25: 117-112

Goodfellow M. and D.E. Minnikin (1991). The genera Nocardia and Rhodococcus. In: *The prokaryotes. A handbook on the biology of bacteria: ecophysiology, isolation, identification, applications.* Starr et al. (Eds), 2nd edition , p. 2016-2027

Graham D.W., J.A. Chaudhary, R.S. Hanson and R.G. Arnold (1993). Factors affecting competition between Type I and Type II methanotrophs in two-organism, continuous-flow reactors. *Micr. Ecol.* 25: 1-17

Grant R.F. (1998). Simulation of methanogenesis in the mathematical model ECOSYS. *Soil Biol. Biochem.* 30: 883-896

Grant R.F. (1999). Simulation of methanotrophy in the mathematical model ecosys. *Soil Biol. Biochem.* 31: 287-297

Groot T.T., P.M. van Bodegom, F. Harren and H. Meijer (2000). Quantification of gas transport through the root-shoot transition zone of rice plant tillers with different ages. *Plant Cell Environ.* (submitted)

Grosskopf R., P.H. Janssen and W. Liesack (1998). Diversity and structure of the methanogenic community in anoxic rice paddy soil microcosms as examined by cultivation and direct 16S rRNA gene sequence retrieval. *Appl. Env. Microbiol.* 64: 960-969

Gujer W. and A.J.B. Zehnder (1983). Conversion processes in anaerobic digestion. *Wat. Sci. Tech.* 15: 127-167

Gupta A., J.R.V. Flora, G.D. Sayles and M.T. Suidan (1994). Methanogenesis and sulfate reduction in chemostats- II. Model development and verification. *Wat. Res.* 28: 795-803

Hanada K. (1995). Tillers. In: *Science of the rice plant. Volume two. Physiology.* T. Matsuo, K. Kumazawa, R. Ishii, K. Ishihara and H. Hirata (Eds), Food and Agriculture Policy Research Center, Tokyo, p. 222-258

Harada J. and K. Yamazaki (1993). Roots. In: *Science of the rice plant. Volume one. Morphology.* T. Matsuo and K. Hoshikawa (Eds), Food and Agriculture Policy Research Center, Tokyo, p. 133-186

Harwood J.H. and S.J. Pirt (1972). Quantitative aspects of growth of the methane oxidizing bacterium *Methylococcus capsulatus* on methane in shake flask and continuous chemostat culture. *J. Appl. Bact.* 35: 597-607

Hassink J. and A.P. Whitmore (1997). A model of the physical protection of organic matter in soils. *Soil Sci. Soc. Am. J.* 61: 131-139

Henckel T., M. Friedrich and R. Conrad (1999). Molecular analyses of the methane-oxidizing microbial community in rice field soil by targeting the genes of the 16SRNA, particulate methane monooxygenase and methanol dehydrogenase. *Appl. Env. Microbiol.* 65: 1980-1990

Hirschfelder J.O., C.F. Curtiss and R.B. Bird (1964). *Molecular theory of gases and liquids*, Wiley, New York, USA

Hoffland E., G.R. Findenegg and J.A. Nelemans (1989). Solubilization of rock phosphate by rape. II. Local root exudation of organic acids as a response to P-starvation. *Plant Soil* 113: 161-165

Holzapfel-Pschorn A. and W. Seiler (1986). Methane emission during a cultivation period from an Italian rice paddy. *J. Geophys. Res.* 91: 11803-11814

Holzapfel-Pschorn A., R. Conrad and W. Seiler (1985). Production, oxidation and emission of methane in rice paddies. *FEMS Microbiol. Ecol.* 31: 343-351

Holzapfel-Pschorn A., R. Conrad and W. Seiler (1986). Effects of vegetation on the emission of methane from submerged paddy soil. *Plant Soil* 92: 223-233

Hosono T. and I. Nouchi (1997). The dependence of methane transport in rice plants on the root zone temperature. *Plant Soil* 191: 233-240

Hossain M. (1996). Recent developments in the Asian rice economy: challenges for rice research. In: *Rice reseach in Asia. Progress and priorities.* R.E. Evenson, R.W. Herdt and M. Hossain (Eds), CAB International, Wallingford, UK, p. 17-33

Houghton J.T., L.G. Meira Filho, J. Bruce, H. Lee, B.A. Callander, E. Haites, N. Harriss and K. Maskell (1995). *Climate change 1994. Radiative forcing of climate change and an evaluation of the IPCC IS92 emissions scenarios.* Cambridge University Press, Cambridge, UK

Houghton J.T., L.G. Meira Filho, B.A. Callander, N. Harris, A. Kattenberg and K. Marskell (1996). *Climate change 1995. The science of climate change.* 1st edition, University Press, Cambridge, UK

Houweling S. (2000). *Global modeling of atmospheric methane sources and sinks.* PhD thesis, Utrecht University, The Netherlands

Howeler R.H. and D.R. Bouldin (1971). The diffusion and consumption of oxygen in submerged soil. *Soil Sci. Soc. Am. Proc.* 35: 202-208

Huang Y., R.L. Sass and F.M. Fisher Jr. (1997). Methane emission from Texas rice paddy soils. 1. Quantitative multi-year dependence of CH_4 emission on soil, cultivar and grain yield. *Global Change Biol.* 3: 479-489

Huang Y., R.L. Sass and F.M. fisher Jr. (1998). A semi-empirical model of methane emission from flooded rice paddy soils. *Global Change Biol.* 4: 247-268

Hunik J.H., C.G. Bos, M.P. van den Hoogen, C.D. de Gooijer and J. Tramper (1994). Co-immobilized *Nitrosomonas europaea* and *Nitrobacter agilis* cells: validation of a dynamic model for simultaneous substrate conversion and growth in k-carrageenan gel beads. *Biotechn. Bioeng.* 43: 1153-1163

Hunter K.S., Y. Wang and P. van Cappellen (1998). Kinetic modeling of microbially-driven redox chemistry of subsurface environments: coupling transport, microbial metabolism and geochemistry. *J. Hydrology* 209: 53-80

Husin Y.A., D. Murdiyarso, M.A.K. Khalil, R.A. Rasmussen, M.J. Shearer, S. Sabiham, A. Sunar and H. Adijuwana (1995). Methane flux from indonesian wetland rice: the effects of water management and rice variety. *Chemosphere* 31: 3153-3180

Ingvorsen K., A.J.B. Zehnder and B.B. Jørgensen (1984). Kinetics of sulfate and acetate uptake by *Desulfobacter postgatei. Appl. Env. Microbiol.* 47: 403-408

Intergovernmental Panel on Climate Change (IPCC) (1995). *IPCC 2nd assessment. Climate change 1995.* Cambridge University Press, Cambridge, UK

International Rice Research Institute (IRRI) (1991). *World rice statistics 1990.* IRRI, Manila, Philippines

Inubushi K. and H. Wada (1987). Easily decomposable organic matter in paddy soils: VII. Effect of various pretreatments on N mineralization in submerged soils. *Soil Sci. Plant Nutr.* 33: 567-576

Inubushi K., H. Wada and Y. Takai (1984). Easily decomposable organic matter in paddy soil. IV. Relationship between reduction process and organic matter decomposition. *Soil Sci. Plant Nutr.* 30: 189-198

Inubushi K., K. Hori, S. Matsumoto and H. Wada (1997). Anaerobic decomposition of organic carbon in paddy soil in relation to methane emission to the atmosphere. *Wat. Sci. Tech.* 36: 523-530

Iwahori K., M. Wang, H. Taki and M. Fujita (1995). Comparative studies on utilization of fatty acids and hydrocarbons in *Nocardia amarae* and *Rhodococcus sp.. J. Ferm. Bioeng.* 79: 186-189

Jackson M.B. and W. Armstrong (1999). Formation of aerenchyma and the processes of plant ventilation in relation to soil flooding and submergence. *Plant Biol.* 1: 274-287

Jähne B., G. Heinz and W. Dietrich (1987). Measurement of the diffusion coefficients of sparingly soluble gases in water. *J. Geophys. Res.* 92: 10767-10776

Jakobsen P., W.H. Patrick Jr. and B.G. Williams (1981). Sulfide and methane formation in soils and sediments. *Soil Sci.* 132: 279-287

James R.T. (1993). Sensitivity analysis of a simulation model of methane flux from the Florida Everglades. *Ecol. Modelling* 68: 119-146

Jenkinson D.S., D.D. Harkness, E.D. Vance, D.E. Adams and A.F. Harrison (1992). Calculating net primary production and annual input of organic matter to soil from the amount and radiocarbon content of soil organic matter. *Soil Biol. Biochem.* 24: 295-308

Jensen C.R., R.J. Luxmoore, S.D. van Gundy and L.H. Stolzy (1969). Root air space measurement by a pycnometer method. *Agron. J.* 61: 474-475

Jetten M.S.M., A.J.M. Stams and A.J.B. Zehnder (1990). Acetate threshold values and acetate activating enzymes in methanogenic bacteria. *FEMS Microbiol. Ecol.* 73: 339-344

Jones D.L., P.R. Darrah and L.V. Kochian (1996). Critical evaluation of organic acid mediated iron dissolution in the rhizosphere and its potential role in root iron uptake. *Plant Soil* 180: 57-66

Jørgensen L. (1985). The methane mono-oxygenase reaction system studies in vivo by membrane inlet mass spectrometry. *Biochem. J.* 225: 441-448

Jørgensen L. and H. Degn (1983). Mass spectrometric measurements of methane and oxygen utilization by methanotrophic bacteria. *FEMS Microbiology Lett.* 20: 331-335

Joulian C., S. Escoffier, J. le Mer, H.U. Neue and P.A. Roger (1997). Populations and potential activities of methanogens and methanotrophs in rice fields: relations with soil properties. *Eur. J. Soil Biol.* 33: 105-116

Journel A.G. and C.J. Huijbregts (1978). *Mining Geostatistics.* Academic Press, New York

Kang S.Y., S. Morita and K. Yamazaki (1994). Root growth and distribution in some Japonica-Indica hybrid and Japonica type rice cultivars under field conditions. *Jpn. J. Crop Sci.* 63: 118-124

Keesman K. and G. van Straten (1990). Set membership approach to identification and prediction of lake eutrophication. *Wat. Resource Res.* 26: 2643-2652

Kerns D.M.H. (1960). The hydration of carbon dioxide. *J. Chem. Educ.* 37: 14-23

Khalil M.A.K., R.A. Rasmussen and M.J. Shearer (1998a). Effects of production and oxidation processes on methane emissions from rice fields. *J. Geophys. Res.* 103: 25233-25239

Khalil M.A.K., R.A. Rasmussen, M.J. Shearer, R.W. Dalluge, L.X. Ren and C.L. Duan (1998b). Measurements of methane emissions from rice fields in China. *J. Geophys. Res.* 103: 25181-25210

Kightley D., D.B. Nedwell and M. Cooper (1995). Capacity for methane oxidation in landfill cover soils measured in laboratory-scale microcosms. *Appl. Env. Microbiol.* 61: 592-601

Kimura M. and K. Minami (1995). Dynamics of methane in rice fields. In: *Climate change and rice.* S. Peng et al. (Eds), Springer Verlag, Berlin, p. 33-45

Kimura M., Y. Miura, A. Watanabe, K. Katoh and H. Haraguchi (1991). Methane emission from paddy field, part I. Effect of fertilization, growth stage and midsummer drainage: Pot experiment. *Environ. Sci.* 4: 265-271

Kimura M., T. Minoda and J. Murase (1993). Water-soluble organic materials in paddy soil ecosystem, part 2. Effects of temperature on contents of total organic materials, organic acids, and methane in leachate from submerged paddy soils amended with rice straw. *Soil Sci. Plant Nutr.* 39: 713-724

King G.M. (1992). Ecological aspects of methane consumption, a key determinant of global methane dynamics. *Adv. Microbiol. Ecol.* 12: 431-468

King G.M. (1996). In situ analyses of methane oxidation associated with the roots and rhizomes of a bur reed, *Sparganium eurycarpum*, in a marine wetland. *Appl. Env. Microbiol.* 62: 4548-4555

King G.M., P. Roslev and H. Skovgaard (1990). Distribution and rate of methane oxidation in sediments of the Florida Everglades. *Appl Env. Microbiol.* 56: 2902-2911

Kirchhof G. and H.B. So (1996). The effect of puddling intensity and compaction on soil properties, rice and mungbean growth: a mini-ricebed study. In: *Management of clay soils for rainfed lowland rice-based cropping systems.* G. Kirchhof and H.B. So (Eds), ACIAR, Canberra, p. 51-70

Kirk G.J.D. (1993). Root ventilation, rhizosphere modification, and nutrient uptake by rice. In: *Systems approaches for agricultural development.* F.W.T. Penning de Vries et al. (Eds), Kluwer academic Publishers, Dordrecht, The Netherlands, p. 221-232

Kirk G.J.D. and J.L. Solivas (1997). On the extent to which root properties and transport through the soil limit nitrogen uptake by lowland rice. *Eur. J. Soil Sci.* 48: 613-621

Kirk G.J.D., A.R. Ahmad and P.H. Nye (1990). Coupled diffusion and oxidation of ferrous iron in soils. II. A model of the diffusion and reaction of O_2, Fe^{2+}, H^+ and HCO_3^- in soils and a sensitivity analysis of the model. *J. Soil Sci.* 41: 411-431

Kirk G.J.D., C.B.M. Begg and J.L. Solivas (1993). The chemistry of the lowland rice rhizosphere. *Plant Soil* 155/156: 83-86

Klemendtsson L., B.H. Svenson, T. Lindberg and T. Rosswall (1977). The use of acetylene inhibition of nitrous oxide reductase in quantifying denitrification in soils. *Swed. J. Agric. Res.* 7: 179-185

Klüber H.D. and R. Conrad (1993). Ferric iron-reducing *Shewanella putrefaciens* and nitrogen fixing *Bradyrhizobium japonicum* with uptake hydrogenase are unable to oxidize atmospheric hydrogen. *FEMS Microbiol. Lett.* 111: 337-342

Klüber H.D. and R. Conrad (1998). Effects of nitrate, nitrite, NO and N_2O on methanogenesis and other redox processes in anoxic rice field soil. *FEMS Microbiol. Ecol.* 25: 301-318

Kludze H.K. and R.D. Delaune (1995a). Straw application effects on methane and oxygen exchange and growth in rice. *Soil Sci. Soc. Am. J.* 59: 824-830

Kludze H.K. and R.D. Delaune (1995b). Gaseous exchange and wetland plant response to soil redox intensity and capacity. *Soil Sci. Soc. Am. J.* 59: 939-945

Kludze H.K., R.D. Delaune and W.H. Patrick Jr. (1993). Aerenchyma formation and methane and oxygen exchange in rice. *Soil Sci. Soc. Am. J.* 57: 386-391

Kludze H.K., R.D. Delaune and W.H. Patrick Jr. (1994). A colorimetric method for assaying dissolved oxygen loss from container-grown rice roots. *Agron. J.* 86: 483-487

Kludze H.K., H.U. Neue, D. Llenaresas and R.S. Lantin (2000). Rice root exudation and its impact on methane production. *Soil Sci. Soc. Am. J.* (in press)

Koyama T. (1963). Gaseous metabolism in lake sediments and paddy soils and the production of atmospheric methane and hydrogen. *J. Geophys. Res.* 68: 3971-3973

Krieg N.R. (Ed.) (1984). *Bergey's manual of systematic bacteriology. Vol I.* Williams& Wilkins, Baltimore, USA

Kristjansson J.K., P. Schönheit and R.K. Thauer (1982). Different Ks values for hydrogen of methanogenic bacteria and sulfate reducing bacteria: An explanation for the apparent inhibition of methanogenesis by sulfate. *Arch. Microbiol.* 131: 278-282

Krooneman J., E.R.B. Moore, J.C.L. van Velzen, R.A. Prins, L.J. Forney and J.C. Gottschal (1996). Competition for oxygen and 3-chlorobenzoate between two aerobic bacteria using different degradation pathways. *FEMS Microbiol. Ecol.* 26: 171-179

Krumböck M. and R. Conrad (1991). Metabolism of position-labelled glucose in anoxic methanogenic paddy soil and lake sediment. *FEMS Microbiol. Ecol.* 85: 247-256.

Kumaraswamy S., B. Ramakrishnan, S.N. Satpathy, A.K. Rath, S. Misra, V.R. Rao and N. Sethunathan (1997). Spatial distribution of methane-oxidizing activity in a flooded rice soil. *Plant Soil* 191: 241-248

Kumazawa K. (1984). Physiological specificity of rice root in relation to oxidizing power and nutrient uptake. In: *Biology of rice.* S. Tsunoda and N. Takahashi (Eds), Sci. Soc. Press/Elsevier, Tokyo/Amsterdam, Japan, p. 117-131

Kun E. and E.B. Kearney (1974). Ammonia. In: *Methods of enzymatic analysis.* Bergmeyer H.U. (Ed), Verlag chemie, Weinheim, Germany, p. 1802-1806

Langø T., T. Mørland and A.O. Brubakk (1996). Diffusion coefficients and solubility coefficients for gases in biological fluids and tissues: A review. *Undersea Hyperbaric Med.* 23: 247-272

Lee K.K., R.W. Holst, I. Watanabe and A. App (1981). Gas transport through rice. *Soil Sci. Plant Nutr.* 27: 151-158

Leffelaar P.A. and W.W. Wessel (1988). Denitrification in a homogeneous, closed system: Experiment and simulation. *Soil Sci.* 146: 335-349

Lelieveld J., P.J. Crutzen and F.J. Dentener (1998). Changing concentration, lifetime and climate forcing of atmospheric methane. *Tellus* 50B: 128-150

Lindau C.W. and P.K. Bollich (1993). Methane emissions from Lousiana 1st and ratoon crop rice. *Soil Sci.* 156: 42-48

Lindau C.W., P.K. Bollich and R.D. Delaune (1995). Effect of rice variety on methane emission from Louisiana rice. *Agr. Ecosys. Env.* 54: 109-114

Lord C.J. III and T.M. Church (1983). The geochemistry of salt marshes: sedimentary ion diffusion, sulfate reduction and pyritization. *Geochim. Cosmochim. Acta* 47: 1381-1391

Lovley D.R. and R.J. Klug (1986). Model for the distribution of sulphate reduction and methanogenesis in freshwater sediments. *Geochim. Cosmochim. Acta* 50: 11-18

Lovley D.R. and E.P. Phillips (1986). Organic matter mineralization with reduction of ferric iron in anaerobic sediments. *Appl. Env. Microbiol.* 51: 683-689

Lovley D.R. and E.P. Phillips (1987). Competitive mechanisms for inhibition of sulfate reduction and methane production in the zone of ferric iron reduction in sediments. *Appl. Env. Microbiol.* 53: 2636-2641

Lovley D.R. and E.P. Phillips (1988). Novel mode of microbial energy metabolism: organic carbon oxidation coupled to dissimilatory reduction of iron or manganese. *Appl. Env. Microbiol.* 54: 1472-1480

Lovley D.R., J.D. Coates, E.L. Blunt-Harris, E.J. Phillips and J.C. Woodward (1996). Humic substances as electron acceptors for microbial respiration. *Nature* 382: 445-448

Lu Y., R. Wassmann, H.U. Neue and C. Huang (1999). Impact of phosphorus supply on root exudation, aerenchyma formation and methane emission of rice plants. *Biogeochemistry* 47: 203-218

Lupton F.S. and J.G. Zeikus (1984). Physiological basis for sulfate-dependent hydrogen competition between sulfidogens and methanogens. *Curr. Microbiol.* 11: 7-11

Luther G.W. III, A. Giblin, R.W. Howarth and R.A. Ryans (1982). Pyrite and oxidized iron mineral phases formed from pyrite oxidation in salt marshes and estuarine sediments. *Geochim. Cosmochim. Acta* 46: 2665-2669

Luxmoore R.J., L.H. Stolzy and J. Letey (1970a). Oxygen diffusion in the soil-plant system I. A model. *Agron. J.* 62: 317-322

Luxmoore R.J., L.H. Stolzy and J. Letey (1970b). Oxygen diffusion in the soil-plant system. II. Respiration rate, permeability and porosity of consecutive excised segments of maize and rice roots. *Agron. J.* 62: 322-324

Masscheleyn P.H., R.D. Delaune and W.H. Patrick Jr. (1993). Methane and nitrous oxide emissions from laboratory measurements of rice soil suspension: Effect of soil oxidation-reduction status. *Chemosphere* 26: 251-260

Matthews E., I. Fung and G. Learner (1991). Methane emission from rice cultivation: Geographic and seasonal distribution of cultivated areas and emissions. *Global Biogeochem. Cycl.* 5: 3-24

Mattson M.D. and G.E. Likens (1990). Air pressure and methane fluxes. *Nature* 347: 718-719

Mattsson M., S. Husted and J.K. Schjoerring (1998). Influence of nitrogen nutrition and metabolism on ammonia volatilization in plants. *Nutr. Cycl. Agroecosys.* 51: 35-40

Mayer H.P. and R. Conrad (1990). Factors influencing the population of methanogenic bacteria and the initiation of methane production upon flooding of paddy soil. *FEMS Microbiol. Ecol.* 7: 103-112

Mc Cartney D.M. and J.A. Oleszkiewizc (1993). Competition between methanogens and sulfate reducers: effect of COD:sulfate ratio and acclimation. *Water Env. Res.* 65: 655-664

McLatchley G.P. and K.R. Reddy (1998). Regulation of organic matter decomposition and nutrient release in a wetland soil. *J. Env. Qual.* 27: 1268-1274

Mer J. le, S. Escoffier, C. Chessel and P.A. Roger (1996). Microbiological aspects of methane emission in a ricefield soil from the Camargue (France):2. Methanotrophy and related microflora. *Eur. J. Soil Biol.* 32: 71-80

Metra-Corton T.M., J.B. Bajita, C.A. Asis Jr. and R.R. Pamplona (1995). Methane emission from an irrigated Philippine paddy field subjected to several fertilizer treatments. *Philipp. J. Crop Sci.* 20: 39-55

Metra-Corton T.M., J.B. Bajita, F.S. Grospe, R.R. Pamplona, C.A. Asis Jr., R. Wassmann and R.S. Lantin (2000). Methane emission from irrigated and intensively managed rice fields in Central Luzon (Philippines). *Nutr. Cycl. Agroecosys.* (in press)

Middleton A.G. and A.W. Lawrence (1977). Kinetics of microbial sulfate reduction. *Res. J. WPCF* 229: 1659-1670

Minami K. (1989). *Effects of agricultural management on methane emission from rice paddies*. NIAES, Japan

Minoda T. and M. Kimura (1994). Contribution of photosynthesized carbon to the methane emitted from paddy fields. *Geophys. Res. Lett.* 21: 2007-2010

Minoda T., M. Kimura and E. Wada (1996). Photosynthates as dominant source of CH_4 and CO_2 in soil water and CH_4 emitted to the atmosphere from paddy fields. *J. Geophys. Res.* D101: 21091-21097

Miura Y., A. Watanabe, J. Murase and M. Kimura (1992). Methane production and its fate in paddy fields. II. Oxidation of methane and its coupled ferric oxide reduction in subsoil. *Soil Sci. Plant Nutr.* 38: 673-679

Monteith J.L. and M.H. Unsworth (1990). *Principles of environmental physics*. 2nd edition. Edward Arnold, London

Murase J. and M. Kimura (1994). Methane production and its fate in paddy fields VI. Anaerobic oxidation of methane in plow layer soil. *Soil Sci. Plant Nutr.* 40: 404-414

Murase J. and M. Kimura (1996). Methane production and its fate in paddy fields IX. Methane flux distribution and decomposition of methane in the subsoil during the growth period of rice plants. *Soil Sci. Plant Nutr.* 42: 187-190

Murase J. and M. Kimura (1997). Anaerobic reoxidation of Mn^{2+}, Fe^{2+}, S_0 and S^{2-} in submerged paddy soils. *Biol. Fertil. Soils* 25: 302-306

Murray R.E., L.L. Parsons and M. Scott Smith (1989). Kinetics of nitrate utilization by mixed populations of denitrifying bacteria. *Appl. Env. Microbiol.* 55: 717-721

Murthy N.B.K., S.P. Kale and K. Raghu (1991). Mineralization of ^{14}C-labeled rice straw in aerobic and anaerobic clay soils as influenced by insecticide treatments. *Soil Biol. Biochem.* 23: 857-859

Nagai S., T. Mori and S. Aiba (1973). Investigation of the energetics of methane-utilizing bacteria in methane- and oxygen-limited chemostat cultures. *J. Appl. Chem. Biotechn.* 23: 549-562

Nedwell D.B. and A. Watson (1995). CH_4 production, oxidation and emission in a U.K. ombrotrophic peat bog: influence of SO_4 from acid rain. *Soil Biol. Biochem.* 27: 893-903

Neue H.U. (1997). Fluxes of methane from rice fields and potential for mitigation. *Soil Use Management* 13: 258-267

Neue H.U. and P.A. Roger (1994). Potential of methane emission in major rice ecologies. In: *Climate Biosphere Interaction*. R.G. Zepp (Ed), Wiley, New York, USA, p. 65-93

Neue H.U. and H.W. Scharpenseel (1987). Decomposition pattern of ^{14}C-labeled rice straw in aerobic and submerged rice soils of the Philippines. *Sci. Total Env.* 62: 431-434

Neu H.U., P. Becker-Heidmann and H.W. Scharpenseel (1990). Organic matter dynamics, soil properties, and cultural practices in rice lands and their relationship to methane production. In: *Soils and the greenhouse effect*. A.F. Bouwman (Ed), Wiley and Sons, New York, USA, p. 457-466

Neue H.U., R. Wassmann, H.K. Kludze, B. Wang and R.S. Lantin (1997). Factors and processes controlling methane emissions from rice fields. *Nutr. Cycl. Agroecosys.* 49: 111-117

Newman E.I. and A. Watson (1977). Microbial abundance in the rhizosphere: A computer model. *Plant Soil* 48: 17-56

Noordwijk M. van and G. Brouwer (1993). Gas-filled porosity in response to temporary low oxygen supply in different growth stages. *Plant Soil* 152: 187-199

Nouchi I. (1990). Mechanisms of methane transport through rice plants. In: *CH₄ and N₂O: Global emissions and controls from rice fields and other agricultural and industrial sources.* NIAES, Japan, p. 87-104

Nouchi I. and Mariko S. (1993). Mechanisms of methane transport by rice plants. In: *Biogeochemistry of global change. Radiatively active trace gases.* R.S. Oremland (Ed.), Chapman & Hall, p. 336-352

Nouchi I., T. Hosono, K. Aoki and K. Minami (1994). Seasonal variation in methane flux from rice paddies associated with methane concentration in soil water, rice biomass and temperature and its modelling. *Plant Soil* 161: 195-208

Nugroho S.G., J. Lumbanraja, H. Suprapto, Sunyoto, W.S. Ardjasa, H. Haraguchi and M. Kimura (1994). Effect of intermittent irrigation on methane emission from an Indonesian paddy field. *Soil Sci. Plant Nutr.* 40: 609-615

Nugroho S.G., J. Lumbaranaja, H. Suprapto, Sunyoto, W.S. Ardjasa, H. Haraguchi and M. Kimura (1996). Three-year measurement of methane emission from an Indonesian paddy field. *Plant Soil* 181: 287-293

Nugroho S.G., Sunyoto, J. Lumbanraja, H. Suprapto, W.S. Ardjasa and M. Kimura (1997). Effect of rice variety on methane emission from an Indonesian paddy field. *Soil Sci. Plant Nutr.* 43: 799-809

Nye P.H. (1972). The measurement and mechanism of ion diffusion in soils. VIII. A theory for the propagation of changes of pH in soils. *J. Soil Sci.* 23: 82-92

O'Connor G.A., W.L. Lindsay and S.R. Olsen (1971). Diffusion of iron and iron chelates in soil. *Soil Sci. Soc. Am. Proc.* 35: 407-410

O'Neill J.G. and J.F. Wilkinson (1977). Oxidation of ammonia by methane-oxidizing bacteria and the effects of ammonia on methane oxidation. *J. Gen. Microbiol.* 100: 407-412

Ogston A.G. (1958). The spaces in a uniform random suspension of fibres. *Trans. Faraday Soc.* 54: 1754-1757

Okabe S., P.H. Nielsen, W.L. Jones and W.G. Characklis (1995). Sulfide product inhibition of *Desulfovibrio desulfuricans* in batch and continuous cultures. *Wat. Res.* 29: 571-578

Oremland R.S. and C.W. Culbertson (1992). Importance of methane-oxidzing bacteria in the methane budget as revealed by the use of a specific inhibitor. *Nature* 356: 421-423

Oremland R.S. and B.F. Taylor (1975). Inhibition of methanogenesis in marine sediments by acetylene and ethylene: validity of the acetylene reduction assay for anaerobic microcosms. *Appl. Env. Microbiol.* 30: 707-709

Ota Y. (1970). Diagnostic methods for the measurement of root activity in rice plant. *Jpn. Agr. Res. Quat.* 5: 1-6

Oude Elferink S.J.W.H., A. Visser, L.W. Hulshoff Pol and A.J.M. Stams (1994). Sulfate reduction in methanogenic bioreactors. *FEMS Microbiol. Rev.* 15: 119-136

Parton W.J., D.S. Schimel, C.V. Cole and D.S. Ojima (1987). Analysis of factors controlling soil organic matter levels in Great Plains grasslands. *Soil Sci. Soc. Am. J.* 51: 1173-1179

Paustian K., W.J. Parton and J. Persson (1992). Modelling soil organic matter in organic-amended and nitrogen fertilized long-term plots. *Soil Sci. Soc. Am. J.* 56: 476-488

Penning de Vries F., P. Jansen, H. ten Berge and A. Bakena (1989). *Simulation of ecophysiological processes of growth in several annual crops.* Pudoc, Wageningen, The Netherlands

Peters V. and R. Conrad (1995). Methanogenic and other strictly anaerobic bacteria in desert soil and other oxic soils. *Appl. Env. Microbiol.* 61: 1673-1676

Pirt S.J. (1965). The maintenance energy of bacteria in growing cultures. *Proc. Royal Soc. London B* 163: 224-231

Ponnamperuma F.N. (1972). The chemistry of submerged soils. Adv. Agron. *24: 29-96*

Powell G.E., M.G. Hilton, D.B. Archer and B.H. Kirsop (1983). Kinetics of methanogenic fermentation of acetate. *J. Chem. Techn. Biotechn.* 33B: 209-220

Raalte M.H. van (1940). On the oxygen supply of rice roots. *Ann. Jar. Bot.* 50: 90-113

Rappoldt C. and D.W.G. van Kraalingen (1996). *The Fortran Simulation Translator. FST version 2.0. Introduction and reference manual.* Quantitative Approaches in Systems Analysis, AB-DLO, The Netherlands

Ratering S. and R. Conrad (1998). Effects of short-term drainage and aeration on the production of methane in submerged rice soil. *Global Change Biol.* 4: 397-407

Reddy K.R. and W.H. Patrick Jr. (1986). Fate of fertilizer nitrogen in the rice root zone. *Soil Sci. Soc. Am. J.* 50: 649-651

Reddy K.R., P.S.C. Rao and W.H. Patrick Jr. (1980). Factors influencing oxygen consumption rates in flooded soils. *Soil Sci. Soc. Am. J.* 44: 741-744

Reddy K.R., W.H. Patrick Jr. and C.W. Lindau (1989). Nitrification-denitrification at the plant root-sediment interface in wetlands. *Limnol. Oceanogr.* 34: 1004-1013

Revsbech N.P., O. Pedersen, W. Reichardt and A. Briones (1999). Microsensor analysis of oxygen and pH in the rice rhizosphere under field and laboratory conditions. *Biol. Fertil. Soils* 29: 379-385

Rickard D.T. (1975). Kinetics and mechanisms of pyrite formation at low temperatures. *Am. J. Sci.* 275: 636-652

Ridgwell A.J., S.J. Marshall and K. Gregson (1999). Consumption of atmospheric methane by soils: a process-based model. *Global Biogeochem. Cycl.* 13: 59-70

Robertson L.A. and J.G. Kuenen (1984). Aerobic denitrification: a controversy revived. Arch. Microbiol. *139: 351-354*

Robinson J.A. and J.M. Tiedje (1984). Competition between sulfate-reducing and methanogenic bacteria for H_2 under resting and growing conditions. *Arch. Microbiol.* 137: 26-32

Roslev P. and G.M. King (1994). Survival and recovery of methanotrophic bacteria starved under oxic and anoxic conditions. *Appl. Env. Microbiol.* 60: 2602-2608

Roslev P. and G.M. King (1995). Aerobic and anaerobic starvation metabolism in methanotrophic bacteria. *Appl. Env. Microbiol.* 61: 1563-1570

Rothfuss F. and R. Conrad (1993). Vertical profiles of CH_4 concentrations, dissolved substrates and processes involved in CH_4 production in a flooded Italian rice field. *Biogeochemistry* 18: 137-152

Rothfuss F. and R. Conrad (1998). Effect of gas bubbles on the diffusive flux of methane in anoxic paddy soil. Limnol. Oceanogr. *43: 1511-1518*

Roy R., H.D. Klüber and R.Conrad (1997). Early initiation of methane production in anoxic rice soil despite the presence of oxidants. *FEMS Microbiol. Ecol.* 24: 311-320

Saini R.C. (1989). Mass loss and nitrogen concentration changes during the decomposition of rice residues under field conditions. *Pedobiologica* 33: 229-235

Sass R.L. and F.M. Fisher (1995). Methane emissions from Texas rice fields: a five-year study. In: *Climate change and rice.* S. Peng et al. (Eds), Springer-Verlag, Berlin, p. 46-59

Sass R.L., F.M. Fisher, P.A. Harcombe and F.T. Turner (1990). Methane production and emission in a Texas rice field. *Global Biogeochem. Cycl.* 4: 47-68

Sass R.L., F.M. Fisher, P.A. Harcombe and F.T. Turner (1991a). Mitigation of methane emissions from rice fields: possible adverse effects of incorporated rice straw. *Global Biogeochem. Cycl.* 5: 275-287

Sass R.L., F.M. Fisher, F.T. Turner and M.F. Jund (1991b). Methane emission from rice fields as influenced by solar radiation, temperature and straw application. *Global Biogeochem. Cycl.* 5: 335-350

Sass R.L., F.M. Fisher, Y.B. Wang, F.T. Turner and M.F. Jund (1992). Methane emission from rice fields: the effect of floodwater management. *Global Biogeochem. Cycl.* 6: 249-262

Satpathy S.N., A.K. Rath, B. Ramakrishan, V.R. Rao, T.K. Adhya and N. Sethunathan (1997). Diurnal variation in methane efflux at different growth stages of tropical rice. *Plant Soil* 195: 267-271

Satpathy S.N., S. Mishra, T.K. Adhya, B. Ramakrishnan, V.R. Rao and N. Sethunathan (1998). Cultivar variation in methane efflux from tropical rice. *Plant Soil* 202: 223-229

Schönheit P., J.K. Kristjansson and R.K. Thauer (1982). Kinetic mechanism for the ability of sulfate reducers to out-compete methanogens for acetate. *Arch. Microbiol.* 132: 285-288

Schulz S. and R. Conrad (1996). Influence of temperature on pathways to methane production in the permanently cold profundal sediment of Lake Constance. *FEMS Microbiol. Ecol.* 20: 1-14

Schütz H., A. Holzapfel-Pschorn, R. Conrad, H. Rennenberg and W. Seiler (1989a). A 3-year continuous record on the influence of daytime, season, and fertilizer treatement on methane emission rates from an Italian rice paddy. *J. Geophys. Res.* 94: 16405-16416

Schütz H., W. Seiler and R. Conrad (1989b). Processes involved in formation and emission of methane in rice paddies. *Biogeochemistry* 7: 33-53

Schütz H., W. Seiler and R. Conrad (1990). Influence of soil temperature on methane emission from rice paddy fields. *Biogeochemistry* 11: 77-95

Segers R. (1998). Methane production and methane consumption: a review of processes underlying wetland methane fluxes. *Biogeochemistry* 41: 23-51

Segers R. (1999). *Wetland methane fluxes: Upscaling from kinetics via a single root and a soil layer to the plot.* PhD thesis, Wageningen University, The Netherlands

Segers R. (2000). Modelling methane fluxes in wetlands with gas transporting plants. 1. Single root scale. *J. Geophys. Res.* (submitted)

Segers R. and S.W.M. Kengen (1998). Methane production as a function of anaerobic carbon mineralization: a process model. *Soil Biol. Biochem.* 30: 1107-1117

Setter T.L., H. Greenway and T. Kupkanchankul (1989). Submergence of rice. II. Adverse effects of low CO_2 concentrations. *Austr. J. Plant Physiol.* 16: 265-278

Setyanto P., A.K. Makarim, A.M. Fagi, R. Wassmann and L.V. Buendia (2000). Crop management affecting methane emissions from irrigated and rainfed rice in Central Java (Indonesia). *Nutr. Cycl. Agroecosys.* (in press)

Sharma B. and R.C. Ahlert (1977). Nitrification and nitrogen removal. *Wat. Res.* 11: 897-925

Sigren L.K., G.T. Byrd, F.M. Fisher and R.L. Sass (1997). Comparison of soil acetate concentrations and methane production, transport, and emission in two rice cultivars. *Global Biogeochem. Cycl.* 11: 1-14

Singh S., R. Batra, M.M. Mishra, K.K. Kapoor and S. Goyal (1992). Decomposition of paddy straw in soil and the effect of straw incorporation in the field on the yield of wheat. *Z. Pflanzenernähr. Bodenk.* 155: 307-311

Sinke A.J.C., A.A. Cornelisse, T.E. Cappenberg and A.J.B. Zehnder (1992). Seasonal variation in sulfate reduction and methanogeneis in peaty sediments of eutrophic lake Loosdrecht, The Netherlands. *Biogeochemistry* 16: 43-61

Sipkema E.M., W. de Koning, K.J. Ganzeveld, D.B. Janssen, A.A.C.M. Beenackers (1998). Experimental pulse technique for the study of microbial kinetics in continuous culture. *J. Biotechn.* 64: 159-176

Slaton N.A., C.A. Beyrouty, B.R. Wells, R.J. Norman and E.E. Gbur (1990). Root growth and distribution of two short-season rice genotypes. *Plant Soil* 121: 269-278

Soetaert K., P.M.J. Herman and J.J. Middelburg (1996). A model of early diagenetic processes from the shelf to abyssal depths. *Geochim. Cosmochim. Acta* 60: 1019-1040

Sørensen J., J.M. Tiedje and R.B. Firestone (1980). Inhibition by sulfide of nitric and nitrous oxide reduction by denitrifying Pseudomonas fluorescens. *Appl. Env. Microbiol.* 39: 105-108

Sorrell B.K. and W. Armstrong (1994). On the difficulties of measuring oxygen release by root systems of wetland plants. *J. Ecol.* 82: 177-183

Stein A., I.G. Staritsky, J. Bouma, A.C. van Eijnsbergen and A.K. Bregt (1991). Simulation of moisture deficits and areal interpolation by universal cokriging. *Wat. Resource Res.* 27: 1963-1973

Stephen K.D., J.R.M. Arah, W. Daulat and R.S. Clymo (1998). Root-mediated gas transport in peat determined by argon diffusion. *Soil Biol. Biochem.* 30: 501-508

Straub K.L., M. Benz, B. Schink and F. Widdel (1996). Anaerobic, nitrate-dependent microbial oxidation of ferrous iron. *Appl. Env. Microbiol.* 62: 1458-1460

Stroosnijder L. (1982). Simulation of the soil water balance. In: *Simulation of plant growth and crop production*. F.W.T. Penning de Vries and H.H. van Laar (Eds), Pudoc simulation monographs, Wageningen, The Netherlands, p. 175-193

Stubner S., T. Wind and R. Conrad (1998). Sulfur oxidation in rice field soil: activity, enumeration, isolation and characterization of thiosulfate-oxidizing bacteria. *Syst. Appl. Microbiol.* 21: 569-578

Sweerts J.P.R.A., D. de Beer, L.P. Nielsen, H. Verdouw, J.C. van den Heuvel, Y. Cohen and T.E. Cappenberg (1990). Denitrification by sulphur oxidizing *Beggiatoa spp.* mats on freshwater sediments. *Nature* 344: 762-763

Takeda K. (1988). Characteristics of a nitrogen-fixing methanotroph, Methylocystis T-1. *Antonie van Leeuwenhoek* 54: 521-523

Tanaka S., A. Yamauchi and Y. Kono (1995). Root system morphology of four rice cultivars: response of different component roots to nitrogen application. *Jpn. J. Crop Sci.* 64: 148-155

Teo Y.H., C.A. Beyrouty, R.J. Norman and E.E. Gbur (1995). Nutrient uptake relationship to root characteristics of rice. *Plant Soil* 171: 297-302

Thauer R.K., K. Jungermann and K. Decker (1977). Energy conservation in chemotrophic anaerobic bacteria. *Bacteriol. Rev.* 41: 100-180

Tros M.E., T.N.P. Bosma, G. Schraa and A.J.B. Zehnder (1996). Measurement of minimum substrate concentration (S_{min}) in a recycling fermentor and its prediction from the kinetic parameters of *Pseudomonas sp. strain B13* from batch and chemostat cultures. *Appl. Env. Microbiol.* 62: 3655-3661

Trüper H.G. and H.G. Schlegel (1964). Sulphur metabolism in Thiorhodaceae I. Quantitative measurements on growing cells of *Chromatium okenii*, *Antonie van Leeuwenhoek* 30: 225-238

Tsutsuki K. and F.N. Ponnamperuma (1987). Behavior of anaerobic decomposition products in submerged soils. Effects of organic material amendment, soil properties, and temperature. *Soil Sci. Plant Nutr.* 33: 13-33

Turner N.C. (1986). Crop water deficits: a decade of progress. *Adv. Agron.* 39: 1-51

Tyler S.C., R.S. Bilek, R.L. Sass and F.M. Fisher (1997). Methane oxidation and pathways of production in a Texas paddy field deduced from measurements of flux, $\delta^{13}C$ and δD of CH_4, *Global Biogeochem. Cycl.* 11: 323-348

Ueckert J., T. Hurek, I. Fendrik and E-G. Niemann (1990). Radial gas diffusion from roots of rice (*Oryza sativa* L.) and Kallar grass (*Leptochloa flusca* L. *Kunth*) and effects of inoculation with azospirillum brasilense Cd.. *Plant Soil* 122: 59-65

Ueki K., A. Ueki, K. Takahashi and M. Iwatsu (1992). The role of sulfate reduction in methanogenic digestion of municipal sewage sludge. *J. Gen. Appl. Microbiol.* 38: 195-207

Vavilin V.A., V.B. Vasiliev, A.V. Pomomarev and S.V. Rytow (1994). Simulation model 'Methane as a tool for effective biogas production during anaerobic conversion of complex organic matter'. *Biores. Techn.* 48: 1-8

Vavilin V.A., S.V. Rytov and L. Ya Lokshina (1996). A description of hydrolysis kinetics in anaerobic degradation of particulate organic matter. *Biores. Techn.* 56: 229-237

Verburg P.H. (2000). *Exploring the spatial and temporal dynamics of land use- with special reference to China.* PhD thesis, Wageningen University, The Netherlands

Verburg P.H., A. Veldkamp and J. Bouma (1999). Land use changes under conditions of high population pressure: the case of Java. *Global Env. Change* 9: 303-312

Verhagen F.J.M., H.J. Laanbroek and J.W. Woldendorp (1995). Competition for ammonium between plant roots and nitrifying and heterotrophic bacteria and the effects of protozoan grazing. *Plant Soil* 170: 241-250

Visser A., I. Beeksma, F. van der Zee, A.J.M. Stams and G. Lettinga (1993). Anaerobic degradation of volatile fatty acids at different sulfate concentrations, *Appl. Microbiol. Biotechnol.* 40: 549-556

Visser A., L.W. Hulshoff Pol and G. Lettinga (1996). Competition of methanogenic and sulfidogenic bacteria. *Wat. Sci. Technol.* 33: 99-110

Voltz M. and R. Webster (1990). A comparison of kriging, cubic splines and classification for predicting soil properties from sample information. *J. Soil Sci.* 41: 473-490

Walinga I., J.J. van der Lee, V.J.G. Houba, W. van Vark and I. Novozamsky (1995). *Plant analysis manual,* Kluwer Academic Publishers, Dordrecht, The Netherlands

Walter B.P., M. Heimann, R.D. Shannon and J.R. White (1996). A process-based model to derive methane emissions from natural wetlands. *Geophys. Res. Lett.* 23: 3731-3734

Wang B., H.U. Neue and H.P. Samonte (1997). Effect of cultivar difference ('IR72', 'IR65598' and 'Dular') on methane emission. *Agr. Ecosys. Env.* 62: 31-40

Wang B., H.U. Neue and H.P. Samonte (1999). Factors controlling diel patterns of methane emission via rice. *Nutr. Cycl. Agroecosys.* 53: 229-235

Wang M-X., A.G. Dai, J. Huang, L. Ren, W. Seiler, H. Schütz, H. Rennenberg, R.A. Rasmussen and M.A.K. Khalil (1992). Sources of methane in China: Rice fields, cattle, coal mining, sewage treatment, other minor sources. In: *Proc. of CH4 and N2O workshop: CH4 and N2O emission from natural and anthropogenic sources and their reduction research plan,* NIAES, Japan, p. 70-88

Wang T. and J.H. Peverly (1999). Iron oxidation states on root surfaces of a wetland plant (*Phragmites australis*). *Soil Sci. Soc. Am. J.* 63: 247-252

Wang Z.P., R.D. Delaune, P.H. Masscheleyn and W.H. Patrick Jr. (1993). Soil redox and pH effects on methane production in a flooded rice soil. *Soil Sci. Soc. Am. J.* 57: 382-385

Wang Z.Y., Y.C. Xu, Z. Li, Y.X. Guo, R. Wassmann, H.U. Neue, R.S. Lantin, L.V. Buendia, Y.P. Ding and Z.Z. Wang (2000). Methane emission from irrigated rice fields in Northen China (Beijing). *Nutr. Cycl. Agroecosys.* (in press)

Wassmann R., H. Schütz, H. Papen, H. Rennenberg, W. Seiler, D. Aiguo, R.X. Shen, Y.S. Wang, X.J. Shangguan and M.X. Wang (1993). Quantification of methane emissions from Chinese rice fields Zhejiang province as influenced by fertilizer treatment. *Biogeochemistry* 20: 83-101

Wassmann R., H.U. Neue, R.S. Lantin, J.B. Aduna, M.C.R. Alberto, M.J. Andales, M.J. Tan, H.A.C. Denier van der Gon, H. Hoffmann, H. Papen, H. Rennenberg and W. Seiler (1994). Temporal patterns of methane emissions from wetland rice fields treated by different modes of N application. *J. Geophys. Res.* 99: 16457-16462

Wassmann R., H.U. Neue, M.C.R. Alberto, R.S. Lantin, C. Bueno, D. Llenaresas, J.R.M. Arah, H. Papen, W. Seiler and H. Rennenberg (1996a). Fluxes and pools of methane in wetlands rice soils with varying organic inputs. *Env. Monitoring Assessment* 42: 163-173

Wassmann R., X.J. Shangguan, M. Tölg, D.X. Cheng, M.X. Wang, H. Papen, H. Rennenberg and W. Seiler (1996b). Spatial and seasonal distribution of organic amendments affecting methane emissions from Chinese rice fields. *Biol. Fertil. Soils* 22: 191-195

Wassmann R., H.U. Neue, C. Bueno, R.S. Lantin, M.C.R. Alberto, L.V. Buendia, K. Bronson, H. Papen and H. Rennenberg (1998). Methane production of different rice soils derived from intrinsic and exogenous substrates. *Plant Soil* 203: 227-237

Watanabe A. and M. Kimura (1995). Methane production and its fate in paddy fields. VIII. seasonal variations in the amount of methane retained in soil. *Soil Sci. Plant Nutr.* 41: 225-233

Watanabe A., K. Katoh and M. Kimura (1993). Effect of rice straw application on CH$_4$ emission from paddy fields. I. Effect of weathering of rice straw in the field during off-crop season. *Soil Sci. Plant Nutr.* 39: 707-712

Watanabe A., K. Katoh and M. Kimura (1994). Effects of rice straw application on CH$_4$ emission from paddy fields. III. Effect of incorporation site of rice straw on CH$_4$ emission rates and their variation among shoots of a rice plant. *Soil Sci. Plant Nutr.* 40: 497-504

Watanabe A., M. Kajiwara, T. Tashiro and M. Kimura (1995a). Influence of rice cultivar on methane emission from paddy fields. *Plant Soil* 176: 51-56

Watanabe A., Y. Satoh and M. Kimura (1995b). Estimation of the increase in CH4 emission from paddy soils by rice straw application. *Plant Soil* 173: 225-231

Watanabe A., M. Yoshida and M. Kimura (1998). Contribution of rice straw carbon to CH$_4$ emission from rice paddies using ^{13}C-enriched rice straw. *J. Geophys. Res.* D103: 8237-8242

Watanabe I. (1984). Decomposition of organic matter in flooded rice soils. In: *Organic matter and rice.* IRRI, Philippines, p. 238-257

Watanabe I., W.L. Barraquio, M.R. de Guzman and D.A. Cabrera (1979). Nitrogen-fixing (acetylene reduction) activity and population of aerobic heterotrophic nitrogen-fixing bacteria associated with wetland rice. *Appl. Env. Microbiol.* 37: 813-819

Watanabe I., T. Hashimoto and A. Shimoyama (1997). Methane-oxidizing activities and methanotrophic populations associated with wetland rice plants. *Biol. Fertil. Soils* 24: 261-265

Watson A. and D.B. Nedwell (1998). Methane production and emission from peat: The influence of anions (sulphate, nitrate) from acid rain. *Atmos. Env.* 32: 3239-3245

Watson A., K.D. Stephen, D.B. Nedwell and J.A. Arah (1997). Oxidation of methane in peat: kinetics of CH$_4$ and O$_2$ removal and the role of plant roots. *Soil Biol. Biochem.* 29: 1257-1267

Webster R. (1985). Quantitative spatial analysis of soil in the field. *Adv. Soil Sci.* 3: 1-70

Westermann P. and B.K. Ahring (1987). Dynamics of methane production, sulfate reduction and denitrification in a permanently waterlogged alder swamp. *Appl. Env. Microbiol.* 53: 2554-2559

Westermann P., B.K. Ahring and R.A. Mah (1989). Temperature compensation in *Methanosarcina barkeri* by modulation of hydrogen and acetate affinity. *Appl. Env. Microbiol.* 55: 1262-1266

Whittenbury R., K.C. Phillips and J.F. Wilkinson (1970). Enrichment, isolation and some properties of methane-utilizing bacteria. *J. Gen. Microbiol.* 61: 205-218

Wilhelm E., R. Battino and R.J. Wilcock (1977). Low-pressure solubility of gases in liquid water. *Chem. Rev.* 77: 219-262

Willigen P. de and M. van Noordwijk (1994). Mass flow and diffusion of nutrients to a root with constant or zero-sink uptake. II. Zero-sink uptake. *Soil Sci.* 157: 171-175

Wind T. and R. Conrad (1995). Sulfur compounds, potential turnover of sulfate and thiosulfate, and numbers of sulfate-reducing bacteria in planted and unplanted paddy soil. *FEMS Microbiol. Ecol.* 18: 257-266

Winfrey M.R. and J.G. Zeikus (1977). Effect of sulfate on carbon and electron flow during microbial methanogenesis in freshwater sediments. *Appl. Env. Microbiol.* 33: 275-281

Witt C., K.G. Cassmann, J.C.G. Ottow and U. Biker (1999). Soil microbial biomass and nitrogen supply in an irrigated lowland rice soil as affected by crop rotation and residue management. *Biol. Fertil. Soils* (in press)

Wopereis M.C.S., T.P. Tuong and M.J. Kropff (1995). Challenges and advances in simulation modeling of rainfed lowland rice systems. In: *Fragile live in fragile ecosystems. Proceedings of the International Rice Research Conference 13-17 February 1995.* IRRI, Los Baños, Philippines, p. 615-631

Yagi K. and K. Minami (1990). Effect of organic matter application on methane emission from some Japanese paddy fields. *Soil Sci. Plant Nutr.* 36: 599-610

Yagi K., H. Tsuruta, K. Kanda and K. Minami (1996). Effect of water management on methane emission from a Japanese rice paddy field: Automated methane monitoring. *Global Biogeochem. Cycl.* 10: 255-267

Yagi K., K. Minami and Y. Ogawa (1998). Effects of water percolation on methane emission from rice paddies: a lysimeter experiment. *Plant Soil* 198: 193-200

Yamauchi A., Y. Kono and J. Tatsumi (1987). Comparison of root system structure of upland rice and maize. *Jpn. J. Crop Sci.* 56: 608-617

Yang H.S. (1996). Modelling organic matter mineralization and exploring options for organic matter management in arable farming in Northern China. *PhD thesis, Wageningen University, The Netherlands*

Yang S-S and H-L Chang (1998). Effect of environmental conditions on methane production and emission from paddy soil. *Agr Ecosys. Env.* 69: 69-80

Yao H. and R. Conrad (1999). Thermodynamics of methane production in different rice paddy soils from China, the Philippines and Italy. *Soil Biol. Biochem.* 31: 463-473

Yu L.X., J.D. Ray, J.C. O'Toole and H.T. Nguyen (1995). Use of was-petrolatum layers for screening rice root penetration. *Crop Sci.* 35: 684-687

Zehnder A.J.B. and K. Wuhrmann (1977). Physiology of *Methanobacterium*, strain AZ. *Arch. Microbiol.* 111: 199-205

Zehnder A.J.B., B.A. Huser, T.D. Brock and K. Wuhrmann (1980). Characterization of an acetate-decarboxylating, non-hydrogen-oxidizing methane bacterium. *Arch. Microbiol.* 124: 1-11

Curriculum vitae

Peter Michiel van Bodegom was born in Vlaardingen March 29th, 1972. He completed secondary school (VWO) at the 'Chr. Sg. Groen van Prinsterer' in Vlaardingen in June 1990. Afterwards, he started his study 'Soil, Water and Atmosphere' at the Wageningen Agricultural University. After the propaedeutic year, which he concluded 'cum laude', he specialised in soil science. During his studies he spent seven months in Kenya at the International Center for Research in Agroforestry to study nutrient dynamics in tree fallows. Back in Wageningen, he wrote a thesis on water, nitrogen and phosphorus balances in various fallow systems encountered in Kenya. He wrote a 2nd thesis on soil chemical aspects of sodic soil formation at fluctuating water tables. In December 1995, he supervised the course on 'Quantitative Evaluation of Fertility of Tropical Soils'. After graduation in January 1996, he started in March 1996 on his PhD research at the department of Microbiology and at the department of Theoretical Production Ecology of Wageningen University, which resulted in this dissertation. Since March 2000, he works as a post doc at the department of Systems Ecology of the Free University in Amsterdam on the effects of raising water tables on the biogeochemistry and vegetation of wet dune slacks.